UNCLASSIFIED

AD NUMBER

AD432026

NEW LIMITATION CHANGE

TO

Approved for public release, distribution unlimited

FROM

Distribution authorized to U.S. Gov't. agencies and their contractors; Administrative/Operational Use; DEC 1963. Other requests shall be referred to Army Missile Command, Redstone Arsenal, AL 35898.

AUTHORITY

GMDRL ltr dtd 1 Aug 1966 per MICOM

THIS PAGE IS UNCLASSIFIED

ARPA ORDER NO. 347-63
PROJECT CODE NO. 7400

GENERAL MOTORS CORPORATION

A COMPARISON OF SEVERAL APPROXIMATIONS FOR

THE DETERMINATION OF PLASMA LAYER PROPERTIES FROM THE MEASURED ELECTROMAGNETIC TRANSMISSION COEFFICIENT

Sponsored By
ADVANCED RESEARCH PROJECTS AGENCY
Monitored By
U.S. ARMY MISSILE COMMAND

CONTRACT NO. DA-04-495-ORD-3567(Z)
HYPERVELOCITY RANGE RESEARCH PROGRAM
A PART OF PROJECT "DEFENDER"

GM DEFENSE RESEARCH LABORATORIES
SANTA BARBARA, CALIFORNIA

AEROSPACE OPERATIONS DEPARTMENT

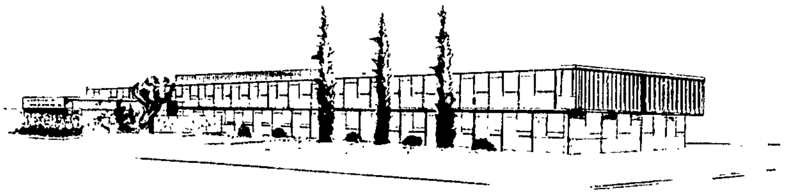

TR63-217G

DECEMBER 1963

ARPA ORDER NO. 347-6?
PROJECT CODE NO. 7400

Copy No 67

A COMPARISON OF SEVERAL APPROXIMATIONS FOR

THE DETERMINATION OF PLASMA LAYER PROPERTIES FROM THE MEASURED ELECTROMAGNETIC TRANSMISSION COEFFICIENT

by

S.V. Zivanovic, H.M. Musal, Jr.,
R.I. Primich and J. Allen

CONTRACT NO. DA-04-495-ORD-3567(Z)
HYPERVELOCITY RANGE RESEARCH PROGRAM
A PART OF PROJECT "DEFENDER"

THIS RESEARCH WAS SUPPORTED BY THE
ADVANCED RESEARCH PROJECTS AGENCY
DEPARTMENT OF DEFENSE
AND WAS MONITORED BY THE
U.S. ARMY MISSILE COMMAND
REDSTONE ARSENAL, ALABAMA

TR63-217G

DECEMBER 1963

FOREWORD

This report is one of a series of related papers covering various aspects of a broad program to investigate the flow-field variables associated with hypersonic-velocity projectiles in free flight under controlled environmental conditions. This research is being conducted in the Flight Physics Range of General Motors Defense Research Laboratories, and is supported by the Advanced Research Projects Agency under Contract No. DA-04-495-ORD-3567 (Z). It is intended that this series of reports, when completed, shall form a background of knowledge of the phenomena involved in the basic study and thus aid in a better understanding of the data obtained in the investigation.

ABSTRACT

Several commonly used approximations of the transmission coefficient of a uniform plasma slab are critically examined and compared with a new approximation developed in this report. It is shown that the new approximation, in addition to being very suitable for use on digital computers, gives much higher accuracy than any other one over most useful values of plasma and collision frequencies. A series of charts shows the regions of validity of each approximation in the plasma frequency-collision frequency plane for various amounts of error and slab thicknesses.

CONTENTS

LIST OF FIGURES

(SEE ALSO TABLE I, SUMMARY OF FIGURES)

LIST OF FIGURES (CONT'D)

LIST OF FIGURES (CONT'D)

LIST OF FIGURES (CONT'D)

LIST OF FIGURES (CONT'd)

INTRODUCTION

In many physical situations it is desirable to measure the electron density and electron collision frequency of an ionized medium, which determine its electromagnetic constitutive parameters, without material contact between the measuring instrument and the plasma. The free-space microwave propagation technique, many variations of which have been described in the literature[(1–3)*] is extremely useful for this purpose. In the most general form of this technique, a microwave beam of known field structure is used to illuminate the plasma and measurements are made of the amplitude and phase of both the transmitted and the reflected fields. The interpretation of these measurements in terms of plasma properties depends on a theoretical model of the plasma-microwave interaction, which is often highly idealized in the interests of analytical simplicity. However, in many instances, good results may be obtained by comparing the measured data with calculations based on the theory of the interaction of a uniform plane electromagnetic wave with a plane parallel-sided homogeneous plasma slab. Even in this simplified case it is sometimes necessary to approximate the exact analytical expressions in order to facilitate numerical interpretation. Several such approximations have been widely used,[(1, 3, 4, 5)] but rarely with any precise knowledge of the error incurred. It is the specific purpose of this report to review these approximations as well as several others,[(6, 7)] to calculate the error compared to the exact theory in each case, and to define the range of validity of each approximation. Errors which result from the lack of similitude between the experimental configuration and the theoretical model are not considered here.

Following a discussion of the desirability of measuring the transmission coefficient of a plane slab as opposed to the reflection coefficient, the various approximate expressions for the transmission coefficient are reviewed in

* Raised numbers in parentheses refer to references, listed at the end of this report.

relation to a new approximation presented in this report. This new approximation has two major features. First, the normalized plasma frequency Ω'_p* and normalized collision frequency Ω'_c as determined from the approximate formulas agree within a few percent with the exact values over most plasma conditions of practical interest. Second, Ω'_p and Ω'_c are given by simple algebraic expressions which can be easily incorporated into digital-computer programs. This latter feature is regarded as an essential criterion in determining whether a given approximation is useful, because in much of microwave plasma diagnostics (especially that devoted to transient events) a large amount of data reduction is required, and thus the use of a digital computer for data processing is necessary. The iterative determination of Ω_p and Ω_c from transcendental equations involving the measured transmission coefficient (which is required if the rigorous expressions are used) requires prohibitively long computer-operation time. An additional feature of this new approximation is that Ω'_p and Ω'_c are expressed as sums of terms containing the measured quantities raised to various powers. From this form the poorer approximations are obtained by neglecting the higher orders of small terms involving the measured quantities. Approximations referred to in the literature[1, 2, 4, 5] are located in this hierarchy and are examined for consistency.

In the examination of each approximation, in addition to the consistency test, Ω'_p and Ω'_c are computed from the approximate formulas and are compared to the exact values over most practical conditions of interest. The approximations considered in addition to the approximation developed in this paper are for a loss-free plasma,[1, 4] a low-loss plasma,[2] and an underdense plasma.[7] Finally, all approximations are compared by plotting prescribed error limits in an Ω_p - Ω_c plane, which illustrates in a graphic way the useful operating range of each approximation.

---

* The prime indicates an approximate quantity and the absence of the prime indicates the exact value.

THE TRANSMISSION AND REFLECTION COEFFICIENTS OF A PLANE PLASMA SLAB

For a uniform plane electromagnetic wave, normally incident on a plane parallel-sided homogeneous plasma slab, the external quantities that are available for measurement are the complex transmission and reflection coefficients. Assuming that the plasma may be regarded as an equivalent dielectric, the expressions for the transmission and reflection coefficients can then be written by referring to any standard derivation of the transmission and reflection coefficients of a dielectric layer (see, for example, References 8 and 9). The transmission coefficient is given by

$$T \equiv \frac{E_t}{E_i} = \frac{4\,N_p \exp\left[-j\,k_v\,d\,(N_p - 1)\right]}{(N_p + 1)^2 - (N_p - 1)^2 \exp(-2\gamma_p d)} \qquad (1)$$

where E_t and E_i are the complex amplitudes of the electric fields of the transmitted and incident waves, respectively, evaluated at the slab interface where the transmitted wave emerges, and

$N_p = \left(1 - \frac{\Omega_p^2}{1 - j\,\Omega_c}\right)^{1/2}$ = complex refractive index of plasma

$\Omega_p = \frac{\omega_p}{\omega} = \frac{1}{\omega}\left(\frac{q^2 n}{\epsilon_v m}\right)^{1/2}$ = normalized plasma frequency

$\Omega_c = \frac{\nu_c}{\omega}$ = normalized collision frequency

ω_p = angular plasma frequency

ν_c = collision frequency of electrons

ω = angular frequency of incident wave

q = charge on an electron

m = mass of an electron

n = electron density

ϵ_v = capacitivity of free space

$k_v \quad = \frac{2\pi}{\lambda_v}$

$\lambda_v \quad$ = free space wavelength of incident wave

$d \quad$ = thickness of the plasma slab

$\gamma_p = j\,k_v\,N_p \quad$ = propagation constant for a plane electromagnetic wave in plasma

The definition of the transmission coefficient in Expression (1) is convenient because the phase of T is then identical to the phase change that would be measured when the plasma slab is introduced into the path of the electromagnetic wave.

Similarly, the reflection coefficient is defined as

$$R \equiv \frac{E_r}{E_i} = \frac{(1 - N_p^{\,2})\left[1 - \exp(-2\gamma_p d)\right]}{(N_p + 1)^2 - (N_p - 1)^2 \exp(-2\gamma_p d)} \qquad (2)$$

where E_r and E_i are the complex amplitudes of the reflected and incident electromagnetic waves, respectively, evaluated at the incident interface of the plasma slab.

The plasma slab exhibits wave propagation characteristics similar to those of the unbounded plasma medium.[10] For negligible collision frequency ($\Omega_c << 1$) transmission occurs for plasma frequencies below the critical plasma frequency ($\Omega_p < 1$). The transmitted wave is virtually cut off for $\Omega_p > 1$. Reflection is low in the transmission region ($\Omega_p < 1$) and high in the cut-off region ($\Omega_p > 1$). Significant fluctuations in both quantities occur as Ω_p approaches unity. As the collision frequency increases, transmission decreases in the transmission region and the cut off near critical plasma frequency ($\Omega_p = 1$) is less well defined. For large Ω_c the transmission and reflection coefficients change very gradually, so that the transmission and cut-off regions can no longer be defined.

If either the complex transmission or reflection coefficient is known, the plasma properties Ω_p and Ω_c can be deduced uniquely providing that the thickness d is known. In cases where d is not known, both coefficients in their complex form are needed. It will be assumed hereafter that d is known.

The measurement of the reflection coefficient presents several experimental difficulties. First, the practical problems which arise in separating the received reflected microwave signal from leakage from the microwave transmitter are considerable. Unless extreme precautions are taken, a fraction of the transmitter signal will be present in the receiver and interference will take place. The resulting signal will depend on the relative phase between the reflected and leakage signals, and this depends on the absolute phase stability of the transmitter. Second, the phase of the reflected signal critically depends on the distance between the transmitter and the reflecting interface. If the phase of the reflection coefficient is to be measured, then this distance must be known absolutely at every instant to a high degree of accuracy. As an example, a physical movement of the plasma interface by a hundredth of a wavelength of the incident wave will cause a spurious phase change of 7.2 degrees. Third, in the transmission region the magnitude of the reflection coefficient is very small and can be (for the purpose of this discussion) approximated by the value $\frac{1}{4} \frac{n}{n_c}$ for $\frac{n}{n_c} << 1$, where n_c is the electron density which would cause cut-off at the frequency ω. Thus, for $\frac{n}{n_c} \leq \frac{1}{10}$ it follows that $|R| < 0.025$. Spurious reflections due to the plasma container, microwave windows, waveguide components, etc., can be easily of this order and will cause severe interference with the reflected signal. Consequently, it is extremely difficult to accurately measure by the reflection technique electron density in the range $\frac{n}{n_c} \leq \frac{1}{10}$. Fourth, the reflection coefficient is extremely sensitive to any ionization gradients in the direction of propagation of the electromagnetic wave. As was mentioned in the Introduction, a uniform plasma slab is an idealized model of the real plasma. The sharp boundaries of the idealized slab are never realized in a practical case, and the presence of a diffuse boundary layer is inevitable. These gradients will act as matching sections to further decrease actual reflection power and therefore introduce additional error unless precise information about these gradients is known.

All of these difficulties can be avoided by measuring the transmission coefficient. Small changes in the transmission coefficient can be measured accurately,* with almost no spurious effects from causes such as diffraction and movement of the plasma interfaces. The transmission coefficient is more sensitive to the total number of electrons along the propagation path than to local gradients of electron density.

The foregoing arguments present sufficient reason for measuring the transmission coefficient rather than the reflection coefficient of a plane slab whenever this is possible. It remains to be shown that the interpretation of the measured transmission coefficient in terms of Ω_p and Ω_c is also much more straightforward in view of the good approximations that can be made to the rigorous Expression (1). This in itself is a sufficiently good reason for using a measurement of the transmission coefficient rather than the reflection coefficient to determine the plasma frequency and collision frequency in a plasma slab.

* For example, for a plasma ten wavelengths thick, $\frac{n}{n_c} \geq 0.001$ can be reliably measured by the transmission technique.(7c)

NEED FOR TRANSMISSION COEFFICIENT APPROXIMATION

In principle, Expression (1) for the transmission coefficient may also be written

$$T = \tau(\Omega_p, \Omega_c, d)\, e^{j\,\theta(\Omega_p, \Omega_c, d)} \tag{3}$$

where $\tau(\Omega_p, \Omega_c, d)$ and $\theta(\Omega_p, \Omega_c, d)$ are transcendental functions of the plasma slab properties as indicated.

If the transmission coefficient is measured by a substitution method,[2] and if A_o and A are the amplitudes of the transmitted wave before and after the insertion of the slab, respectively, and if φ is the phase shift of the transmitted wave caused by the insertion of the slab in the beam, then

$$T = \frac{A}{A_o}\, e^{j\varphi} \tag{3a}$$

From Expressions (3) and (3a) it can be seen that

$$\frac{A}{A_o} = \tau(\Omega_p, \Omega_c, d) \tag{4}$$

$$\varphi = \theta(\Omega_p, \Omega_c, d) \tag{5}$$

In principle, these equations may be inverted to give Ω_p and Ω_c in terms of A/A_o, φ, and d. However, because of the complexity of $\tau(\Omega_p, \Omega_c, d)$ and $\theta(\Omega_p, \Omega_c, d)$ in this case, the inversion cannot be carried out explicitly.

In some situations it is practical to use a graphical solution. T can be computed rigorously from Expression (1) and τ and θ can be plotted as functions of Ω_p and Ω_c for various values of d. The measured values are located on the appropriate graph and the corresponding values of Ω_p and Ω_c are then read off.[9,12]

If data reduction requires the use of digital computers, the solution for Ω_p and Ω_c in terms of the measurable quantities has to be obtained through transcendental equations, requiring an iterative approach which, for a large number of data points, proves to be prohibitive in time and cost. An alternative procedure is then required; one such procedure, the use of manageable approximate formulas which can be easily inverted to give Ω_p' and Ω_c' explicitly, will now be pursued.

APPROXIMATIONS TO THE TRANSMISSION COEFFICIENT

In all of the transmission coefficient approximations referred to in the literature[1, 2, 4, 5] it was assumed (usually implicitly) that propagation through the plasma slab is unaffected by the presence of the boundaries. In addition to this assumption, the propagation constant of the plasma medium was then independently approximated. Musal[7] used only an approximate form for the propagation constant in the exact expression for the transmission coefficient, which includes the effect of the boundaries, and was able to derive a useful approximate transmission coefficient. In contrast, Zivanovic[6] used the exact expression for the propagation constant and only neglected the effects of the boundaries, from which a different approximate transmission coefficient was obtained. It was found that this last approximation is more widely applicable than all the earlier ones, since they can be derived from it as a series of successively poorer approximations.

In all the approaches discussed in this report, it is the transmission coefficient that is approximated. The approximate transmission coefficient is then inverted to explicitly express Ω_p' and Ω_c' in terms of the amplitude and phase angle of the measured transmission coefficient. It is important to recognize that a given approximation in the transmission coefficient can cause an error in Ω_p' and Ω_c' which cannot be explicitly predicted in analytic form. It is therefore necessary to examine the accuracy of the expressions for Ω_p' and Ω_c' numerically. This can be done as follows. Values of Ω_p, Ω_c, and d for a plasma slab are assigned and the exact transmission coefficient is calculated from Expression (1). Using this value for the transmission coefficient, Ω_p' and Ω_c' are then calculated from the inverted approximate expressions. It is then possible to compare Ω_p' and Ω_c' with Ω_p and Ω_c and to see directly the error caused by the approximate expressions.

There are a number of ways in which the error caused by the approximate expressions may be shown graphically. In this report, two methods are used. First, the relative errors in both Ω_p' and Ω_c' are plotted as functions of Ω_p' and Ω_c'. The choice of Ω_p' and Ω_c' (rather than Ω_p and Ω_c) as the independent variables was made because Ω_p' and Ω_c' are the quantities that are calculated and hence available, whereas Ω_p and Ω_c are not known in the actual measurement situation. Second, a mapping of the $\Omega_p - \Omega_c$ plane into the $\Omega_p' - \Omega_c'$ plane is given. These charts can be used to determine the exact values of Ω_p and Ω_c when the approximate values of Ω_p' and Ω_c' are known. These charts illustrate very lucidly, by the deviation of the $\Omega_p - \Omega_c$ lines from the $\Omega_p' - \Omega_c'$ grid, the parameter regions in which the approximate values are in large error. Both types of error representation are given for each approximation (non-reflecting boundary, underdense plasma, and low-loss plasma) for Ω_p' and Ω_c' in the range from zero to 0.95 and for d/λ_v in the range from one to ten in steps of one.

THE NONREFLECTIVE BOUNDARY APPROXIMATION (NRBA)

After some rearrangement, Expression (1) may be written in the form

$$T = \frac{\exp\left[jk_v d(1-Np)\right]}{1+F} \tag{6}$$

where

$$F \equiv \frac{1}{4}\Omega_p^4\left[1-\exp(-2\gamma_p d)\right]\frac{(1-j\Omega_c)^{-2}}{\sqrt{1-\frac{\Omega_p^2}{1-j\Omega_c}}\left[1+\sqrt{1-\frac{\Omega_p^2}{1-j\Omega_c}}\right]^2} \tag{6a}$$

The factor F is due to the multiple reflections from the slab boundaries.

Defining quantities a and b (not to be confused with the attenuation and phase constants α_p and β_p of the plasma!) as

$$a \equiv \frac{\lambda_v}{2\pi d} \ \ell n \ \frac{A}{A_o} = - \frac{1}{k_v d} \ \ell n \ \frac{A}{A_o} \tag{7}$$

$$b \equiv \frac{\varphi \lambda_v}{2\pi d} = \frac{\varphi}{k_v d} \tag{8}$$

the measured transmission coefficient given in Expression (3) can be written as

$$T = \exp\left[k_v d(-a+jb)\right] \tag{9}$$

Equating Expressions (9) and (6) results in

$$\exp\left[k_v d\ (-a+jb)\right] = \frac{1}{1+F} \ \exp\left[j\ k_v d\ (1-N_p)\right] \tag{10}$$

It is seen from (6a) that, for small Ω_p, F can be neglected compared with unity due to the Ω_p^4 factor. When Ω_p is close to unity the transmission coefficient depends exponentially on Ω_p, and neglecting F would be compensated by only a slight change of Ω_p in the exponential. Zivanovic[(6)] sets $F = 0$ and obtains an approximate transmission coefficient, given by

$$T' = \exp\left[jk_v d(1-N'_p)\right] \tag{11}$$

Equation (10) then reduces (with $F = 0$) to the form

$$-a + jb = j\ (1 - N'_p) = j\left[1 - \left(1 - \frac{\Omega_p'^2}{1 - j\Omega_c'}\right)^{1/2}\right] \tag{12}$$

and, after some manipulation, this can be inverted to give

$$\Omega_p'^2 = 2b - b^2 + 2\ \frac{a^2}{b} \ \frac{(1-b)^2}{1 - \frac{1}{2} b + \frac{1}{2} \frac{a^2}{b}} \tag{13}$$

$$\Omega'_c = \frac{a}{b} \frac{1 - b}{1 - \frac{1}{2} b + \frac{1}{2} \frac{a^2}{b}} \tag{14}$$

Here a and b and consequently Ω'_p and Ω'_c can be easily calculated from the directly measured quantities A_0, A, and φ using Equations (7), (8), (13) and (14). The values of Ω_p and Ω_c as functions of Ω'_p and Ω'_c are presented in Figures 1 to 10 and the relative errors incurred by this approximation are shown in Figures 11 to 30. It can be seen that the agreement between the exact and approximate values is excellent for a wide range of plasma frequency ($0 \le \Omega_p \le 0.95$), collision frequency ($0 \le \Omega_c \le 0.95$) and thickness of the medium ($\lambda_v \le d \le 10\ \lambda_v$).

THE UNDERDENSE PLASMA APPROXIMATION (UDPA)

Musal[7] has shown that when

$$\left| \frac{\Omega_p^2}{1 - j\,\Omega_c} \right|^2 << 1 \tag{15}$$

then γ'_p can be written as

$$\gamma'_p = j\,k_v \left(1 - \frac{1}{2} \frac{\Omega'^2_p}{1 - j\,\Omega'_c} \right) \tag{16}$$

Substituting Expression (16) into Expression (1) and making use of approximation (15) reduces the expression for T to

$$T' = \exp\left[k_v d \left(- \frac{1}{2} \frac{\Omega'_c\,\Omega'^2_p}{1 + \Omega'^2_c} + j\,\frac{1}{2} \frac{\Omega'^2_p}{1 + \Omega'^2_c} \right) \right] \tag{17}$$

Equating Expressions (17) and (9), one gets

$$\frac{1}{2} \frac{\Omega'_c\,\Omega'^2_p}{1 + \Omega'^2_c} = a \tag{18}$$

$$\frac{1}{2}\,\frac{\Omega_p'^2}{1+\Omega_c'^2} = b \tag{19}$$

where again a and b are defined by (7) and (8) in terms of the measured quantities A_o, A and φ.

Equations (18) and (19) can be solved for Ω_p' and Ω_c' to give

$$\Omega_p'^2 = 2b + 2\frac{a^2}{b} \tag{20}$$

$$\Omega_c' = \frac{a}{b} \tag{21}$$

Expressions (20) and (21) can be obtained from the more accurate Expressions (13) and (14) by retaining only terms of the first order in a and b in a power series expansion. This is consistent with the initial approximation (15) which implicitly neglects higher-order terms.

The graphs representing Ω_p and Ω_c for the underdense approximation as functions of Ω_p' and Ω_c' are given in Figures 31 to 40. The errors incurred in both Ω_p' and Ω_c' are given in Figures 41 to 60. The approximation is excellent within the limits of Assumption (15); the error increases when Ω_p' approaches unity. As can be seen from the graphs, this approximation is very good even for very large values of collision frequency.

Goldstein[5] has derived Equations (18) and (19) by simply approximating γ_p and neglecting multiple reflections from the beginning.

THE LOW-LOSS PLASMA APPROXIMATION (LLPA)

Whitmer,[2] neglecting multiple reflections and assuming that $\Omega_c^2 << 1$ and $\Omega_p^4 << 1$, has derived the following approximation for γ_p :

$$\gamma'_p = k_v \left[\frac{\Omega'_c \ \Omega'^{\,2}_p}{(1 - \Omega'^{\,2}_p)^{1/2}} - j \ (1 - \Omega'^{\,2}_p)^{1/2} \right] \tag{22}$$

Substitution of this into Expression (11) for the reflectionless transmission coefficient results in

$$T' = \exp \left[k_v d \left\{ -\frac{1}{2} \ \frac{\Omega \ \Omega'_c \ \Omega'^{\,2}_p}{(1 - \Omega'^{\,2}_p)^{1/2}} + j \left[1 - (1 - \Omega'^{\,2}_p)^{1/2} \right] \right\} \right] \tag{23}$$

Comparison of Expression (23) with the measured transmission coefficient as given in Expression (9) gives

$$\frac{1}{2} \ \frac{\Omega'_c \ \Omega'^{\,2}_p}{(1 - \Omega'^{\,2}_p)^{1/2}} = a \tag{24}$$

$$1 - (1 - \Omega'^{\,2}_p)^{1/2} = b \tag{25}$$

which can be readily inverted to yield

$$\Omega'^{\,2}_p = 2b - b^2 \tag{26}$$

$$\Omega'_c = \frac{a}{b} \ \frac{1 - b}{1 - \frac{1}{2} b} \tag{27}$$

Comparing these to Expressions (13) and (14), one inconsistency is noted. Whitmer's approximation is equivalent to neglecting the second order of a and hence Expression (27) is consistent with (14). However, the third term in Expression (13) contains a dominant factor $2a^2/b$, which is not necessarily of smaller order than a but has been neglected in Expression (26). Computations of Ω'_p and Ω'_c based on Expressions (26) and (27) bear out the suggestion that the third term in Expression (13) should not have been neglected. The results are shown in Figures 61 to 70. and the errors in Ω'_p and Ω'_c are given in Figures 71 to 90. There is no doubt that large errors arise when Ω_c is not close to zero. These could be reduced considerably by making a more consistent approximation, as indicated above.

Wharton[1a] has used a similar approximation, except that in his expression for β_p he has retained a term in Ω_c^2 as a part of a series expansion. This would lead to the presence of a third term in Expression (26) similar to that in Expression (13). However, because of the series expansion, the conversion of Wharton's α_p and β_p to Ω'_p and Ω'_c cannot be carried out.

THE LOSSLESS PLASMA APPROXIMATION

With $\Omega_c = 0$, Equation (13) becomes

$$\Omega'^2_p = 2b - b^2 \tag{28}$$

which is equal to Whitmer's Expression (26). Equation (28) (in a slightly different form) has been widely used in microwave interferometry.[1, 4] This is just a special case of both non-reflective boundaries and low-loss plasma approximations.

The values of Ω'_p from Equation (28) can be obtained either from the charts representing the nonreflective boundary approximation or the low-loss approximation for the special case of $\Omega_c = 0$.

COMPARISON OF APPROXIMATIONS

There is little doubt that the new approximation presented here leads to values of Ω_p' and Ω_c' that agree with the exact values well within the error limits normally encountered in microwave diagnostic experiments. The expressions for Ω_p' and Ω_c' are simple enough that they can be incorporated readily into any digital-computing program. Thus, from the point of view of interpreting experimental data, this approximation satisfies all practical requirements.

Since the other approximations can be derived from this approximation by neglecting the higher order terms in it, they can be no better than it. However, it is of interest to compare them numerically; this can be done most conveniently by plotting constant-error contours in the $\Omega_p - \Omega_c$ plane for both the plasma frequency and the collision frequency for the various approximations. Percentage-error contours are shown in Figures 91 to 106. Referring to Figures 91 thru 98, which show the one-percent-error contours, it can be seen that the new approximation covers most of the useful range of Ω_p and Ω_c. The lossless approximation (Wharton) includes most of the Ω_p axis ($\Omega_c = 0$), whereas the low-loss approximation (Whitmer)extends this coverage into a finite strip adjacent to the Ω_p axis ($\Omega_c^2 << 1$). On the other hand, the underdense approximation (Musal) covers a strip adjacent to the Ω_c axis ($\Omega_p^2 << 1$). In this sense, the underdense approximation and the low-loss approximation are complementary. Similar behavior prevails for other fixed percentage-error contours, as shown in the remaining figures.

REFERENCES

1. C. B. Wharton:

   a. "Microwave Diagnostics for Controlled Fusion Research," Plasma Physics, McGraw-Hill, 1961, Ch. 12

   b. "A Survey of Plasma Instrumentation," IRE Trans. NS-8, 56, 1961

   c. "Plasma Diagnostics," Paper 63-367, Fifth Biennial Gas Dynamics Symposium, AIAA, Northwestern University, August 14–16, 1963

2. R. F. Whitmer, "Microwave Studies of the Electron Loss Processes in Gaseous Discharges," Phys. Rev., 104, 572,1956

3. R. G. Jahn, "Microwave Probing of Ionized-Gas Flows," Phys. Fluids 5, 678, 1962

4. C. B. Wharton and D. Slager, "Microwave Determination of Plasma Density Profiles," J. A. P. 31, 428, 1960

5. L. Goldstein, "Electrical Discharge in Gases and Modern Electronics," Advances in Electronics and Electron Physics, Academic Press Inc., 1955, p. 401

6. S. Zivanovic, Unpublished work, GM Defense Research Laboratories, Santa Barbara, California

7. H. M. Musal, Jr., Unpublished work, discussed in the following reports:

   a. "Instrumentation, Calibration and Data Reduction Methods," GM Defense Research Laboratories Technical Report TR62-213, Santa Barbara, California, December 1962

   b. R. A. Hayami and R. I. Primich, "Ionization in Hypersonic Wakes," GM Defense Research Laboratories Technical Report TR62-209D, Santa Barbara, California, December 1962

   c. R. I. Primich and R. A. Hayami, "Millimeter Wavelength Focused Probes and Focused, Resonant Probes for Use in Studying Ionized Wakes behind Hypersonic-Velocity Projectiles," GM Defense Research Laboratories Technical Report TR63-217C, Santa Barbara, California, July 1963; Presented at the Millimeter and Submillimeter Wavelength Conference, Orlando, Florida, January 1963

8. W. M. Cady, M. B. Karelitz and L. A. Turner, "Radar Scanners and Radomes," Radiation Laboratory Series, McGraw-Hill, 1948, p. 354

9. I. P. French, G. G. Cloutier and M. P. Bachynski, "The Absorptivity Spectrum of a Uniform Anisotropic Plasma Slab," Can. J. Phys. 39, 1273, 1961

10. M. P. Bachynski, T. W. Johnston, and I. P. Shkarofsky, "Electromagnetic Properties of High Temperature Air," Proc. IRE, 48, 347, 1960

11. A. I. Carswell, M. P. Bachynski and G. G. Cloutier, "Microwave Measurements of Electromagnetic Properties of Plasma Flow-Fields," Paper 63-385, Fifth Biennial Gas Dynamics Symposium, AIAA, Northwestern University, August 14–16, 1963

12. S. Zivanovic, "Transmission and Reflection Coefficients of Uniform Plasma Slabs as a Function of Plasma Frequency, Collision Frequency and Thickness of the Slab," GM Defense Research Laboratories Technical Report TR62-209I, Santa Barbara, California, December 1962

TABLE I

SUMMARY OF FIGURES

	Ω_p and Ω_c vs Ω'_p and Ω'_c			$\frac{\Omega'_p-\Omega_p}{\Omega_p}$ vs Ω'_p			$\frac{\Omega'_c-\Omega'_c}{\Omega_c}$ vs Ω'_c		
	Approximation			Approximation			Approximation		
	NRBA	UDPA	LLPA	NRBA	UDPA	LLPA	NRBA	UDPA	LLPA
d = 1	1	31	61	11	41	71	21	51	81
d = 2	2	32	62	12	42	72	22	52	82
d = 3	3	33	63	13	43	73	23	53	83
d = 4	4	34	64	14	44	74	24	54	84
d = 5	5	35	65	15	45	75	25	55	85
d = 6	6	36	66	16	46	76	26	56	86
d = 7	7	37	67	17	47	77	27	57	87
d = 8	8	38	68	18	48	78	28	58	88
d = 9	9	39	69	19	49	79	29	59	89
d = 10	10	40	70	20	50	80	30	60	90

	ERROR <1%		ERROR < 8%	
	Ω_p	Ω_c	Ω_p	Ω_c
d = 1	91	92	99	100
d = 3	93	94	101	102
d = 5	95	96	103	104
d = 10	97	98	105	106

NOTE

NUMBERS REFER TO FIGURES; PAGE NUMBERS ARE SAME AS FIGURE NUMBERS

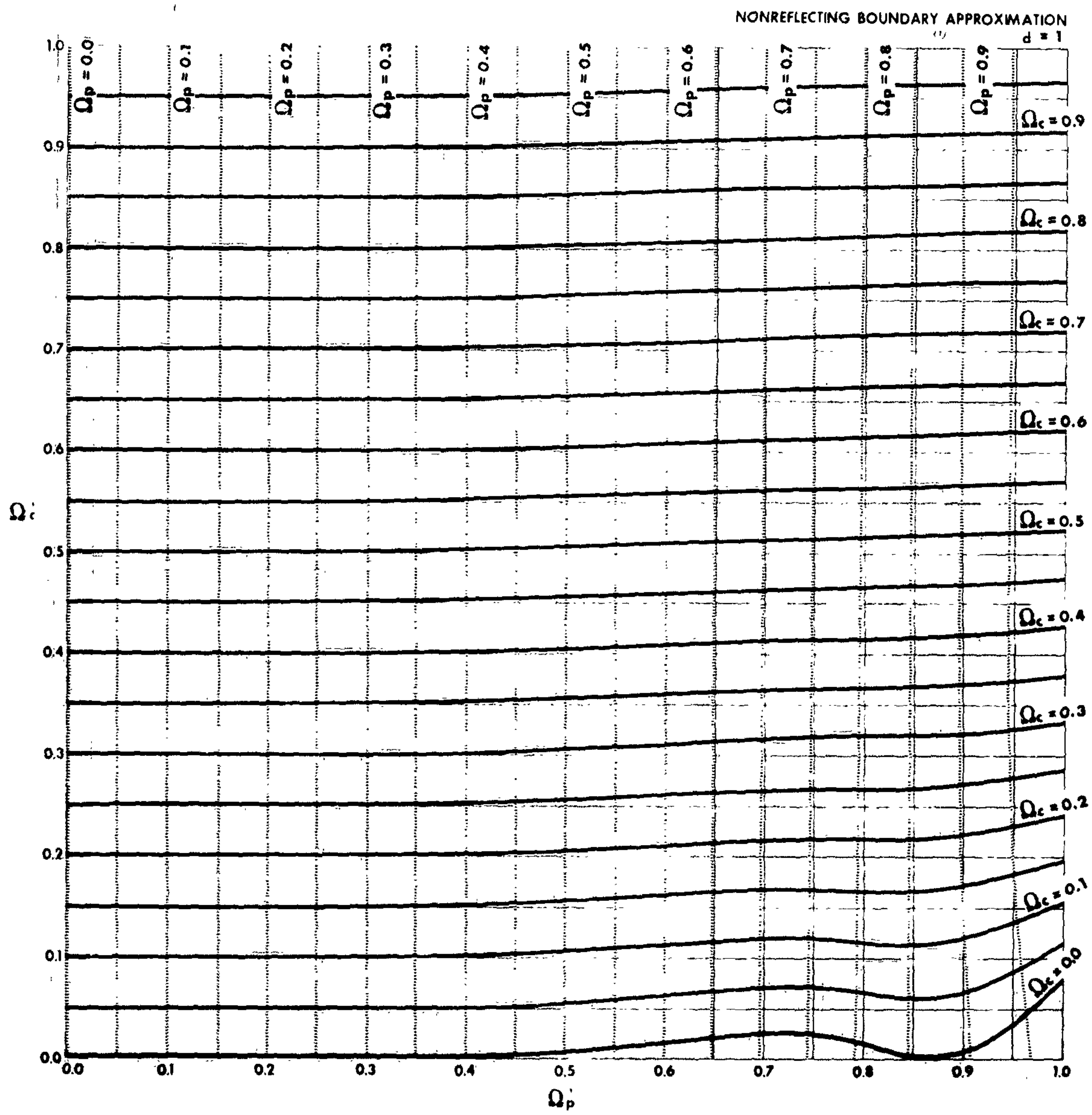

Figure 1 Exact Values, as Functions of the Calculated Values, of the Normalized Plasma and Collision Frequencies for the Nonreflective Boundary Approximation (NRBA), for a Value of the Normalized Thickness of the Plasma Layer d = 1.

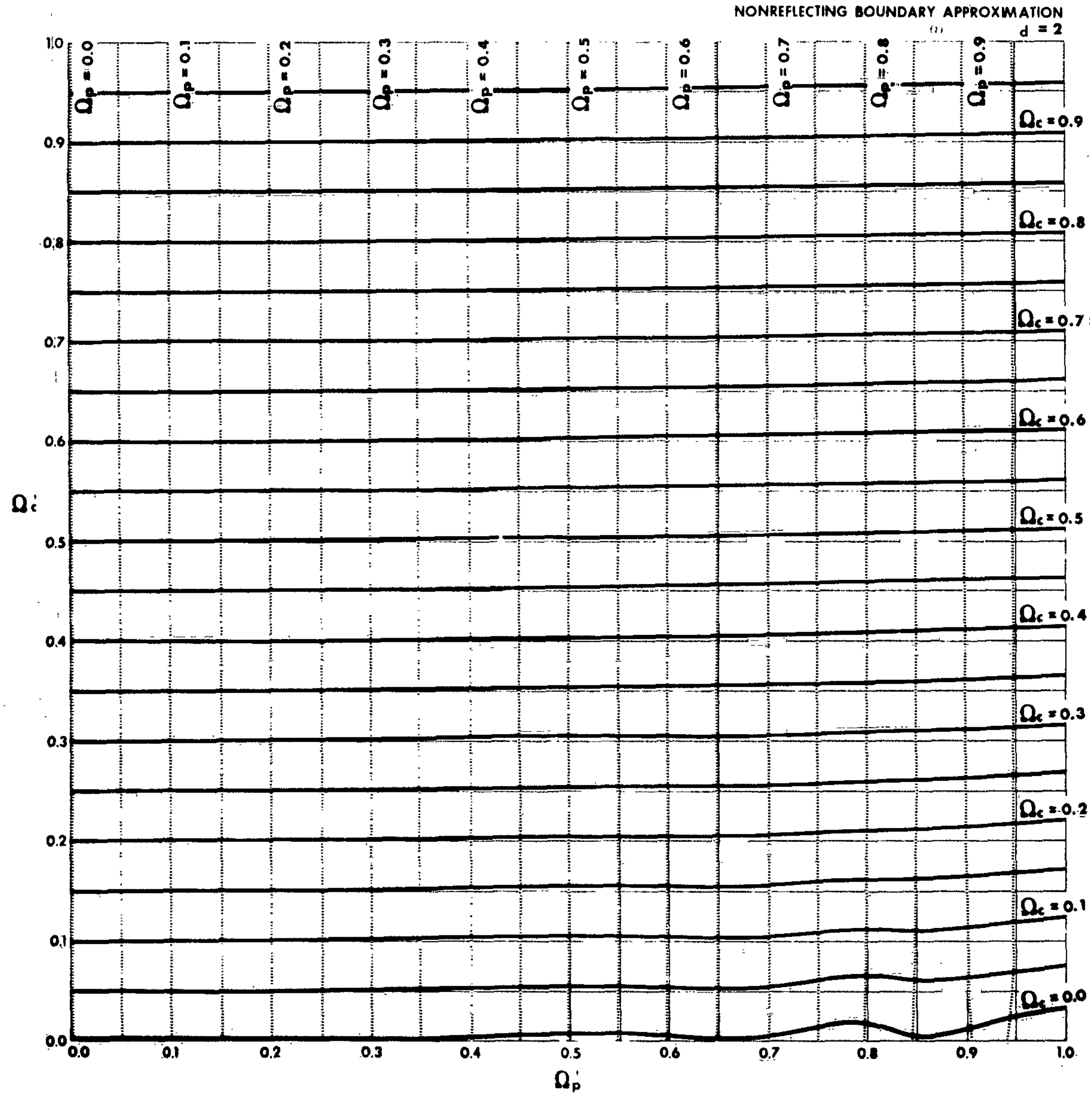

Figure 2 Exact Values, as Functions of the Calculated Values, of the Normalized Plasma and Collision Frequencies for the Nonreflective Boundary Approximation (NRBA), for a Value of the Normalized Thickness of the Plasma Layer d = 2

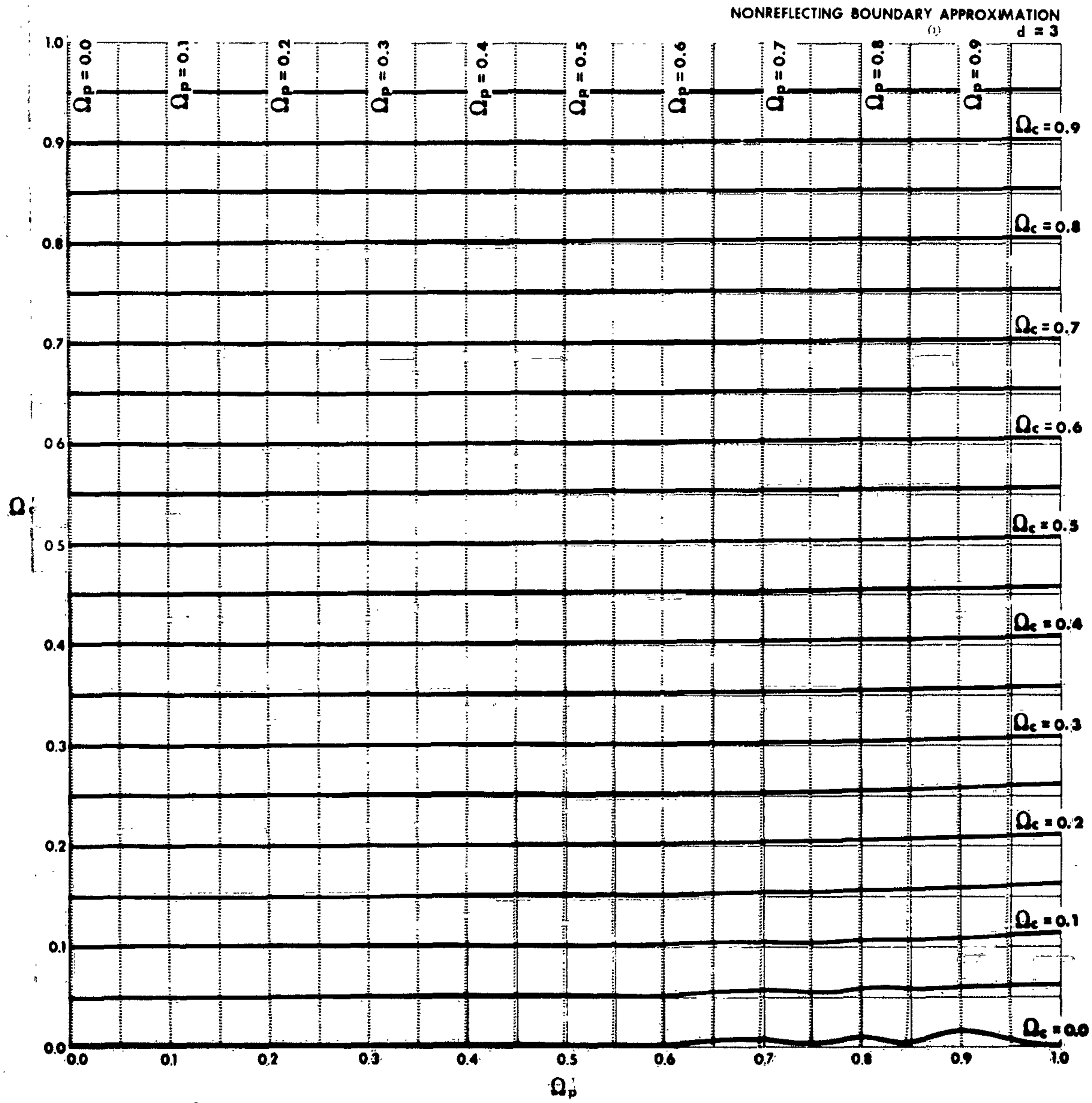

Figure 3 Exact Values, as Functions of the Calculated Values, of the Normalized Plasma and Collision Frequencies for the Nonreflective Boundary Approximation (NRBA), for a Value of the Normalized Thickness of the Plasma Layer d = 3

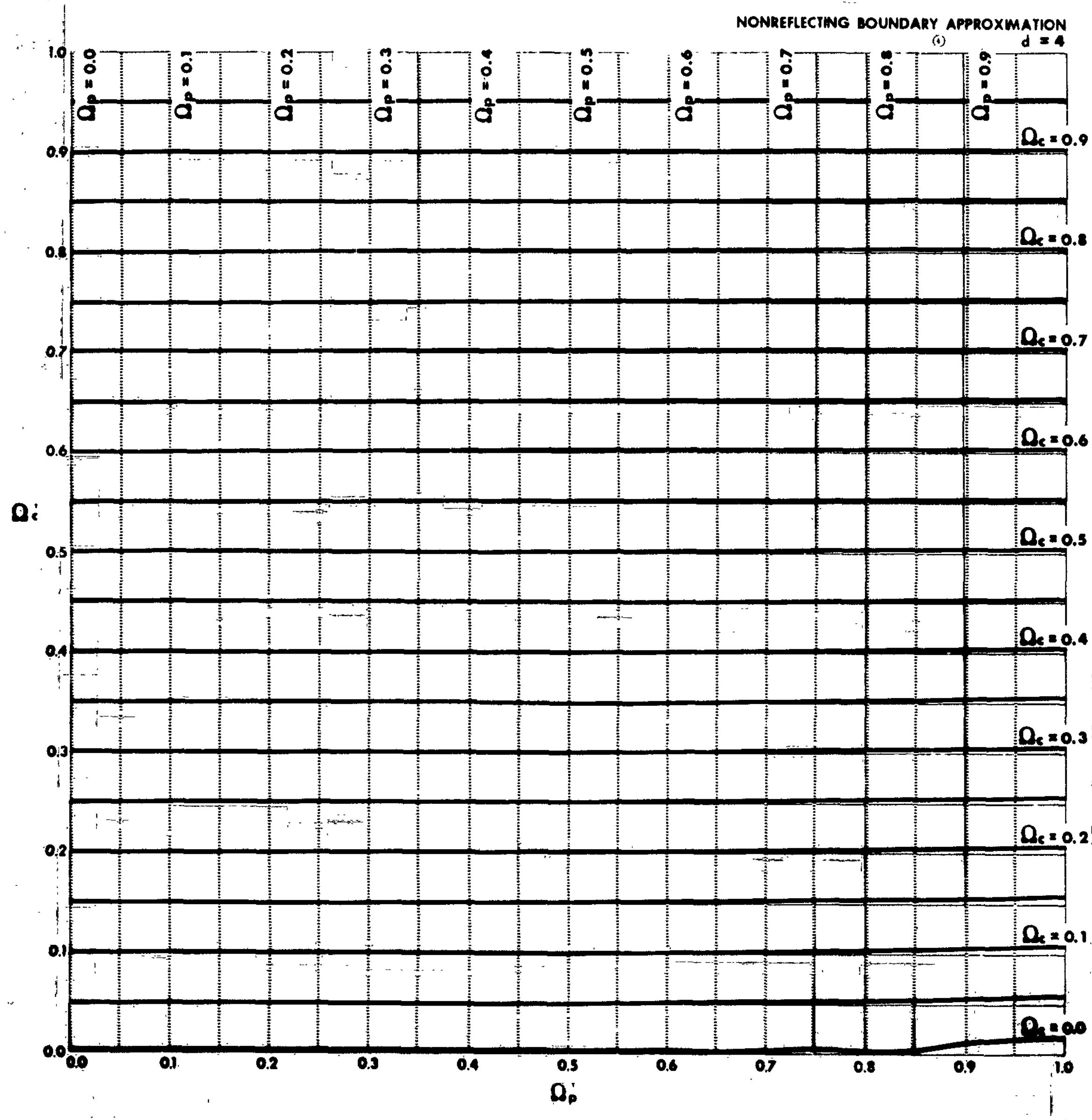

Figure 4 Exact Values, as Functions of the Calculated Values, of the Normalized Plasma and Collision Frequencies for the Nonreflective Boundary Approximation (NRBA), for a Value of the Normalized Thickness of the Plasma Layer d = 4

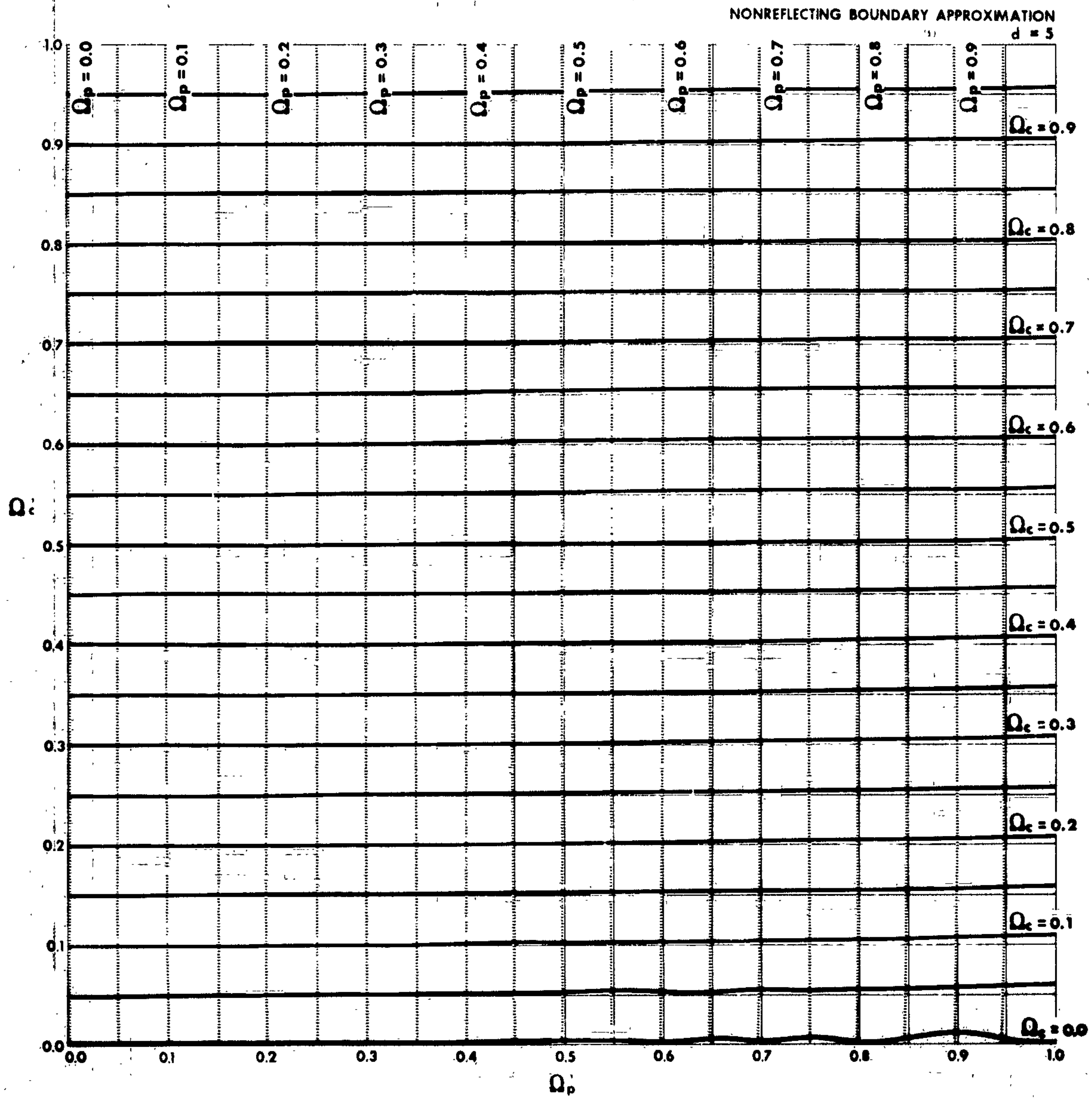

Figure 5 Exact Values, as Functions of the Calculated Values, of the Normalized Plasma and Collision Frequencies for the Nonreflective Boundary Approximation (NRBA), for a Value of the Normalized Thickness of the Plasma Layer d = 5

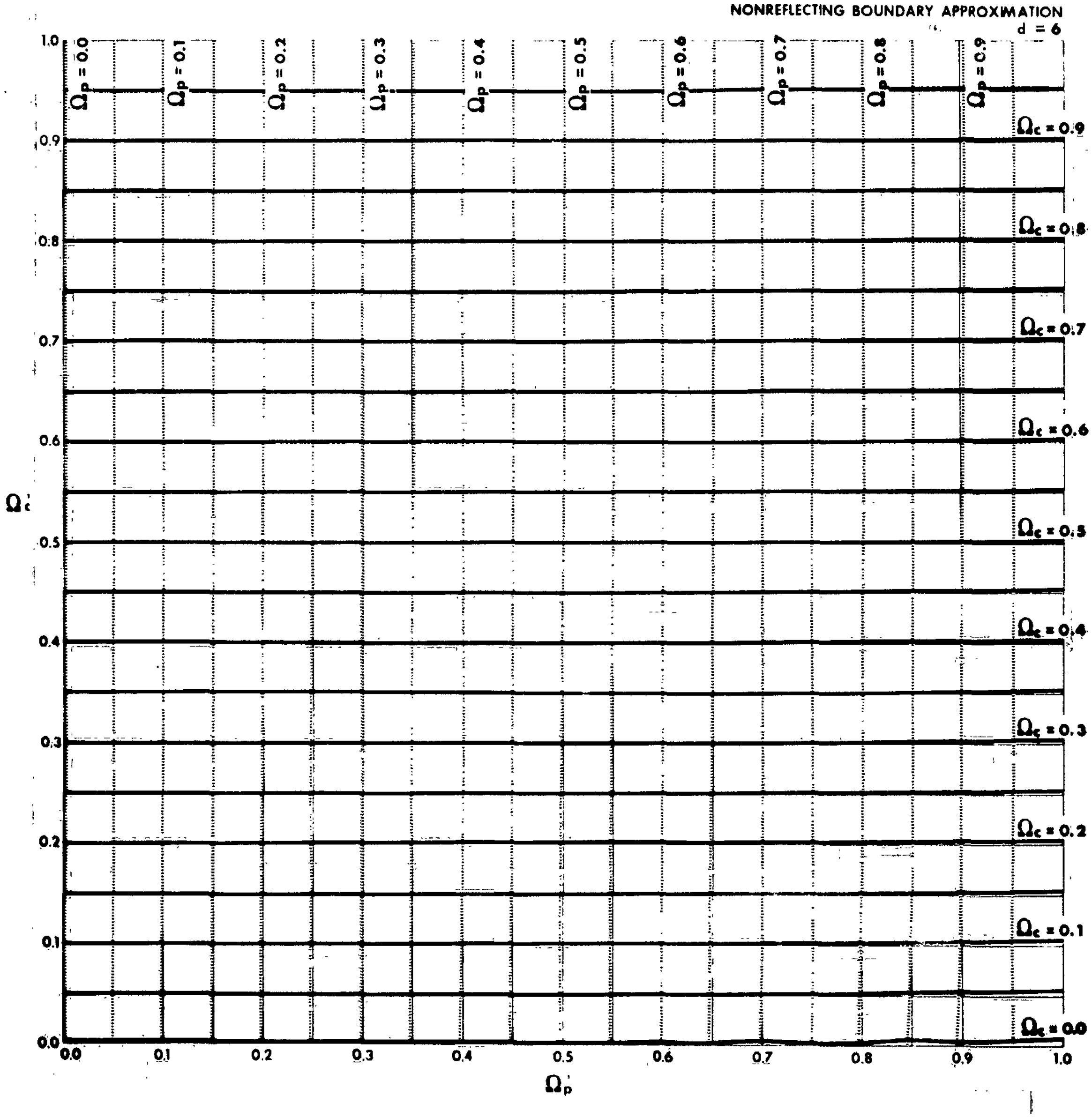

Figure 6 Exact Values, as Functions of the Calculated Values, of the Normalized Plasma and Collision Frequencies for the Nonreflective Boundary Approximation (NRBA), for a Value of the Normalized Thickness of the Plasma Layer d = 6

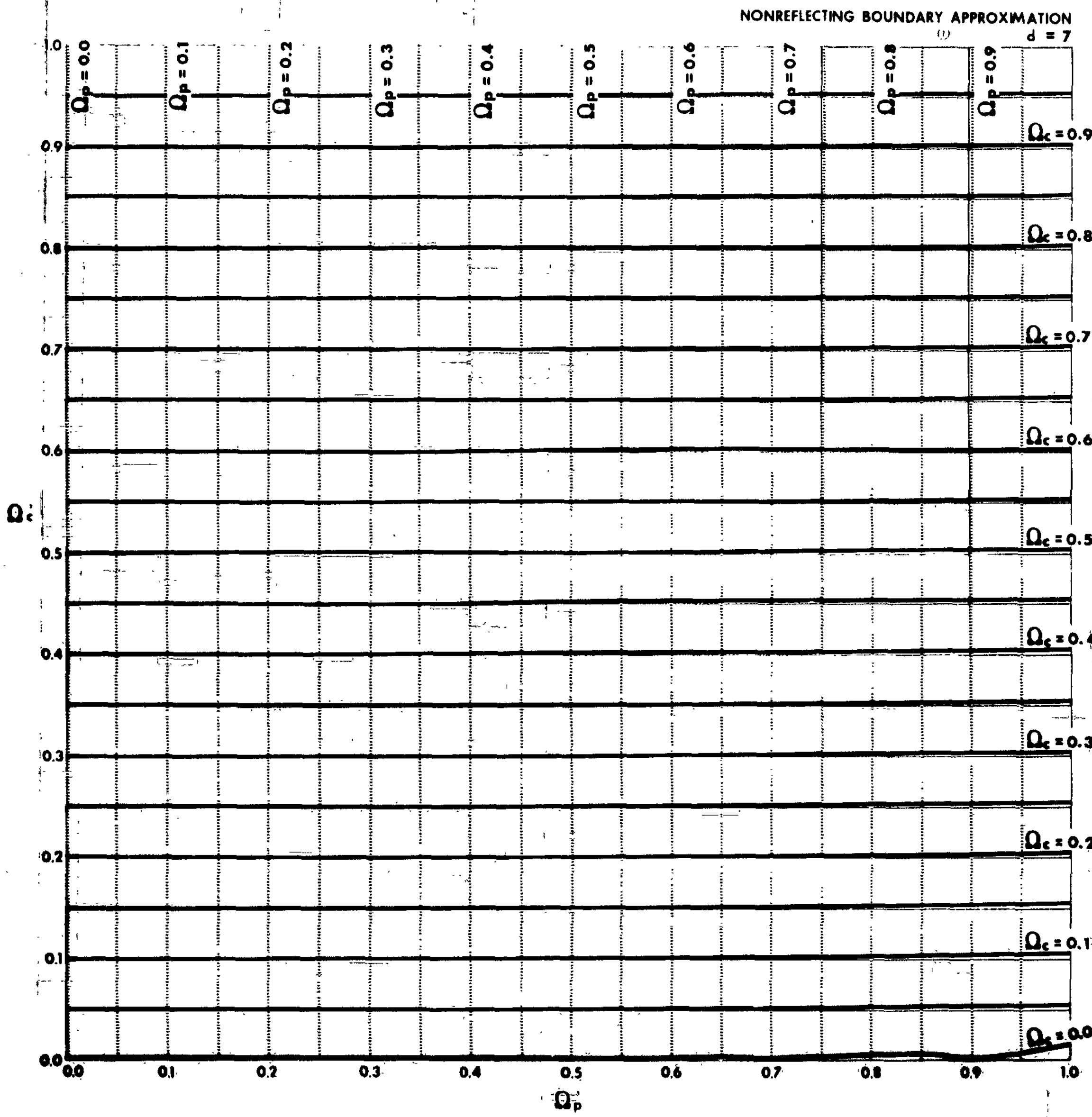

Figure 7 Exact Values, as Functions of the Calculated Values, of the Normalized Plasma and Collision Frequencies for the Nonreflective Boundary Approximation (NRBA), for a Value of the Normalized Thickness of the Plasma Layer d = 7

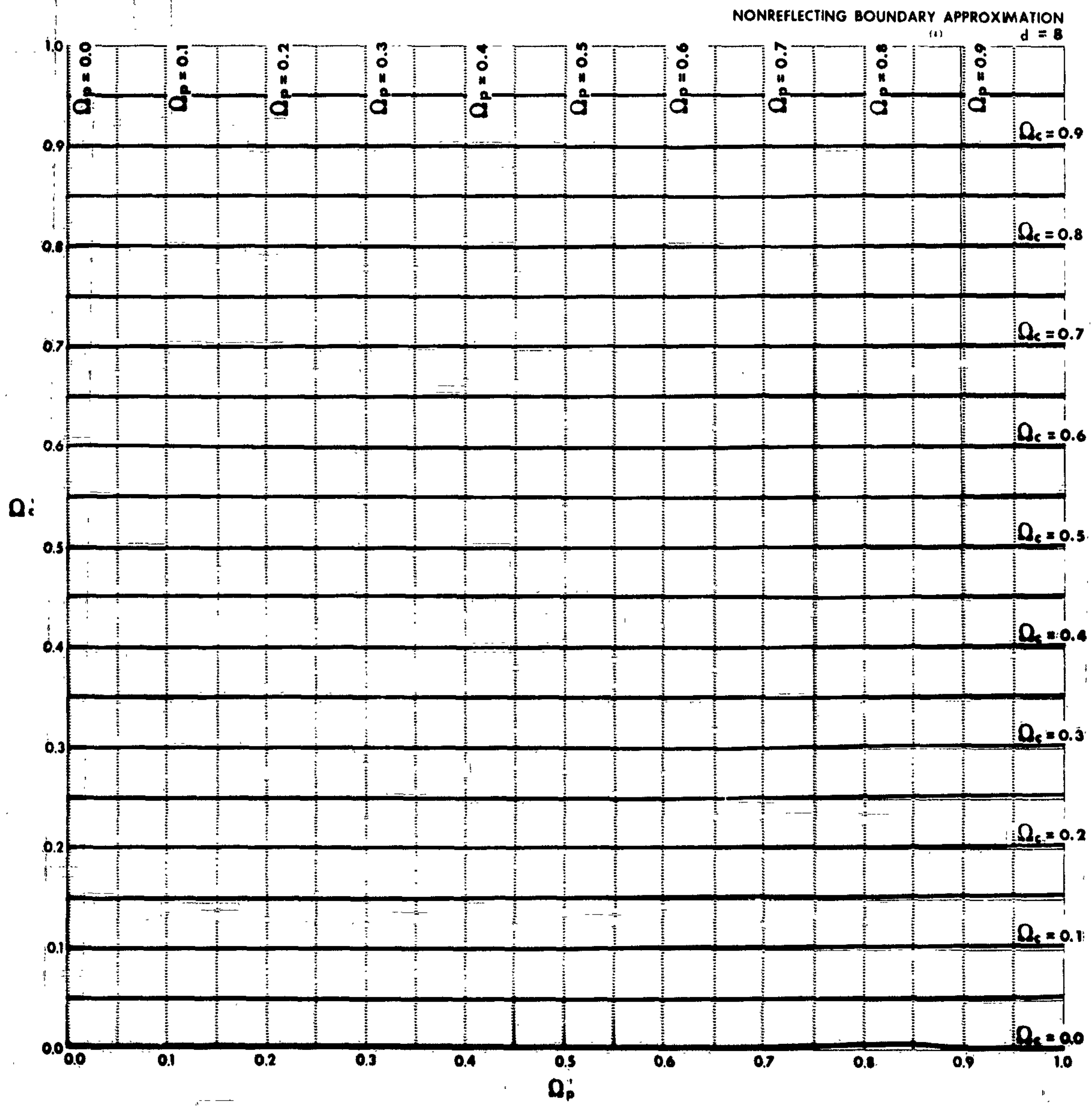

Figure 8 Exact Values, as Functions of the Calculated Values, of the Normalized Plasma and Collision Frequencies for the Nonreflective Boundary Approximation (NRBA), for a Value of the Normalized Thickness of the Plasma Layer d = 8

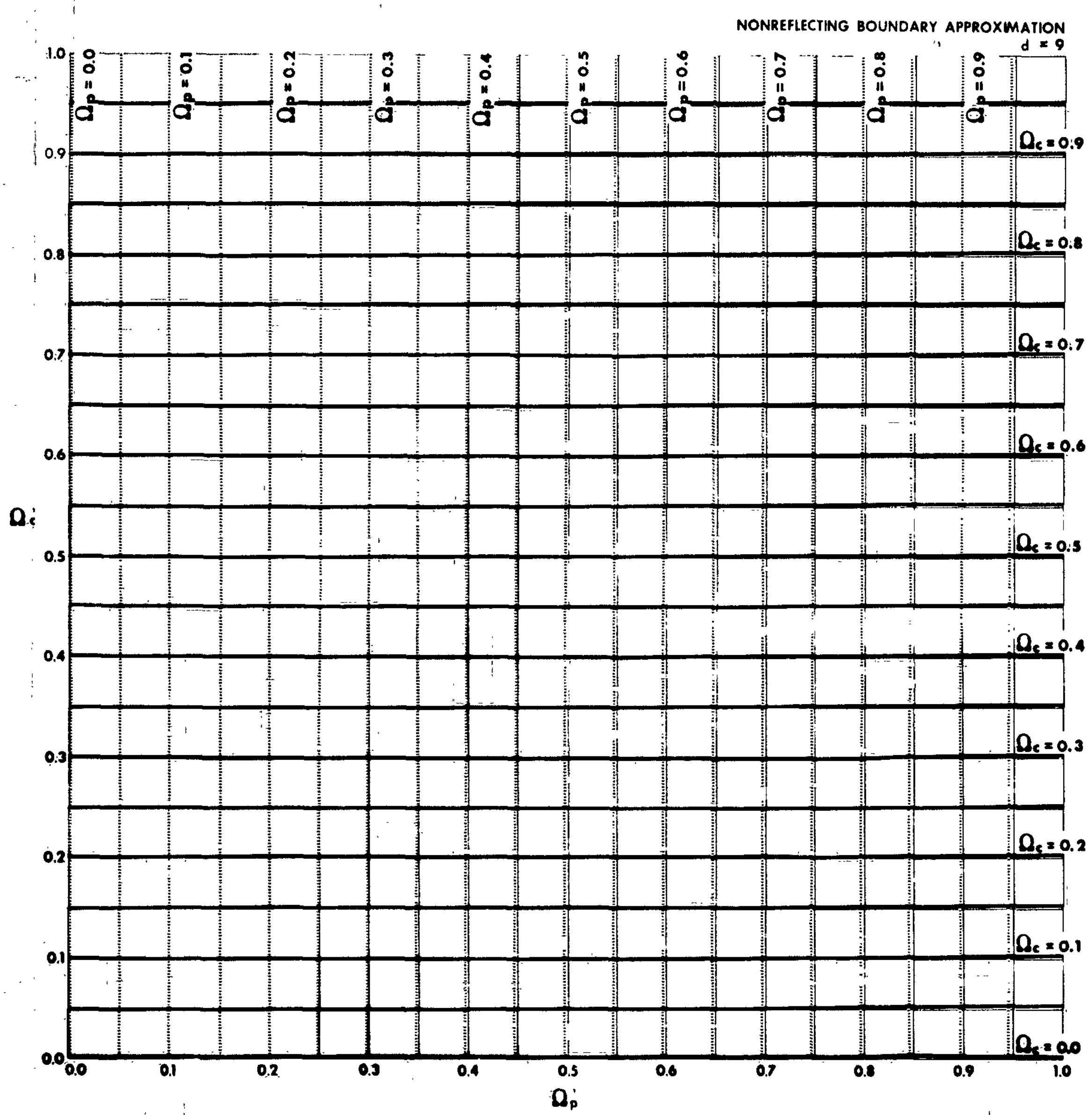

Figure 9 Exact Values, as Functions of the Calculated Values, of the Normalized Plasma and Collision Frequencies for the Nonreflective Boundary Approximation (NRBA), for a Value of the Normalized Thickness of the Plasma Layer d = 9

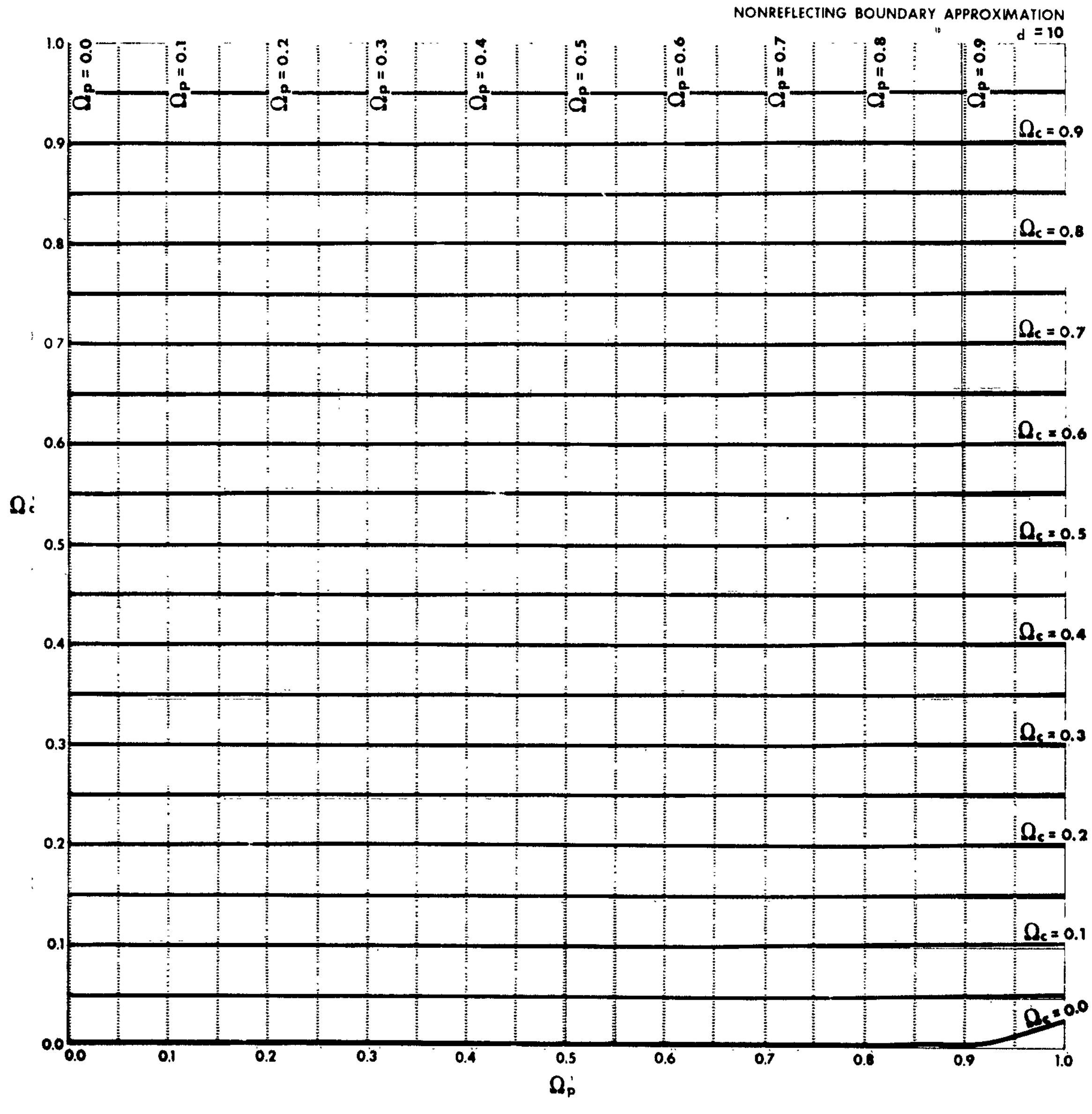

Figure 10 Exact Values, as Functions of the Calculated Values, of the Normalized Plasma and Collision Frequencies for the Nonreflective Boundary Approximation (NRBA), for a Value of the Normalized Thickness of the Plasma Layer d = 10

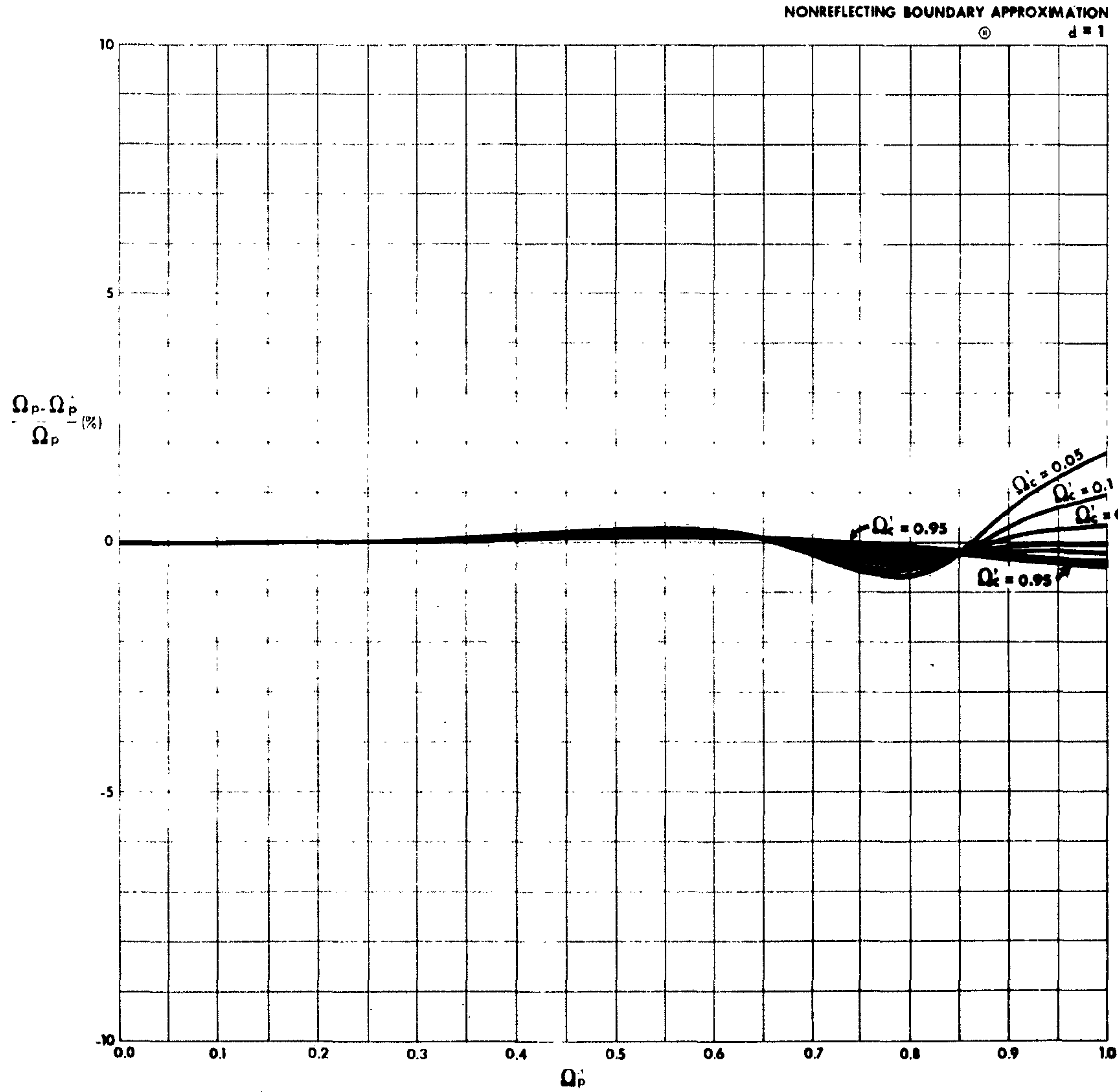

Figure 11 Percentage Error in Normalized Plasma Frequency for the Nonreflective Boundary Approximation (NRBA) as a Function of Measured Plasma Frequency for Various Values of Measured Collision Frequency, for a Value of the Normalized Thickness of the Plasma Layer d = 1

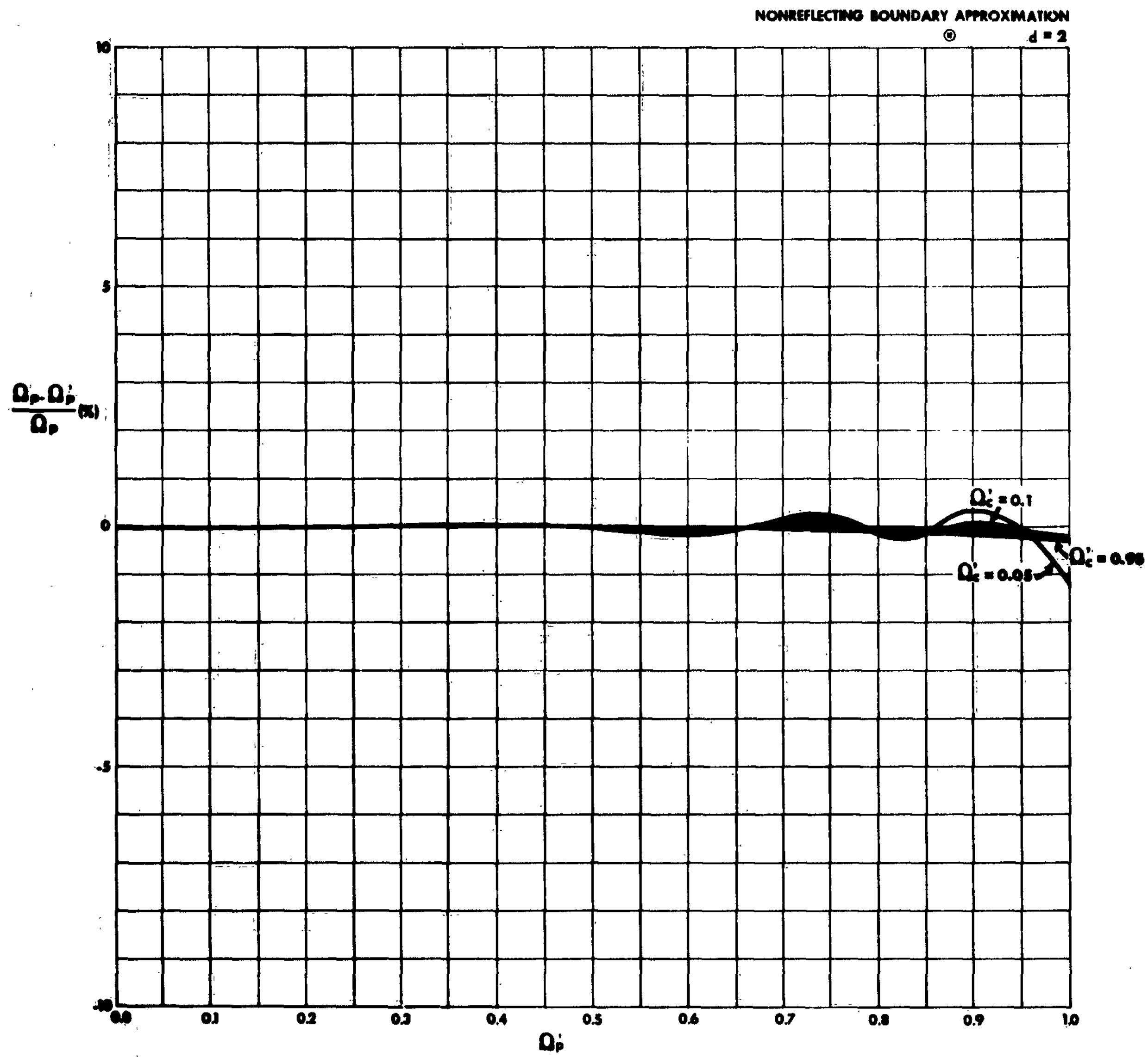

Figure 12 Percentage Error in Normalized Plasma Frequency for the Nonreflective Boundary Approximation (NRBA) as a Function of Measured Plasma Frequency for Various Values of Measured Collision Frequency, for a Value of the Normalized Thickness of the Plasma Layer d = 2

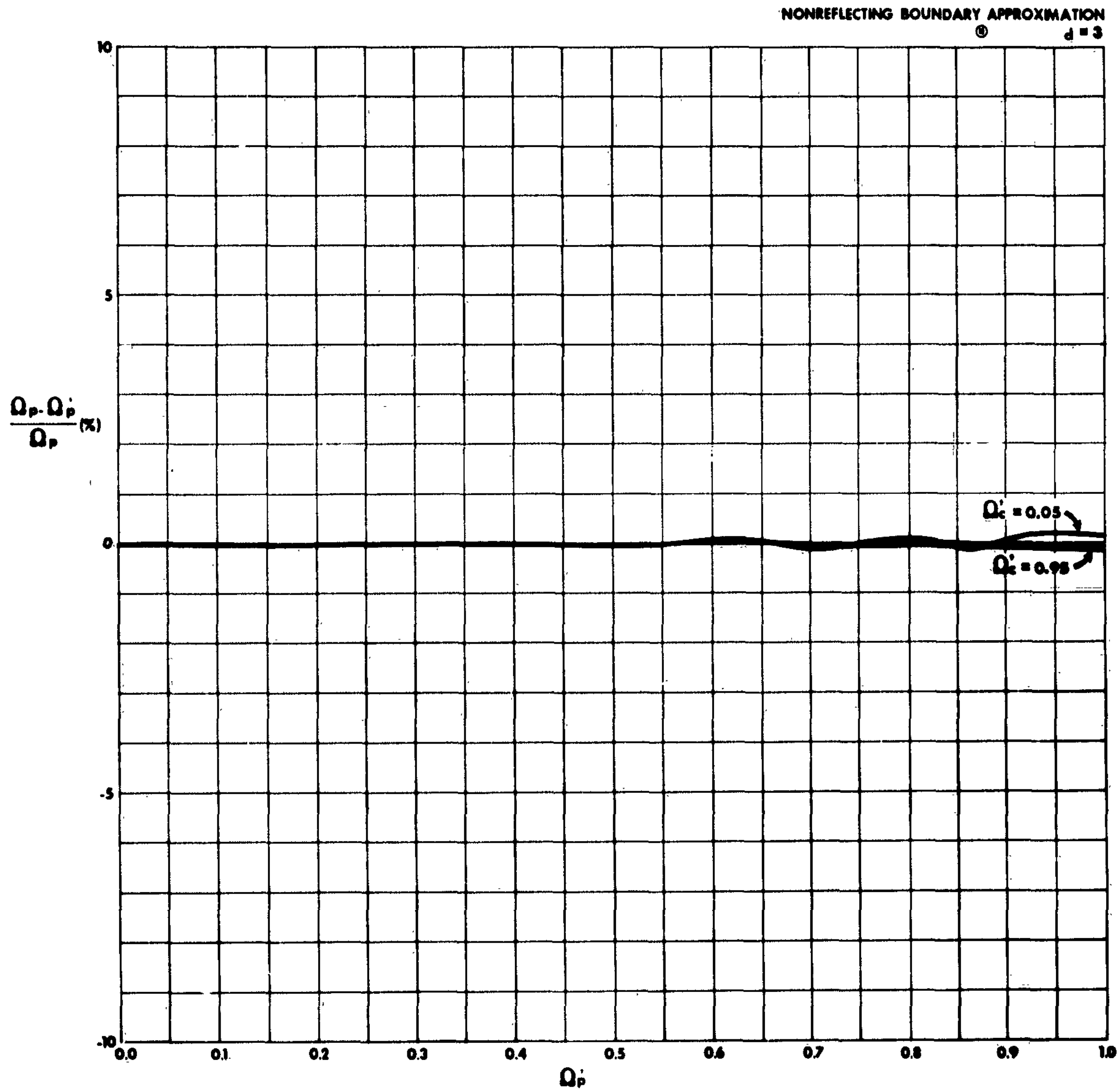

Figure 13 Percentage Error in Normalized Plasma Frequency for the Non-reflective Boundary Approximation (NRBA) as a Function of Measured Plasma Frequency for Various Values of Measured Collision Frequency, for a Value of the Normalized Thickness of the Plasma Layer d = 3

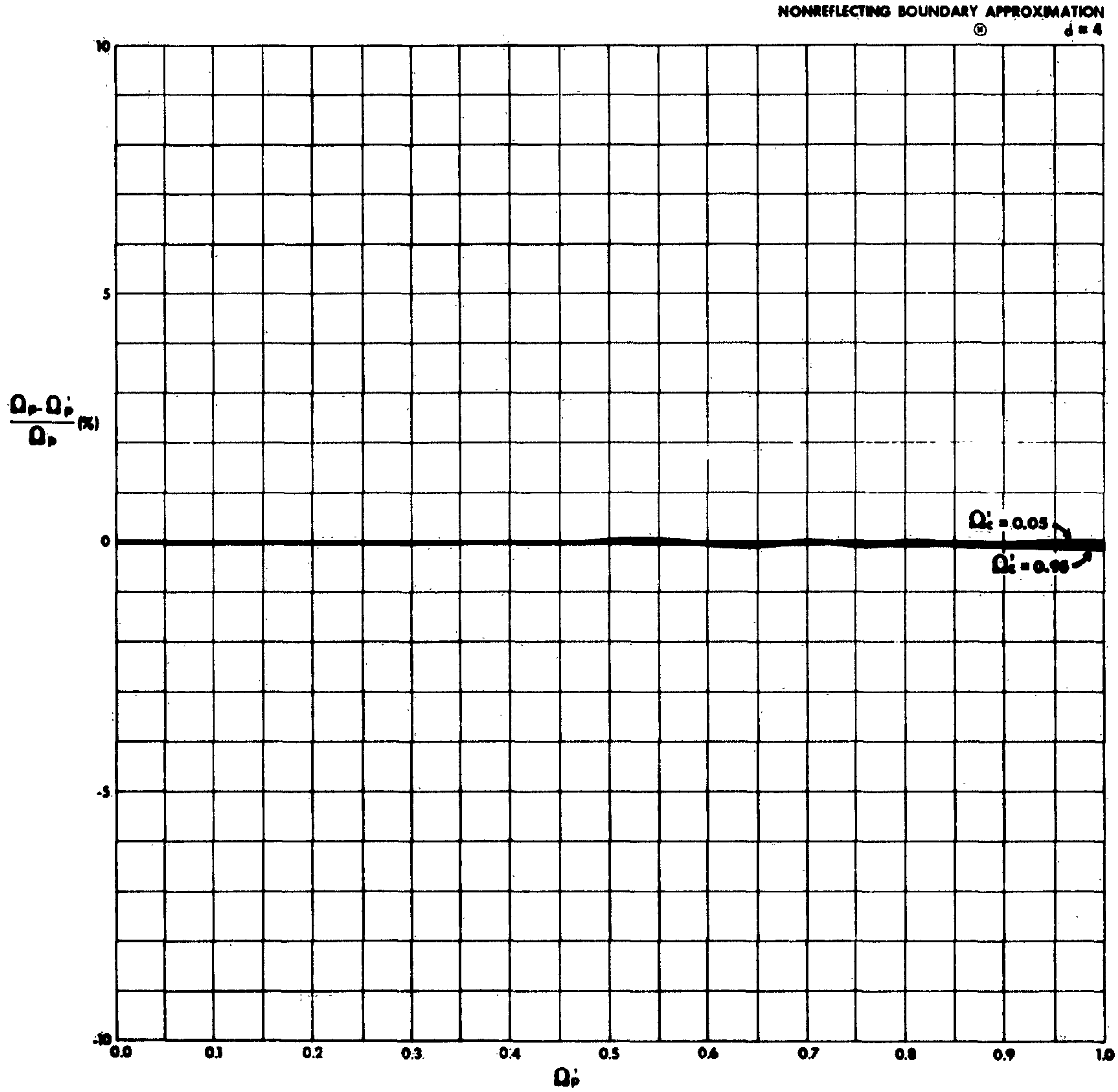

Figure 14 Percentage Error in Normalized Plasma Frequency for the Nonreflective Boundary Approximation (NRBA) as a Function of Measured Plasma Frequency for Various Values of Measured Collision Frequency, for a Value of the Normalized Thickness of The Plasma Layer d = 4

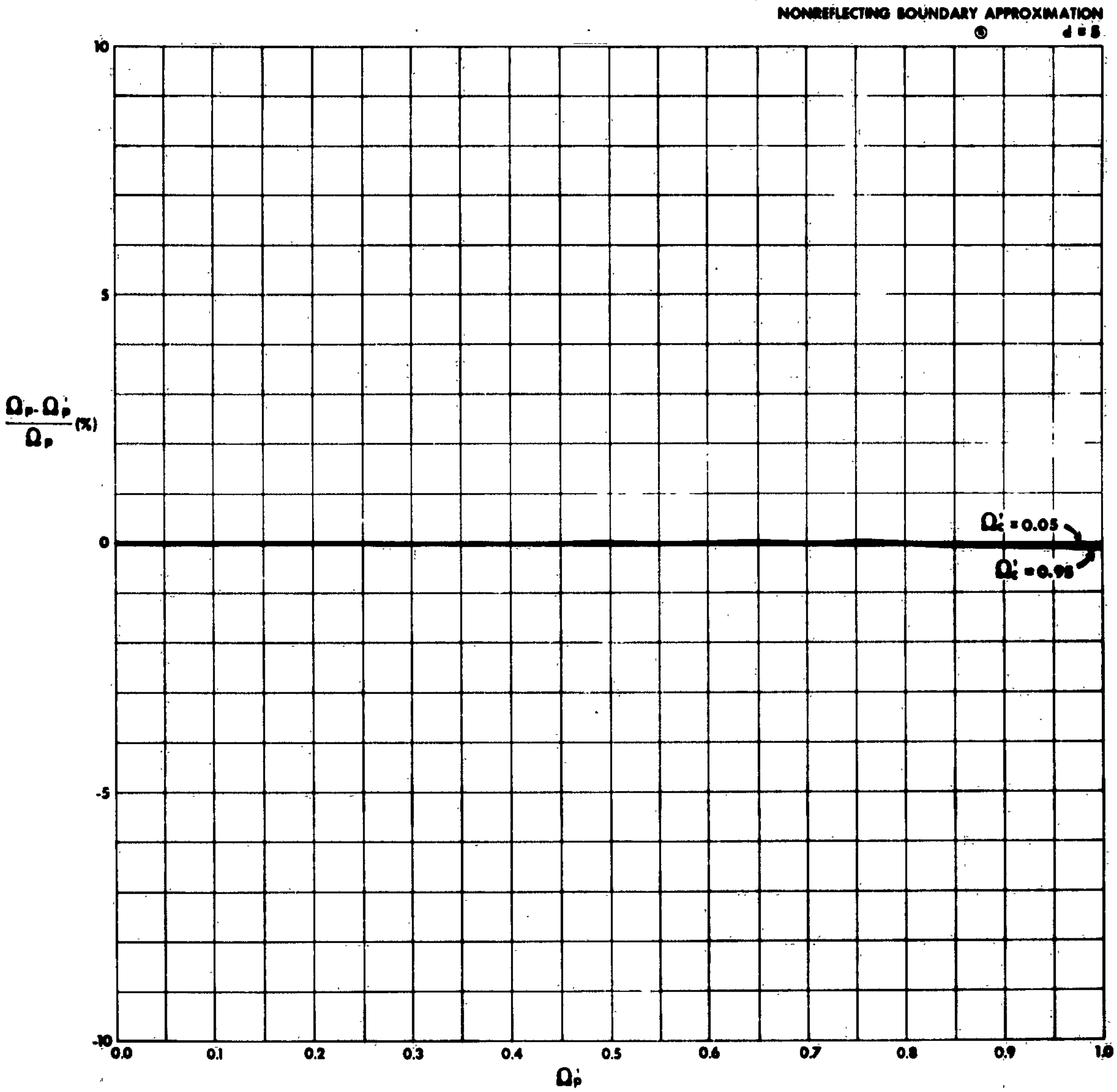

Figure 15 Percentage Error in Normalized Plasma Frequency for the Nonreflective Boundary Approximation (NRBA) as a Function of Measured Plasma Frequency for Various Values of Measured Collision Frequency, for a Value of the Normalized Thickness of the Plasma Layer d = 5

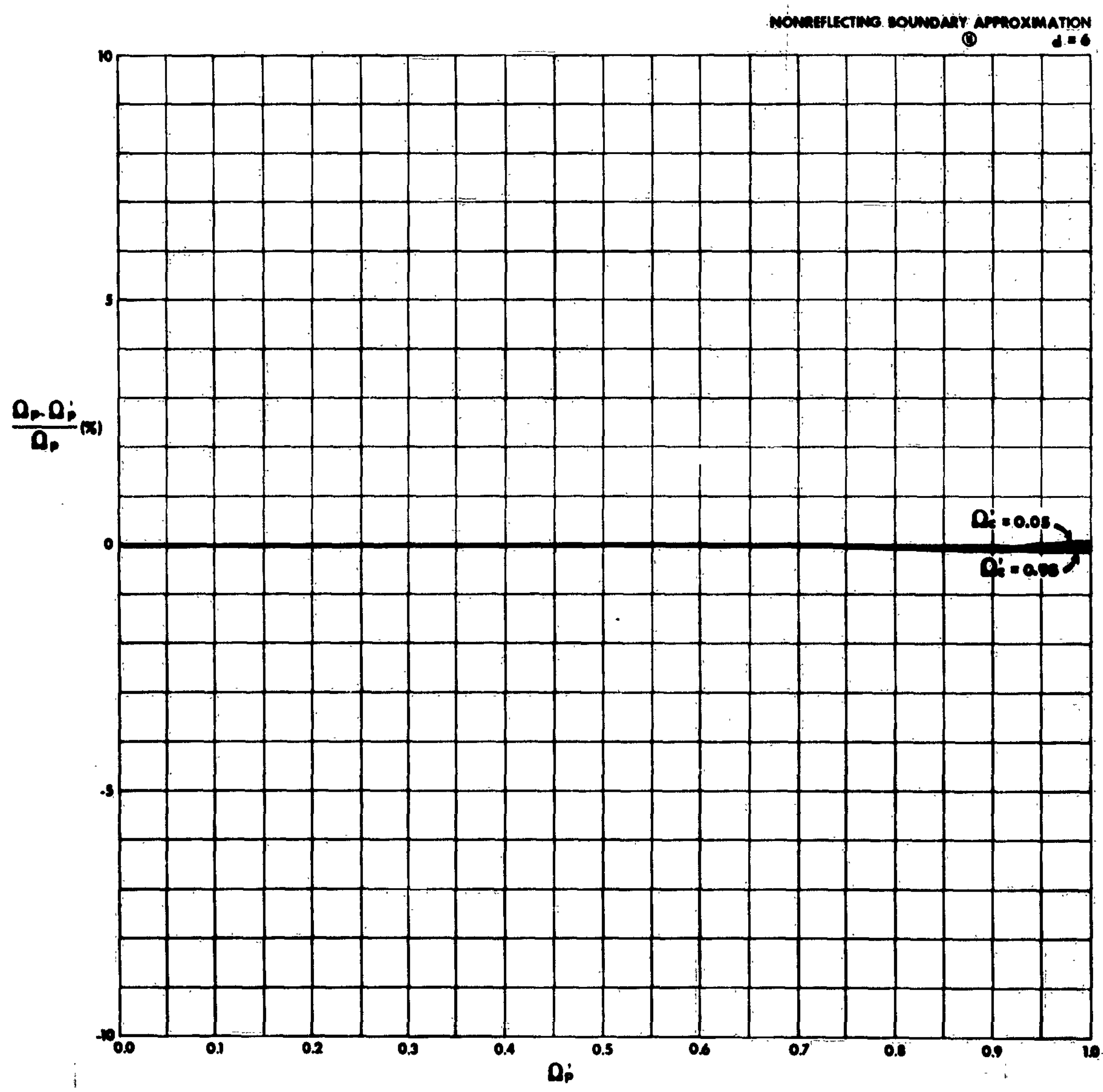

Figure 16 Percentage Error in Normalized Plasma Frequency for the Nonreflective Boundary Approximation (NRBA) as a Function of Measured Plasma Frequency for Various Values of Measured Collision Frequency, for a Value of the Normalized Thickness of the Plasma Layer d = 6

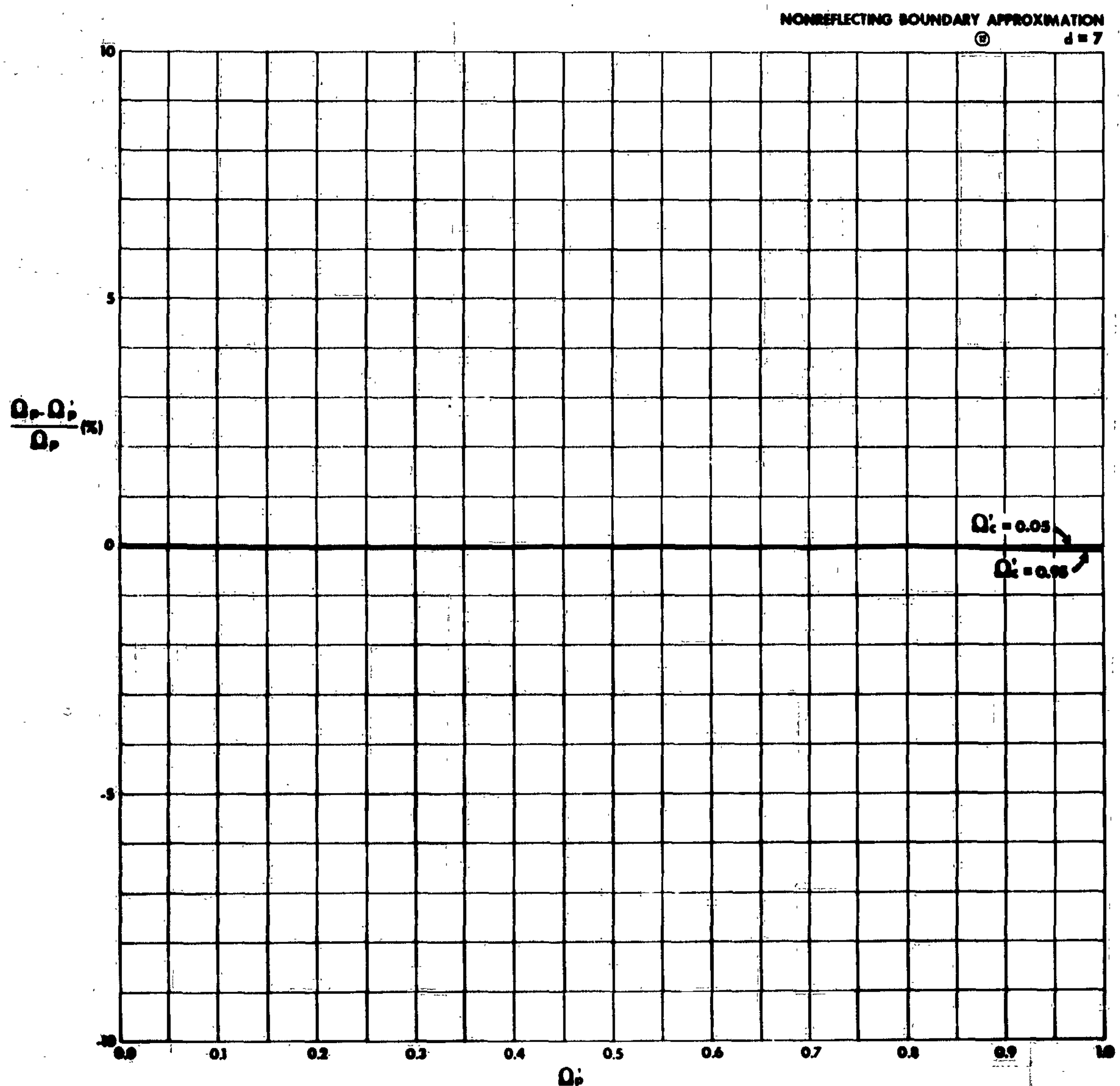

Figure 17 Percentage Error in Normalized Plasma Frequency for the Non-reflective Boundary Approximation (NRBA) as a Function of Measured Plasma Frequency for Various Values of Measured Collision Frequency, for a Value of the Normalized Thickness of the Plasma Layer d = 7

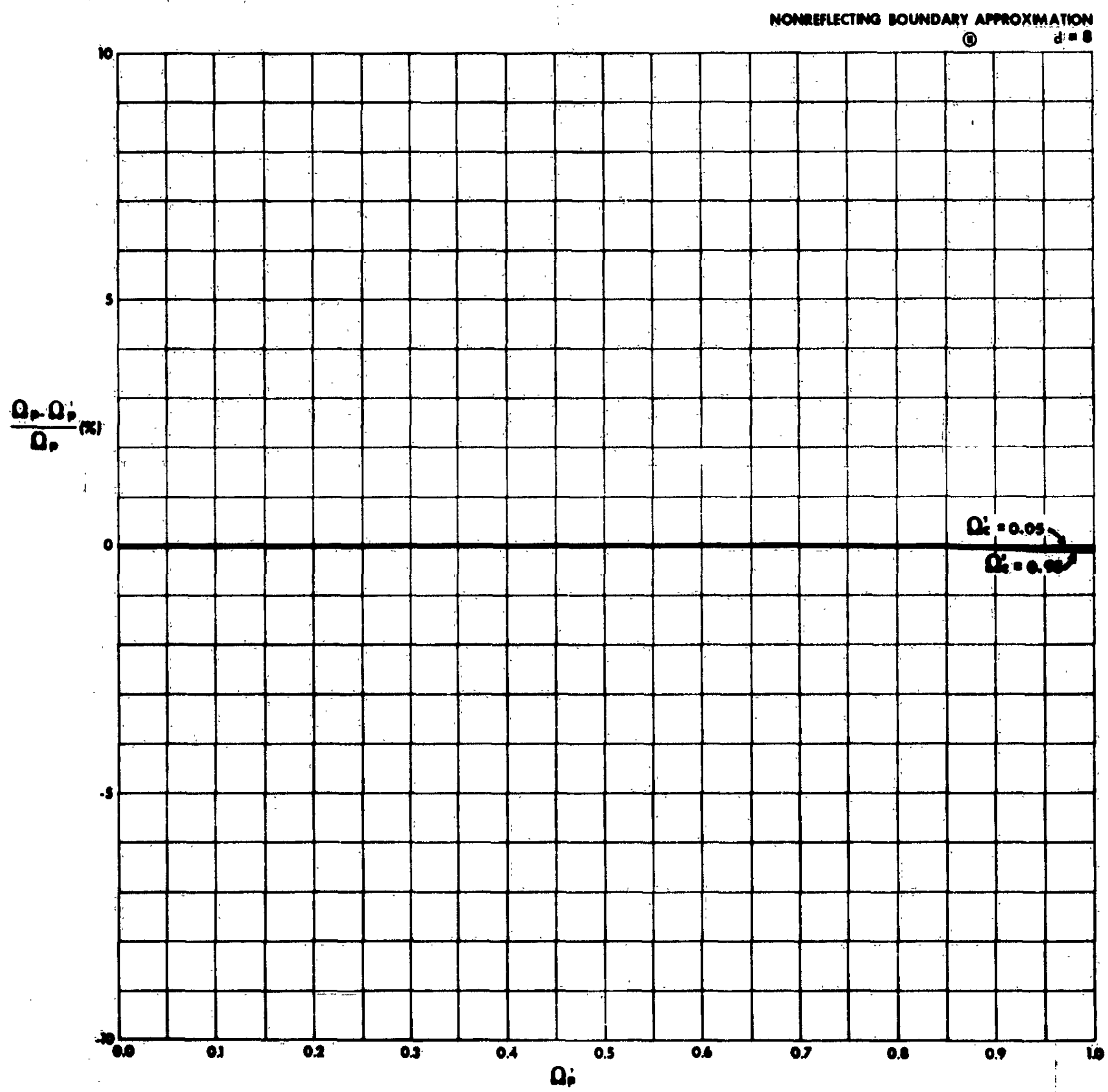

Figure 18 Percentage Error in Normalized Plasma Frequency for the Non-reflective Boundary Approximation (NRBA) as a Function of Measured Plasma Frequency for Various Values of Measured Collision Frequency, for a Value of the Normalized Thickness of the Plasma Layer d = 8

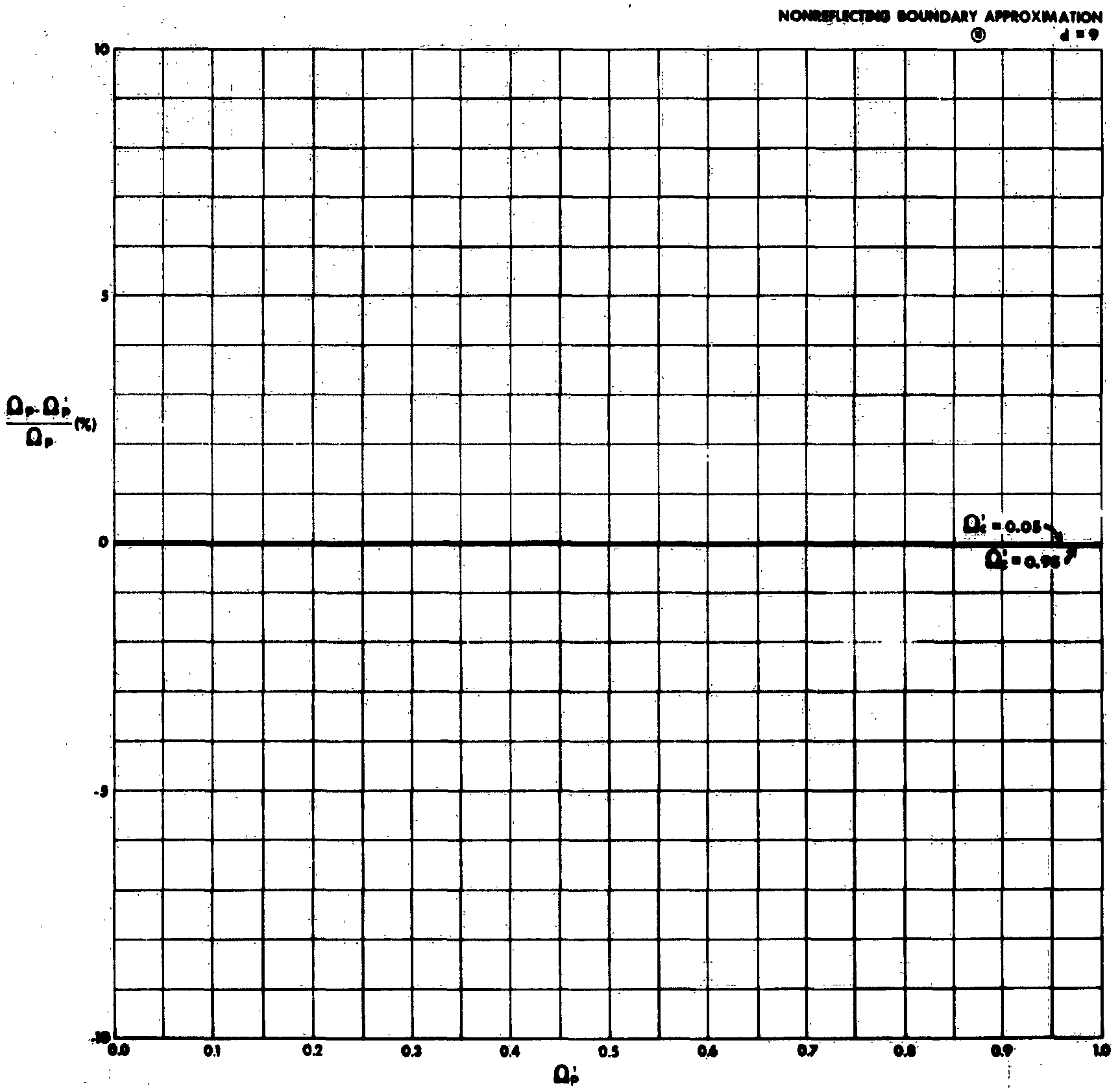

Figure 19 Percentage Error in Normalized Plasma Frequency for the Nonreflective Boundary Approximation (NRBA) as a Function of Measured Plasma Frequency for Various Values of Measured Collision Frequency, for a Value of the Normalized Thickness of the Plasma Layer d = 9

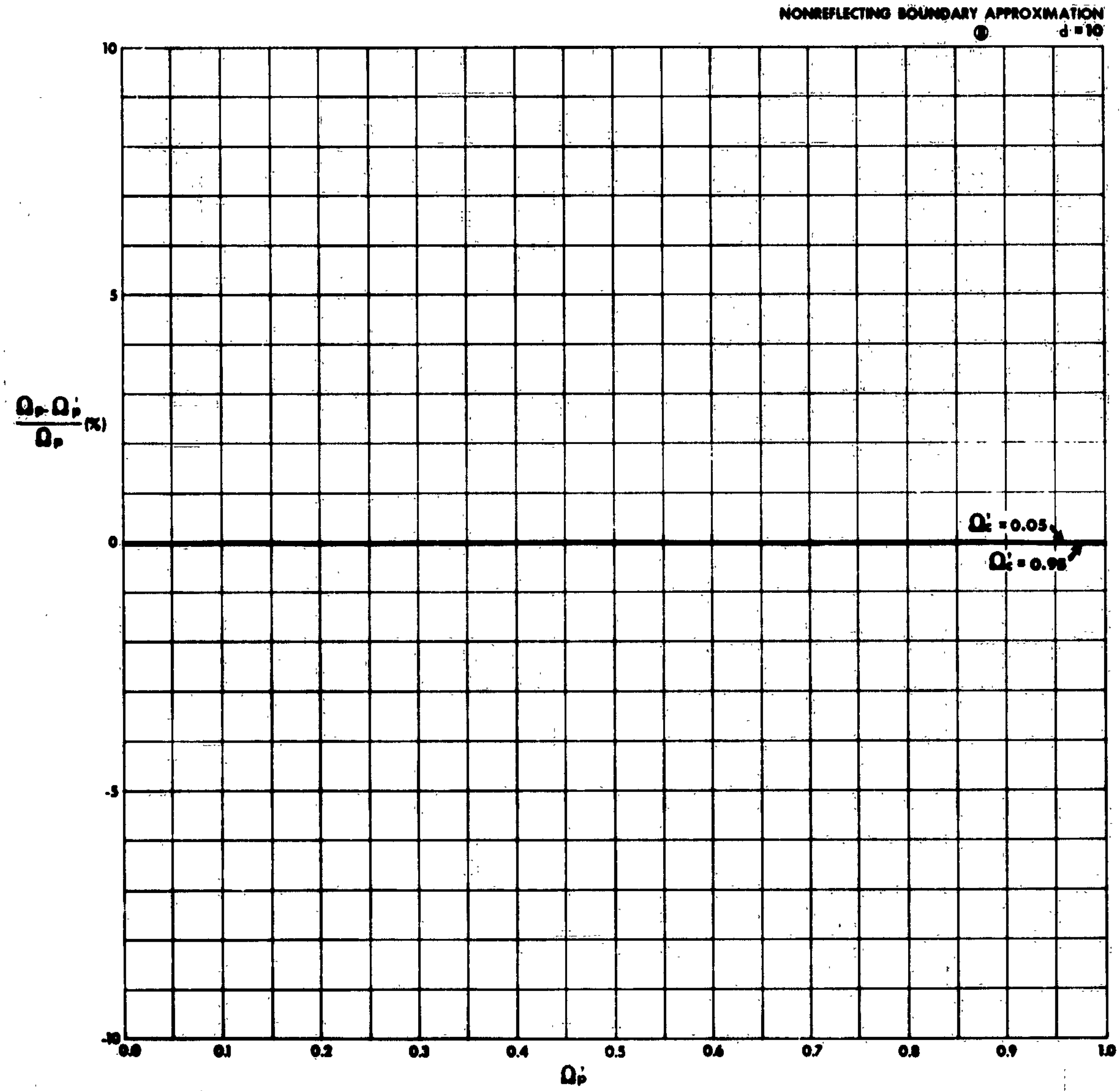

Figure 20 Percentage Error in Normalized Plasma Frequency for the Non-reflective Boundary Approximation (NRBA) as a Function of Measured Plasma Frequency for Various Values of Measured Collision Frequency, for a Value of the Normalized Thickness of the Plasma Layer d = 10

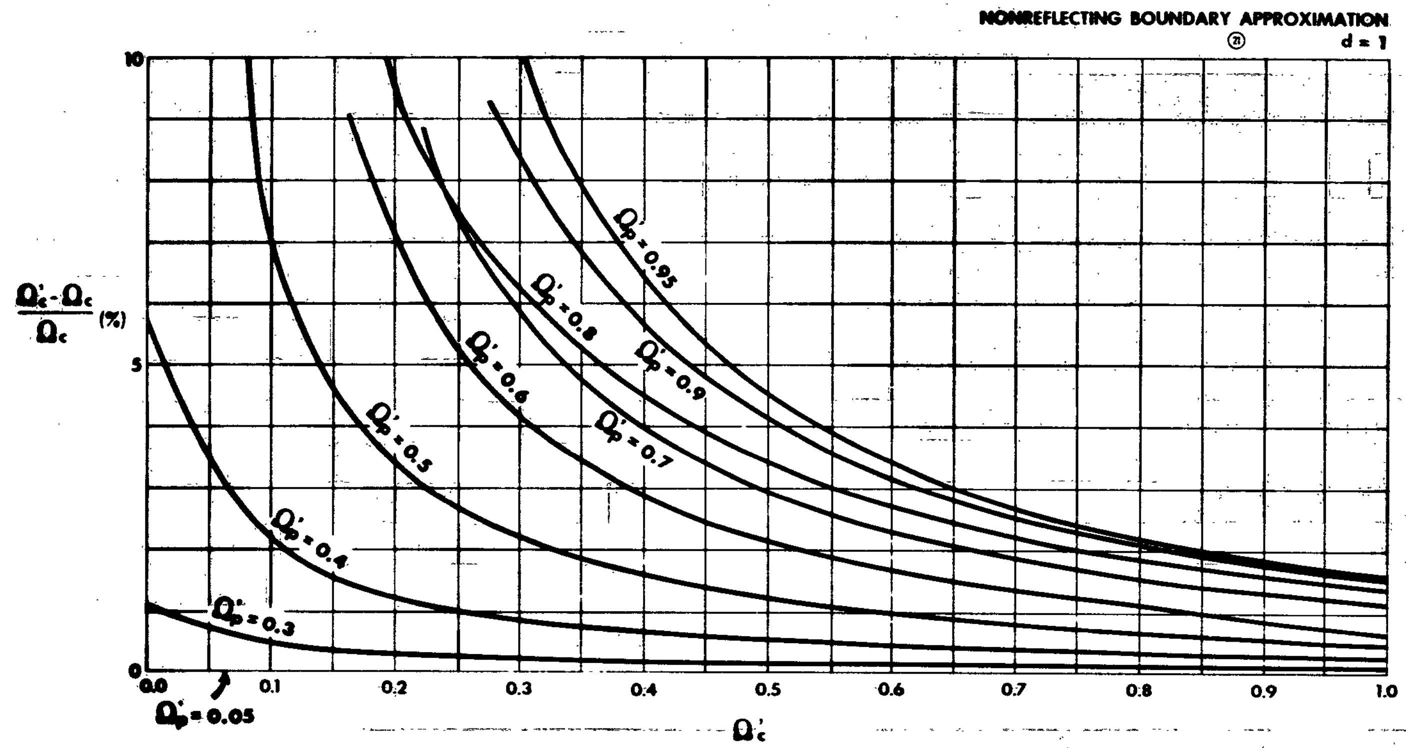

Figure 21 **Percentage Error in Normalized Collision Frequency for the Non-reflective Boundary Approximation (NRBA) as a Function of the Measured Collision Frequency for Various Values of the Measured Plasma Frequency, for a Value of the Normalized Thickness of the Plasma Layer d = 1**

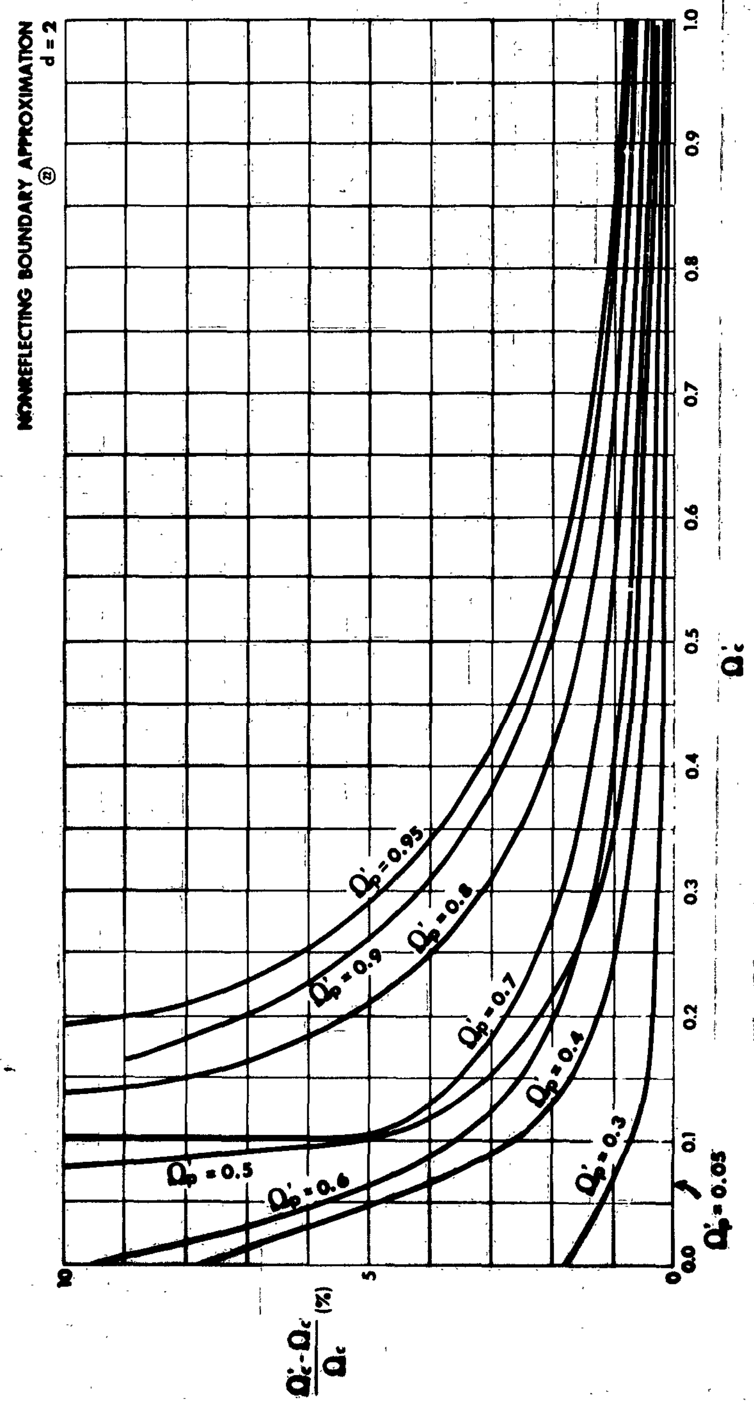

Figure 22 Percentage Error in Normalized Collision Frequency for the Nonreflective Boundary Approximation (NRBA) as a Function of the Measured Collision Frequency for Various Values of the Measured Plasma Frequency, for a Value of the Normalized Thickness of the Plasma Layer d = 2

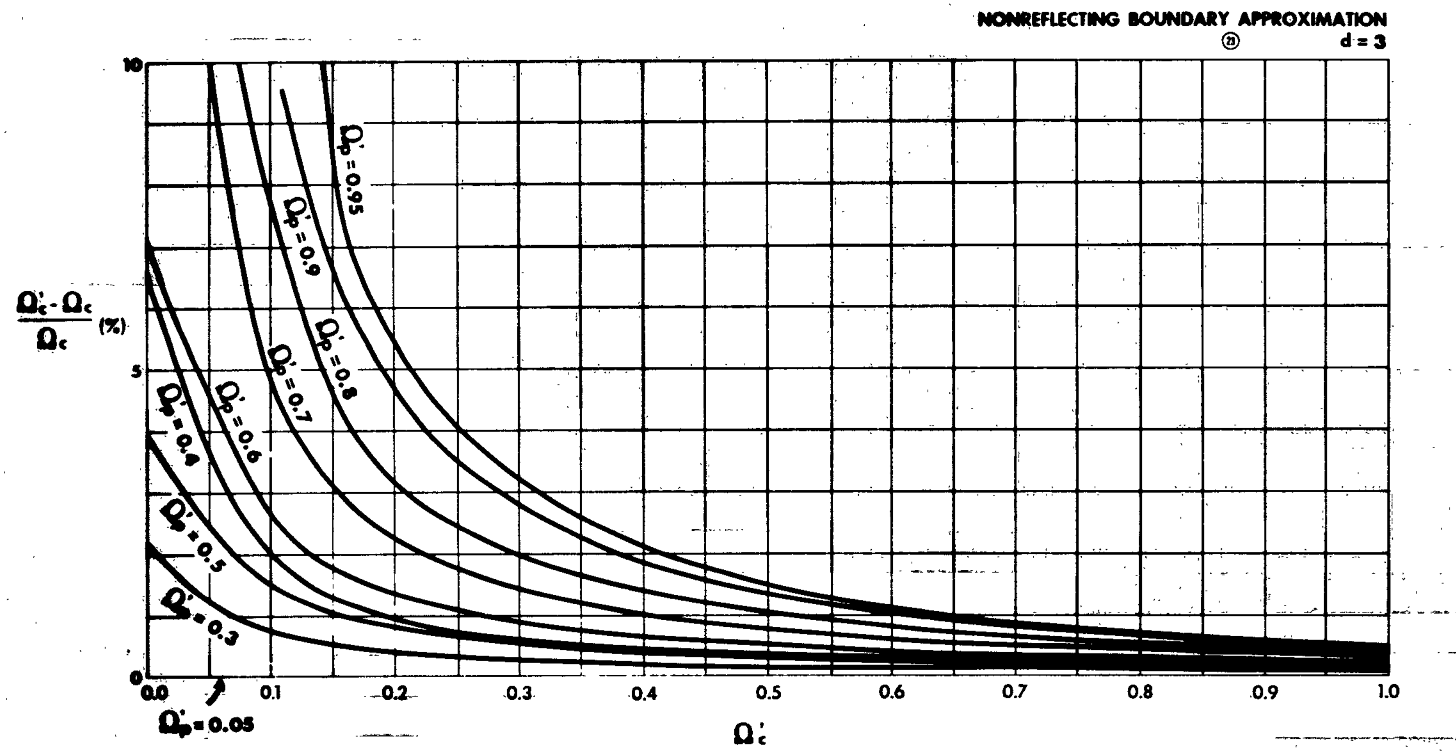

Figure 23 Percentage Error in Normalized Collision Frequency for the Nonreflective Boundary Approximation (NRBA) as a Function of the Measured Collision Frequency for Various Values of the Measured Plasma Frequency, for a Value of the Normalized Thickness of the Plasma Layer d = 3

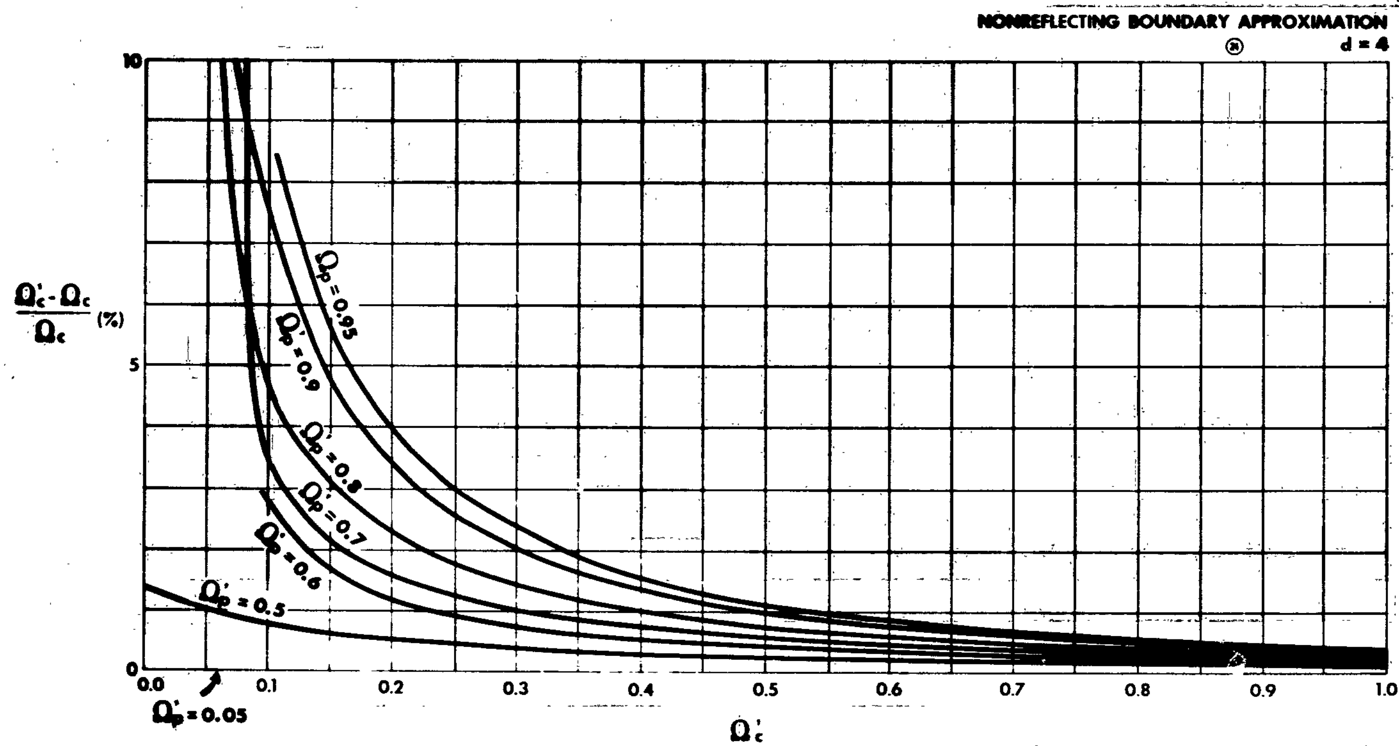

Figure 24 Percentage Error in Normalized Collision Frequency for the Nonreflective Boundary Approximation (NRBA) as a Function of the Measured Collision Frequency for Various Values of the Measured Plasma Frequency, for a Value of the Normalized Thickness of the Plasma Layer d = 4

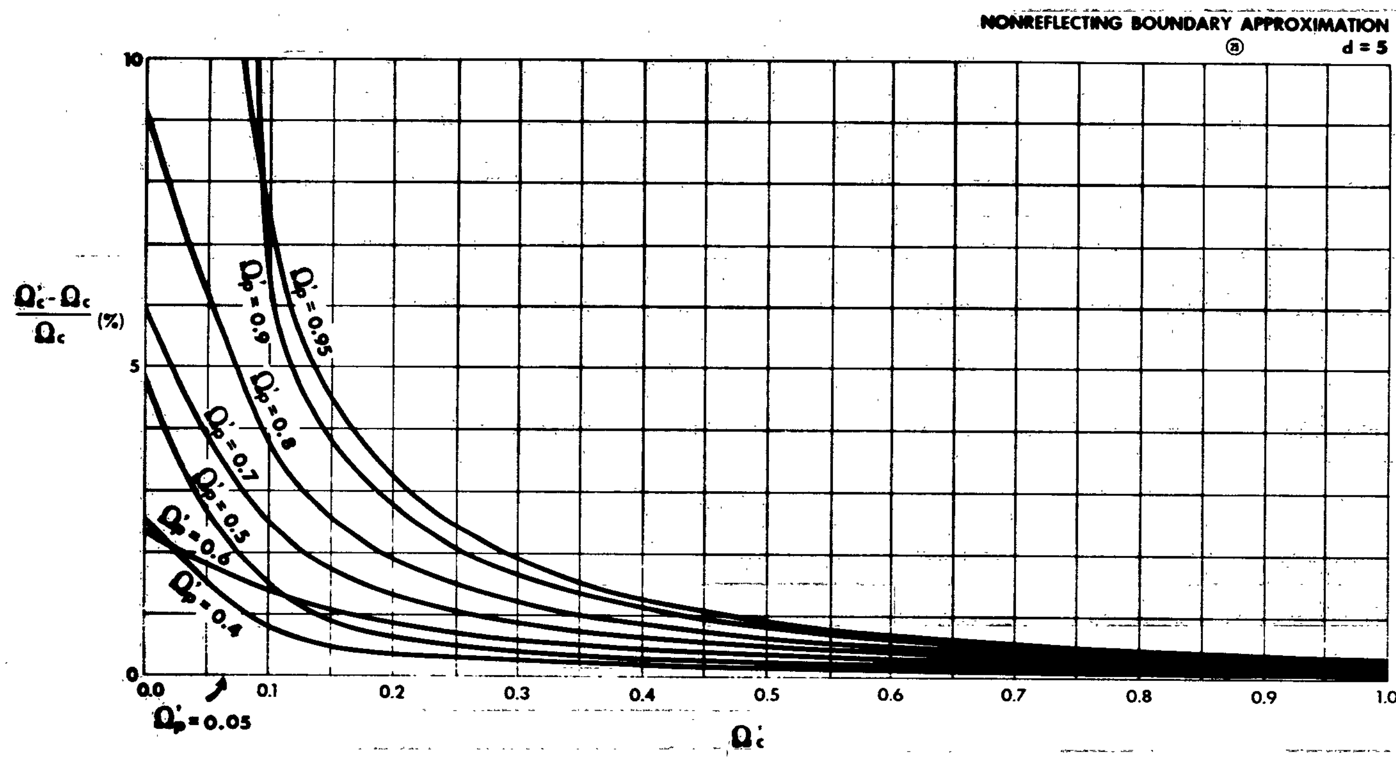

Figure 25 Percentage Error in Normalized Collision Frequency for the Nonreflective Boundary Approximation (NRBA) as a Function of the Measured Collision Frequency for Various Values of the Measured Plasma Frequency, for a Value of the Normalized Thickness of the Plasma Layer d = 5

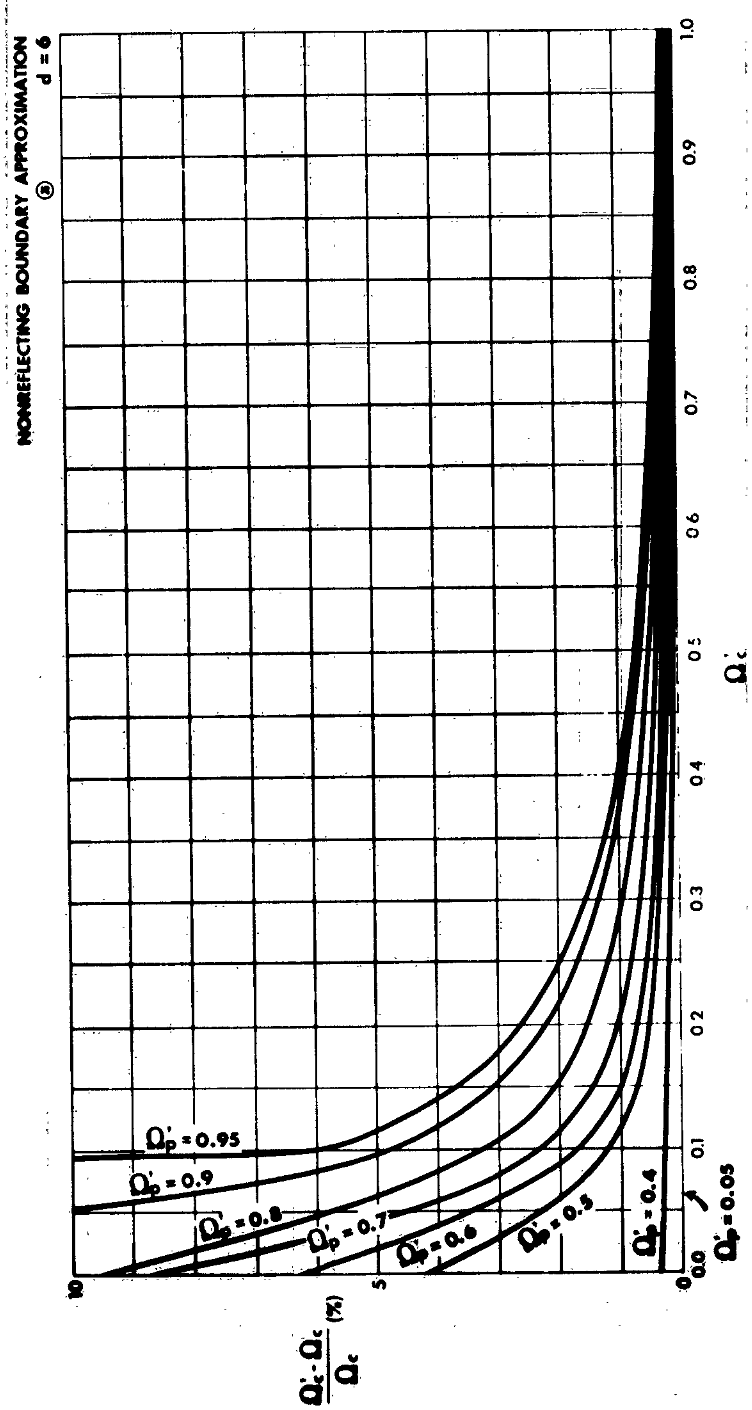

Figure 26 Percentage Error in Normalized Collision Frequency for the Nonreflective Boundary Approximation (NRBA) as a Function of the Measured Collision Frequency for Various Values of the Measured Plasma Frequency, for a Value of the Normalized Thickness of the Plasma Layer d = 6

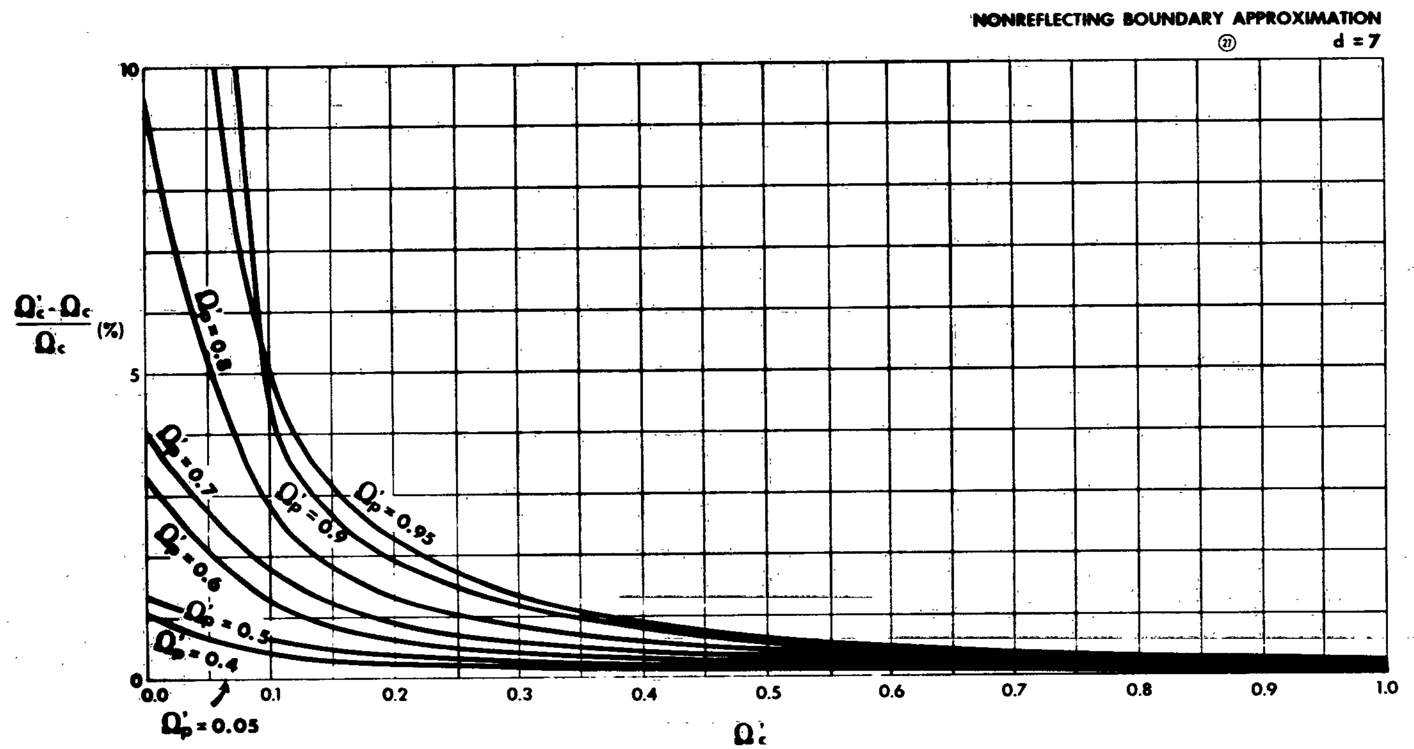

Figure 27 Percentage Error in Normalized Collision Frequency for the Non-reflective Boundary Approximation (NRBA) as a Function of the Measured Collision Frequency for Various Values of the Measured Plasma Frequency, for a value of the Normalized Thickness of the Plasma Layer d = 7

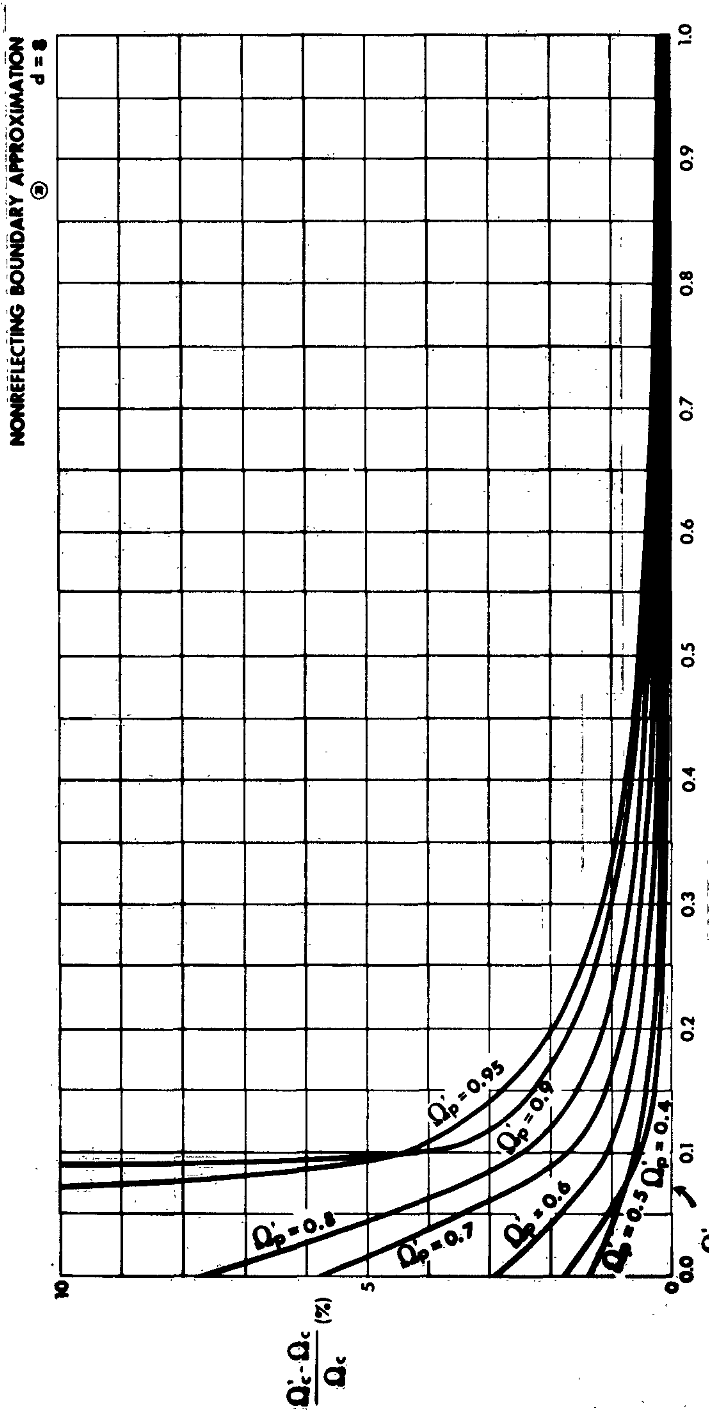

Figure 28 Percentage Error in Normalized Collision Frequency for the Non-reflective Boundary Approximation (NRBA) as a Function of the Measured Collision Frequency for Various Values of the Measured Plasma Frequency, for a Value of the Normalized Thickness of the Plasma Layer d = 8

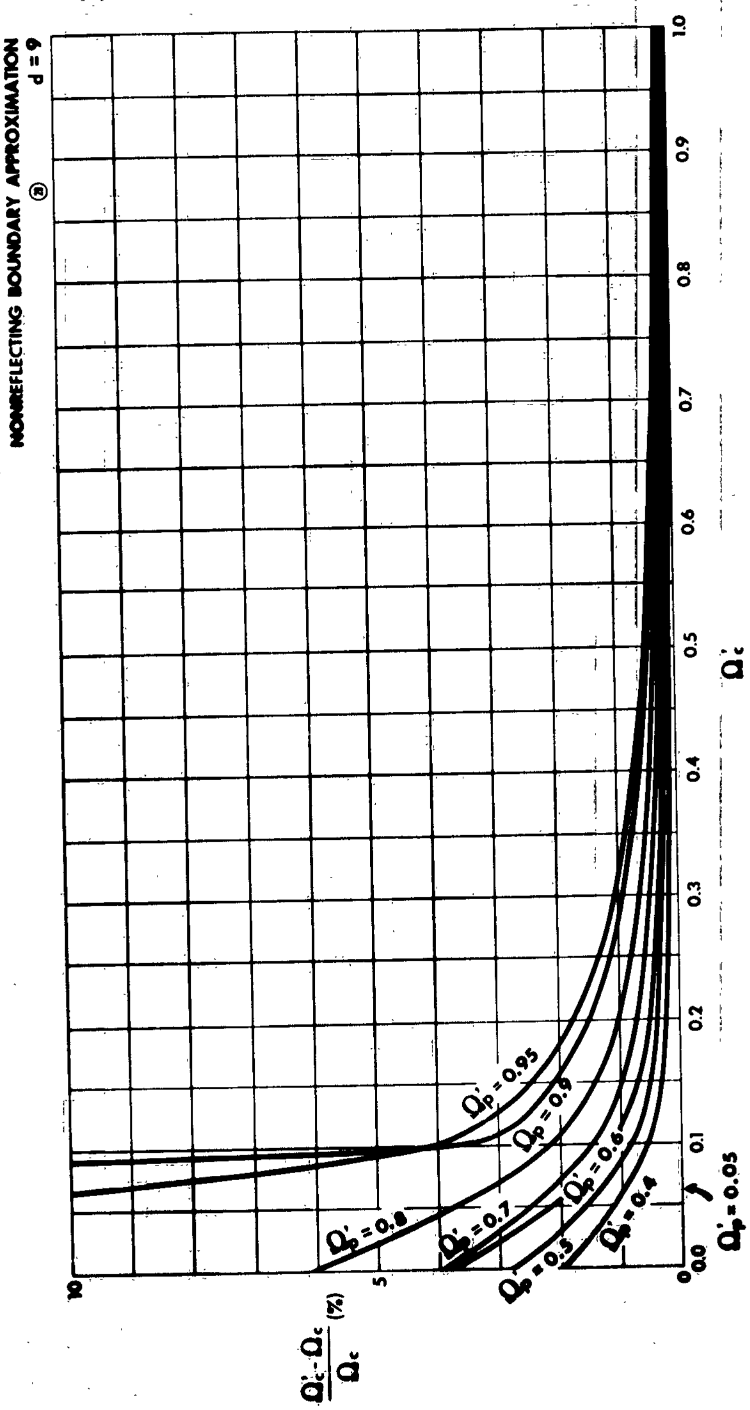

Figure 29 Percentage Error in Normalized Collision Frequency for the Nonreflective Boundary Approximation (NRBA) as a Function of the Measured Collision Frequency for Various Values of the Measured Plasma Frequency, for a Value of the Normalized Thickness of the Plasma Layer d = 9

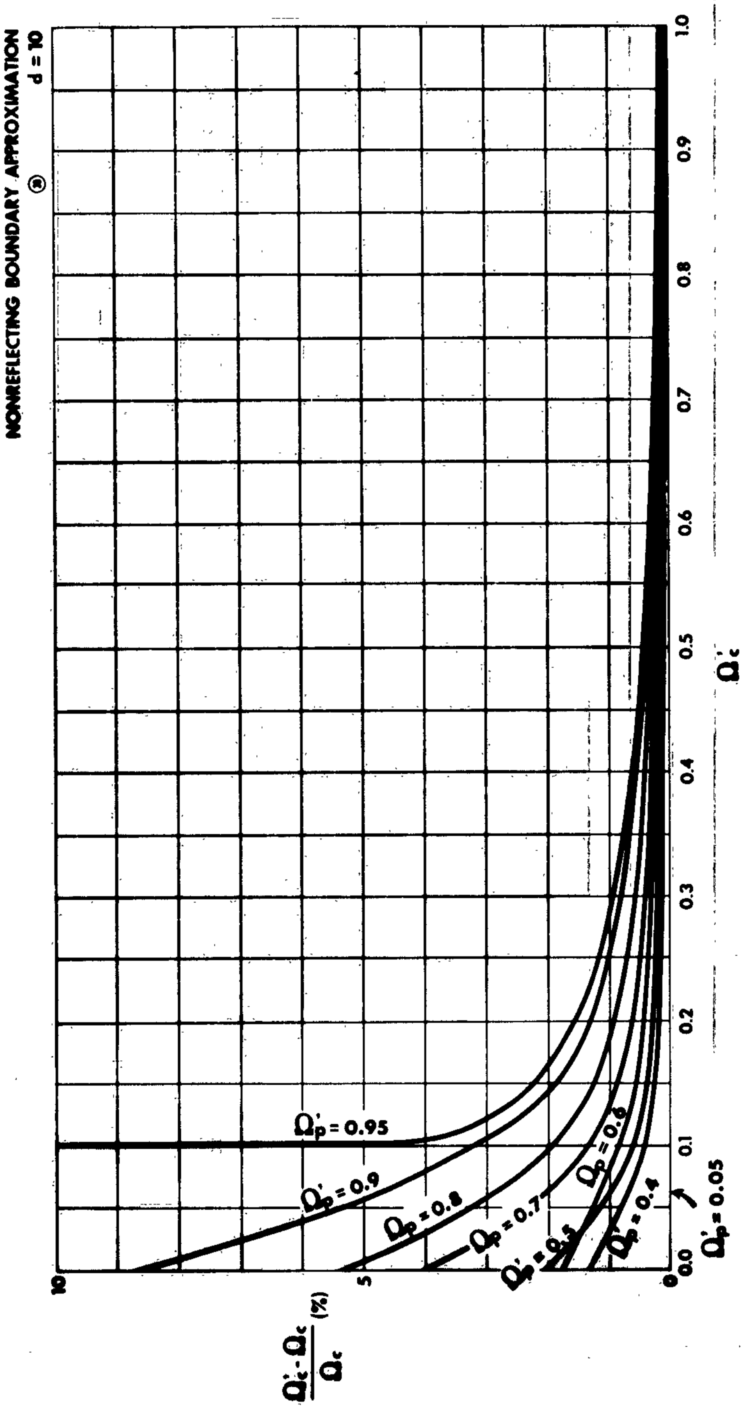

Figure 30 Percentage Error in Normalized Collision Frequency for the Nonreflective Boundary Approximation (NRBA) as a Function of the Measured Collision Frequency for Various Values of the Measured Plasma Frequency, for a Value of the Normalized Thickness of the Plasma Layer d = 10

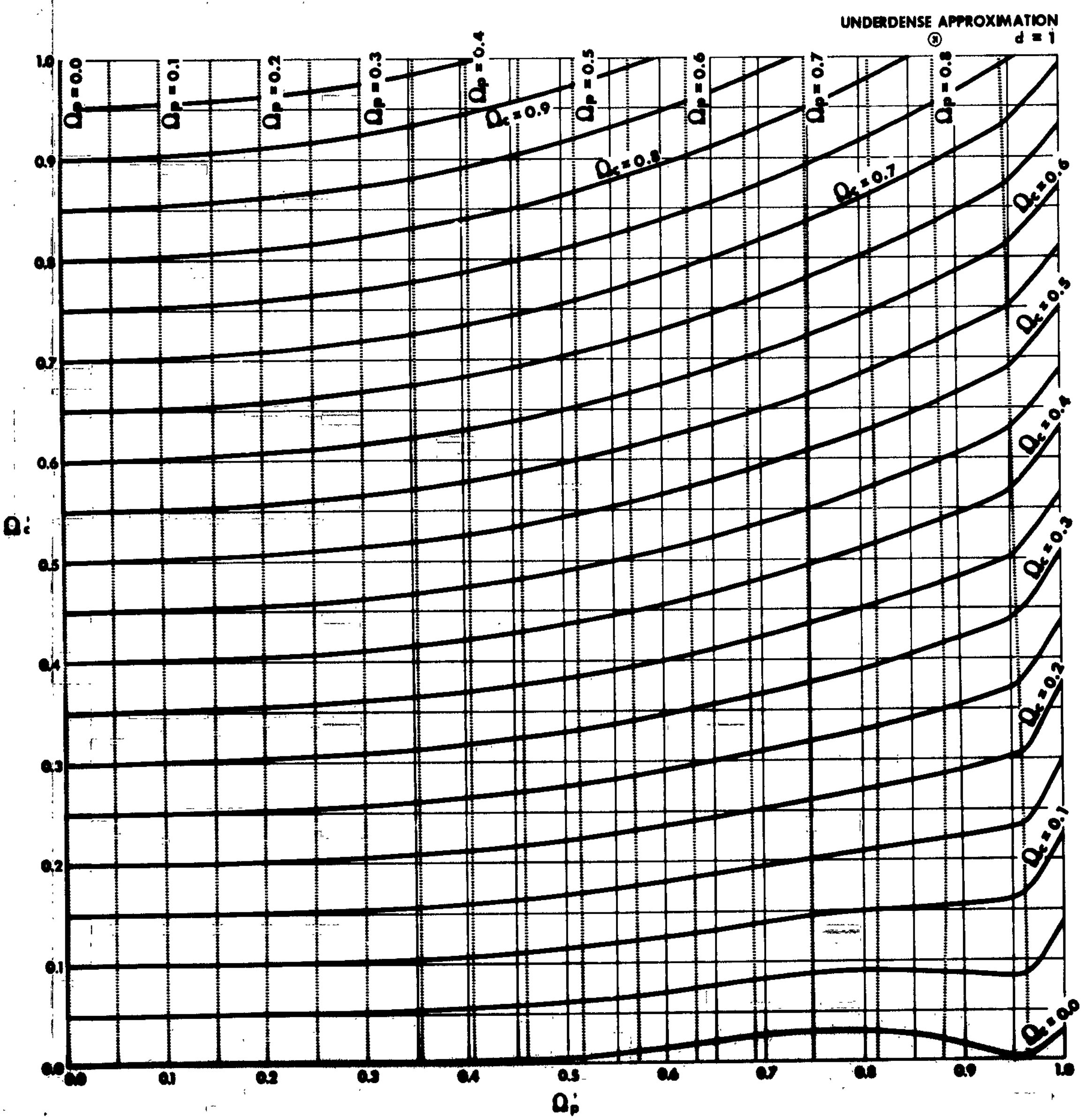

Figure 31 Exact Values, as Functions of the Calculated Values, of the Normalized Plasma and Collision Frequencies for the Underdense Plasma Approximation (UDPA), for a Value of the Normalized Thickness of the Plasma Layer d = 1

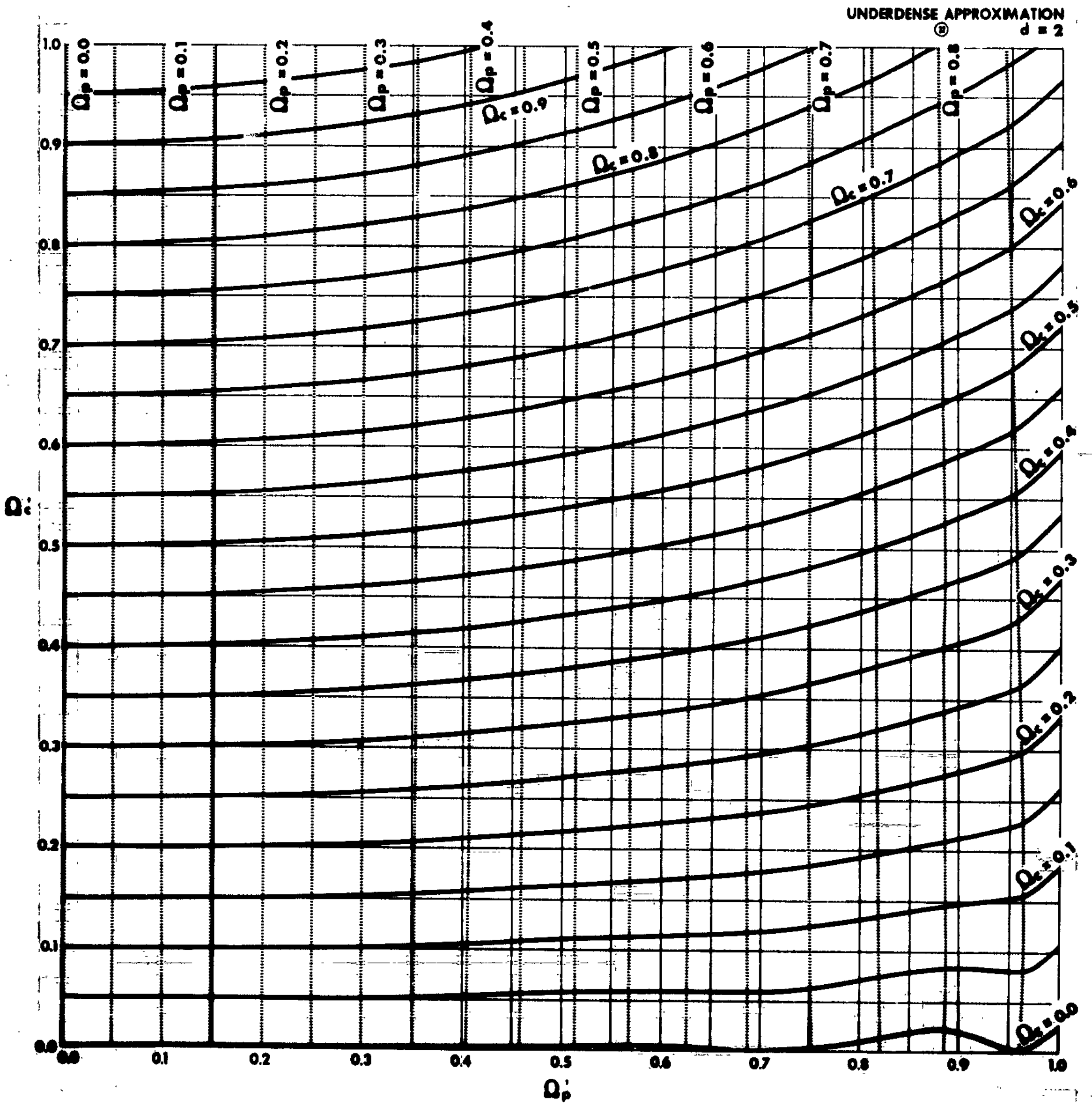

Figure 32 Exact Values, as Functions of the Calculated Values, of the Normalized Plasma and Collision Frequencies for the Underdense Plasma Approximation (UDPA), for a Value of the Normalized Thickness of the Plasma Layer d = 2

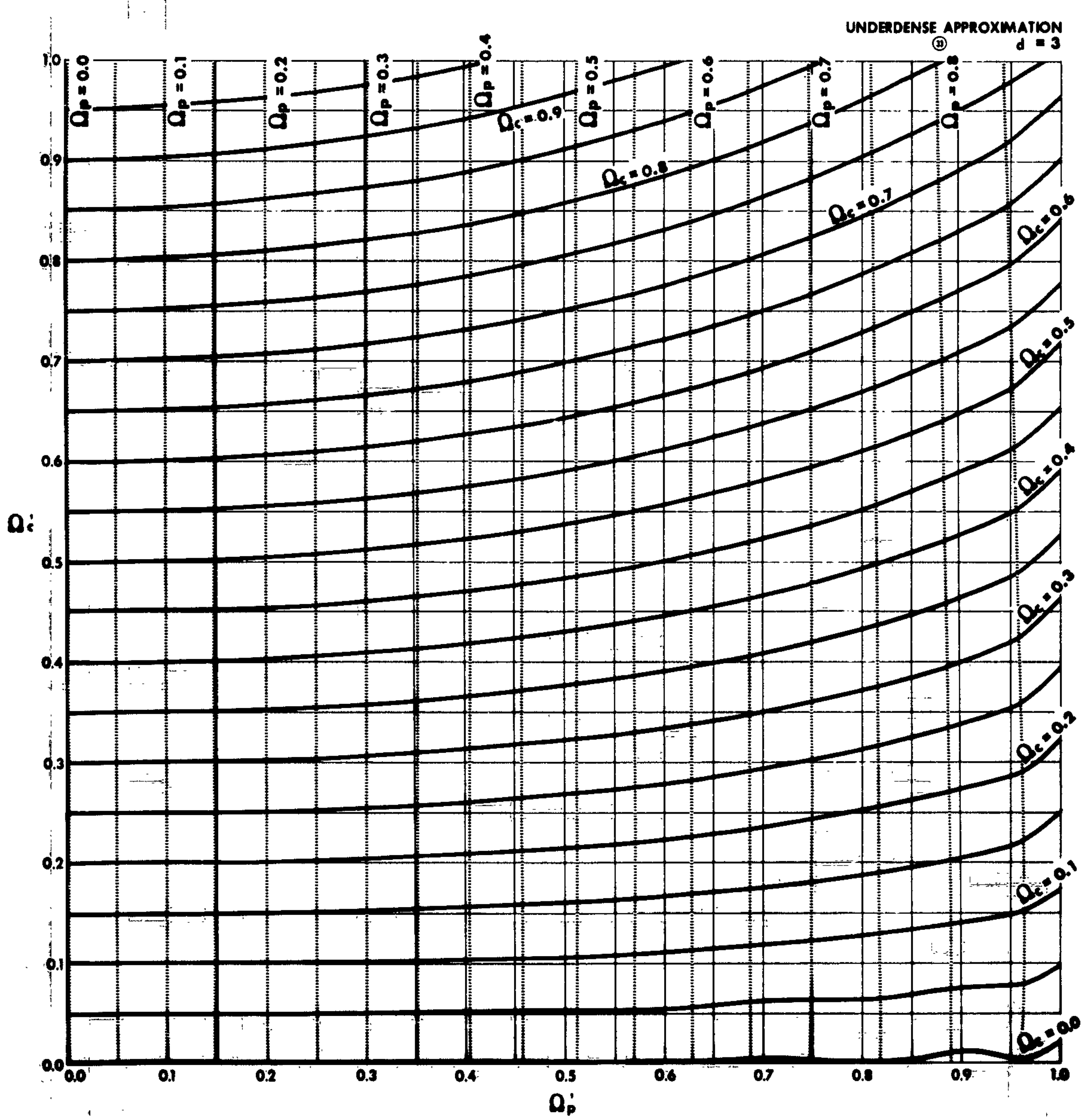

Figure 33 Exact Values, as Functions of the Calculated Values, of the Normalized Plasma and Collision Frequencies for the Underdense Plasma Approximation (UDPA), for a Value of the Normalized Thickness of the Plasma Layer d = 3

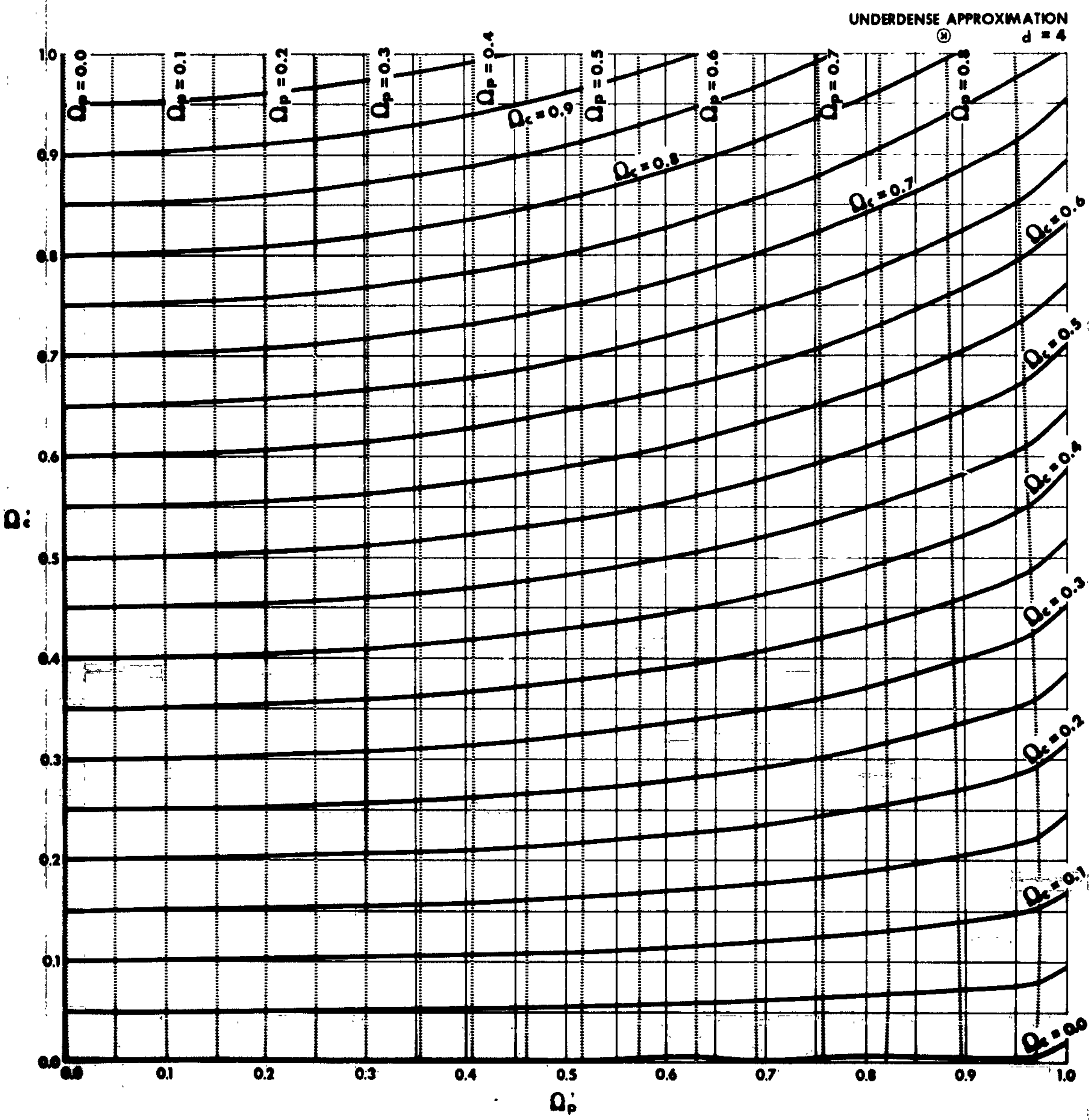

Figure 34 Exact Values, as Functions of the Calculated Values, of the Normalized Plasma and Collision Frequencies for the Underdense Plasma Approximation (UDPA), for a Value of the Normalized Thickness of the Plasma Layer d = 4

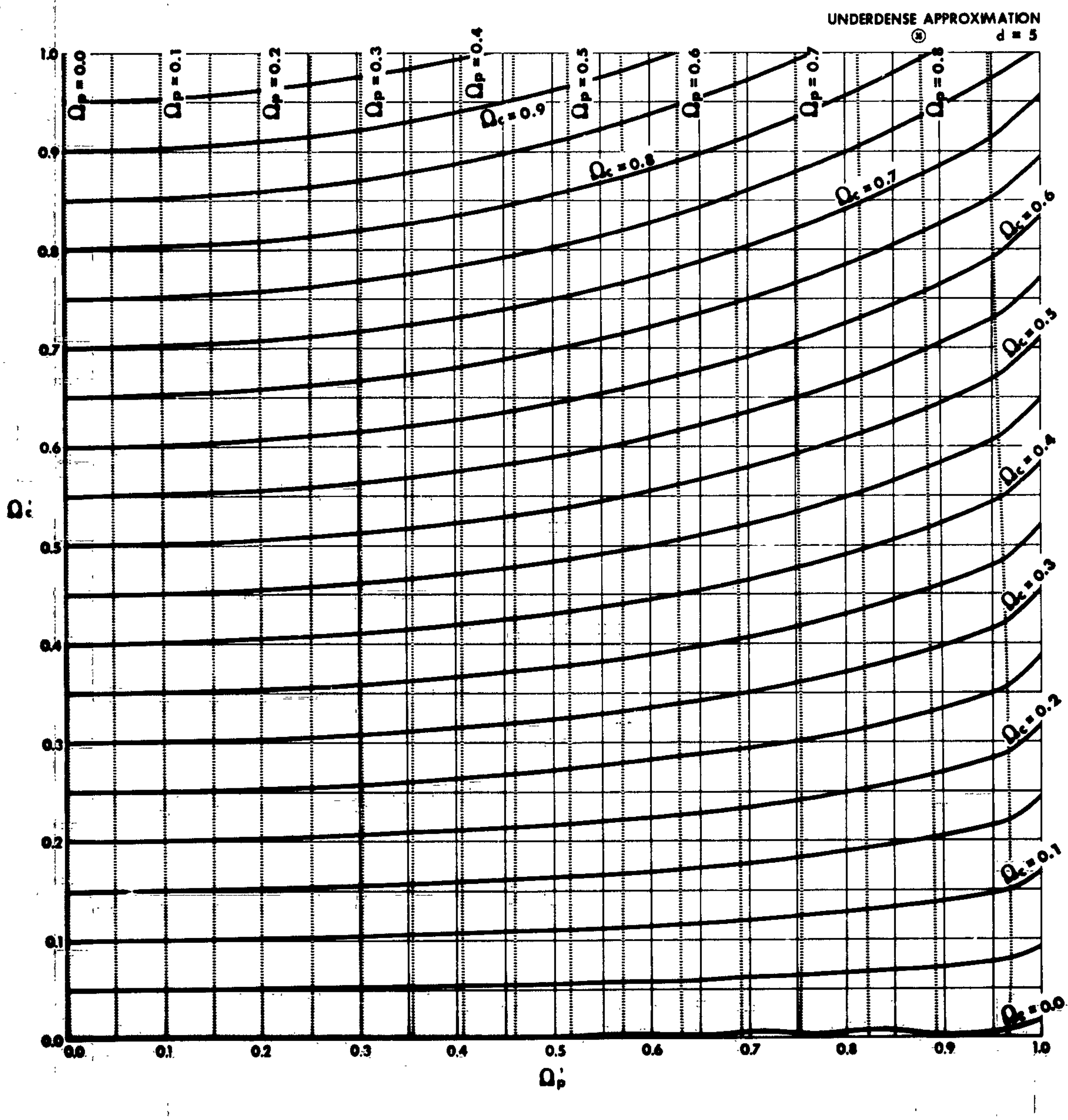

Figure 35 Exact Values, as Functions of the Calculated Values, of the Normalized Plasma and Collision Frequencies for the Underdense Plasma Approximation (UDPA), for a Value of the Normalized Thickness of the Plasma Layer d = 5

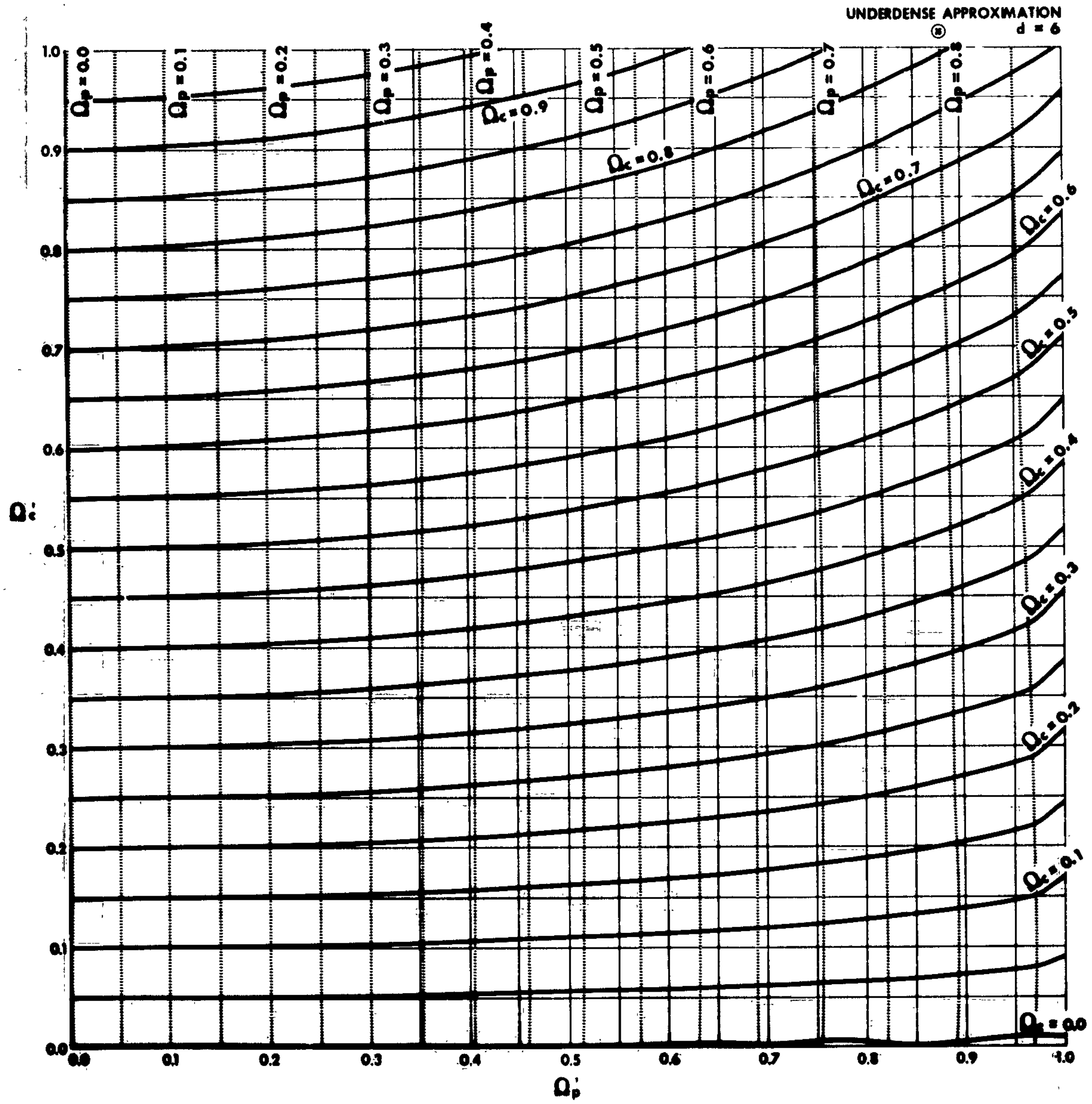

Figure 36 Exact Values, as Functions of the Calculated Values, of the Normalized Plasma and Collision Frequencies for the Underdense Plasma Approximation (UDPA), for a Value of the Normalized Thickness of the Plasma Layer d = 6

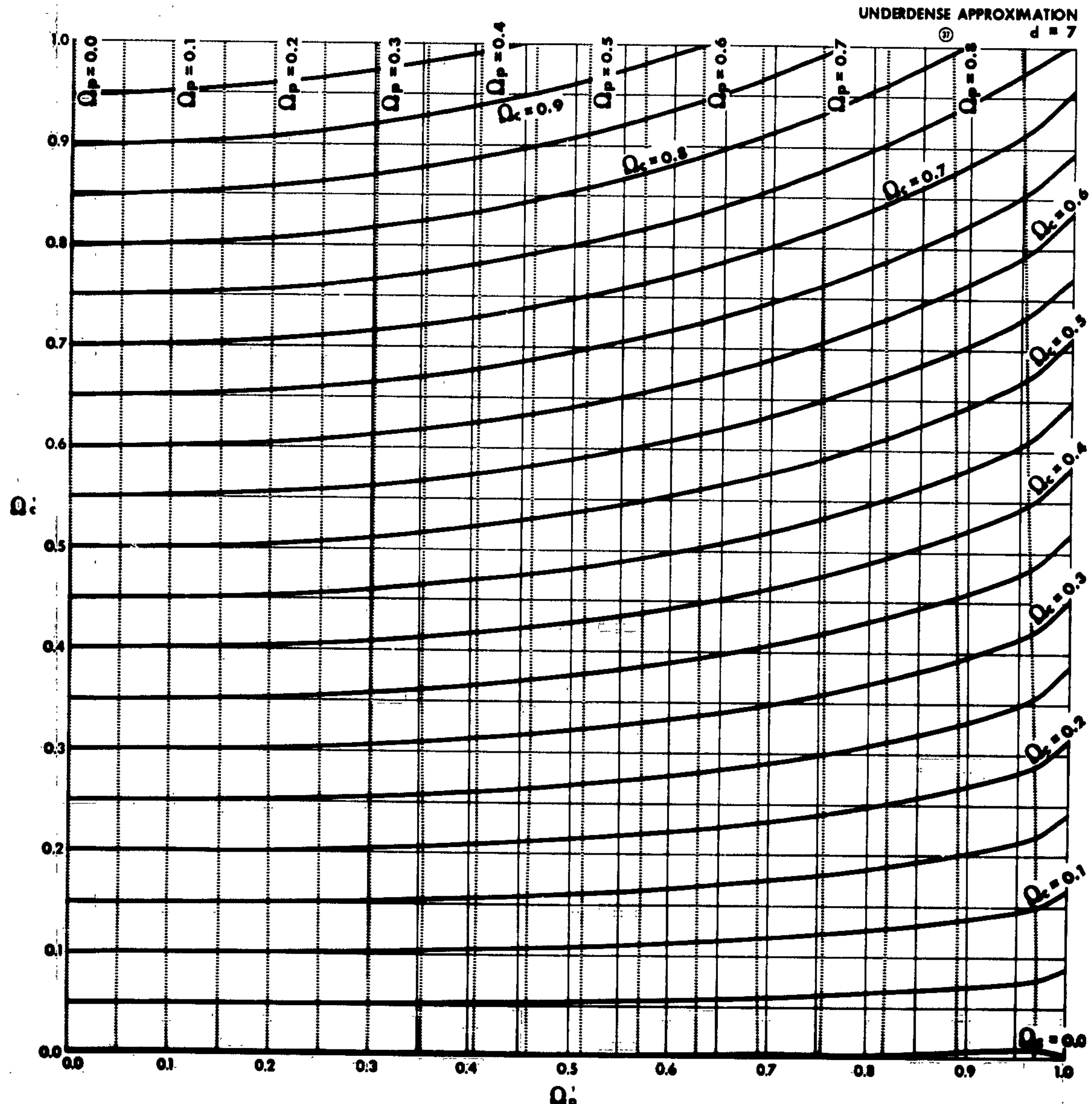

Figure 37 Exact Values, as Functions of the Calculated Values, of the Normalized Plasma and Collision Frequencies for the Underdense Plasma Approximation (UDPA), for a Value of the Normalized Thickness of the Plasma Layer d = 7

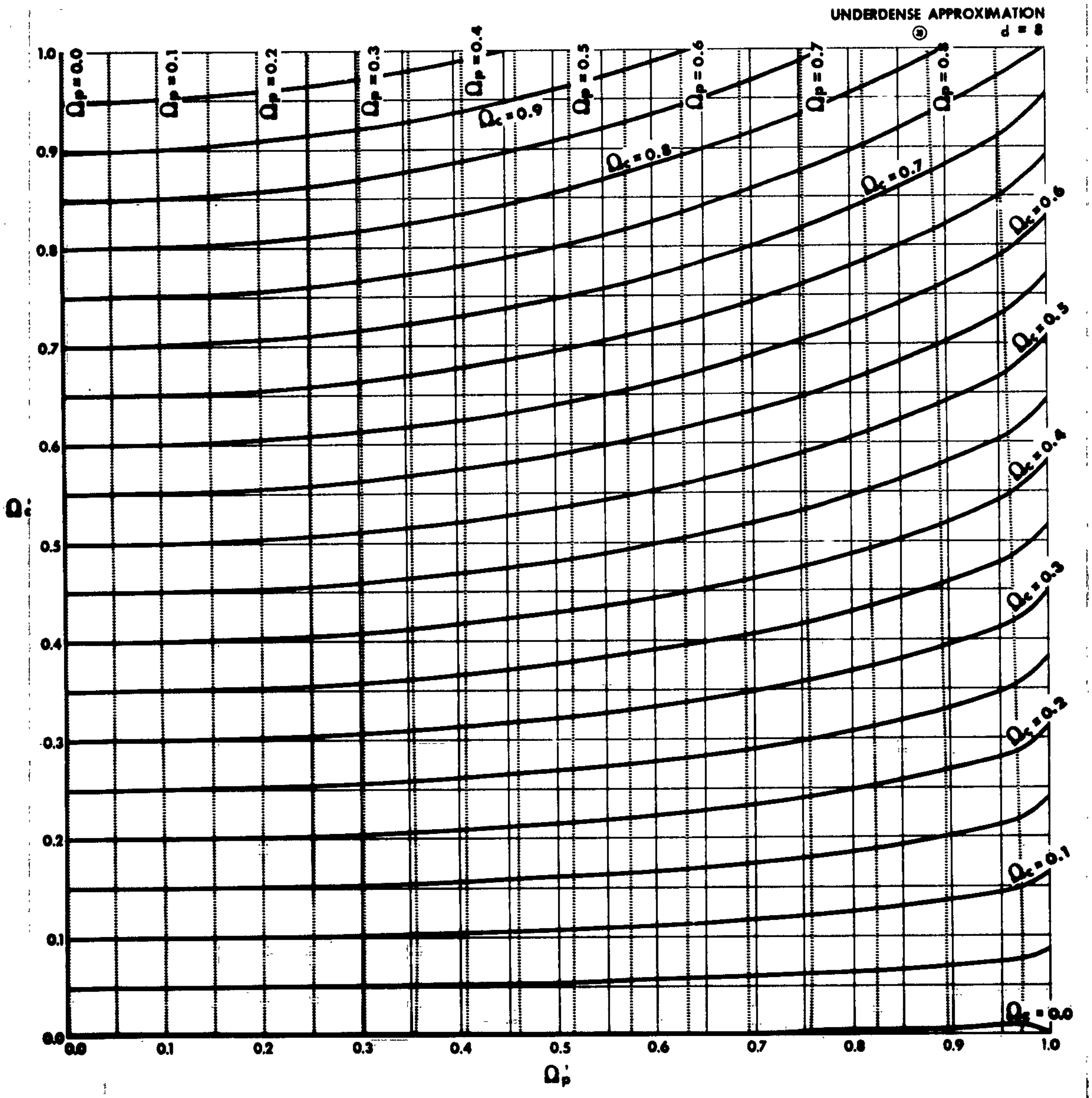

Figure 38 Exact Values, as Functions of the Calculated Values, of the Normalized Plasma and Collision Frequencies for the Underdense Plasma Approximation (UDPA), for a Value of the Normalized Thickness of the Plasma Layer d = 8

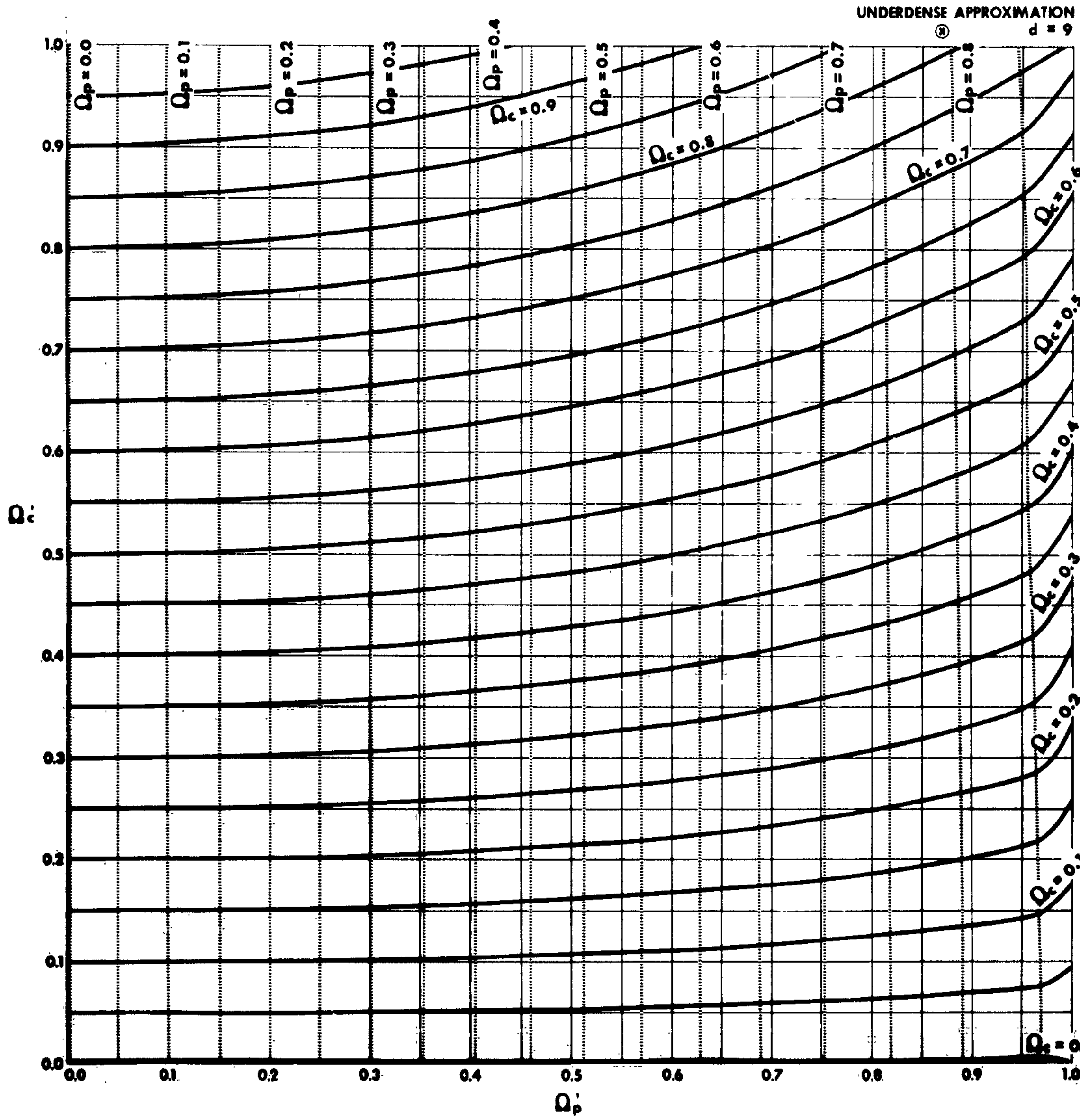

Figure 39 Exact Values, as Functions of the Calculated Values, of the Normalized Plasma and Collision Frequencies for the Underdense Plasma Approximation (UDPA), for a Value of the Normalized Thickness of the Plasma Layer d = 9

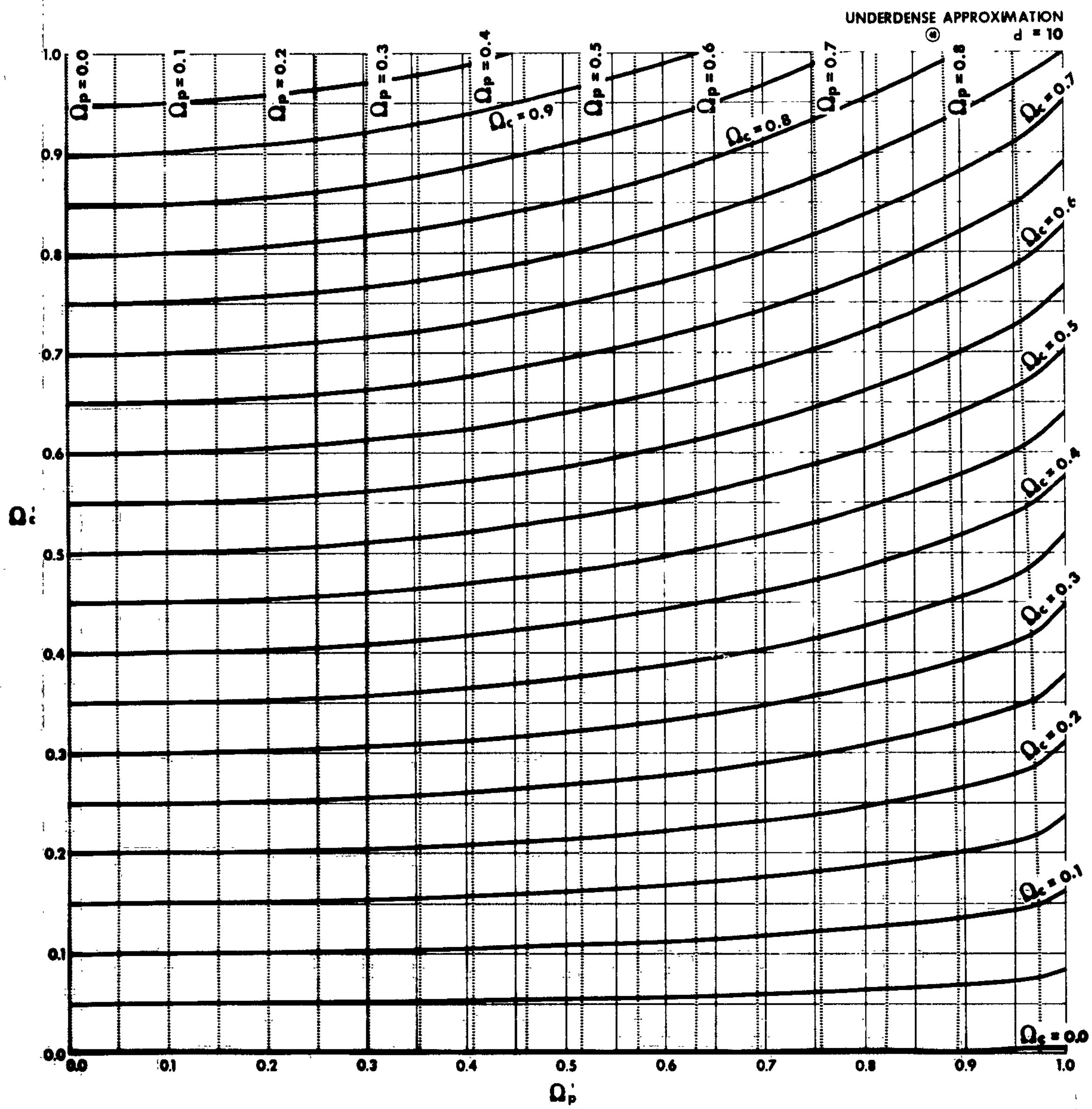

Figure 40 Exact Values, as Functions of the Calculated Values, of the Normalized Plasma and Collision Frequencies for the Underdense Plasma Approximation (UDPA), for a Value of the Normalized Thickness of the Plasma Layer d = 10

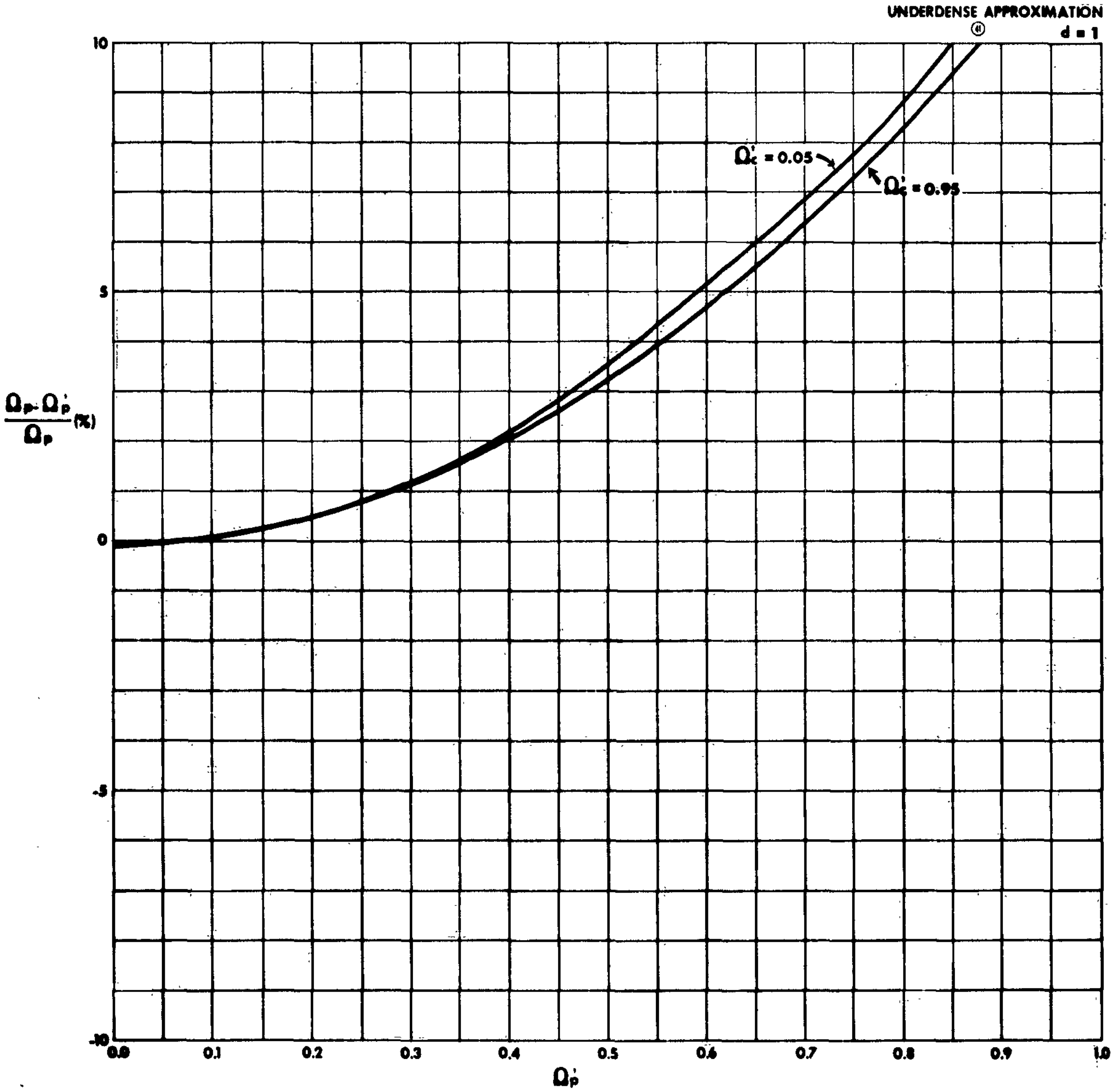

Figure 41 Percentage Error in Normalized Plasma Frequency for the Underdense Plasma Approximation (UDPA) as a Function of Measured Plasma Frequency for Various Values of Measured Collision Frequency, for a Value of the Normalized Thickness of the Plasma Layer d = 1

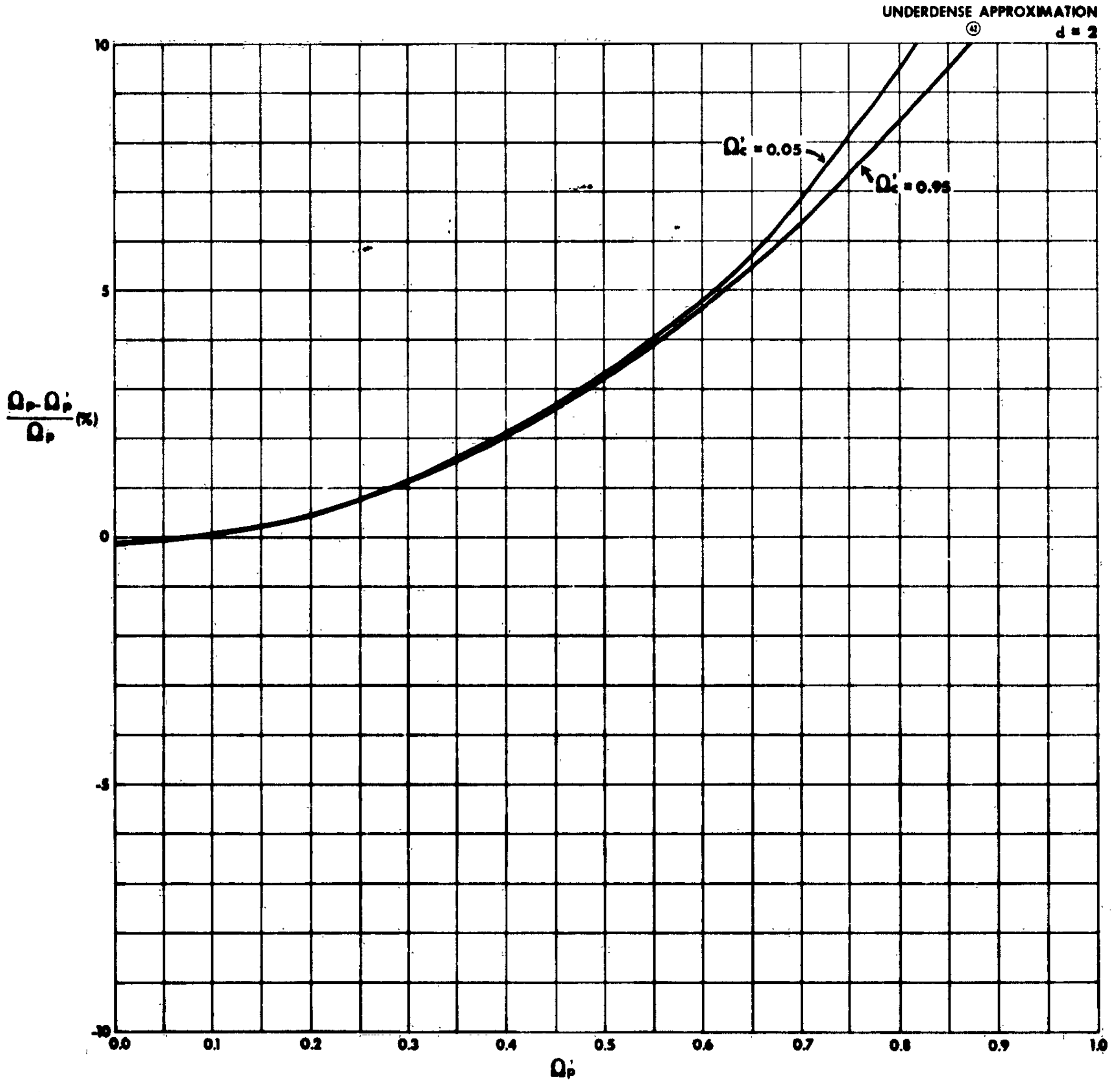

Figure 42 Percentage Error in Normalized Plasma Frequency for the Underdense Plasma Approximation (UDPA) as a Function of Measured Plasma Frequency for Various Values of Measured Collision Frequency, for a Value of the Normalized Thickness of the Plasma Layer d = 2

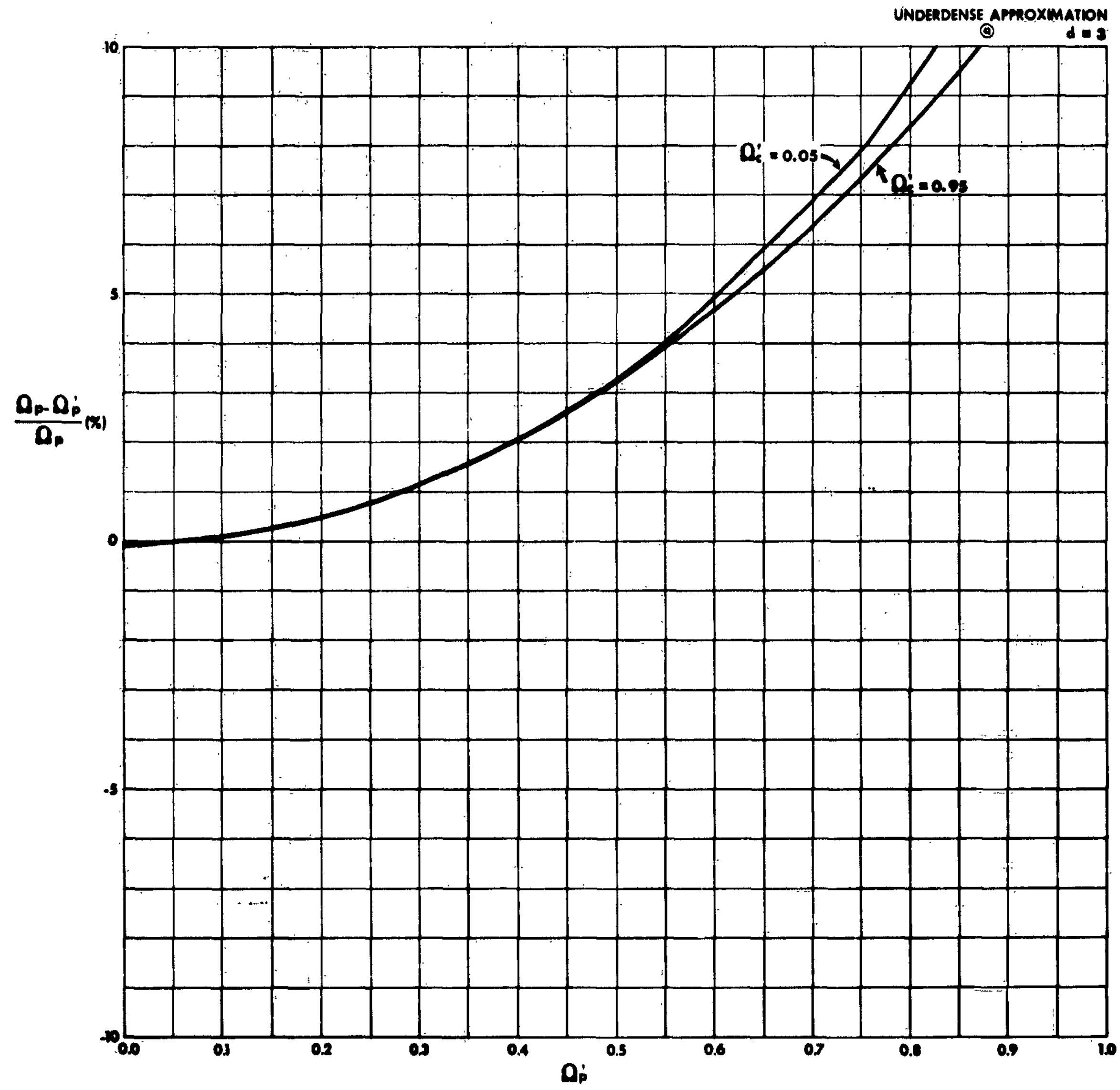

Figure 43 Percentage Error in Normalized Plasma Frequency for the Underdense Plasma Approximation (UDPA) as a Function of Measured Plasma Frequency for Various Values of Measured Collision Frequency, for a Value of the Normalized Thickness of the Plasma Layer d = 3

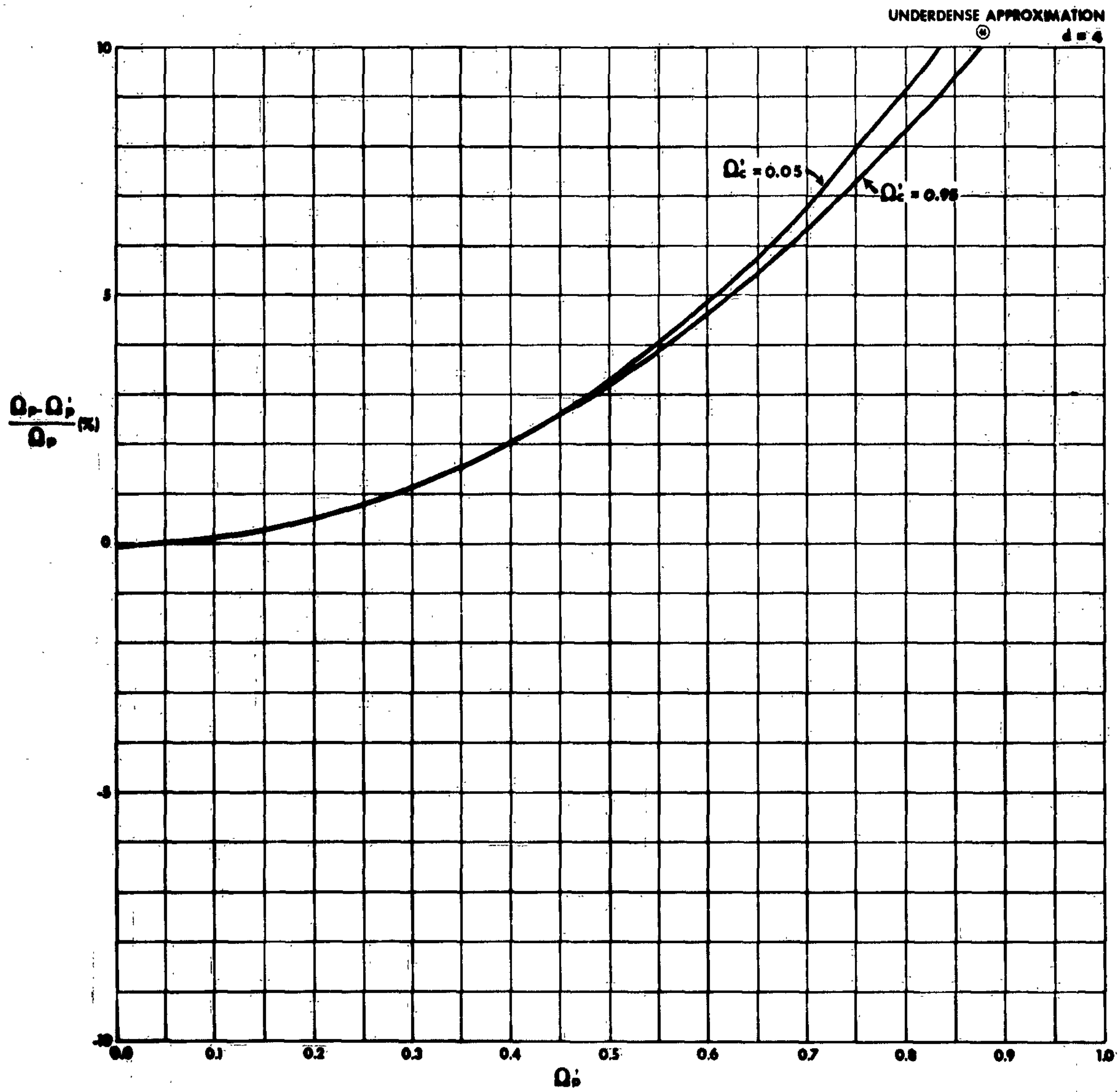

Figure 44 Percentage Error in Normalized Plasma Frequency for the Underdense Plasma Approximation (UDPA) as a Function of Measured Plasma Frequency for Various Values of Measured Collision Frequency, for a Value of the Normalized Thickness of the Plasma Layer d = 4

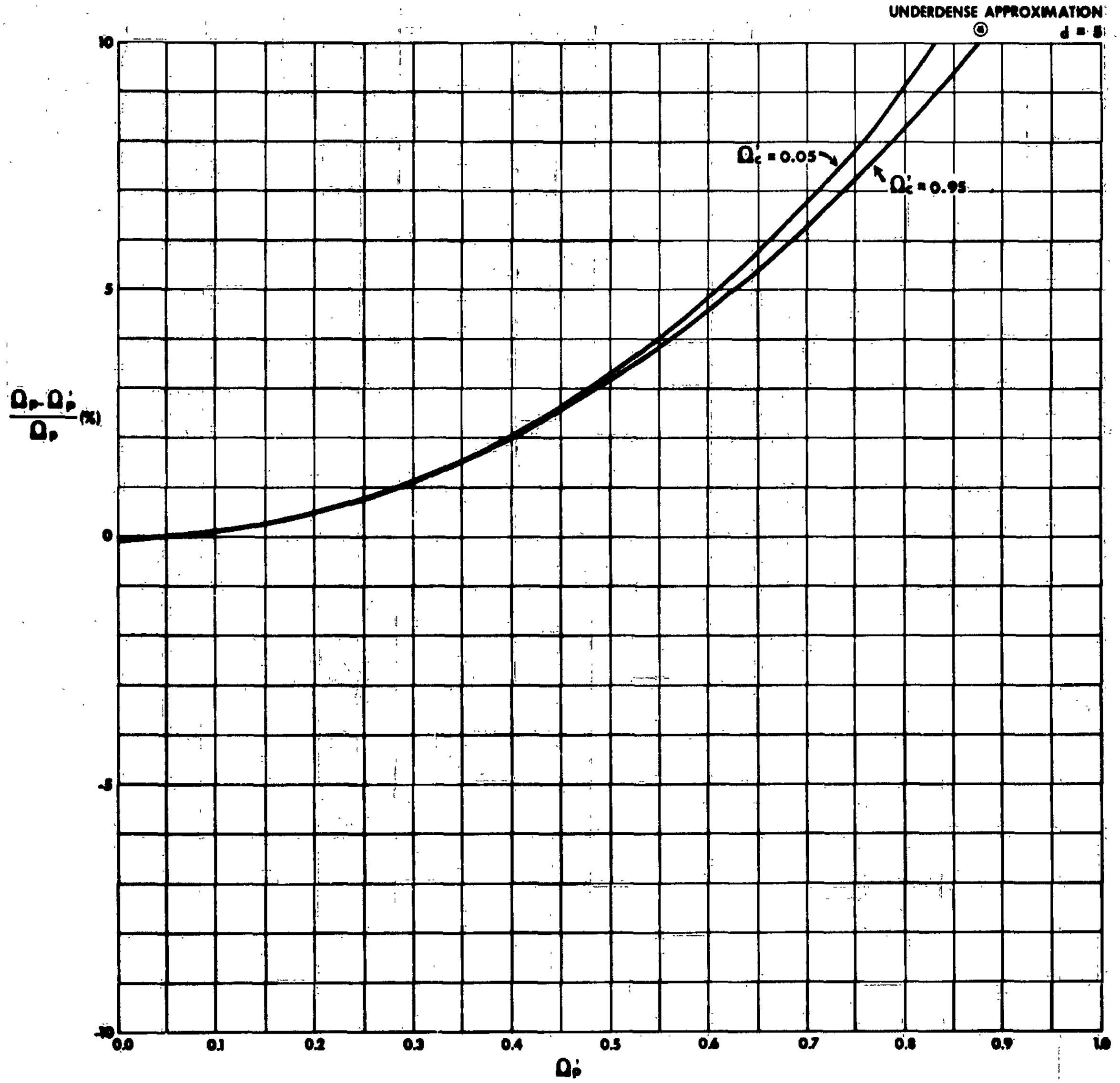

Figure 45 Percentage Error in Normalized Plasma Frequency for the Underdense Plasma Approximation (UDPA) as a Function of Measured Plasma Frequency for Various Values of Measured Collision Frequency, for a Value of the Normalized Thickness of the Plasma Layer d = 5

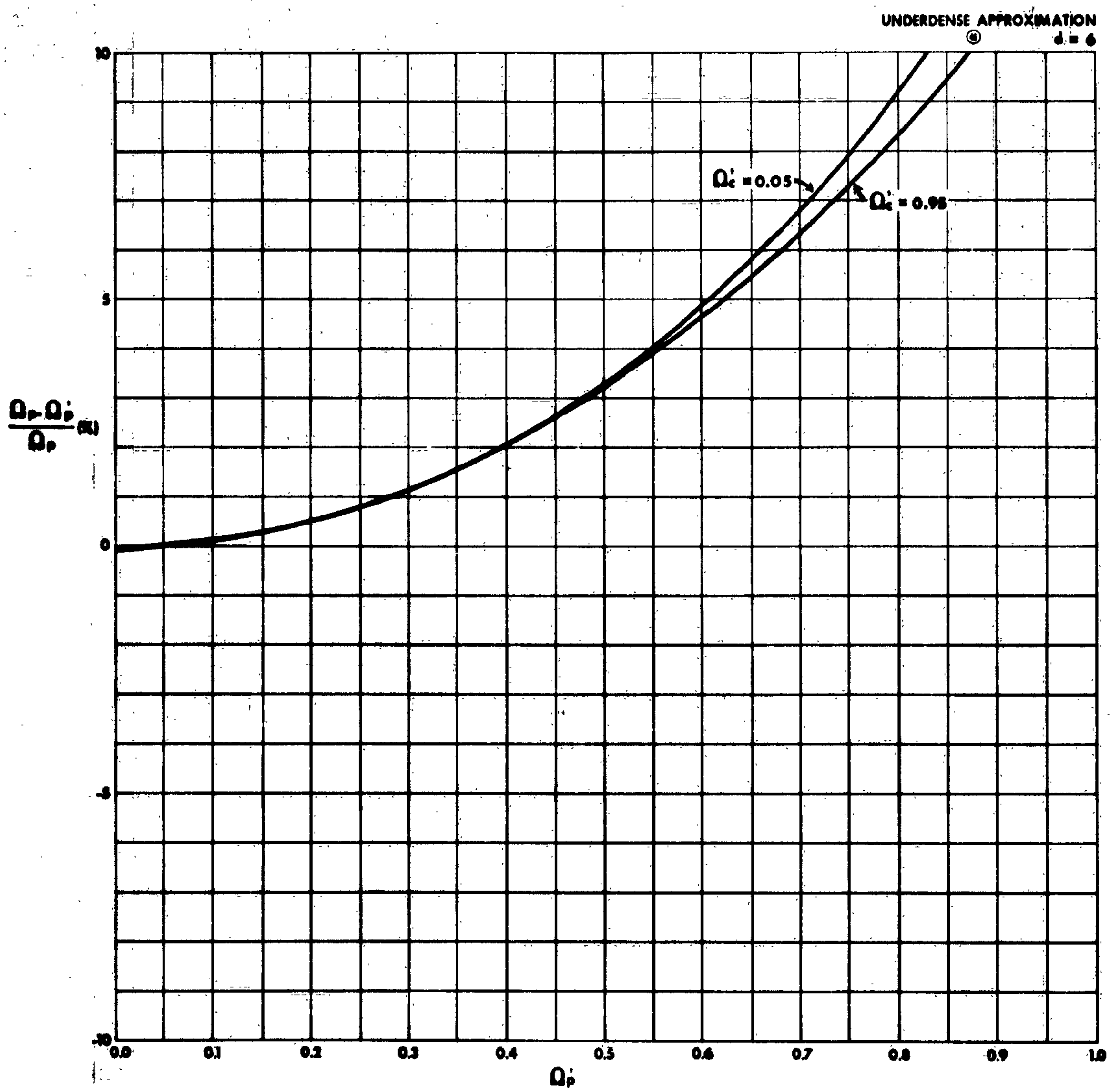

Figure 46 Percentage Error in Normalized Plasma Frequency for the Underdense Plasma Approximation (UDPA) as a Function of Measured Plasma Frequency for Various Values of Measured Collision Frequency, for a Value of the Normalized Thickness of the Plasma Layer d = 6

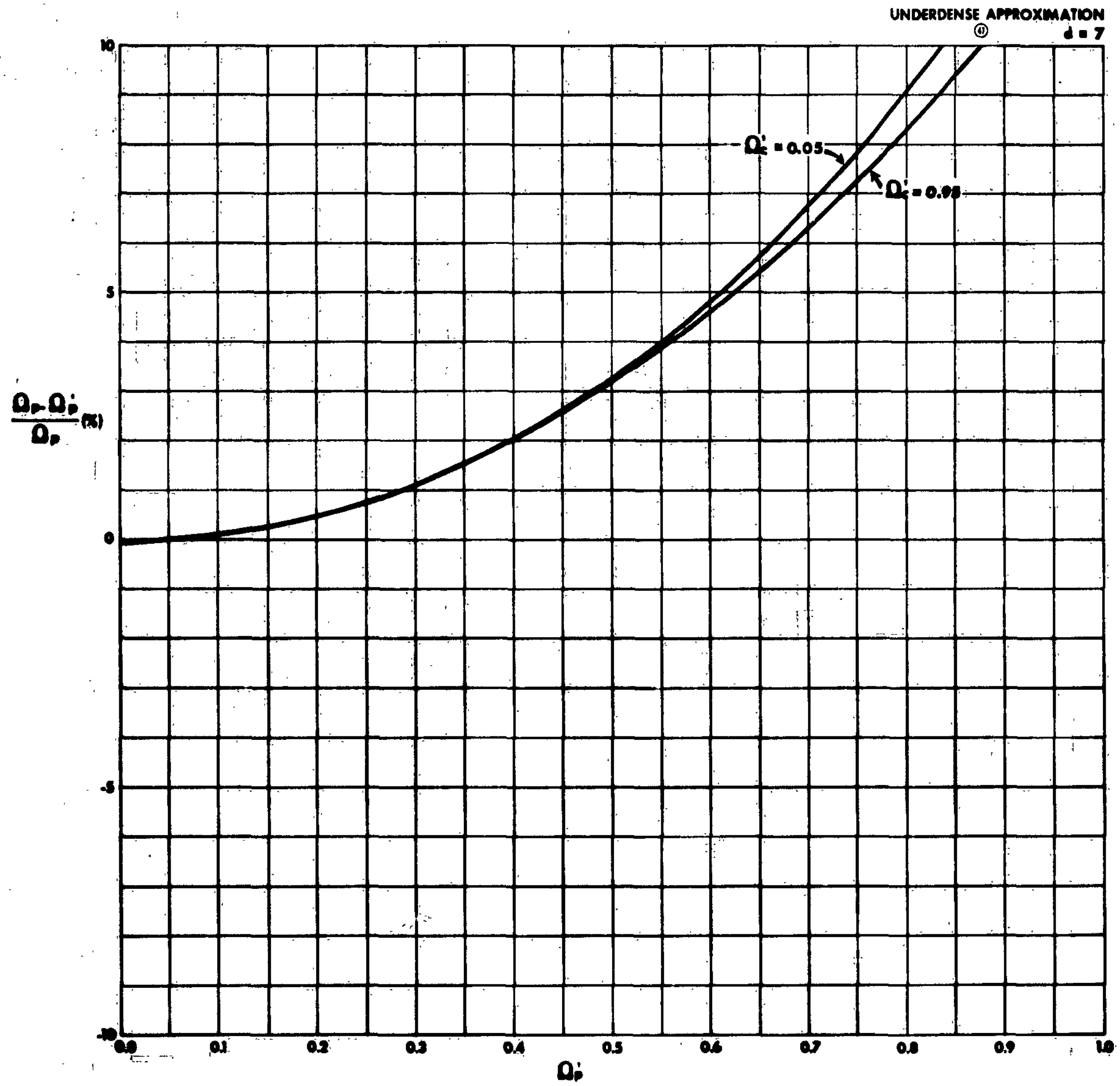

Figure 47 Percentage Error in Normalized Plasma Frequency for the Underdense Plasma Approximation (UDPA) as a Function of Measured Plasma Frequency for Various Values of Measured Collision Frequency, for a Value of the Normalized Thickness of the Plasma Layer $d = 7$

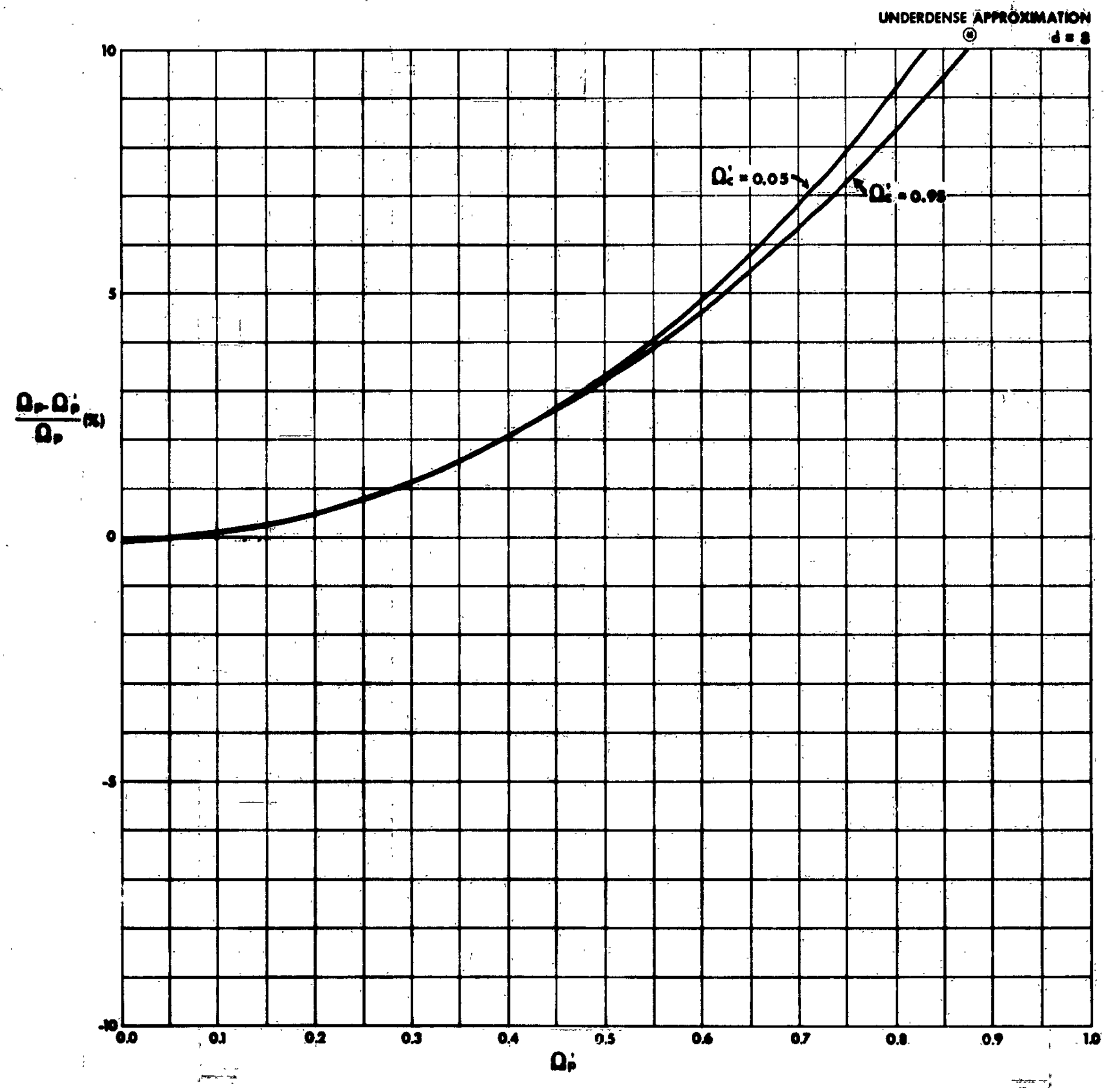

Figure 48 Percentage Error in Normalized Plasma Frequency for the Underdense Plasma Approximation (UDPA) as a Function of Measured Plasma Frequency for Various Values of Measured Collision Frequency, for a Value of the Normalized Thickness of the Plasma Layer d = 8

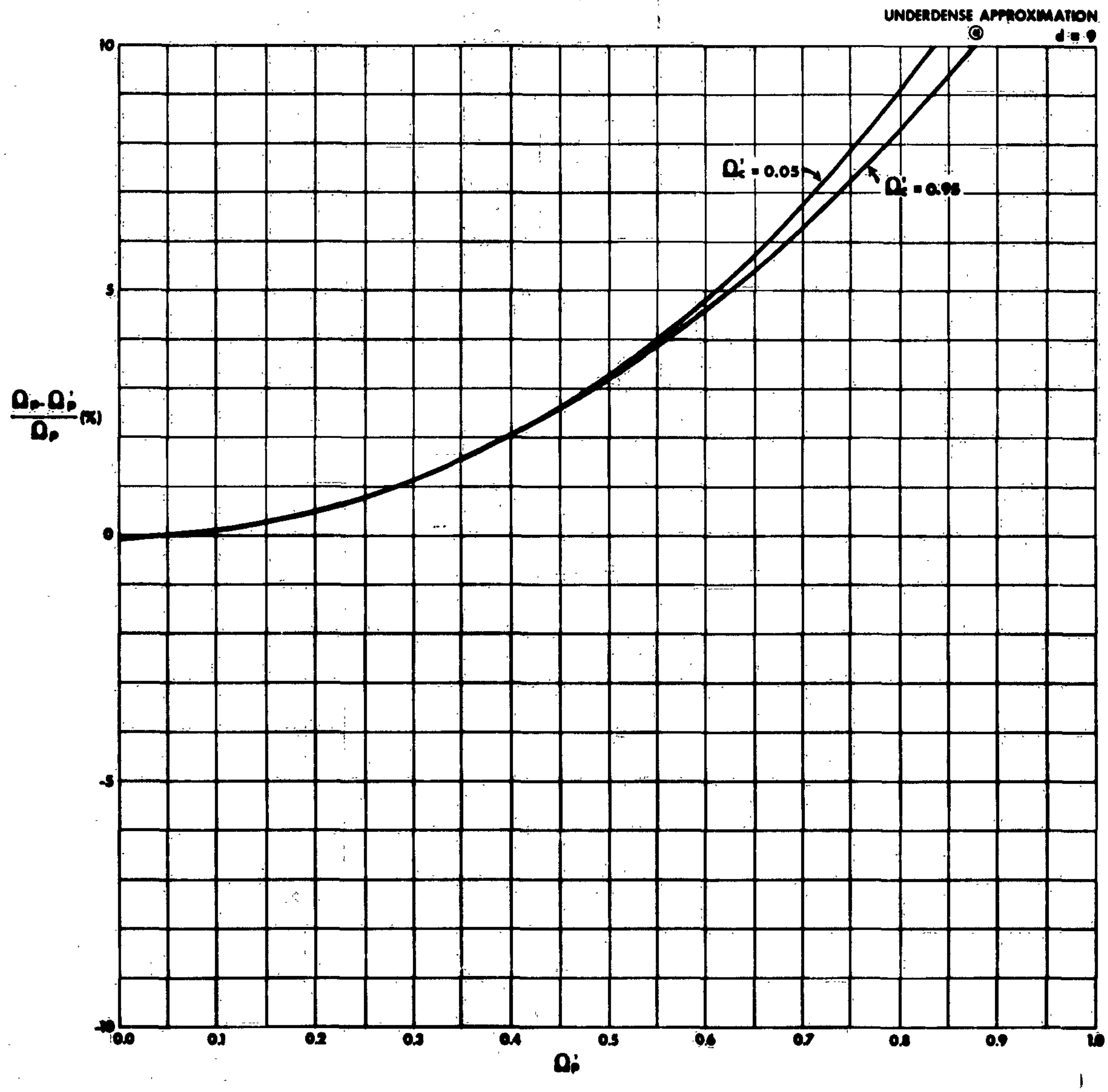

Figure 40 Percentage Error in Normalized Plasma Frequency for the Underdense Plasma Approximation (UDPA) as a Function of Measured Plasma Frequency for Various Values of Measured Collision Frequency, for a Value of the Normalized Thickness of the Plasma Layer d = 9

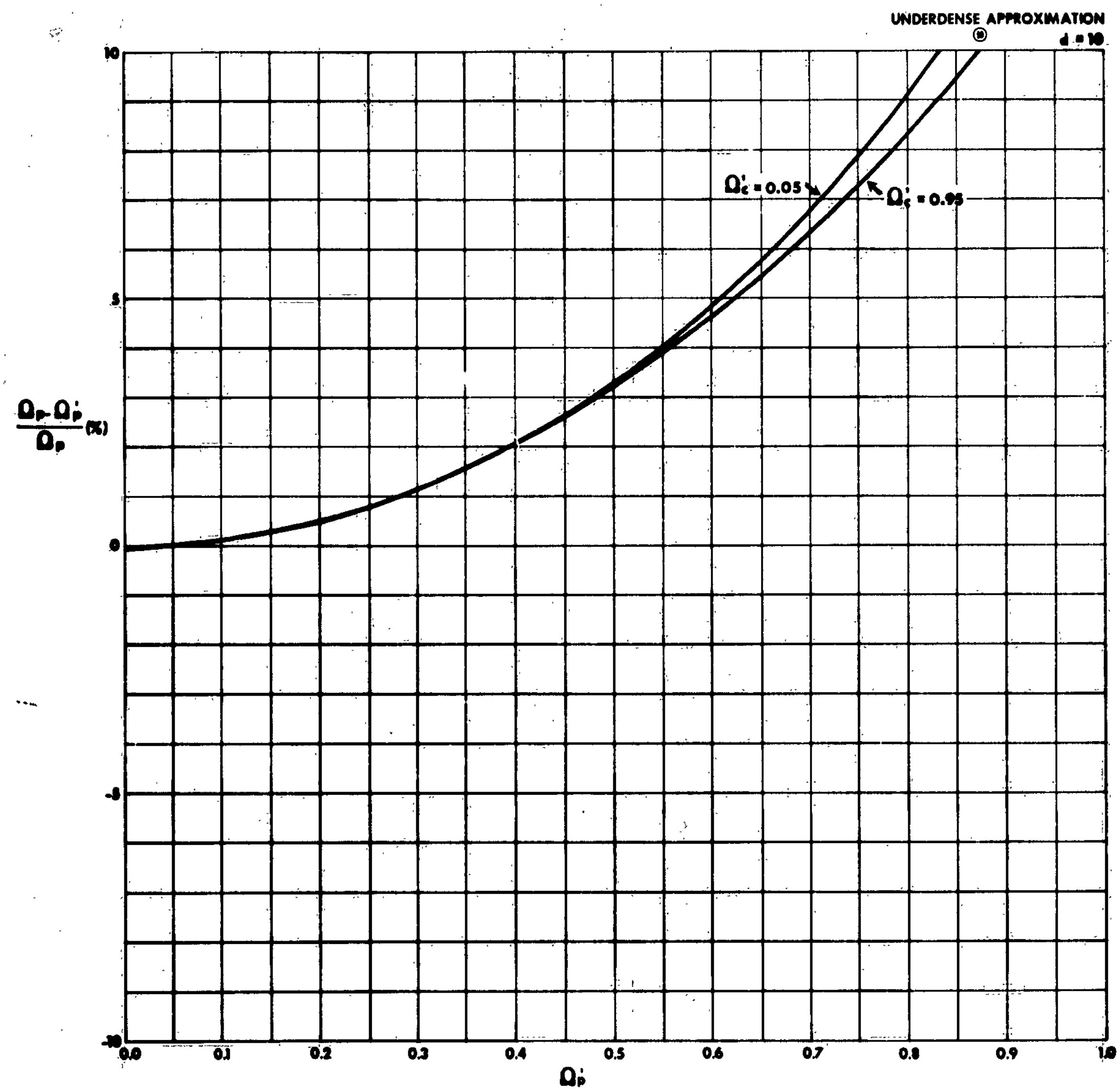

Figure 50 Percentage Error in Normalized Plasma Frequency for the Underdense Plasma Approximation (UDPA) as a Function of Measured Plasma Frequency for Various Values of Measured Collision Frequency, for a Value of the Normalized Thickness of the Plasma Layer d = 10

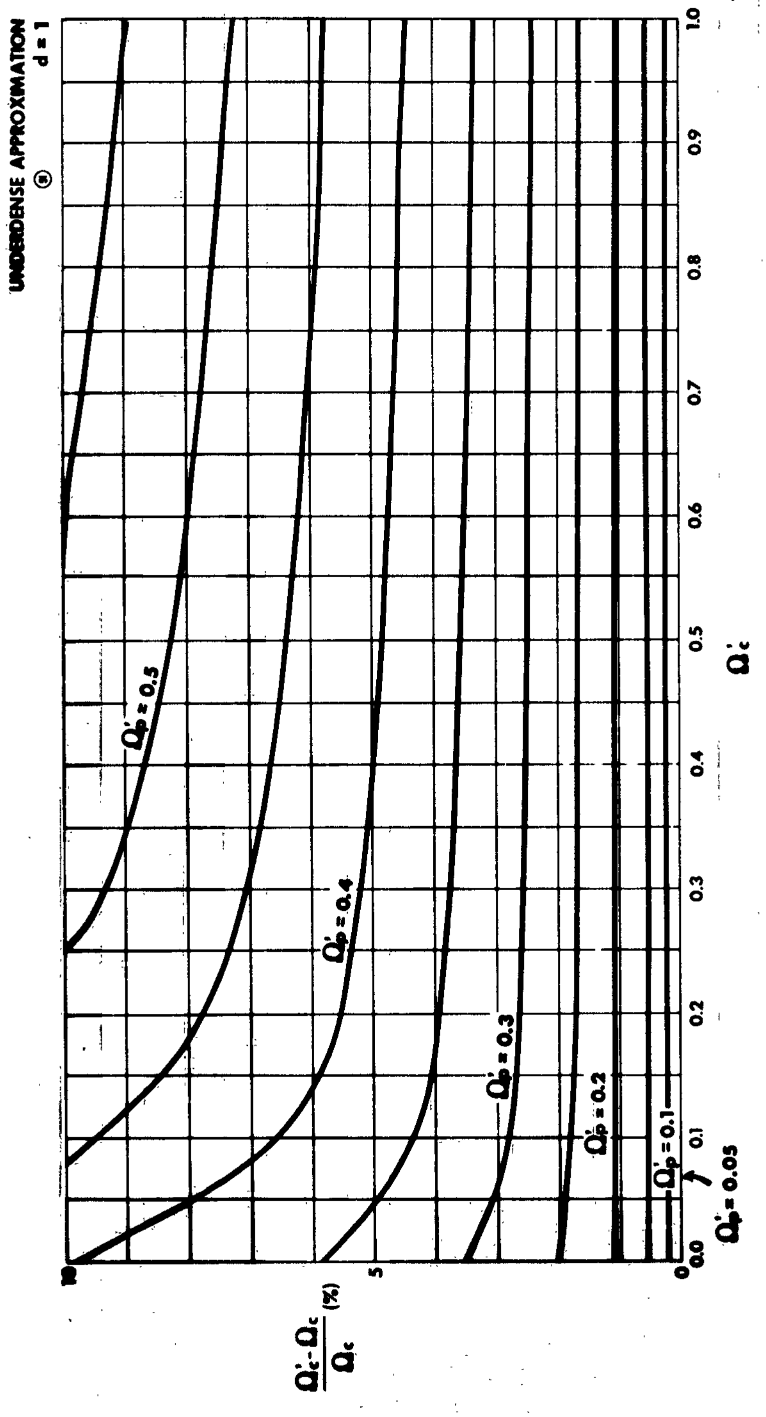

Figure 51 Percentage Error in Normalized Collision Frequency for the Underdense Plasma Approximation (UDPA) as a Function of the Measured Collision Frequency for Various Values of the Measured Plasma Frequency, for a Value of the Normalized Thickness of the Plasma Layer d = 1

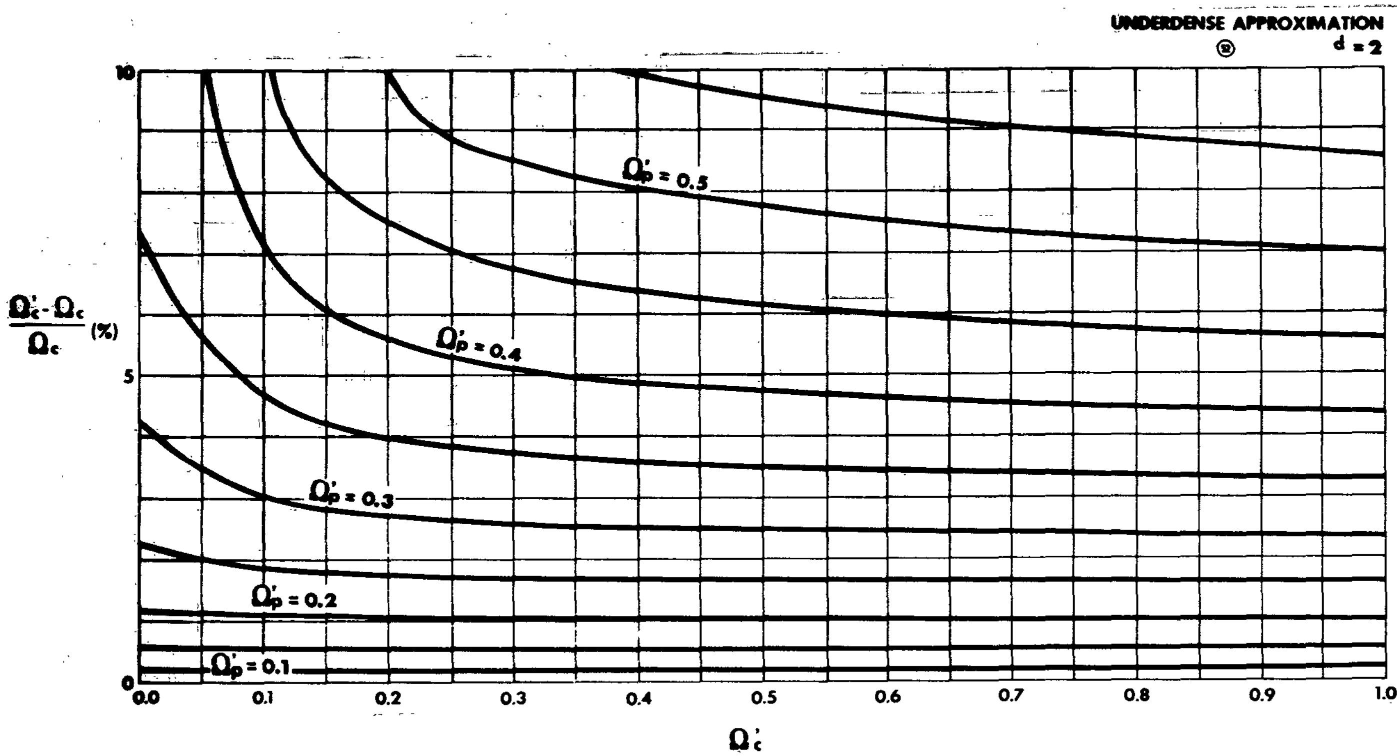

Figure 52 Percentage Error in Normalized Collision Frequency for the Underdense Plasma Approximation (UDPA) as a Function of the Measured Collision Frequency for Various Values of the Measured Plasma Frequency, for a Value of the Normalized Thickness of the Plasma Layer d = 2

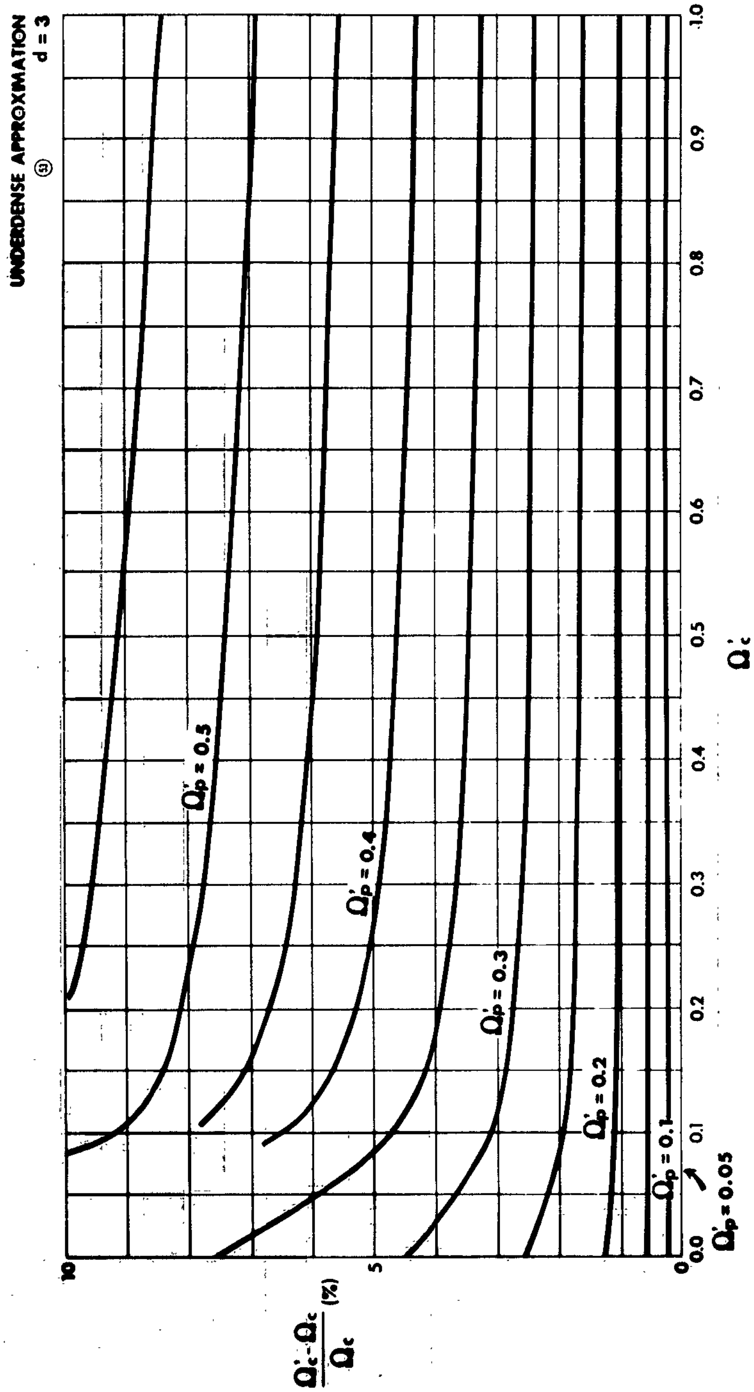

Figure 53 Percentage Error in Normalized Collision Frequency for the Underdense Plasma Approximation (UDPA) as a Function of the Measured Collision Frequency for Various Values of the Measured Plasma Frequency, for a Value of the Normalized Thickness of the Plasma Layer d = 3

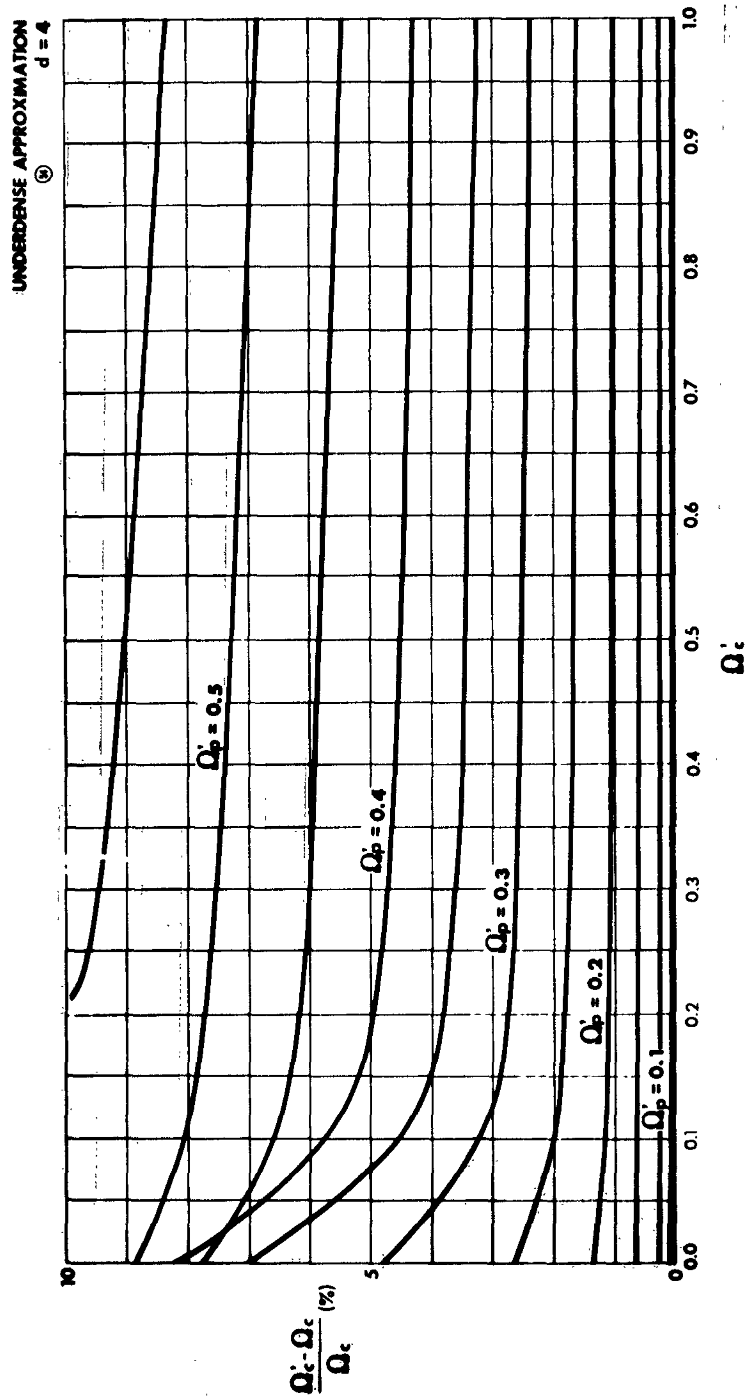

Figure 54 Percentage Error in Normalized Collision Frequency for the Underdense Plasma Approximation (UDPA) as a Function of the Measured Collision Frequency for Various Values of the Measured Plasma Frequency, for a Value of the Normalized Thickness of the Plasma Layer d = 4

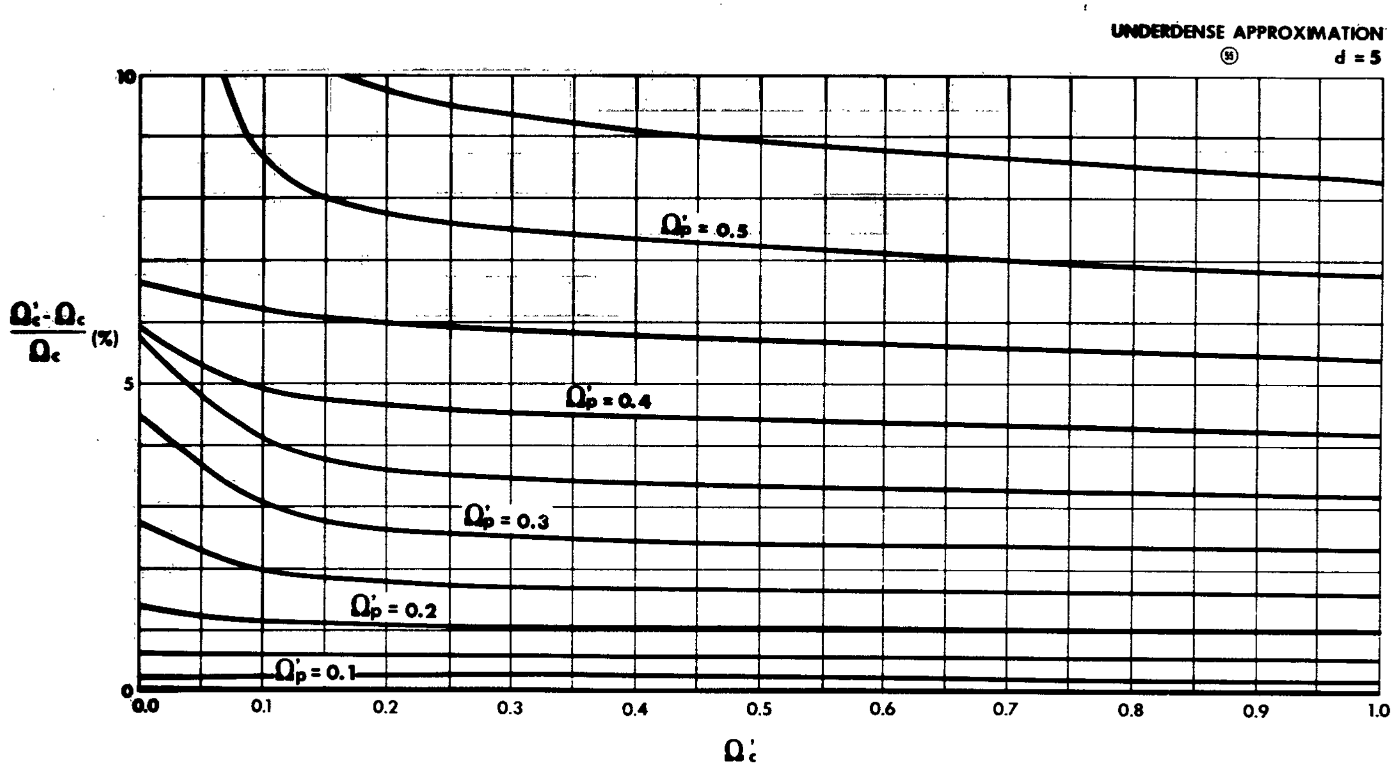

Figure 55 Percentage Error in Normalized Collision Frequency for the Underdense Plasma Approximation (UDPA) as a Function of the Measured Collision Frequency for Various Values of the Measured Plasma Frequency, for a Value of the Normalized Thickness of the Plasma Layer d = 5

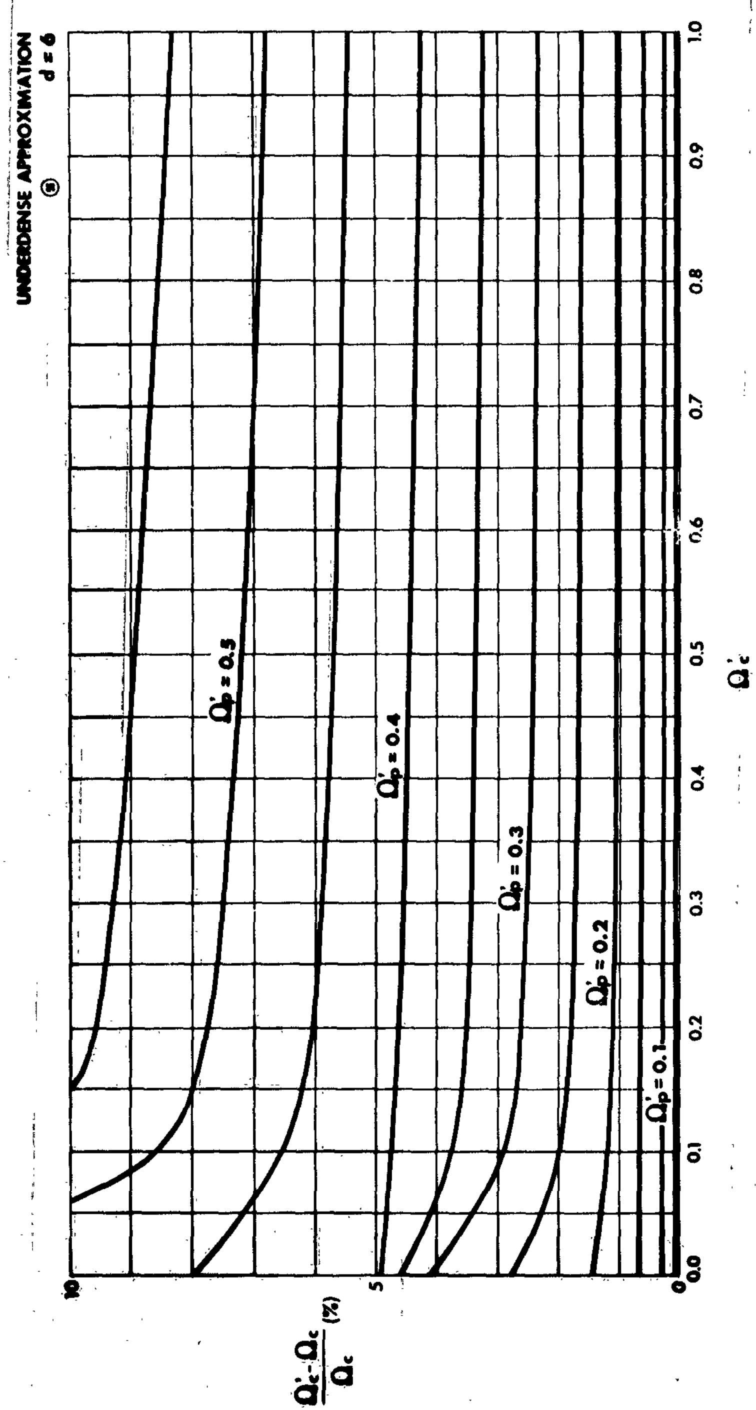

Figure 56 Percentage Error in Normalized Collision Frequency for the Underdense Plasma Approximation (UDPA) as a Function of the Measured Collision Frequency for Various Values of the Measured Plasma Frequency, for a Value of the Normalized Thickness of the Plasma Layer d = 6

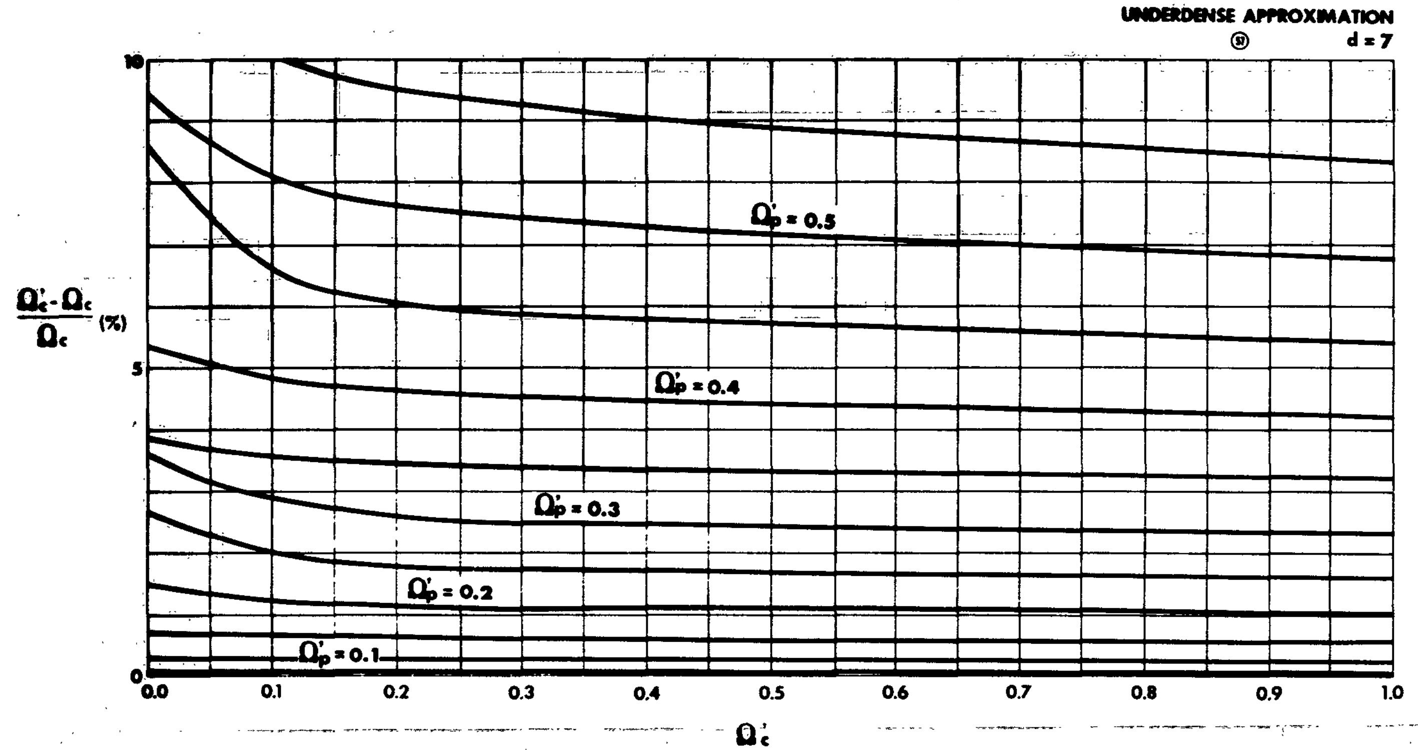

Figure 57 Percentage Error in Normalized Collision Frequency for the Underdense Plasma Approximation (UDPA) as a Function of the Measured Collision Frequency for Various Values of the Measured Plasma Frequency, for a Value of the Normalized Thickness of the Plasma Layer d = 7

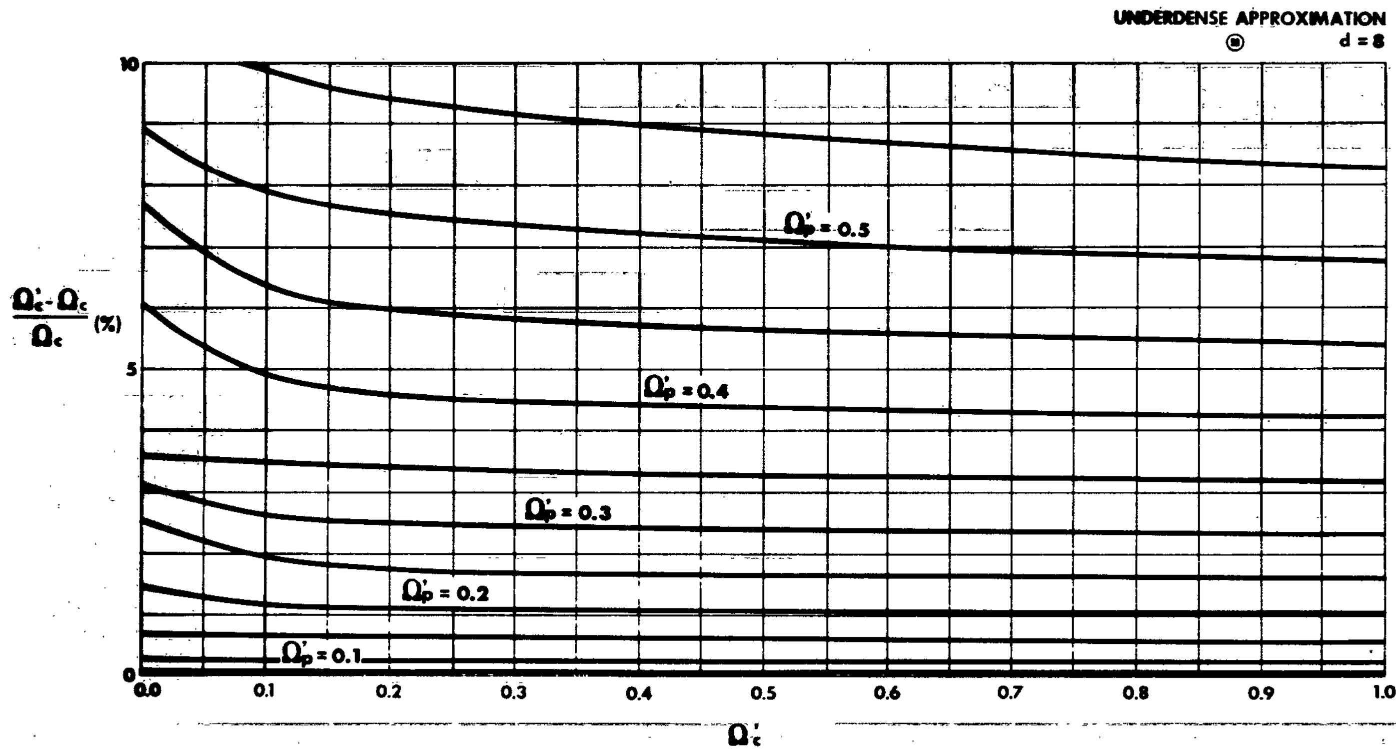

Figure 58 Percentage Error in Normalized Collision Frequency for the Underdense Plasma Approximation (UDPA) as a Function of the Measured Collision Frequency for Various Values of the Measured Plasma Frequency, for a Value of the Normalized Thickness of the Plasma Layer d = 8

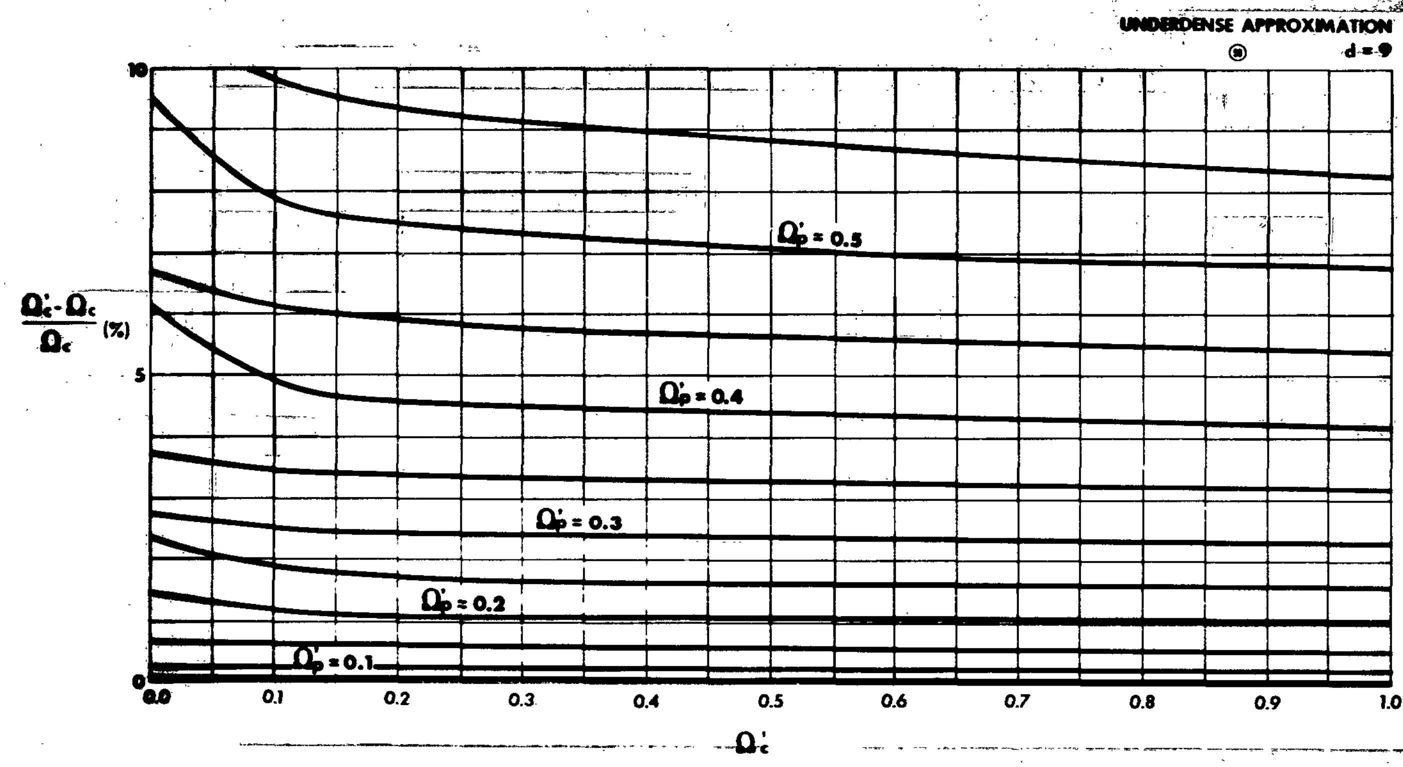

Figure 59 Percentage Error in Normalized Collision Frequency for the Underdense Plasma Approximation (UDPA) as a Function of the Measured Collision Frequency for Various Values of the Measured Plasma Frequency, for a Value of the Normalized Thickness of the Plasma Layer d = 9

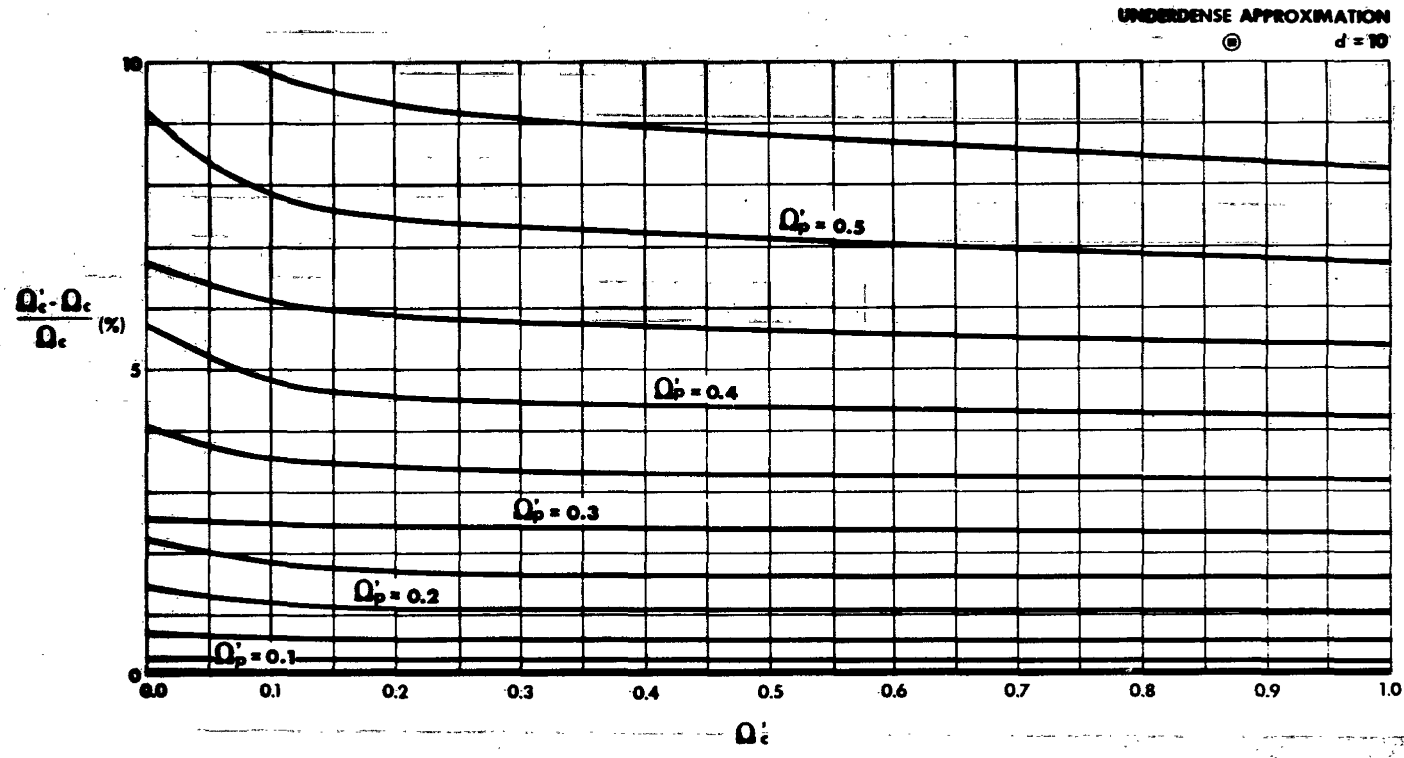

Figure 60 Percentage Error in Normalized Collision Frequency for the Underdense Plasma Approximation (UDPA) as a Function of the Measured Collision Frequency for Various Values of the Measured Plasma Frequency, for a Value of the Normalized Thickness of the Plasma Layer d = 10

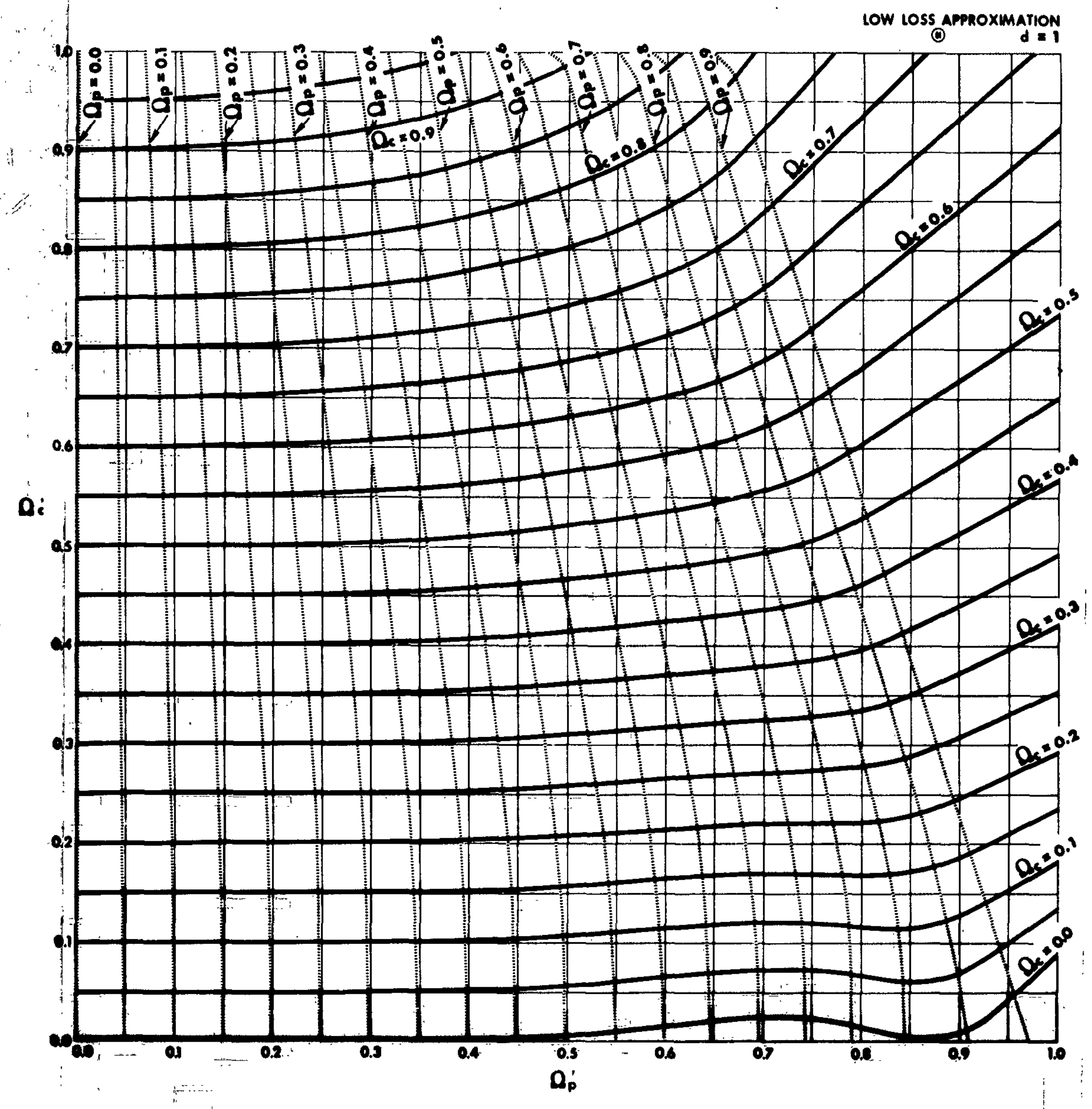

Figure 61 Exact Values, as Functions of the Calculated Values, of the Normalized Plasma and Collision Frequencies for the Low-Loss Plasma Approximation (LLPA), for a Value of the Normalized Thickness of the Plasma Layer d = 1

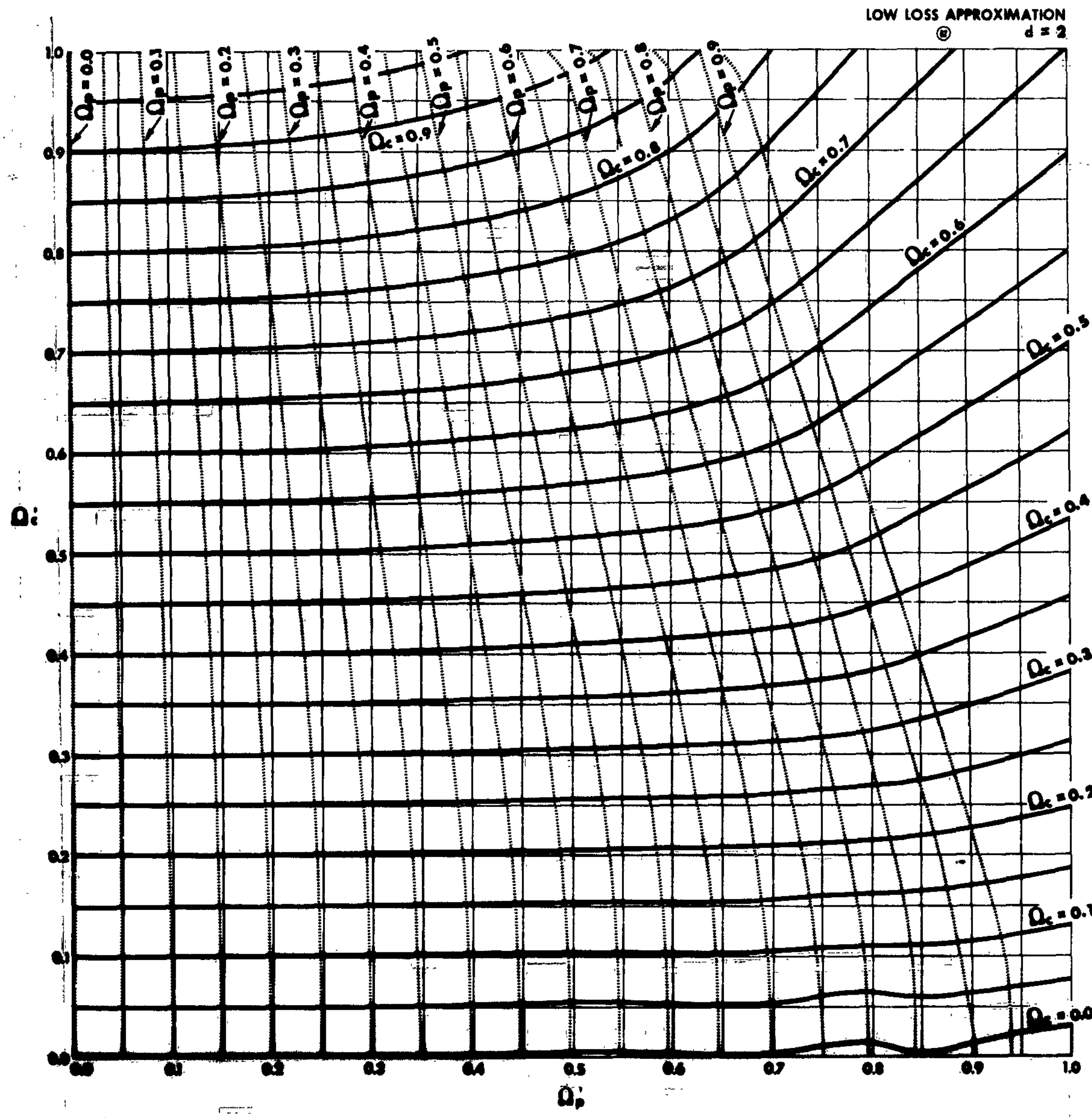

Figure 62 Exact Values, as Functions of the Calculated Values, of the Normalized Plasma and Collision Frequencies for the Low-Loss Plasma Approximation (LLPA), for a Value of the Normalized Thickness of the Plasma Layer d = 2

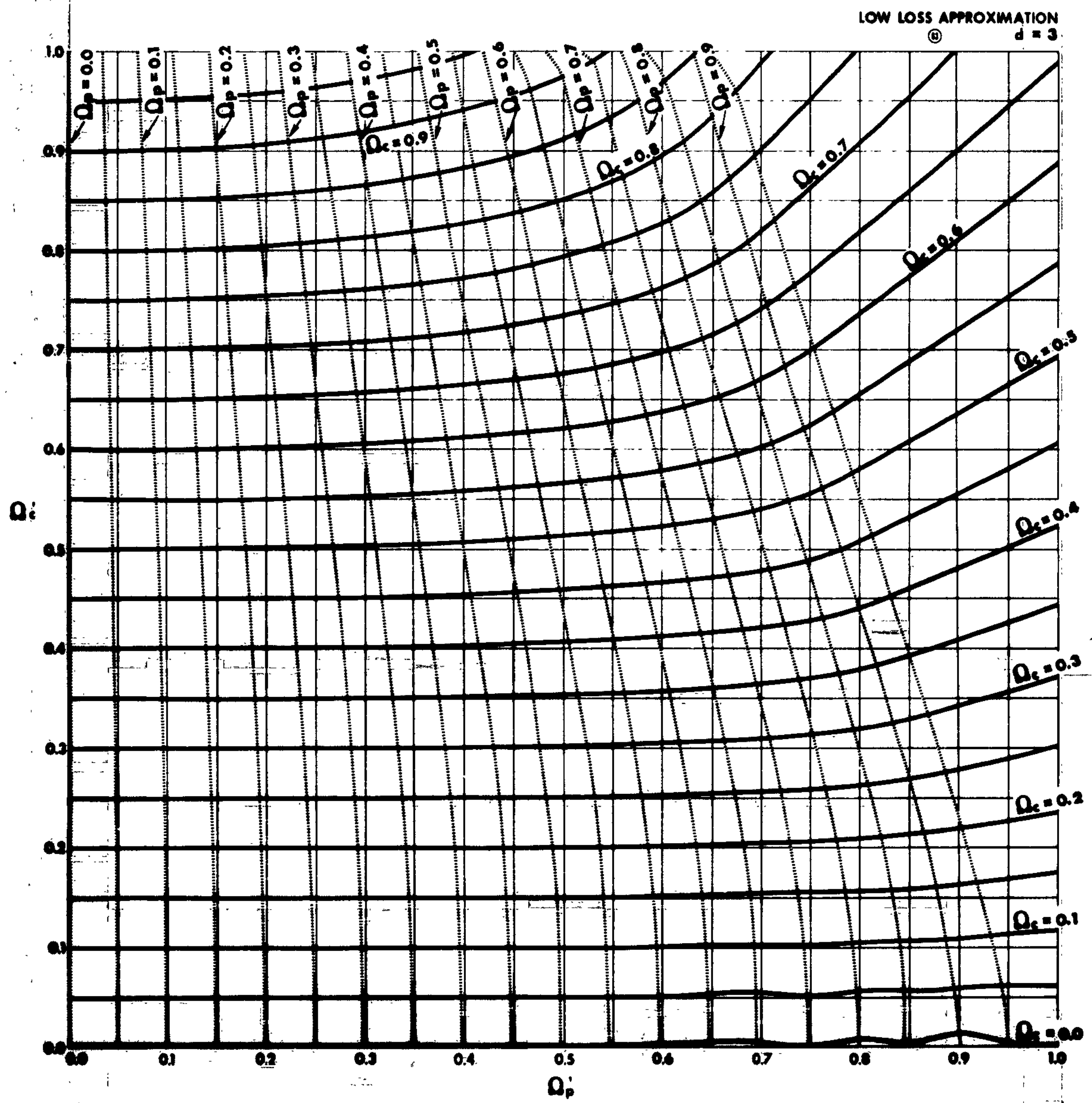

Figure 63 Exact Values, as Functions of the Calculated Values, of the Normalized Plasma and Collision Frequencies for the Low-Loss Plasma Approximation (LLPA), for a Value of the Normalized Thickness of the Plasma Layer d = 3

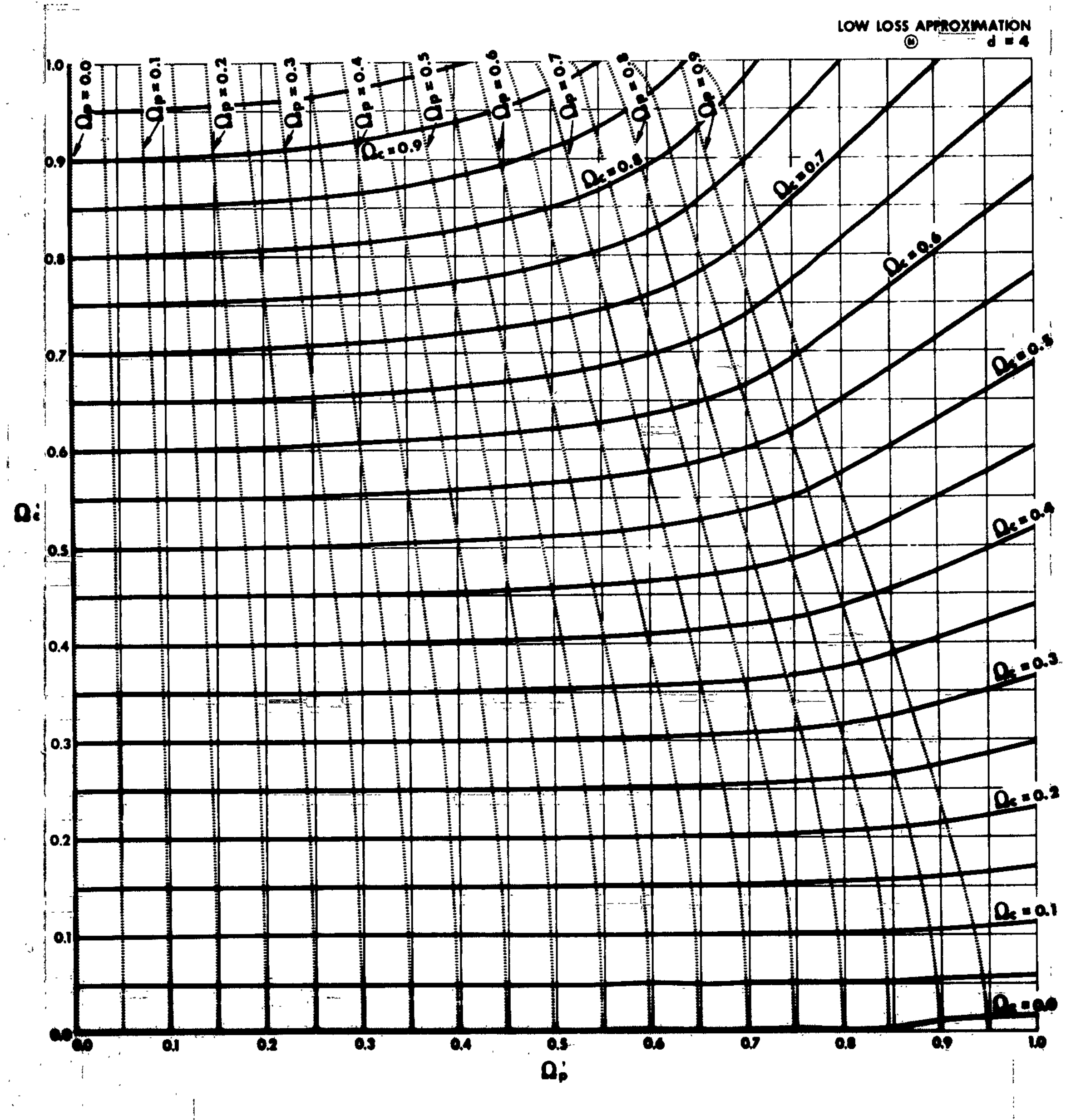

Figure 64 Exact Values, as Functions of the Calculated Values, of the Normalized Plasma and Collision Frequencies for the Low-Loss Plasma Approximation (LLPA), for a Value of the Normalized Thickness of the Plasma Layer d = 4

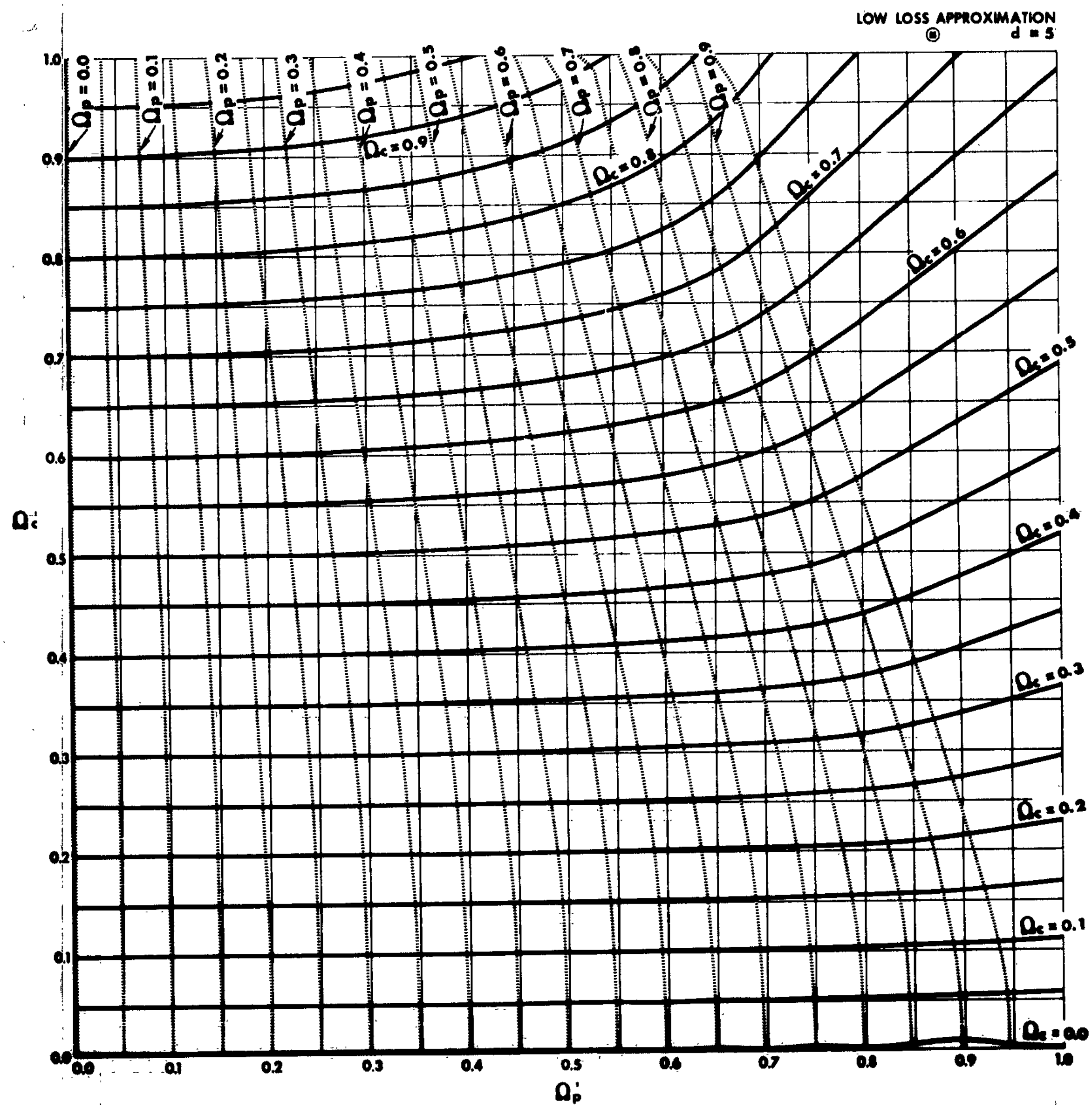

Figure 65 Exact Values, as Functions of the Calculated Values, of the Normalized Plasma and Collision Frequencies for the Low-Loss Plasma Approximation (LLPA), for a Value of the Normalized Thickness of the Plasma Layer d = 5

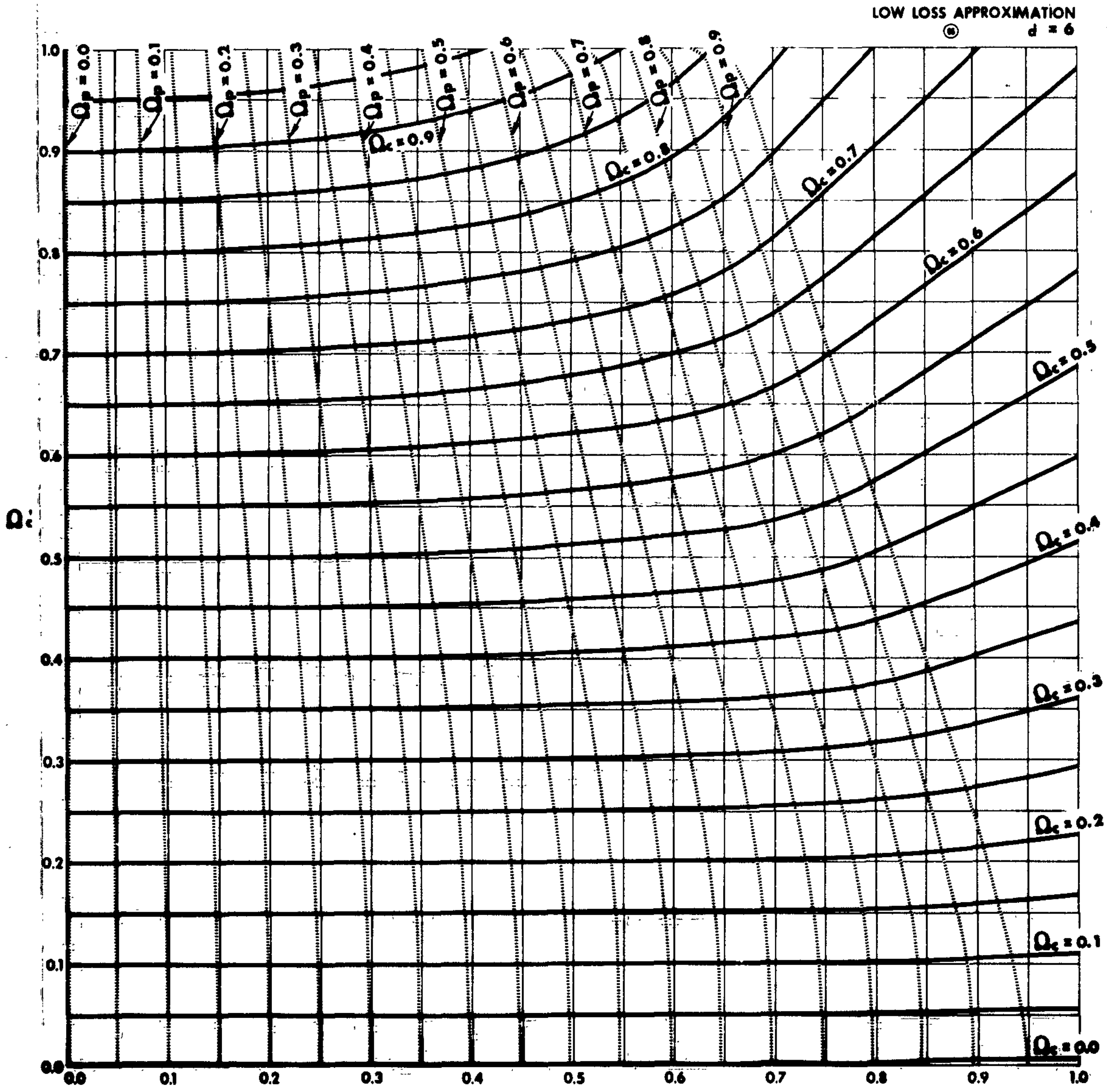

Figure 66 Exact Values, as Functions of the Calculated Values, of the Normalized Plasma and Collision Frequencies for the Low-Loss Plasma Approximation (LLPA), for a Value of the Normalized Thickness of the Plasma Layer d = 6

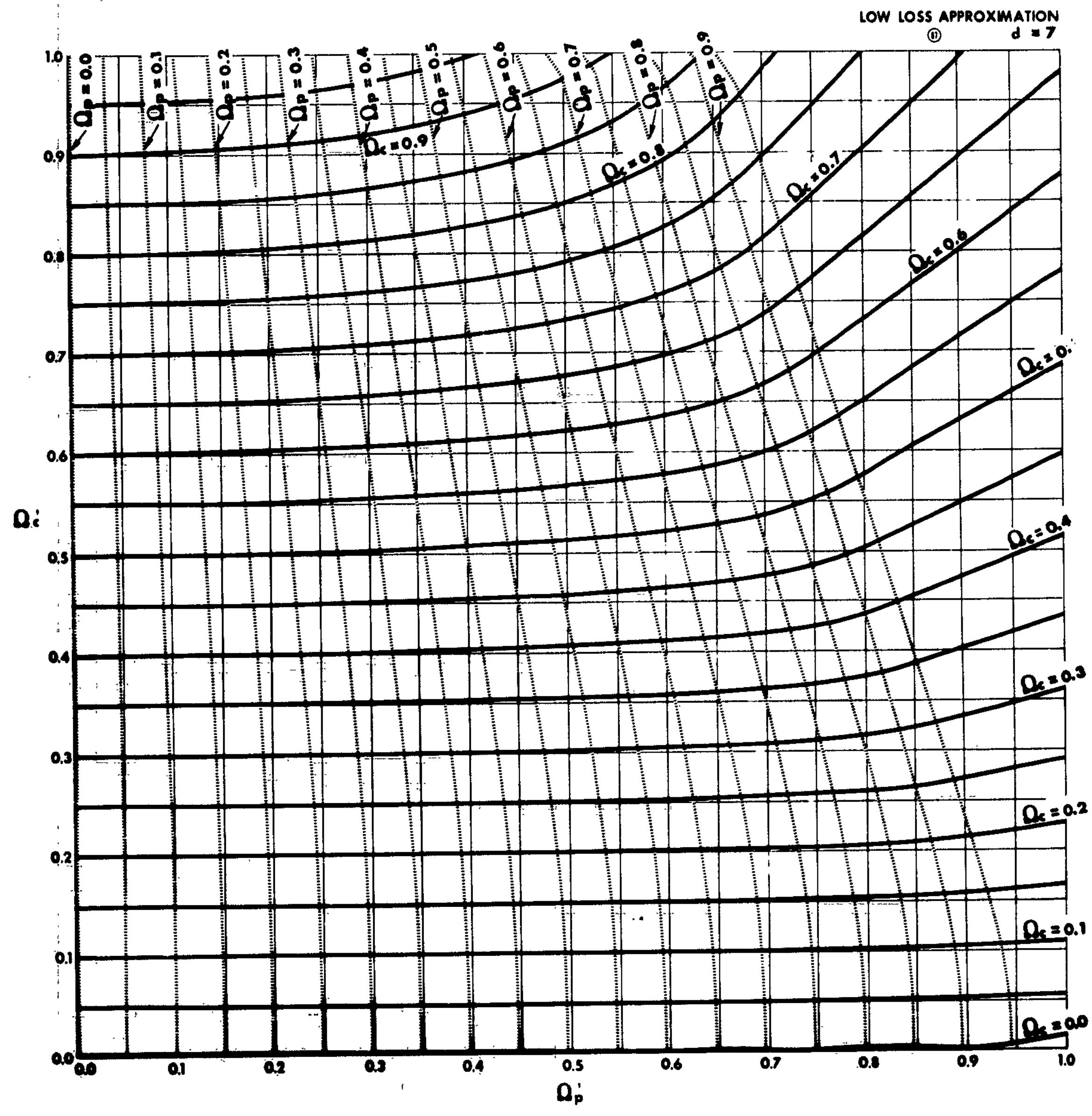

Figure 67 Exact Values, as Functions of the Calculated Values, of the Normalized Plasma and Collision Frequencies for the Low-Loss Plasma Approximation (LLPA), for a Value of the Normalized Thickness of the Plasma Layer d = 7

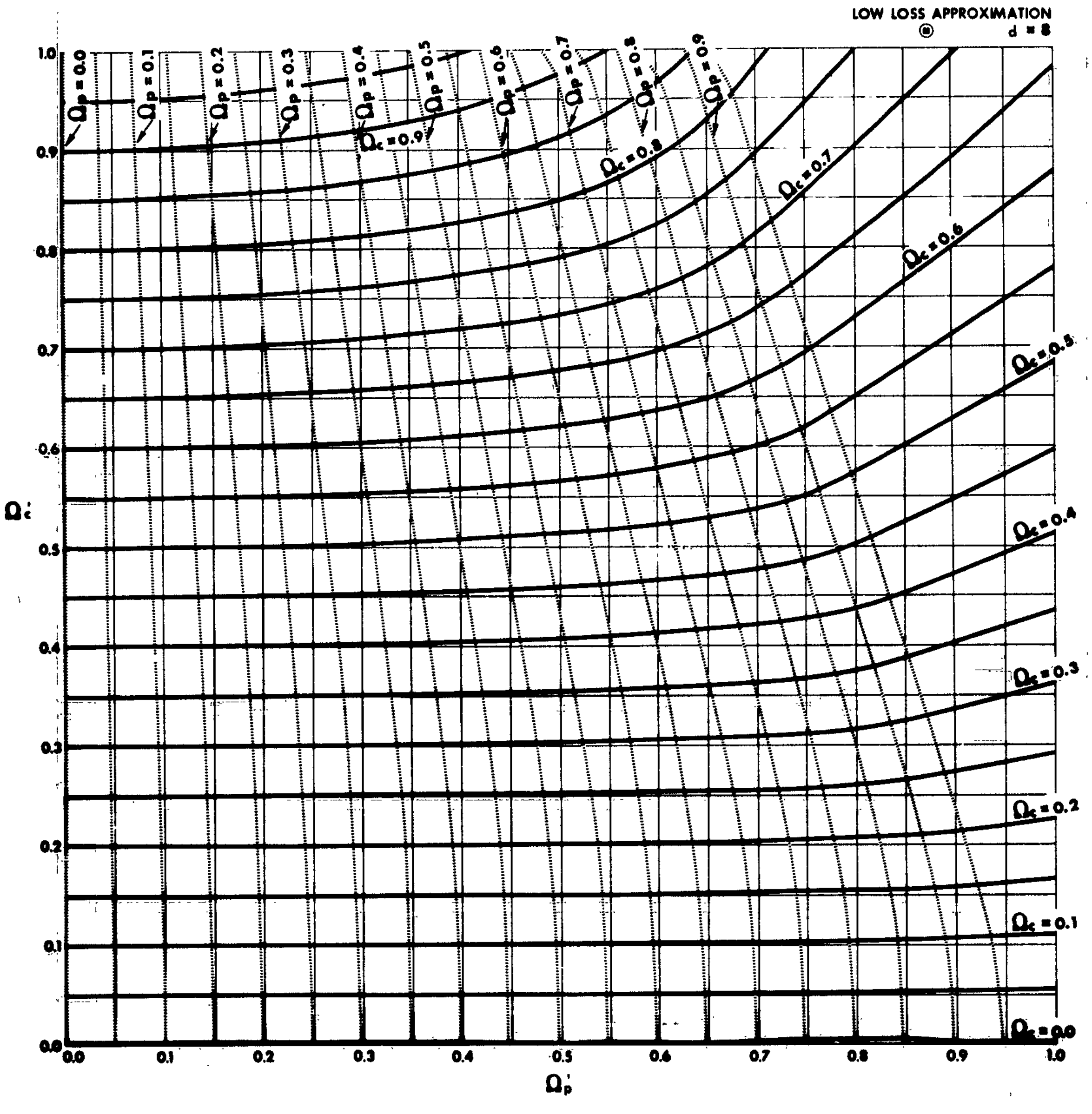

Figure 68 Exact Values, as Functions of the Calculated Values, of the Normalized Plasma and Collision Frequencies for the Low-Loss Plasma Approximation (LLPA), for a Value of the Normalized Thickness of the Plasma Layer d = 8

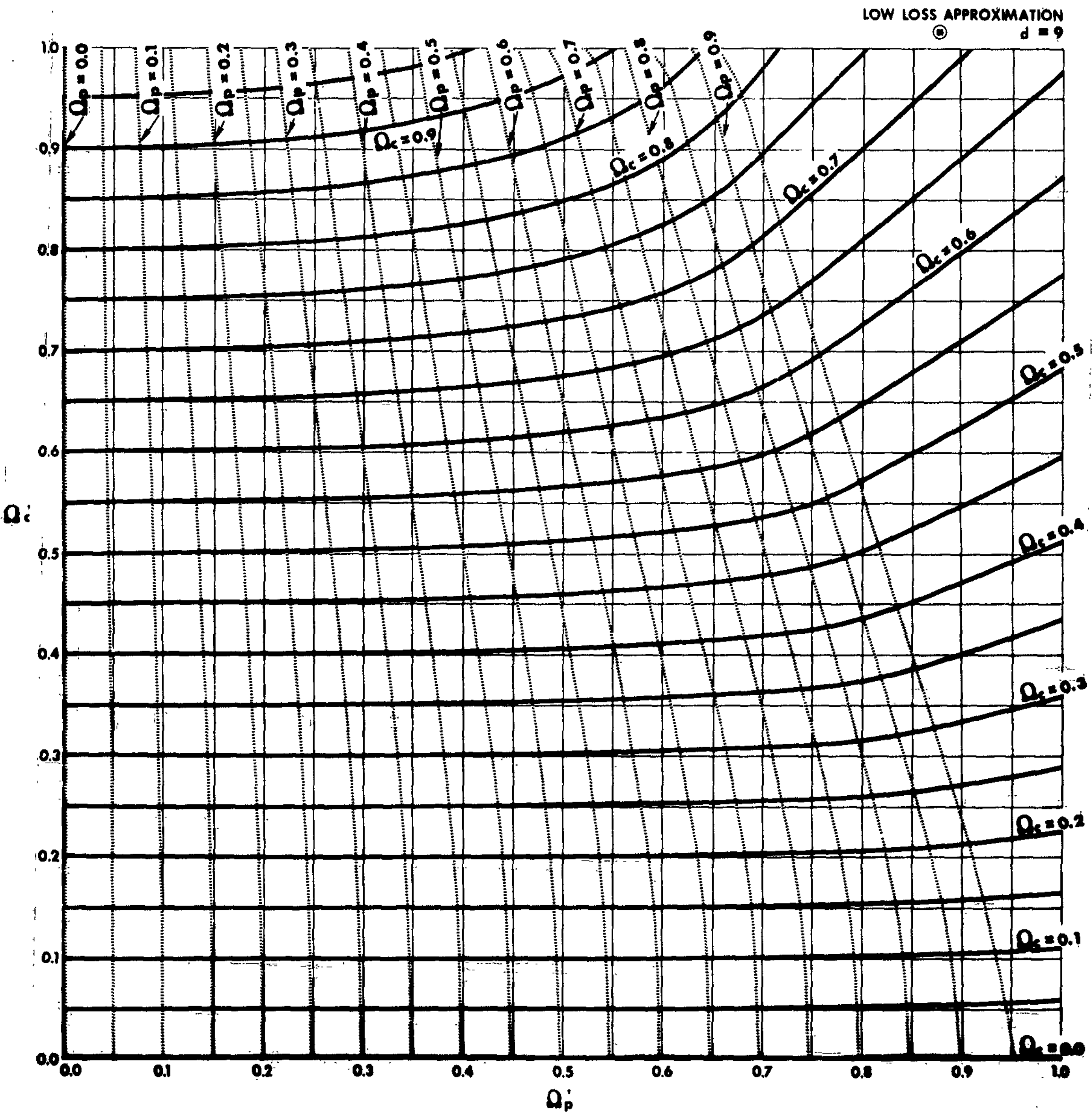

Figure 69 Exact Values, as Functions of the Calculated Values, of the Normalized Plasma and Collision Frequencies for the Low-Loss Plasma Approximation (LLPA), for a Value of the Normalized Thickness of the Plasma Layer d = 9

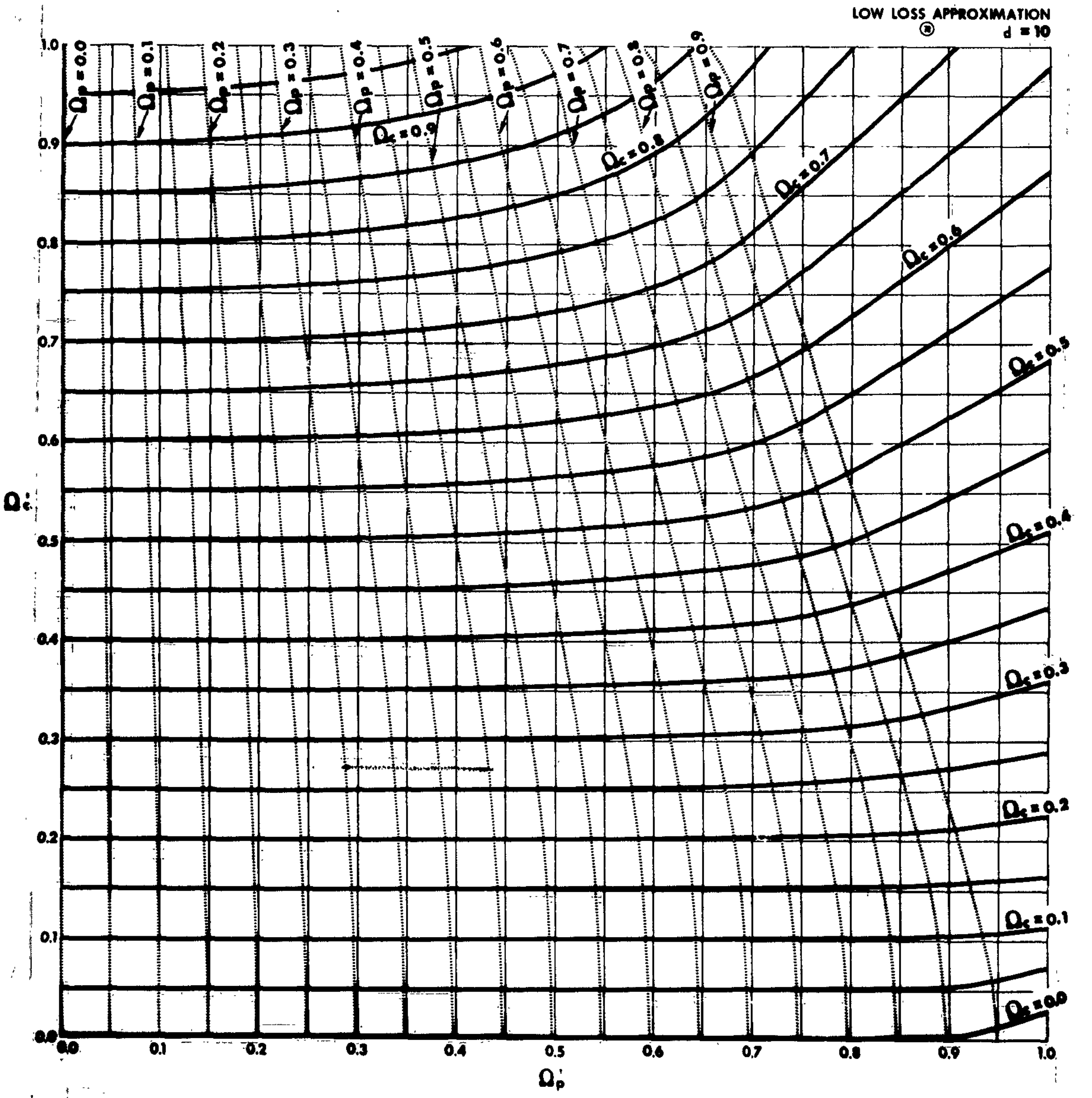

Figure 70 Exact Values, as Functions of the Calculated Values, of the Normalized Plasma and Collision Frequencies for the Low-Loss Plasma Approximation (LLPA), for a Value of the Normalized Thickness of the Plasma Layer d = 10

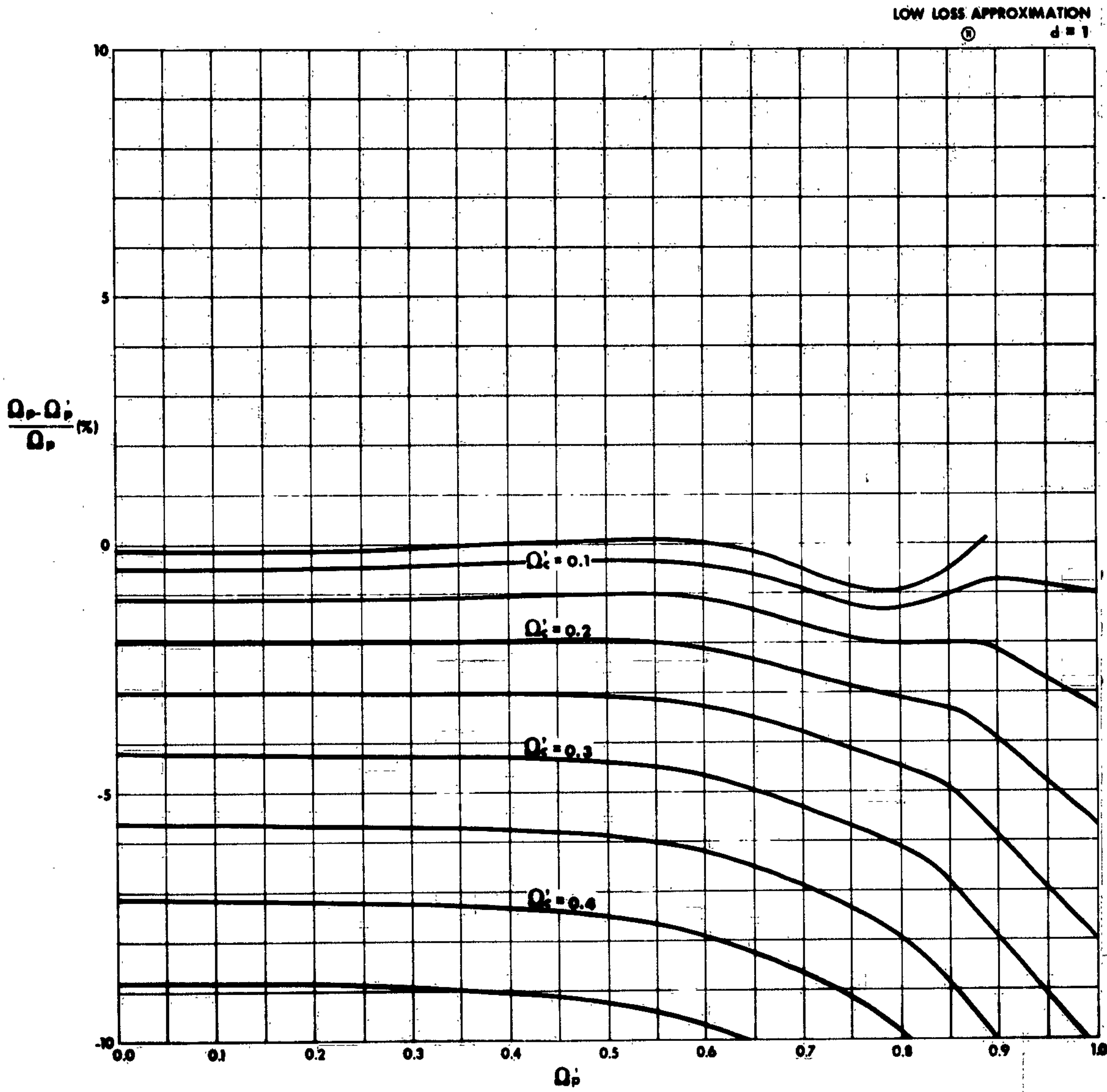

Figure 71 Percentage Error in Normalized Plasma Frequency for the Low-Loss Approximation (LLPA) as a Function of Measured Plasma Frequency for Various Values of Measured Collision Frequency, for a Value of the Normalized Thickness of the Plasma Layer d = 1

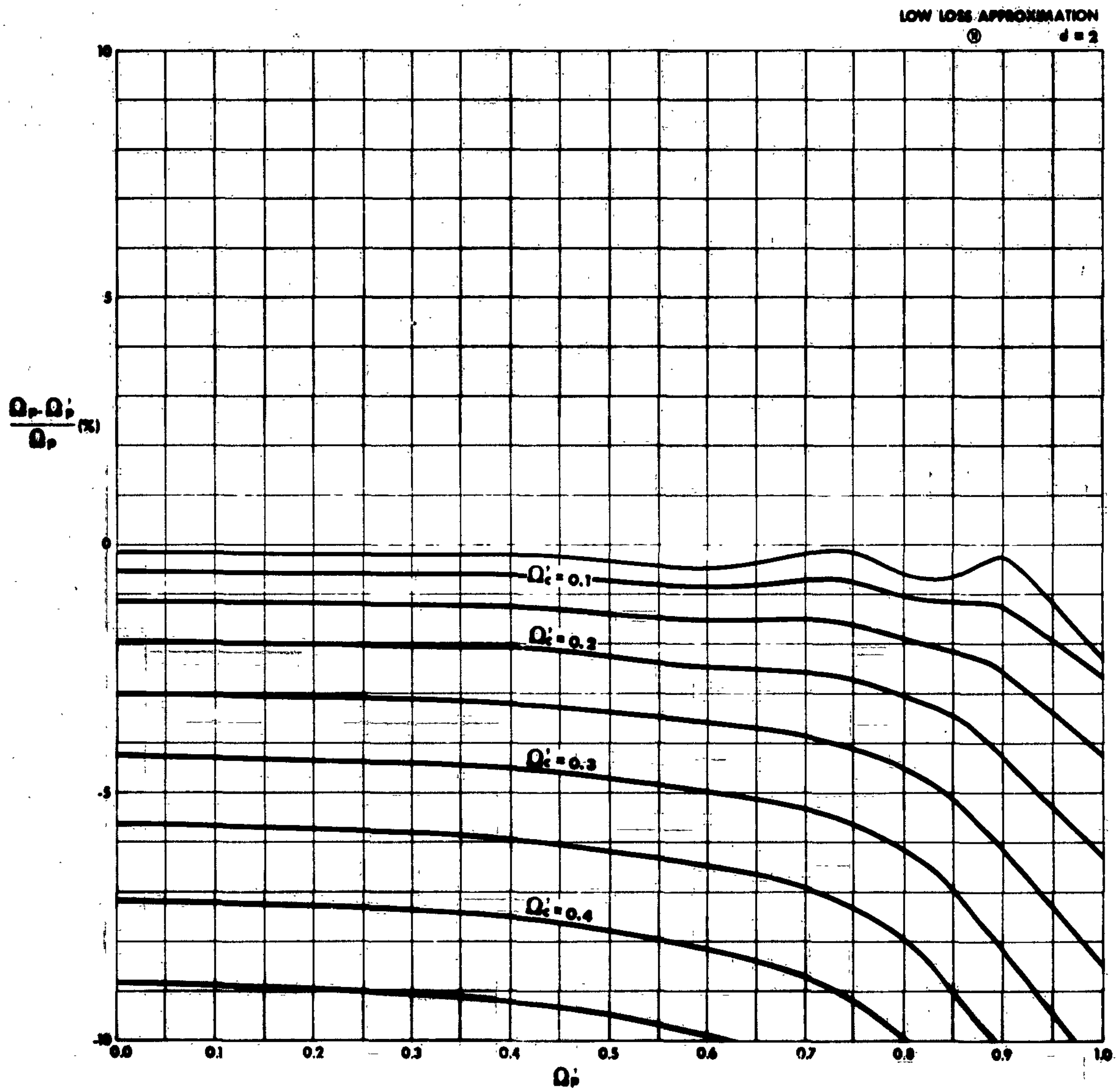

Figure 72 Percentage Error in Normalized Plasma Frequency for the Low-Loss Approximation (LLPA) as a Function of Measured Plasma Frequency for Various Values of Measured Collision Frequency, for a Value of the Normalized Thickness of the Plasma Layer d = 2

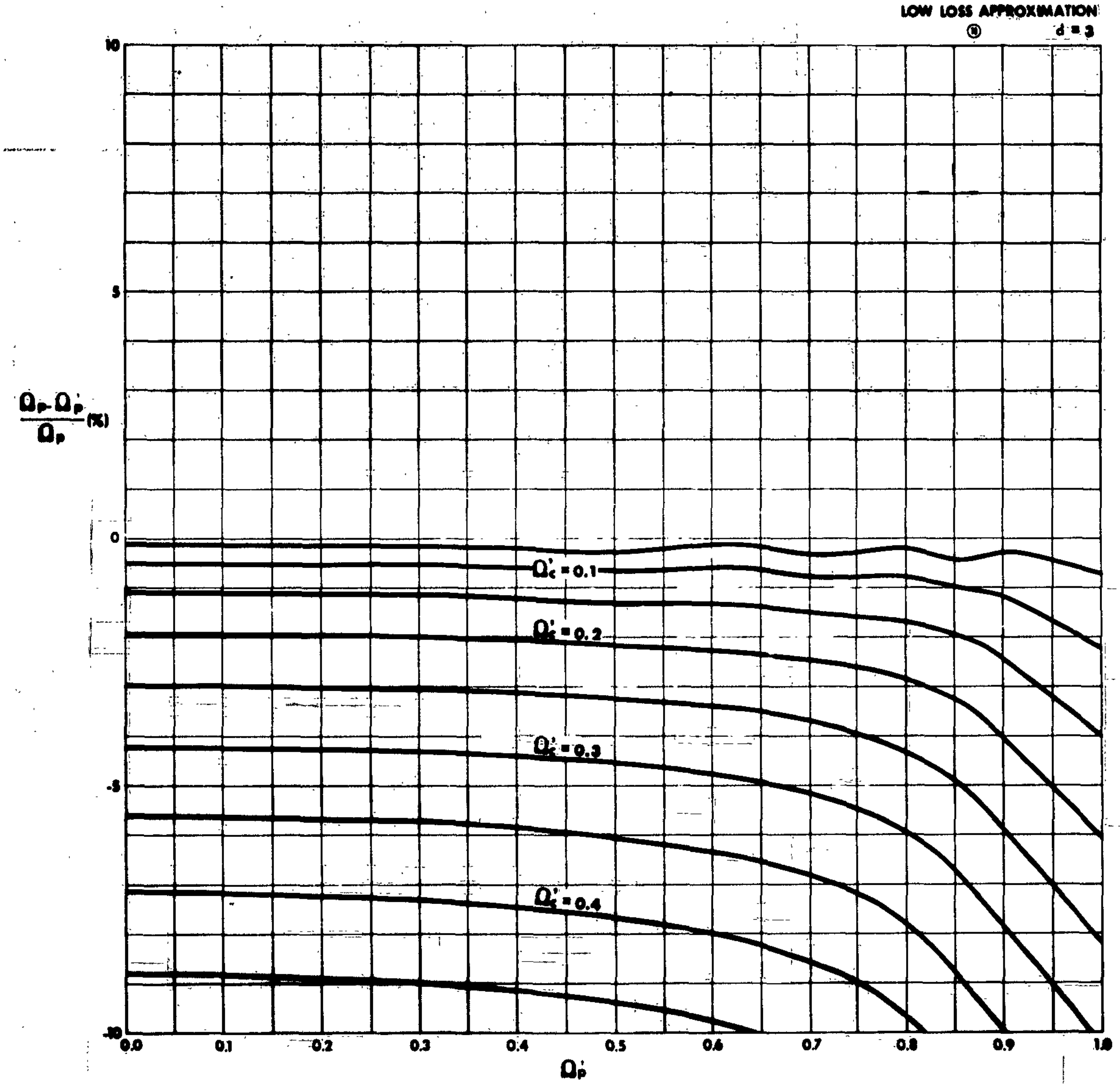

Figure 73 Percentage Error in Normalized Plasma Frequency for the Low-Loss Approximation (LLPA) as a Function of Measured Plasma Frequency for Various Values of Measured Collision Frequency, for a Value of the Normalized Thickness of the Plasma Layer d = 3

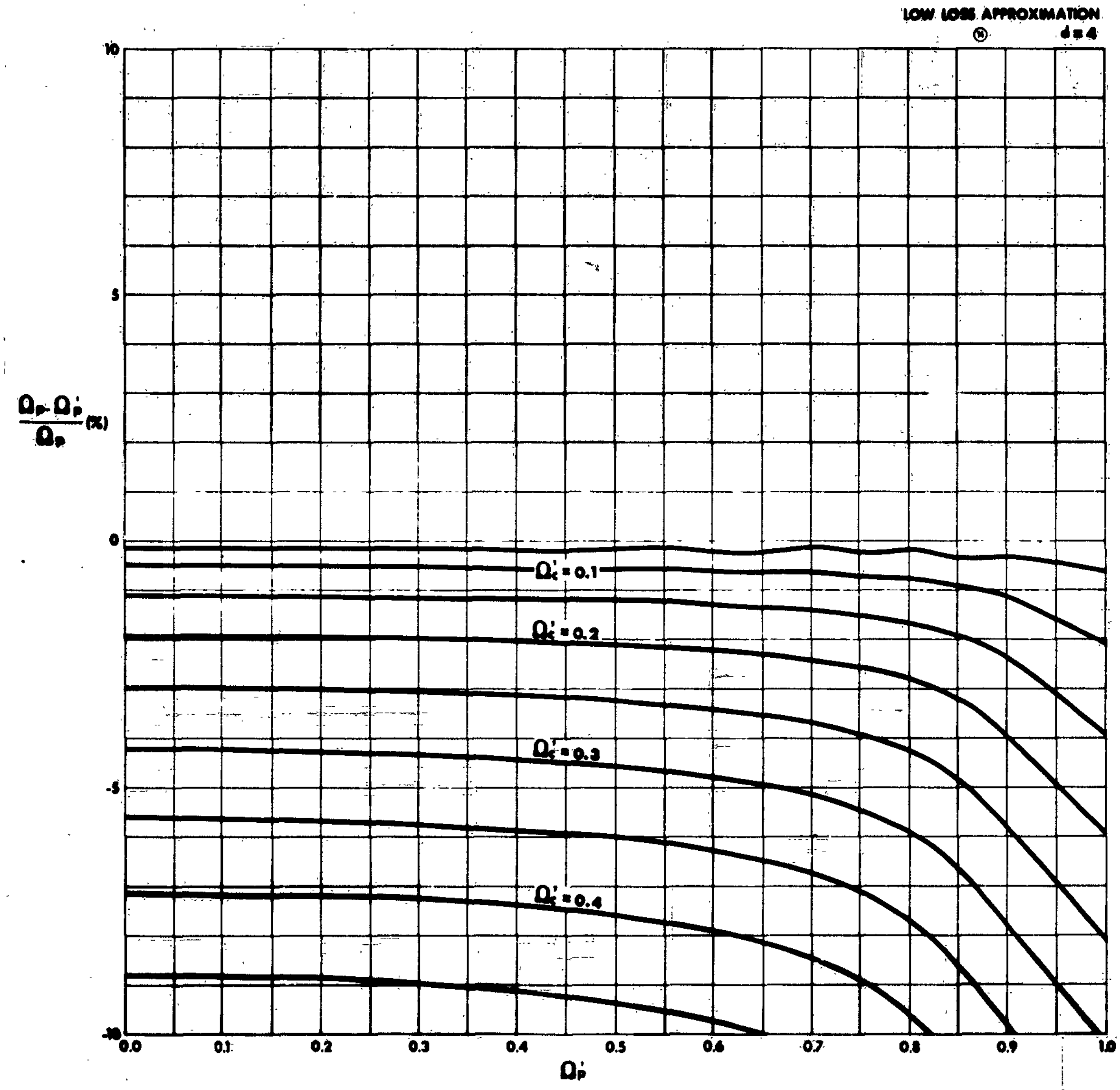

Figure 74 Percentage Error in Normalized Plasma Frequency for the Low-Loss Approximation (LLPA) as a Function of Measured Plasma Frequency for Various Values of Measured Collision Frequency, for a Value of the Normalized Thickness of the Plasma Layer d = 4

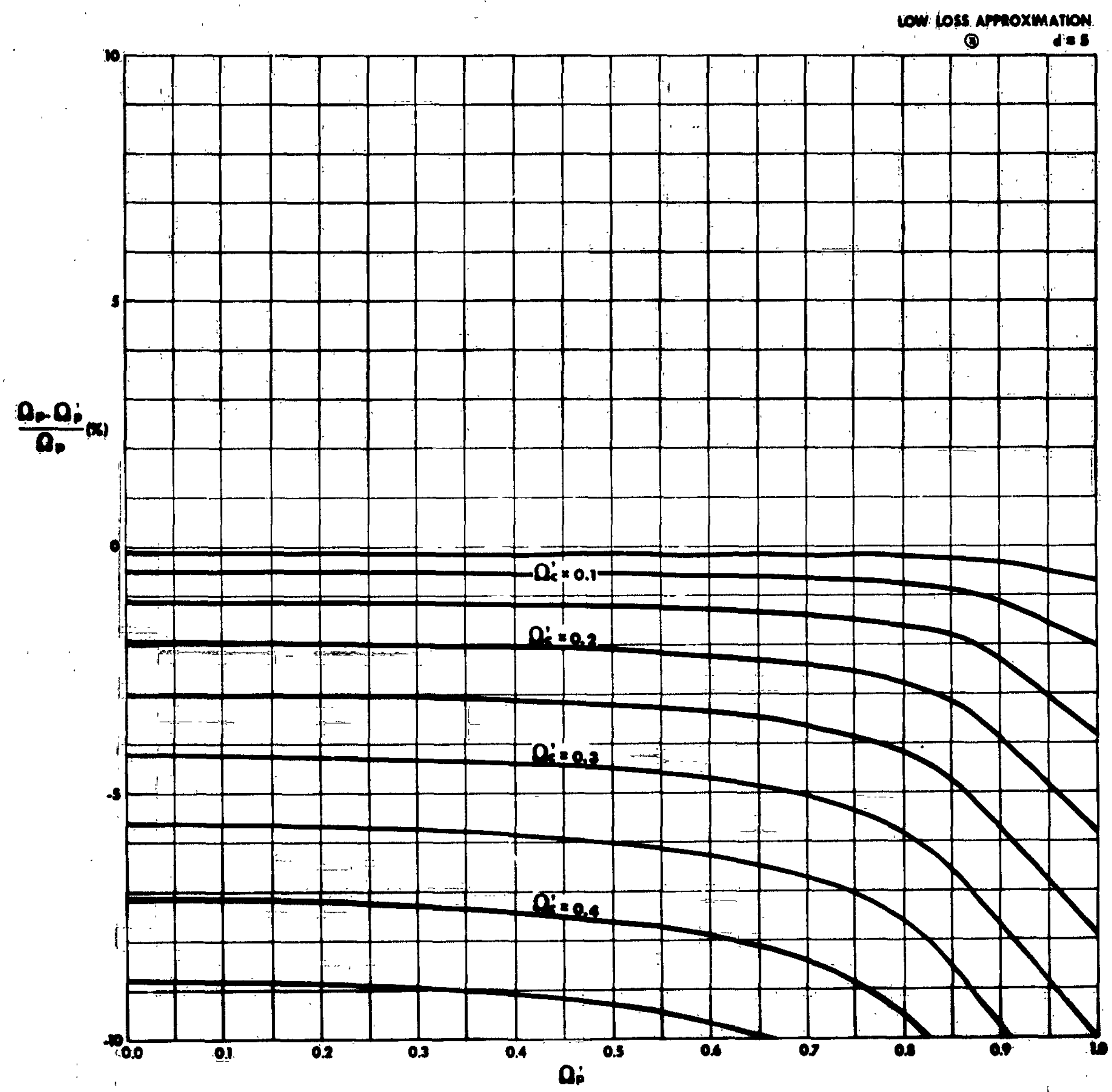

Figure 75 Percentage Error in Normalized Plasma Frequency for the Low-Loss Approximation (LLPA) as a Function of Measured Plasma Frequency for Various Values of Measured Collision Frequency, for a Value of the Normalized Thickness of the Plasma Layer d = 5

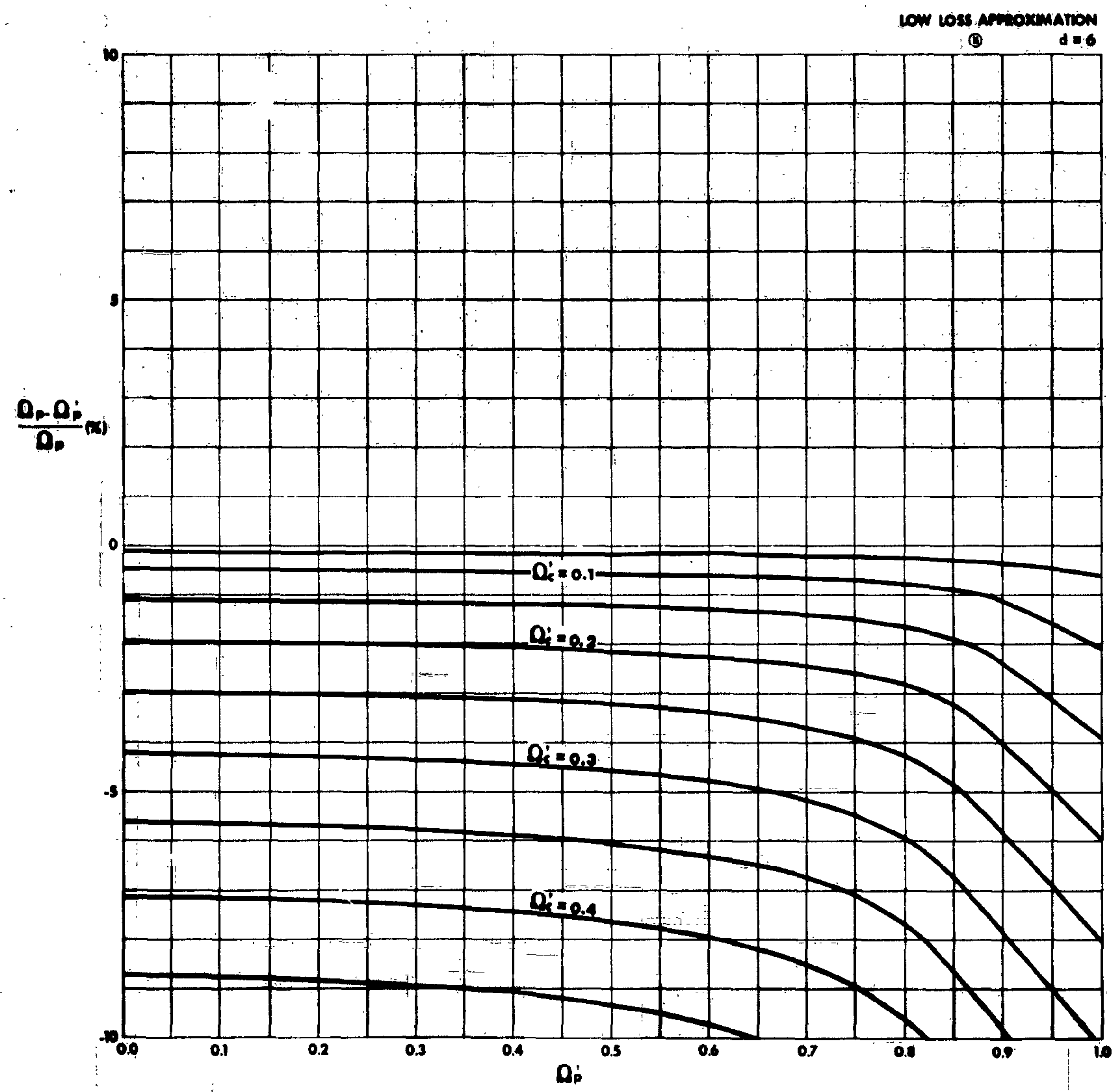

Figure 76 Percentage Error in Normalized Plasma Frequency for the Low-Loss Approximation (LLPA) as a Function of Measured Plasma Frequency for Various Values of Measured Collision Frequency, for a Value of the Normalized Thickness of the Plasma Layer d = 6

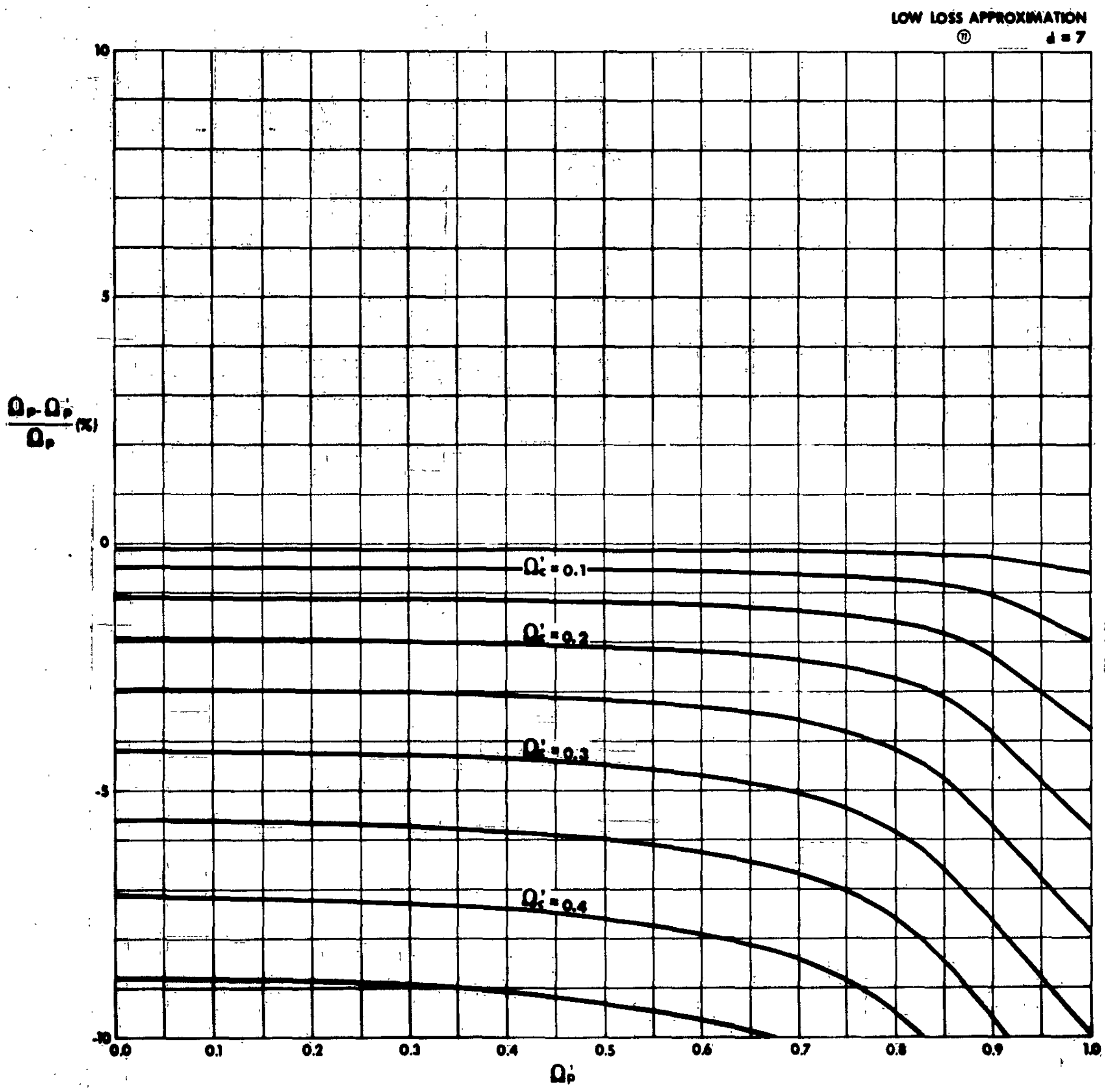

Figure 77 Percentage Error in Normalized Plasma Frequency for the Low-Loss Approximation (LLPA) as a Function of Measured Plasma Frequency for Various Values of Measured Collision Frequency, for a Value of the Normalized Thickness of the Plasma Layer d = 7

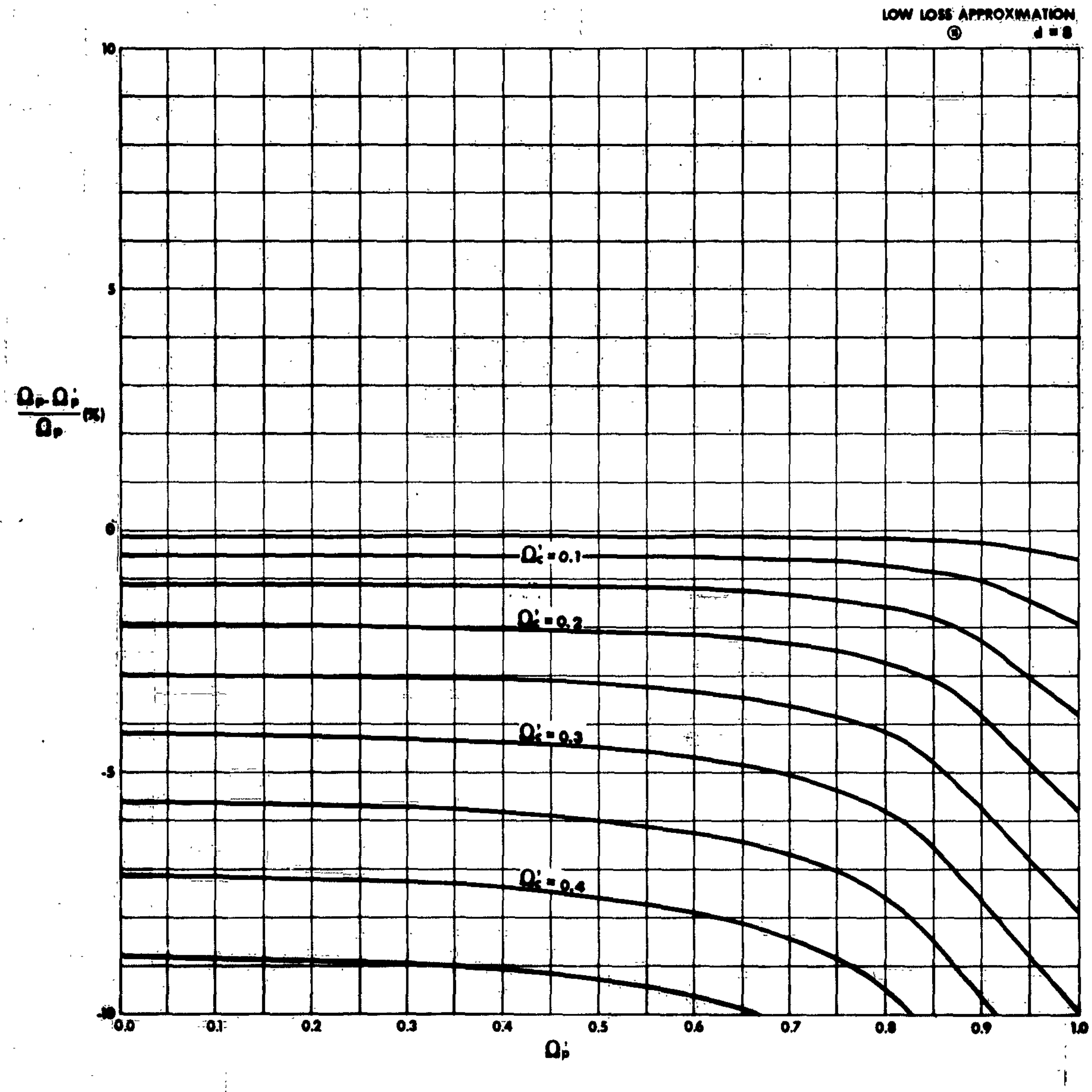

Figure 78 Percentage Error in Normalized Plasma Frequency for the Low-Loss Approximation (LLPA) as a Function of Measured Plasma Frequency for Various Values of Measured Collision Frequency, for a Value of the Normalized Thickness of the Plasma Layer d = 8

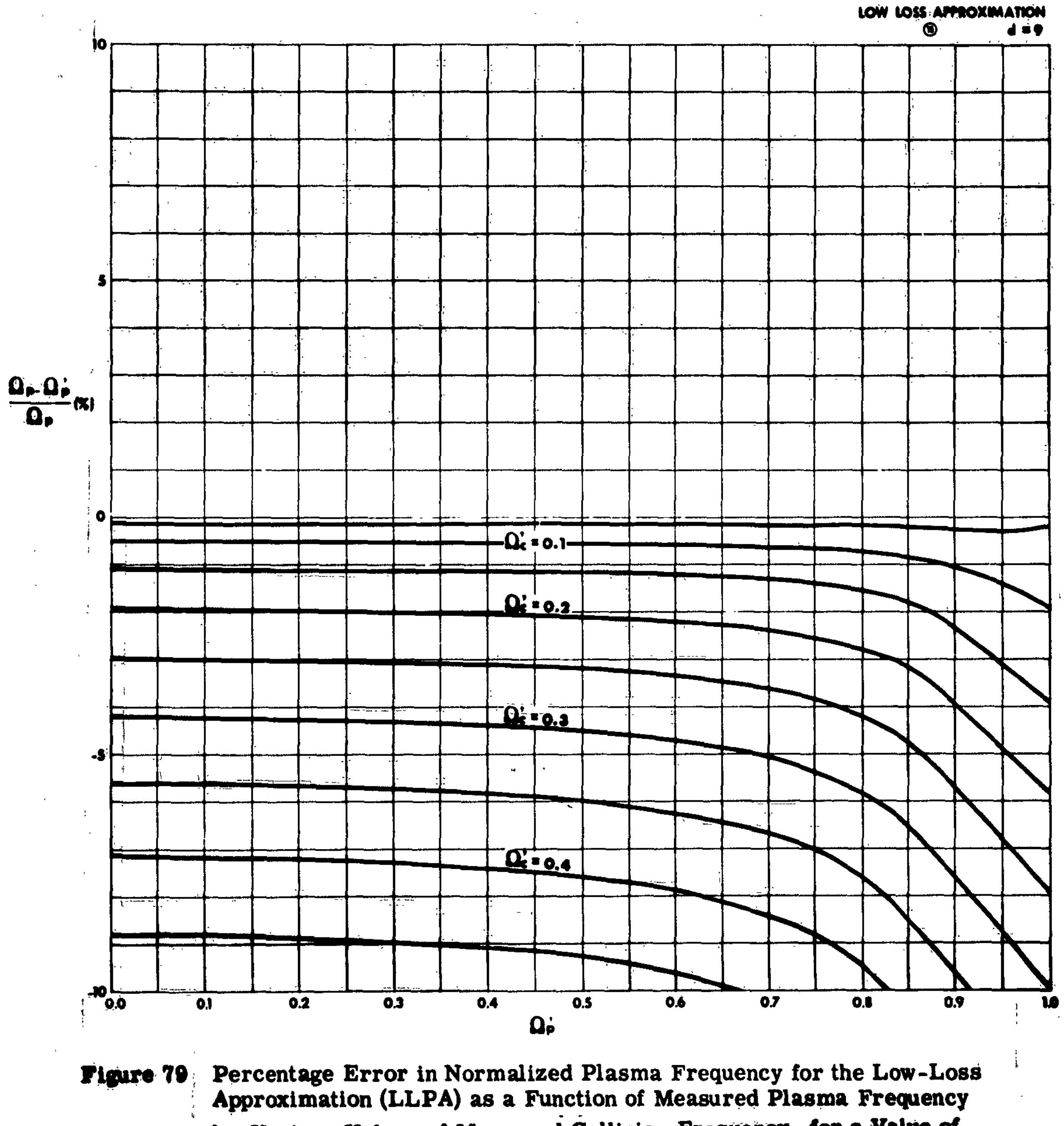

Figure 79 Percentage Error in Normalized Plasma Frequency for the Low-Loss Approximation (LLPA) as a Function of Measured Plasma Frequency for Various Values of Measured Collision Frequency, for a Value of the Normalized Thickness of the Plasma Layer d = 9

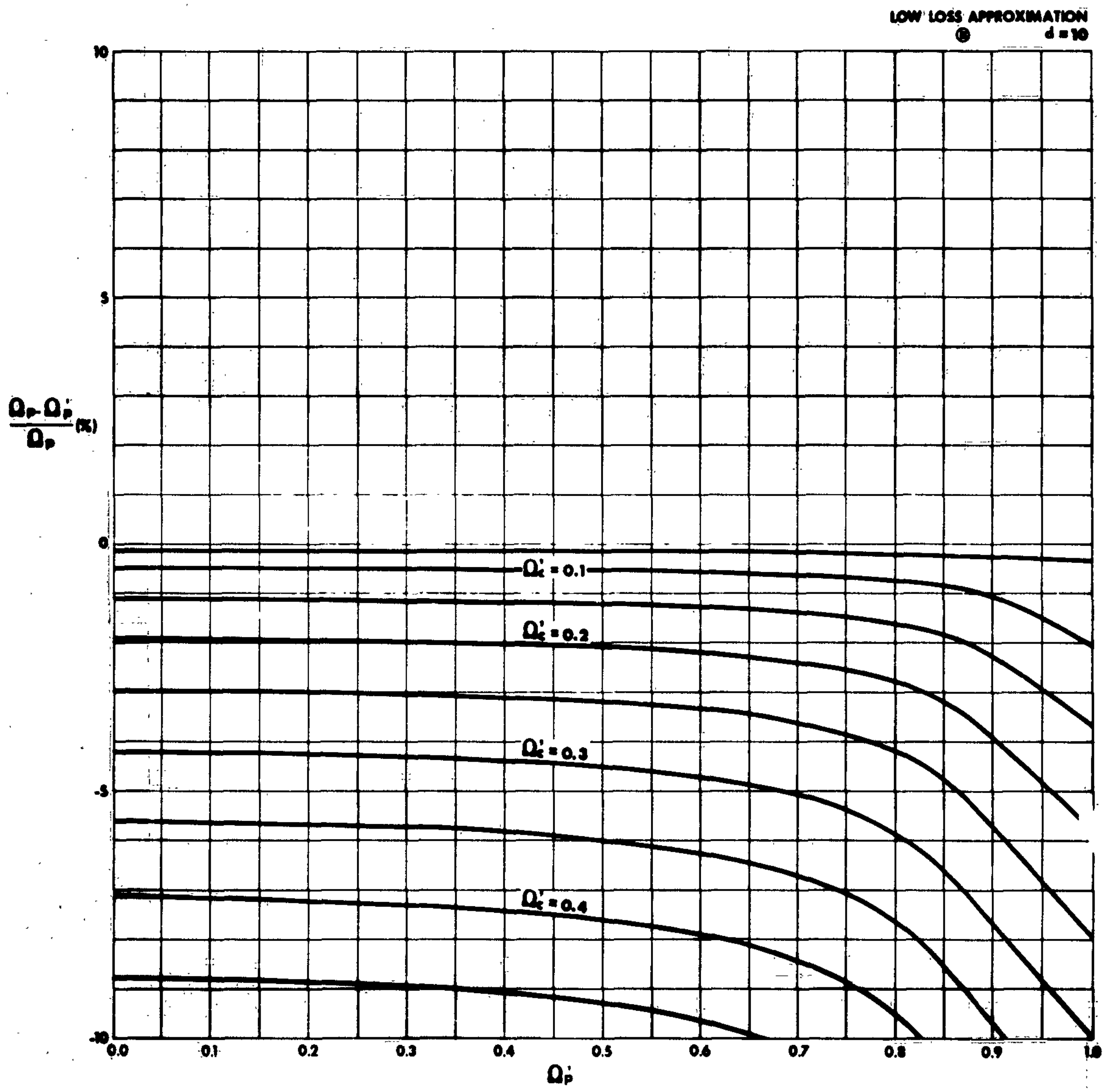

Figure 80 Percentage Error in Normalized Plasma Frequency for the Low-Loss Approximation (LLPA) as a Function of Measured Plasma Frequency for Various Values of Measured Collision Frequency, for a Value of the Normalized Thickness of the Plasma Layer d = 10

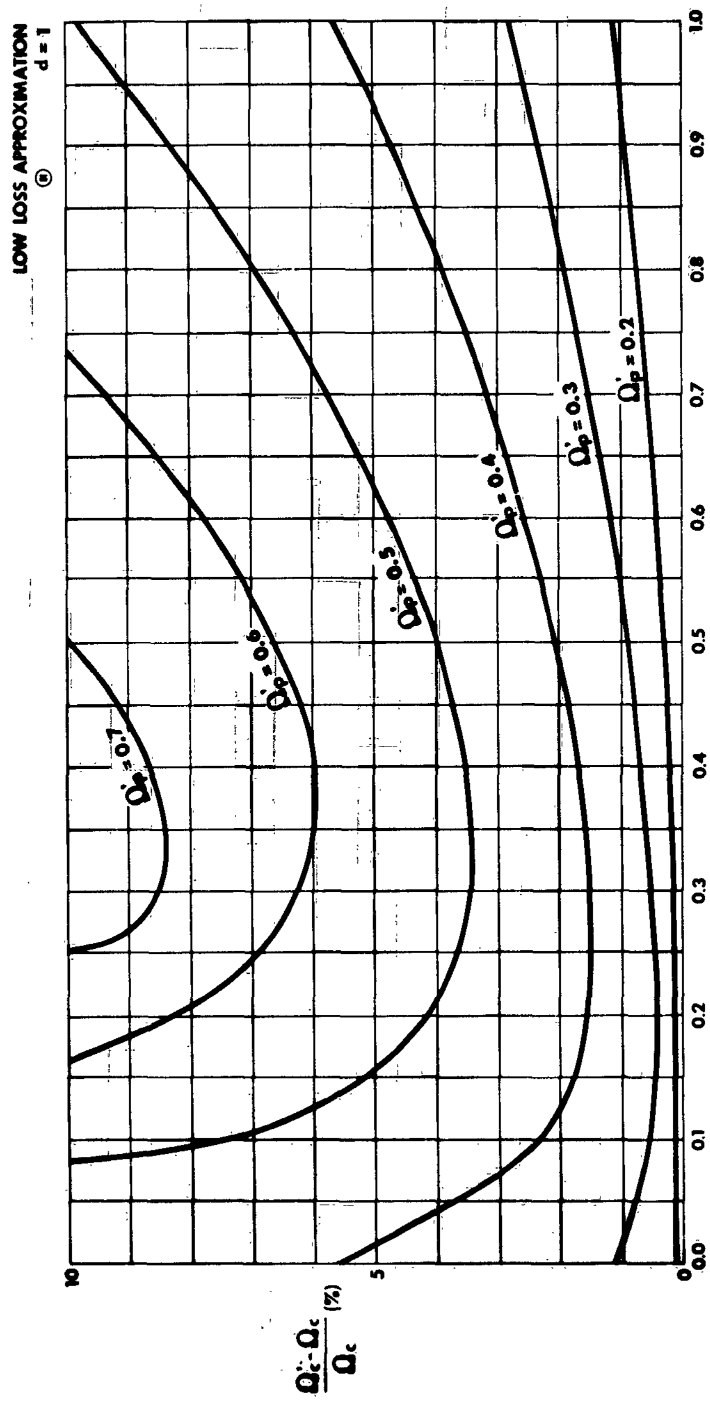

Figure 81 Percentage Error in Normalized Collision Frequency for the Low-Loss Approximation (LLPA) as a Function of the Measured Collision Frequency for Various Values of the Measured Plasma Frequency, for a Value of the Normalized Thickness of the Plasma Layer d = 1

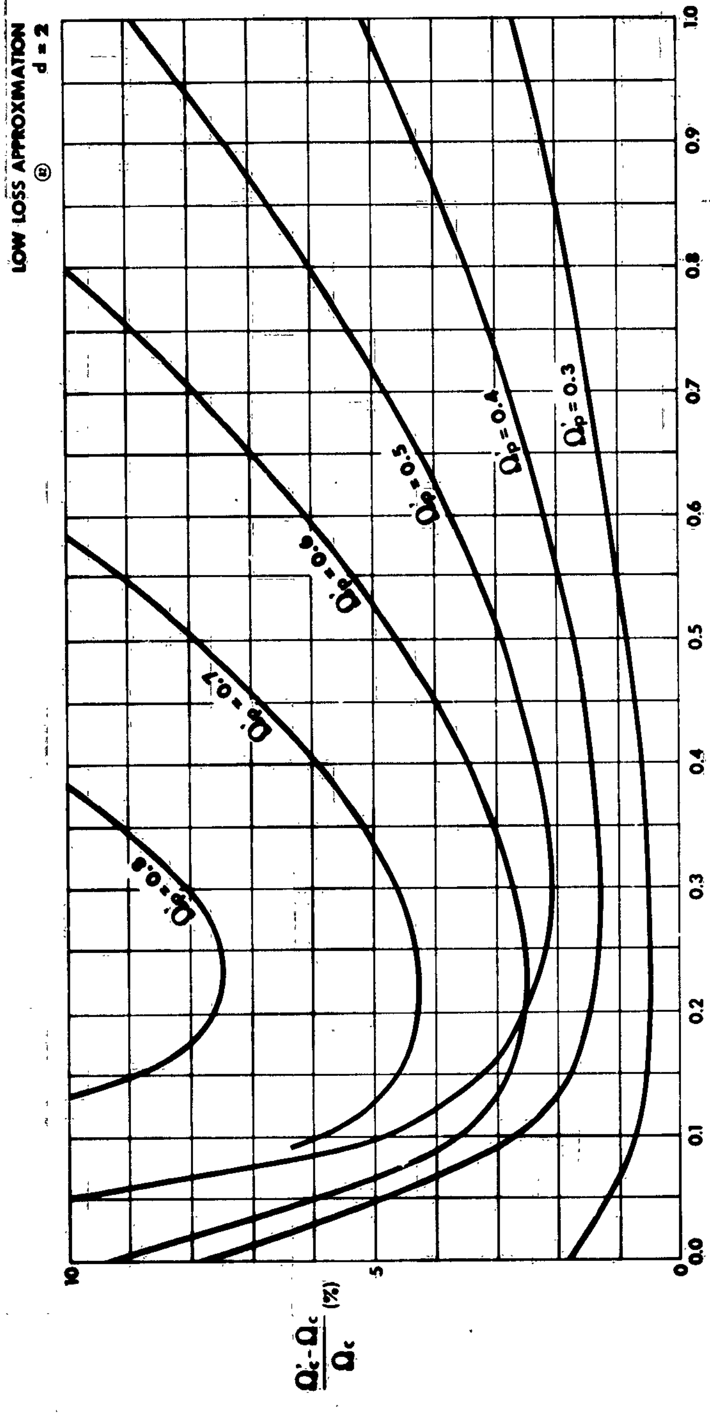

Figure 82 Percentage Error in Normalized Collision Frequency for the Low-Loss Approximation (LLPA) as a Function of the Measured Collision Frequency for Various Values of the Measured Plasma Frequency, for a Value of the Normalized Thickness of the Plasma Layer d = 2

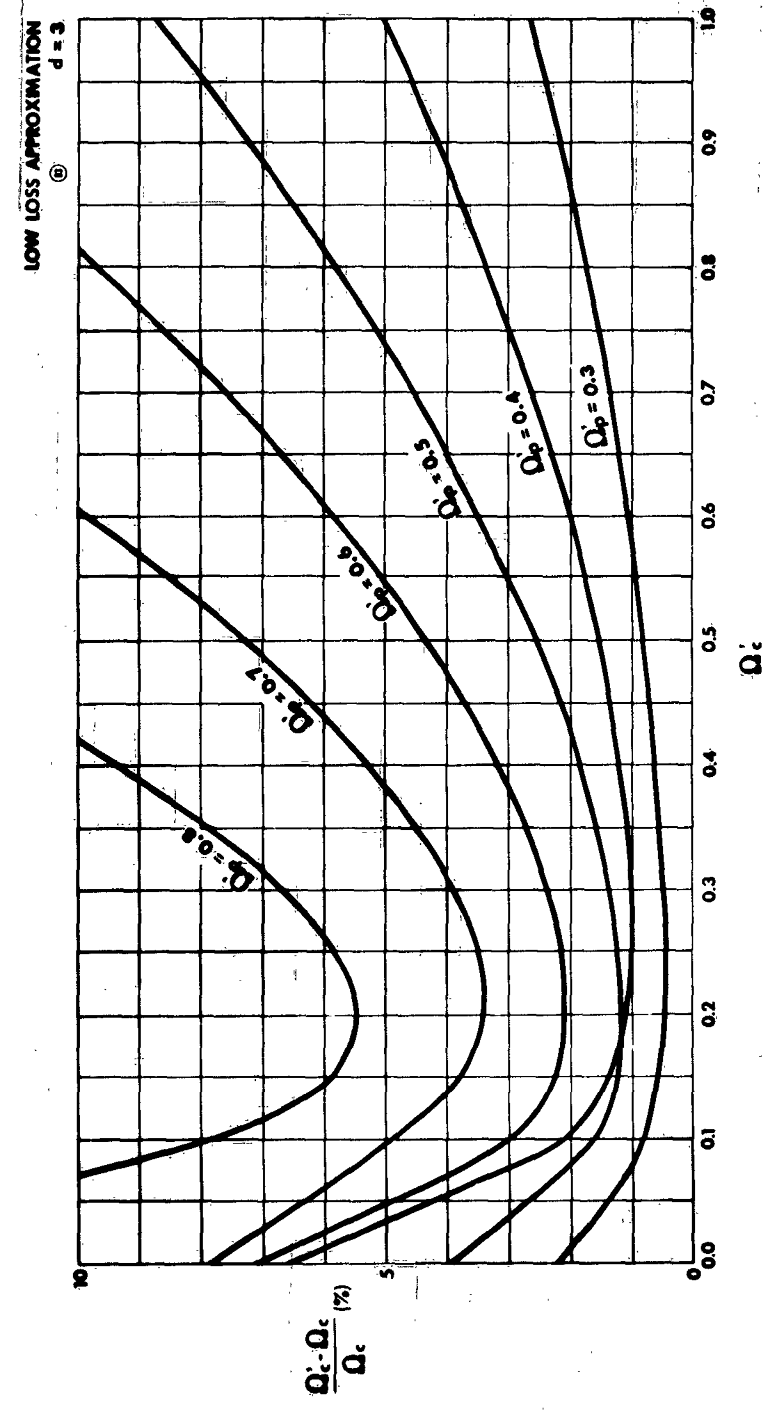

Figure 83 Percentage Error in Normalized Collision Frequency for the Low-Loss Approximation (LLPA) as a Function of the Measured Collision Frequency for Various Values of the Measured Plasma Frequency, for a Value of the Normalized Thickness of the Plasma Layer d = 3

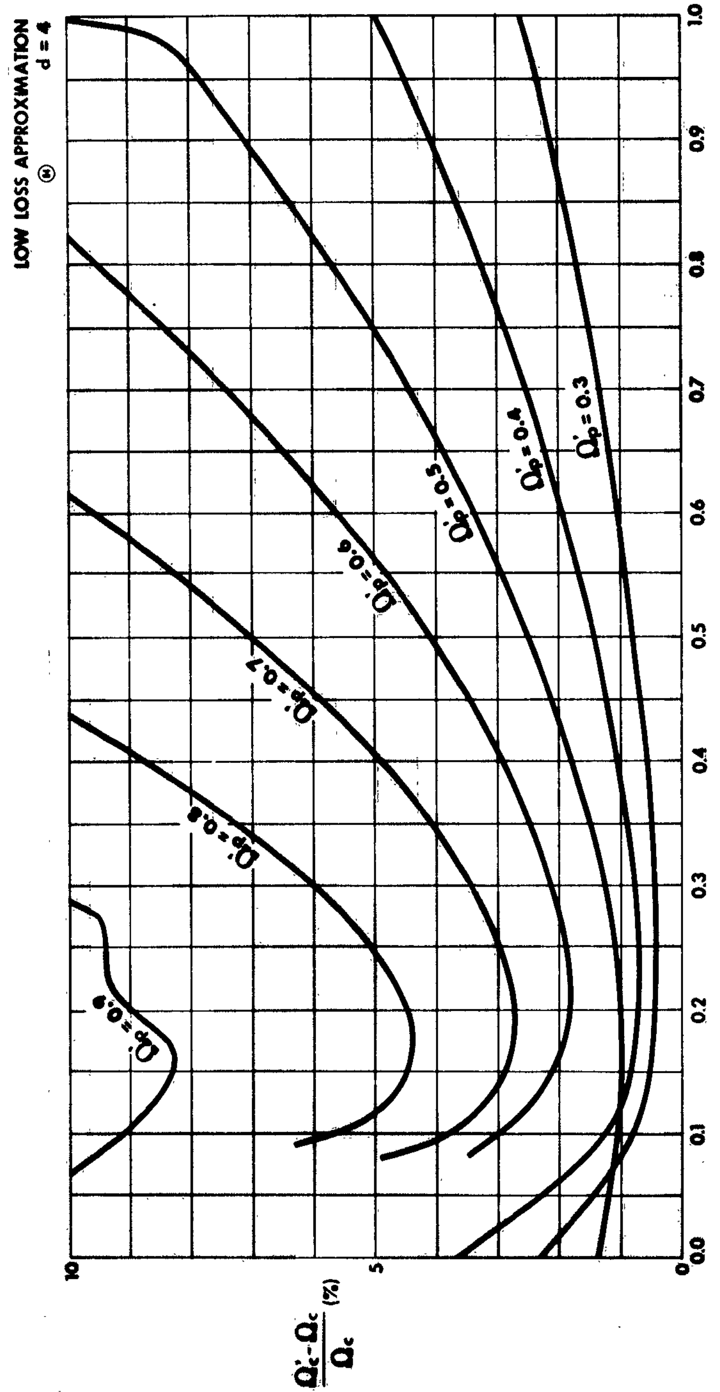

Figure 84 Percentage Error in Normalized Collision Frequency for the Low-Loss Approximation (LLPA) as a Function of the Measured Collision Frequency for Various Values of the Measured Plasma Frequency, for a Value of the Normalized Thickness of the Plasma Layer d = 4

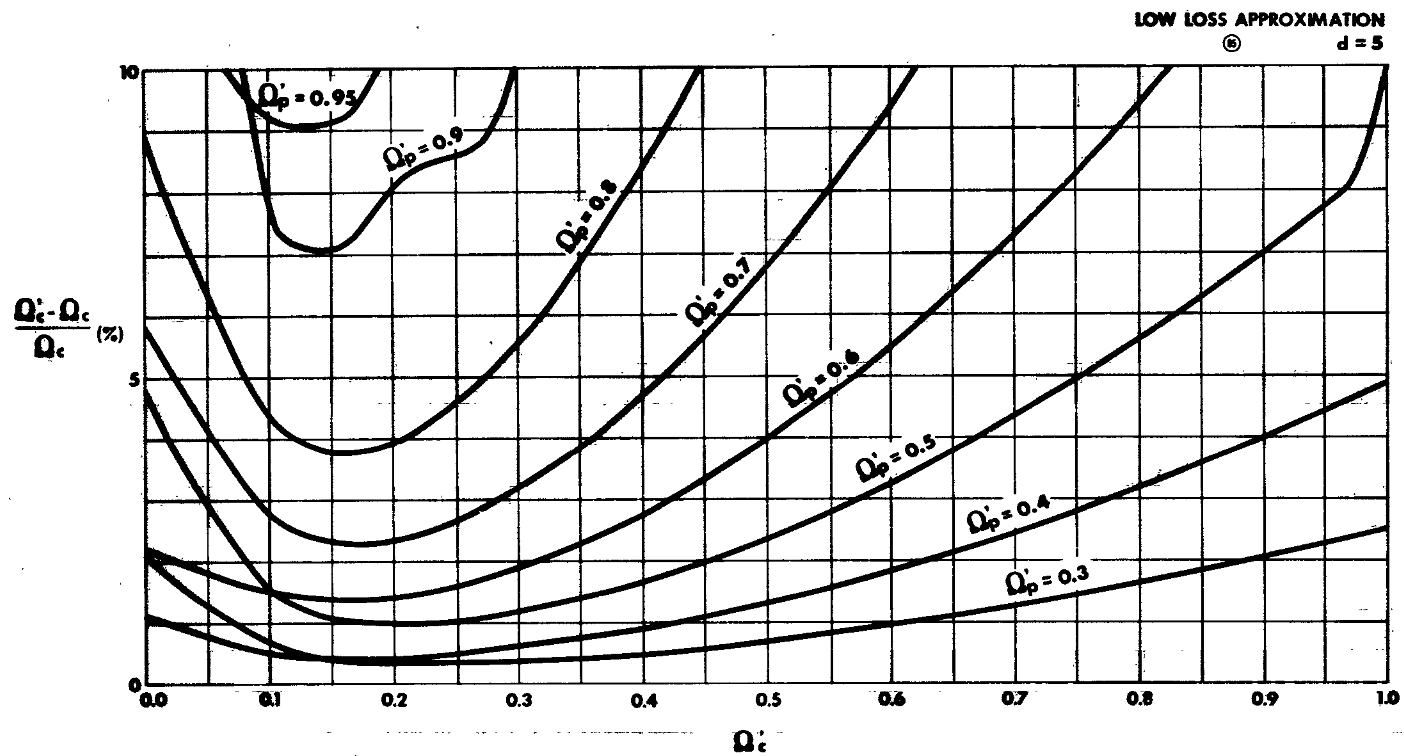

Figure 85 **Percentage Error in Normalized Collision Frequency for the Low-Loss Approximation (LLPA) as a Function of the Measured Collision Frequency for Various Values of the Measured Plasma Frequency, for a Value of the Normalized Thickness of the Plasma Layer d = 5**

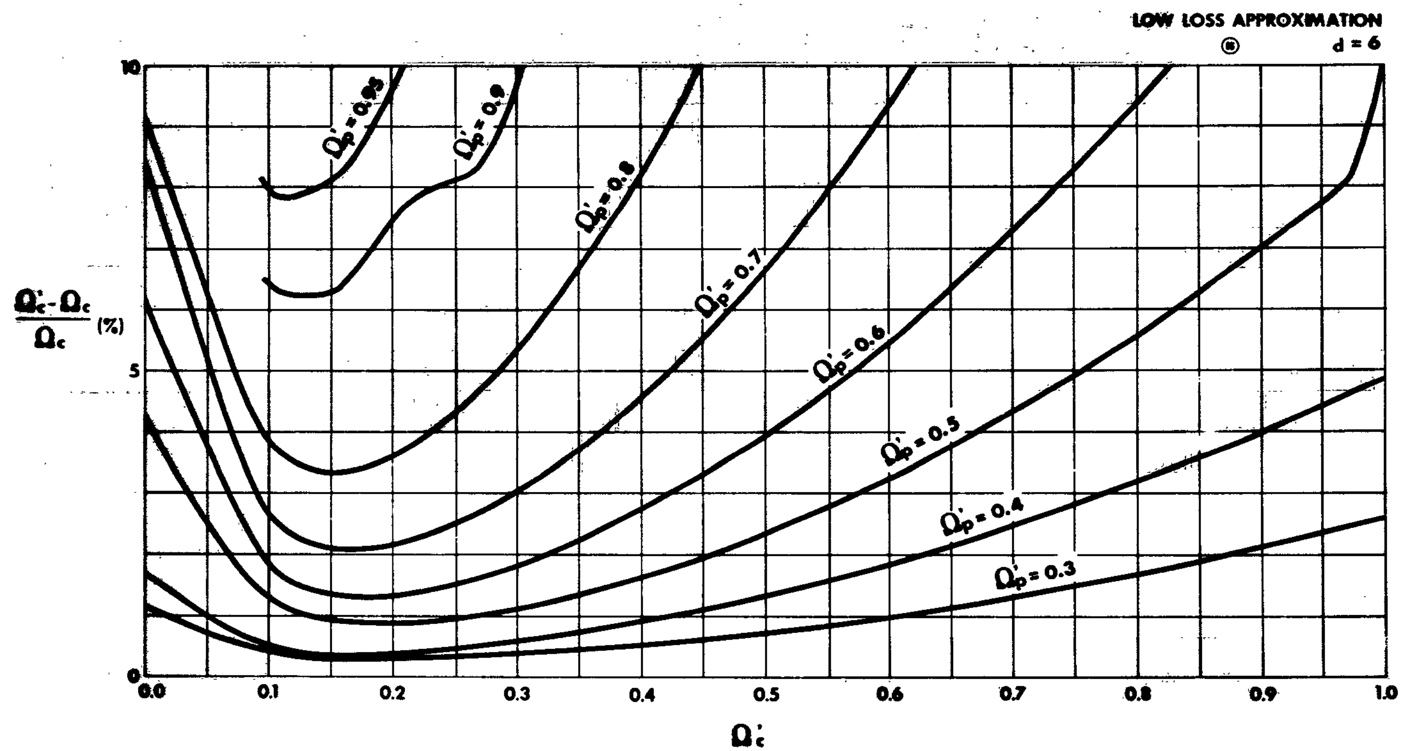

Figure 86 Percentage Error in Normalized Collision Frequency for the Low-Loss Approximation (LLPA) as a Function of the Measured Collision Frequency for Various Values of the Measured Plasma Frequency, for a Value of the Normalized Thickness of the Plasma Layer d = 6

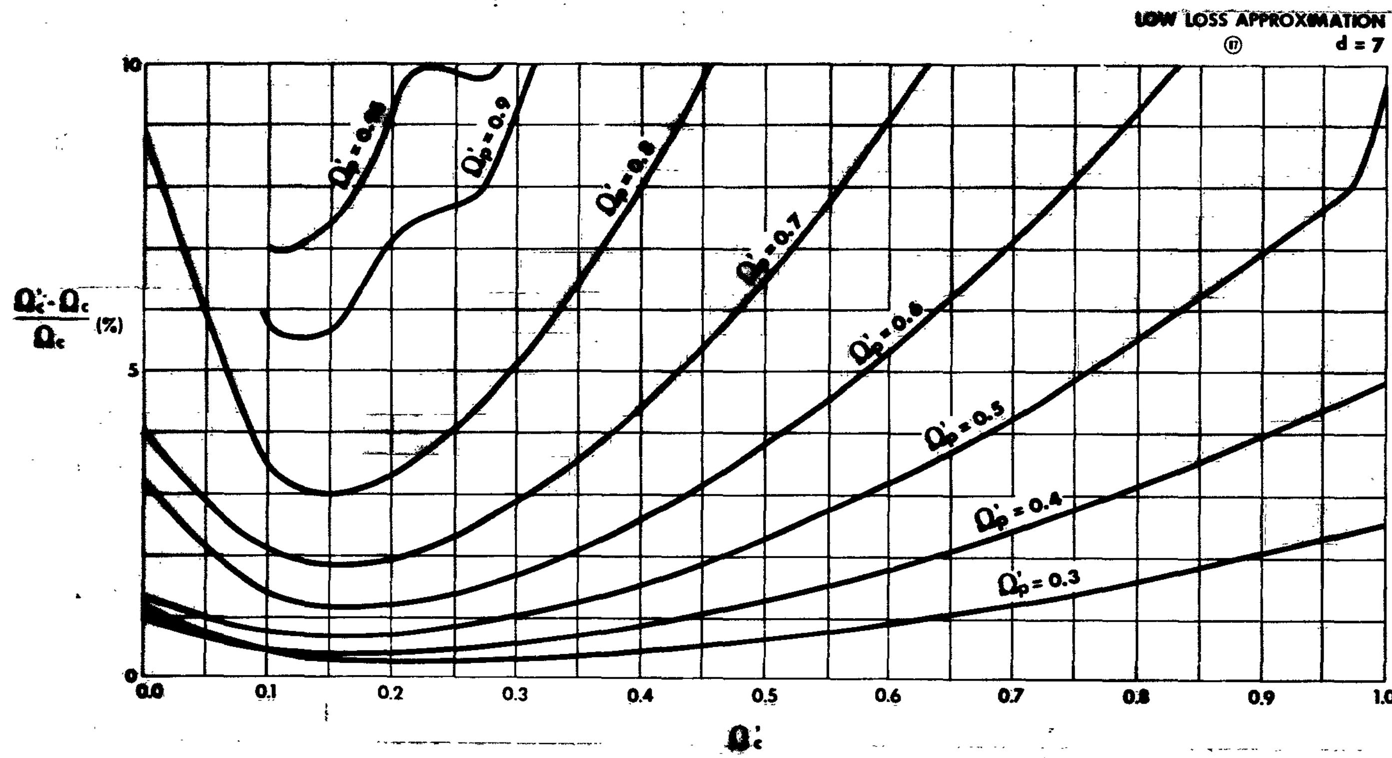

Figure 87 Percentage Error in Normalized Collision Frequency for the Low-Loss Approximation (LLPA) as a Function of the Measured Collision Frequency for Various Values of the Measured Plasma Frequency, for a Value of the Normalized Thickness of the Plasma Layer d = 7

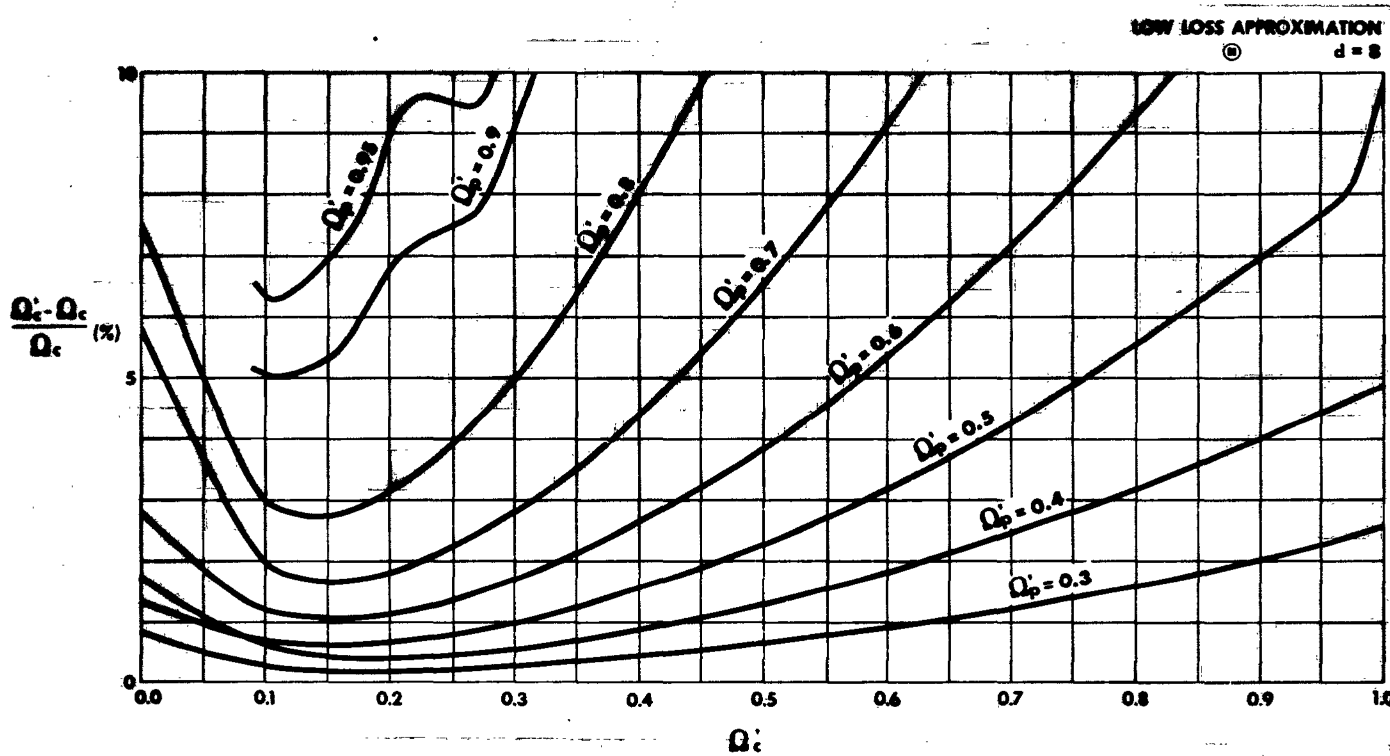

Figure 88 Percentage Error in Normalized Collision Frequency for the Low-Loss Approximation (LLPA) as a Function of the Measured Collision Frequency for Various Values of the Measured Plasma Frequency, for a Value of the Normalized Thickness of the Plasma Layer d = 8

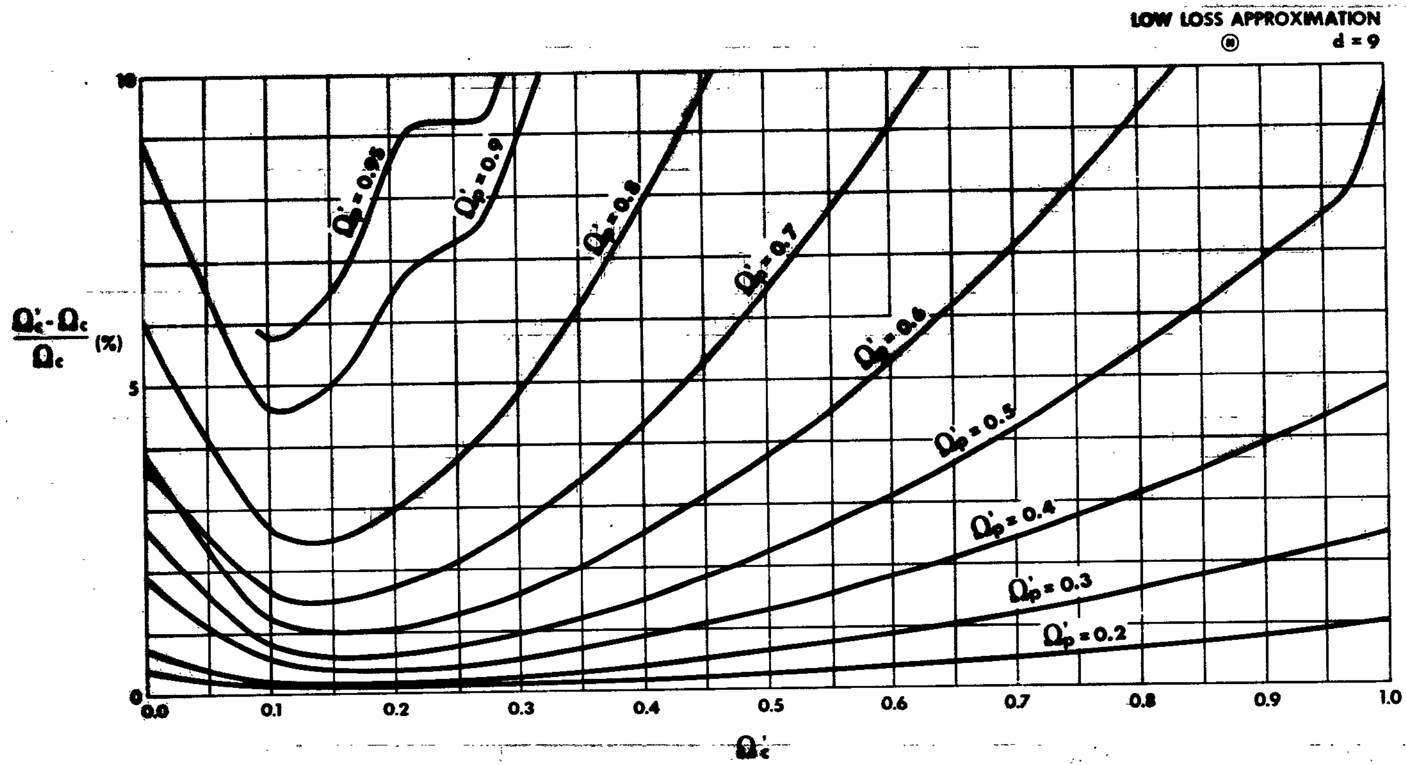

Figure 89 **Percentage Error in Normalized Collision Frequency for the Low-Loss Approximation (LLPA) as a Function of the Measured Collision Frequency for Various Values of the Measured Plasma Frequency, for a Value of the Normalized Thickness of the Plasma Layer d = 9**

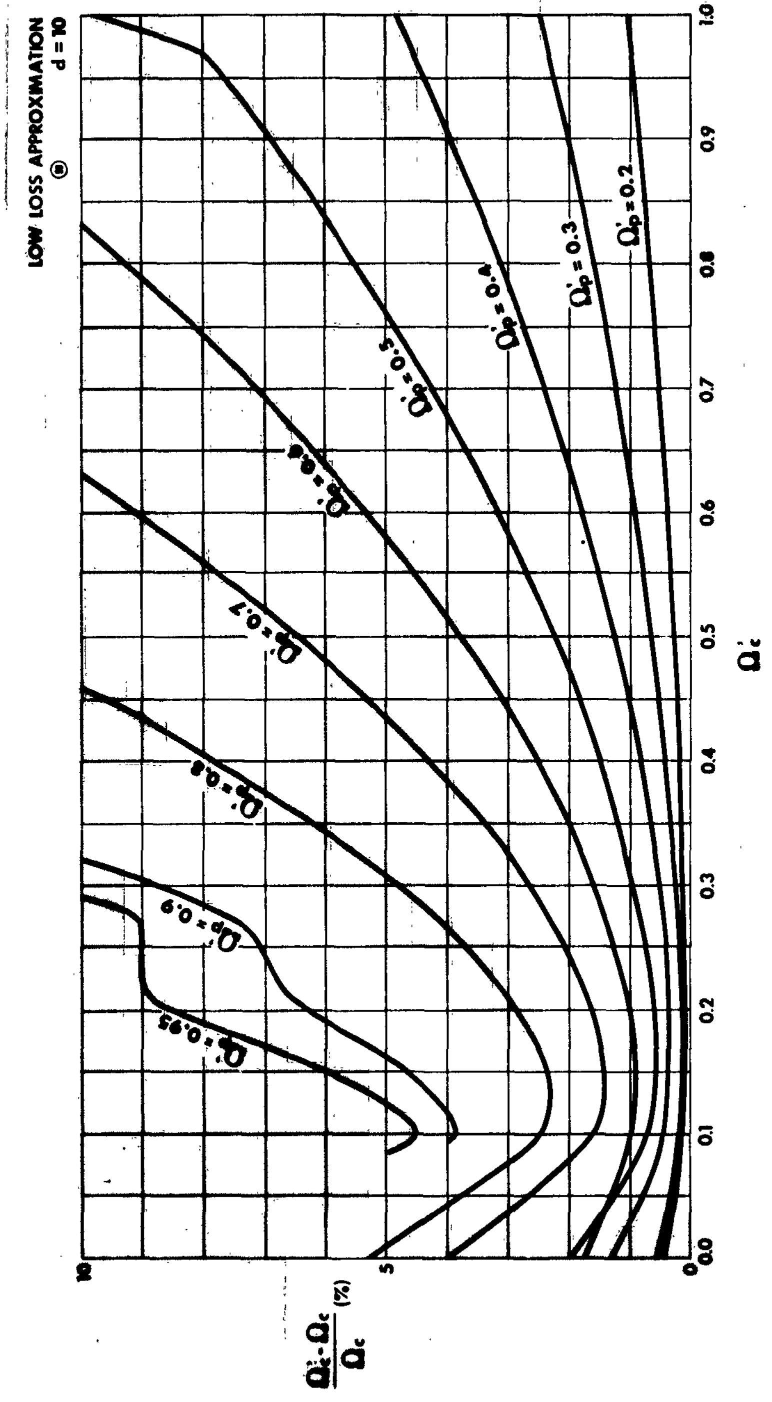

Figure 90 Percentage Error in Normalized Collision Frequency for the Low-Loss Approximation (LLPA) as a Function of the Measured Collision Frequency for Various Values of the Measured Plasma Frequency, for a Value of the Normalized Thickness of the Plasma Layer d = 10

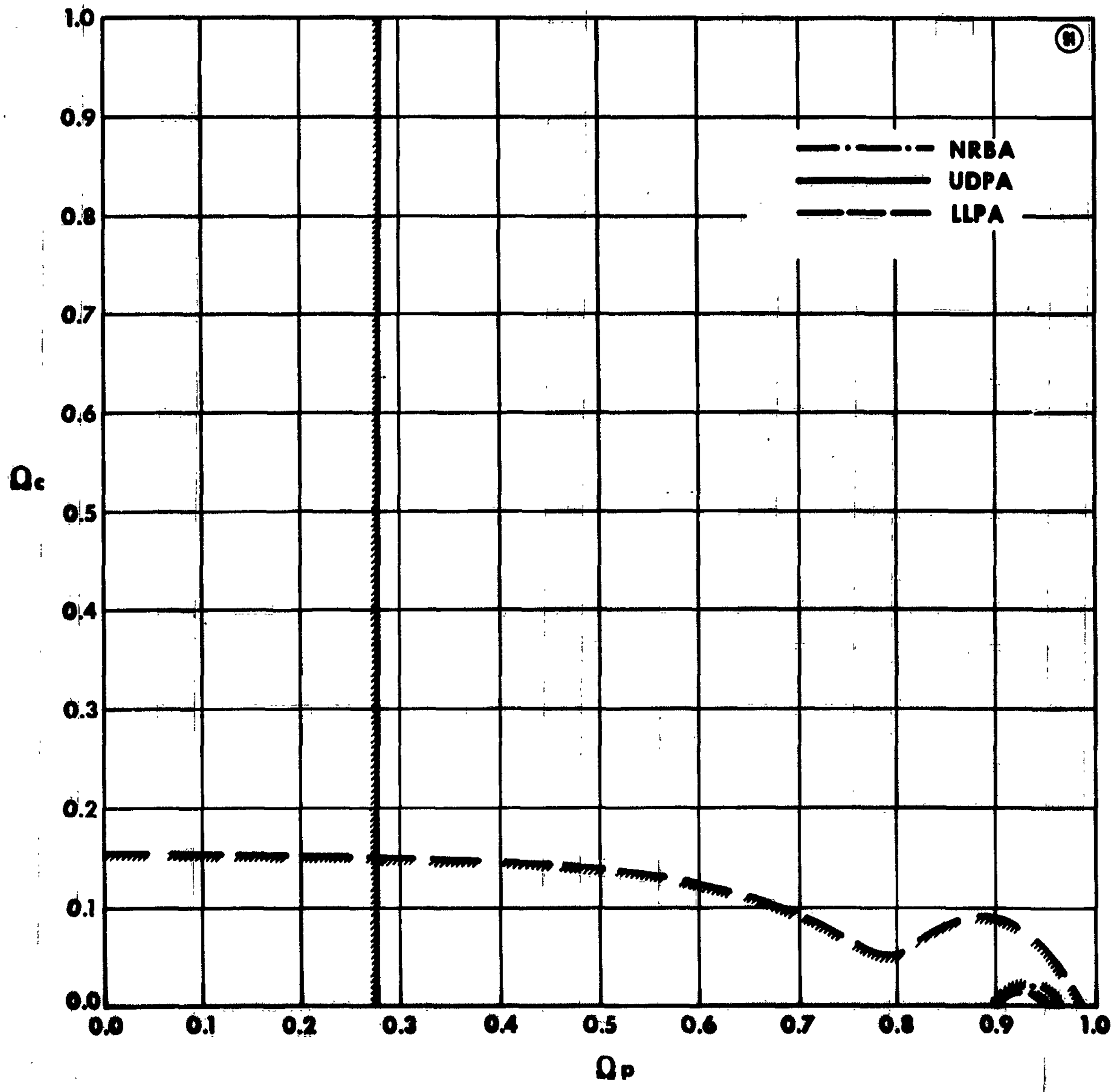

Figure 91 Comparison between Nonreflective Boundary Approximation (NRBA), Underdense Plasma Approximation (UDPA) and Low-Loss Plasma Approximation, for a Value of the Normalized Thickness of the Plasma Layer d = 1, Showing Regions where the Error in Plasma Frequency is less than 1%

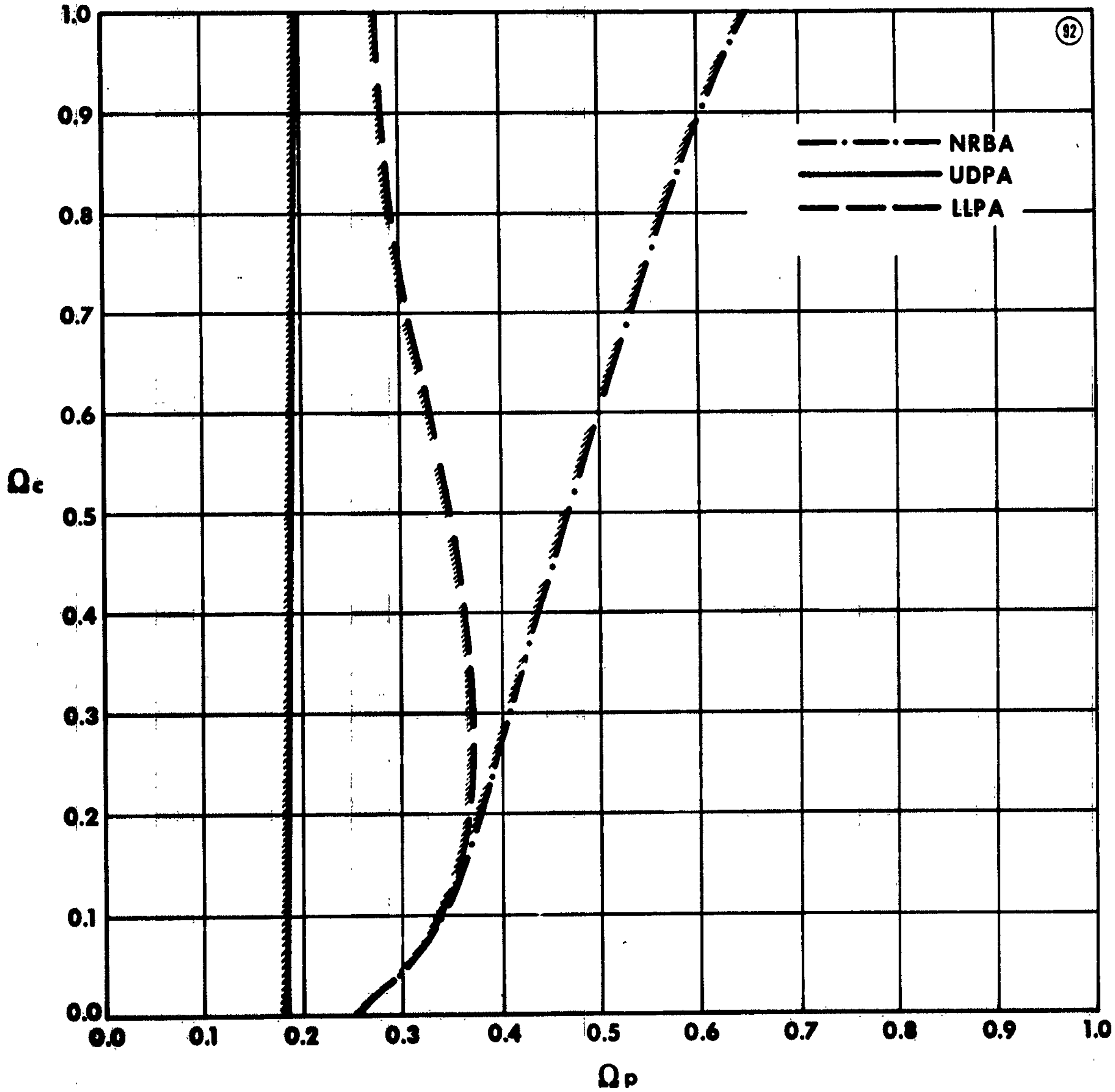

Figure 92 Comparison between Nonreflective Boundary Approximation (NRBA), Underdense Plasma Approximation (UDPA) and Low-Loss Plasma Approximation, for a value of the Normalized Thickness of the Plasma Layer d = 1, Showing Regions where the Error in Collision Frequency is less than 1%

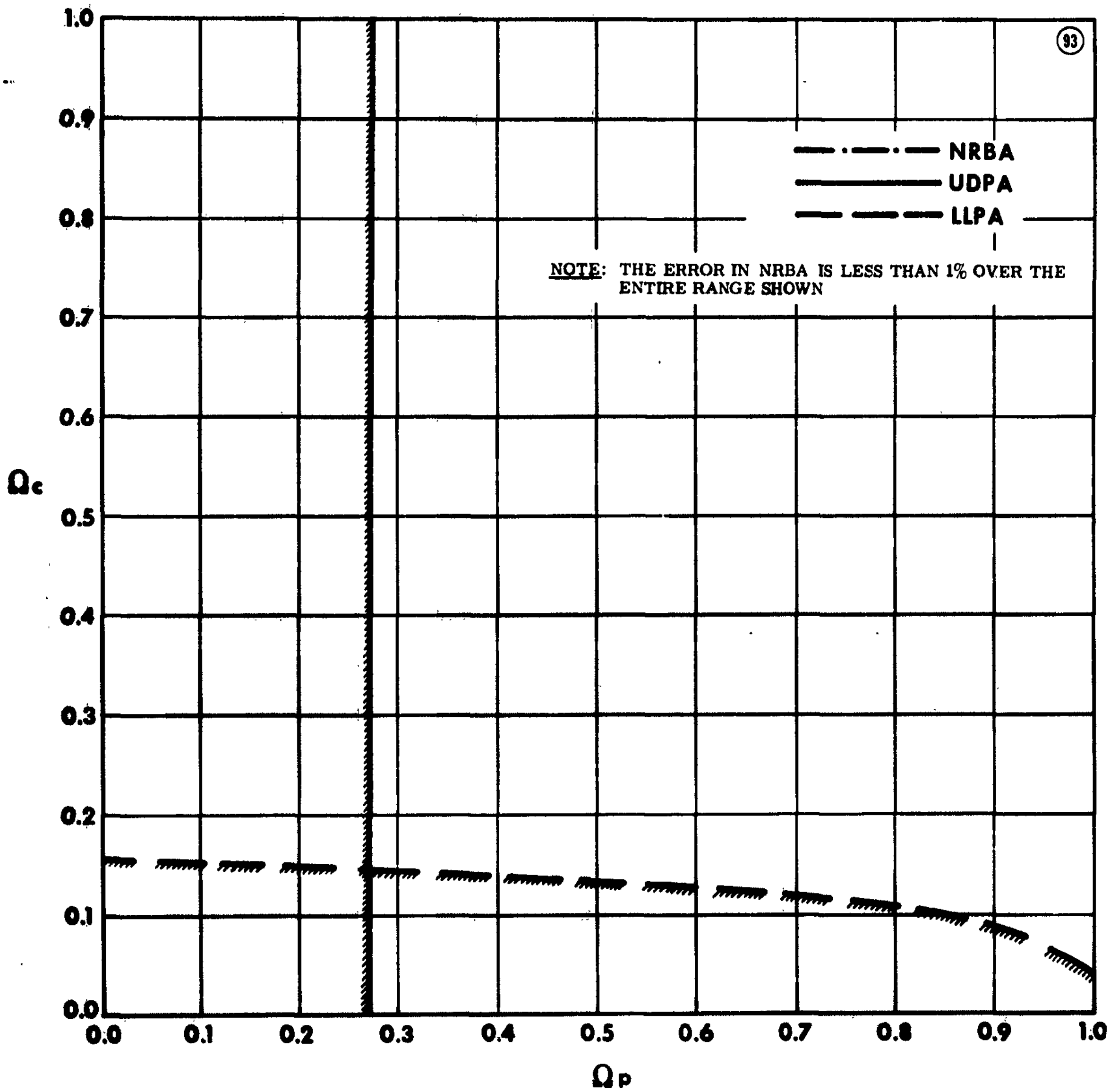

Figure 93 Comparison between Nonreflective Boundary Approximation (NRBA), Underdense Plasma Approximation (UDPA) and Low-Loss Plasma Approximation, for a value of the Normalized Thickness of the Plasma Layer d = 3, Showing Regions where the Error in Plasma Frequency is less than 1%

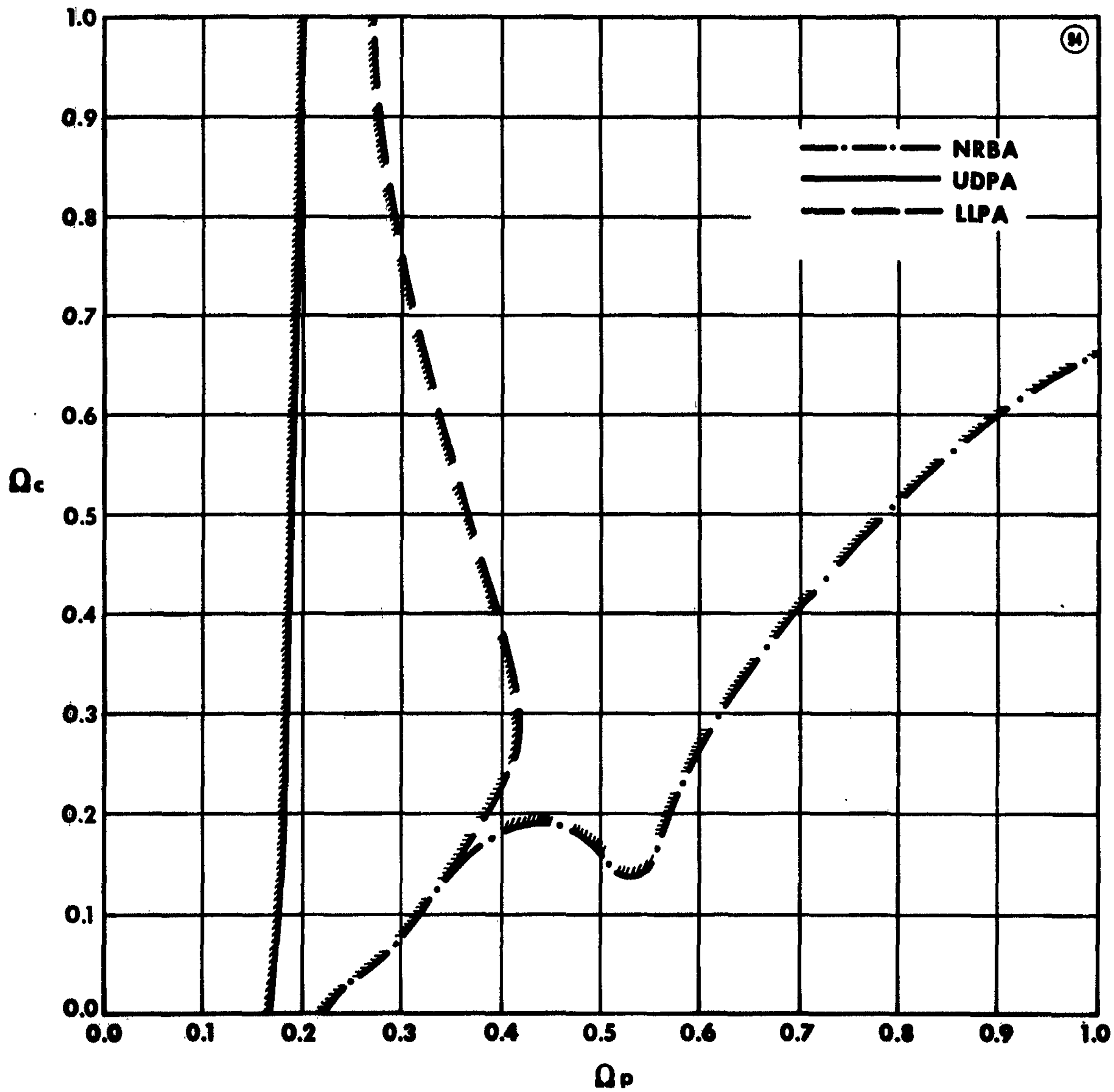

Figure 94 Comparison between Nonreflective Boundary Approximation (NRBA), Underdense Plasma Approximation (UDPA) and Low-Loss Plasma Approximation, for a Value of the Normalized Thickness of the Plasma Layer d = 3, Showing Regions where the Error in Collision Frequency is less than 1%

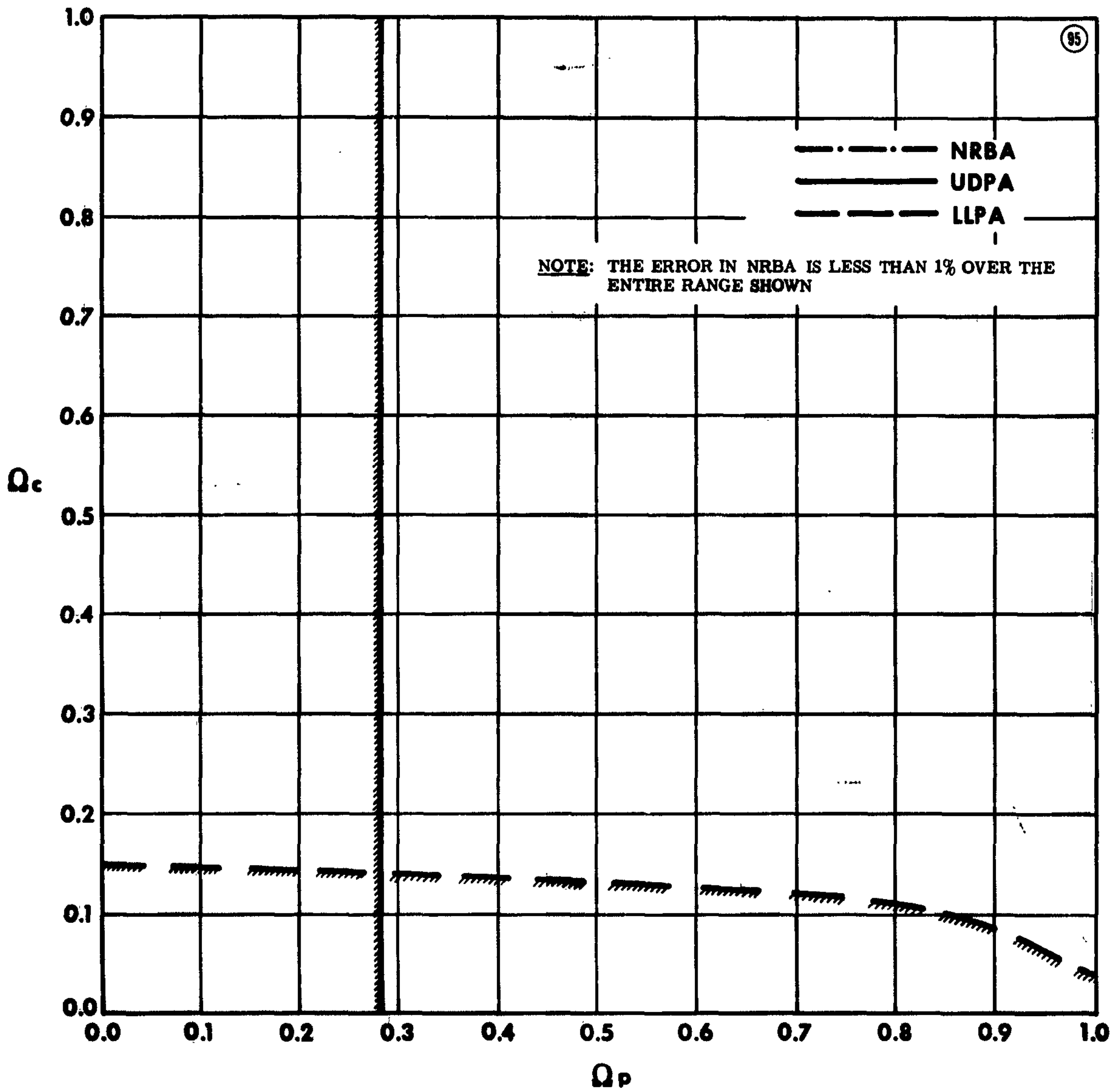

Figure 95 Comparison between Nonreflective Boundary Approximation (NRBA), Underdense Plasma Approximation (UDPA) and Low-Loss Plasma Approximation, for a Value of the Normalized Thickness of the Plasma Layer d = 5, Showing Regions Where the Error in Plasma Frequency is less than 1%

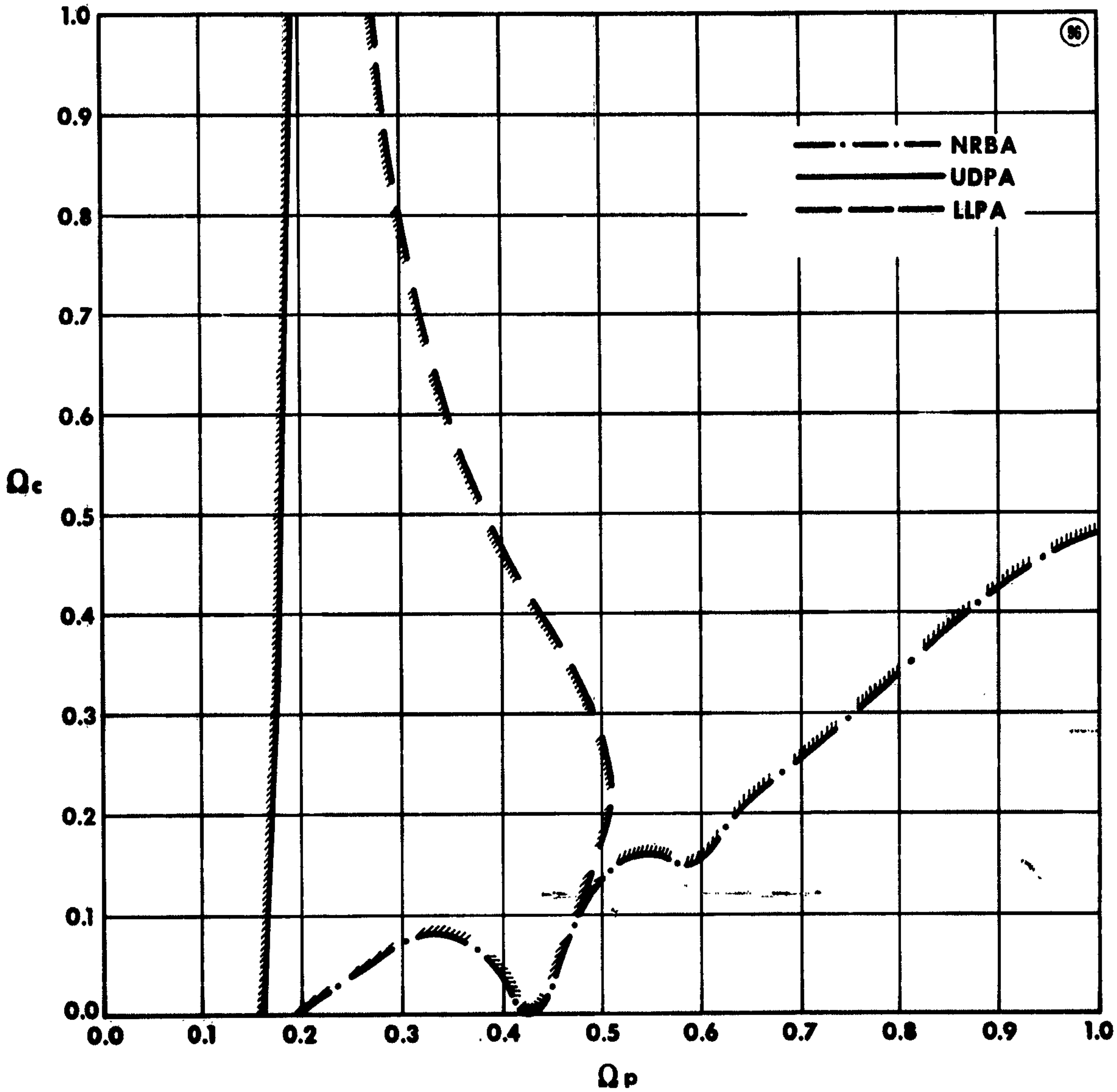

Figure 96 Comparison between Nonreflective Boundary Approximation (NRBA), Underdense Plasma Approximation (UDPA) and Low-Loss Plasma Approximation, for a Value of the Normalized Thickness of the Plasma Layer d = 5, Showing Regions where the Error in Collision Frequency is less than 1%

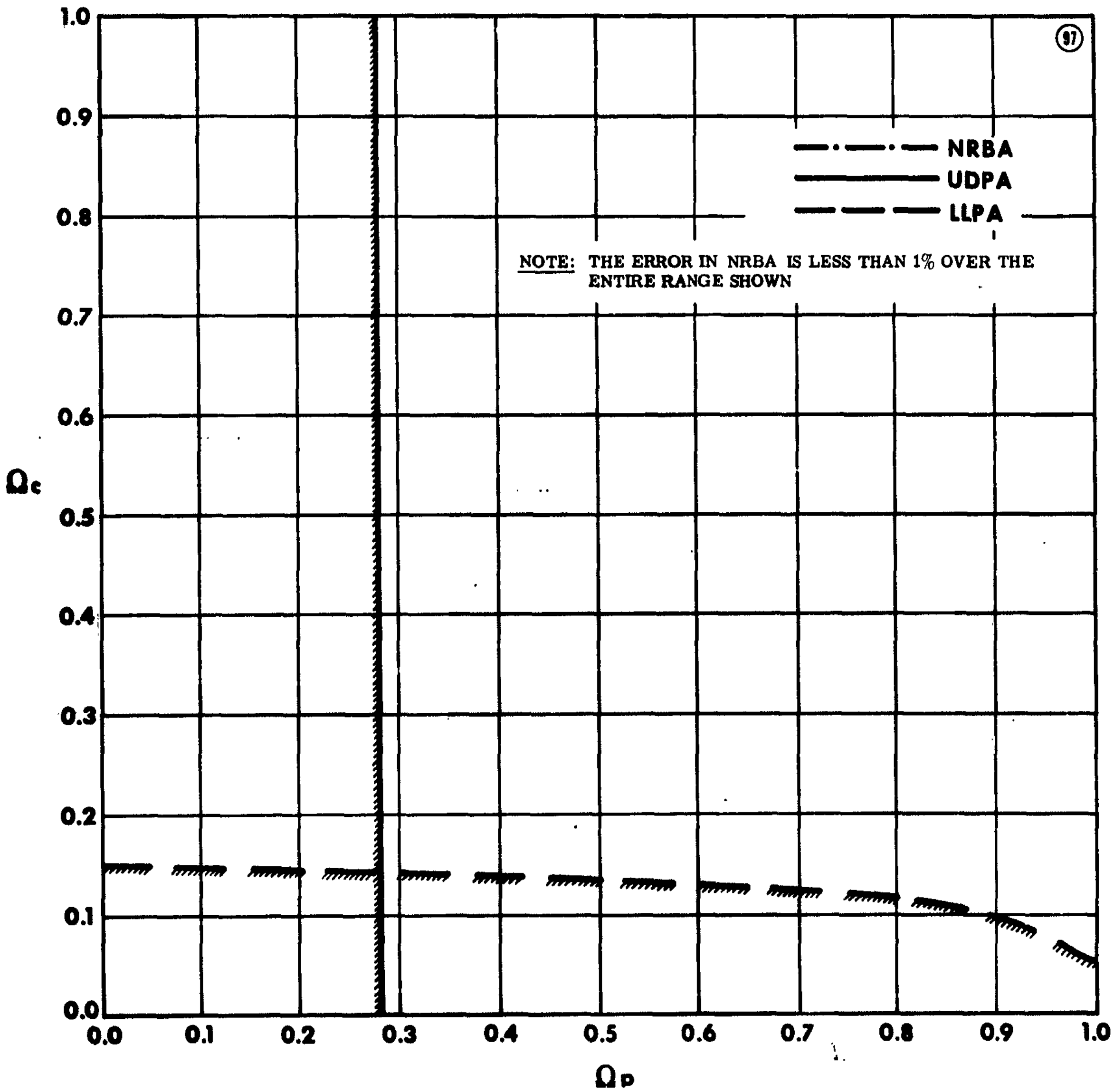

Figure 97 Comparison between Nonreflective Boundary Approximation (NRBA), Underdense Plasma Approximation (UDPA) and Low-Loss Plasma Approximation, for a Value of the Normalized Thickness of the Plasma Layer d = 10, Showing Regions where the Error in Plasma Frequency is less than 1%

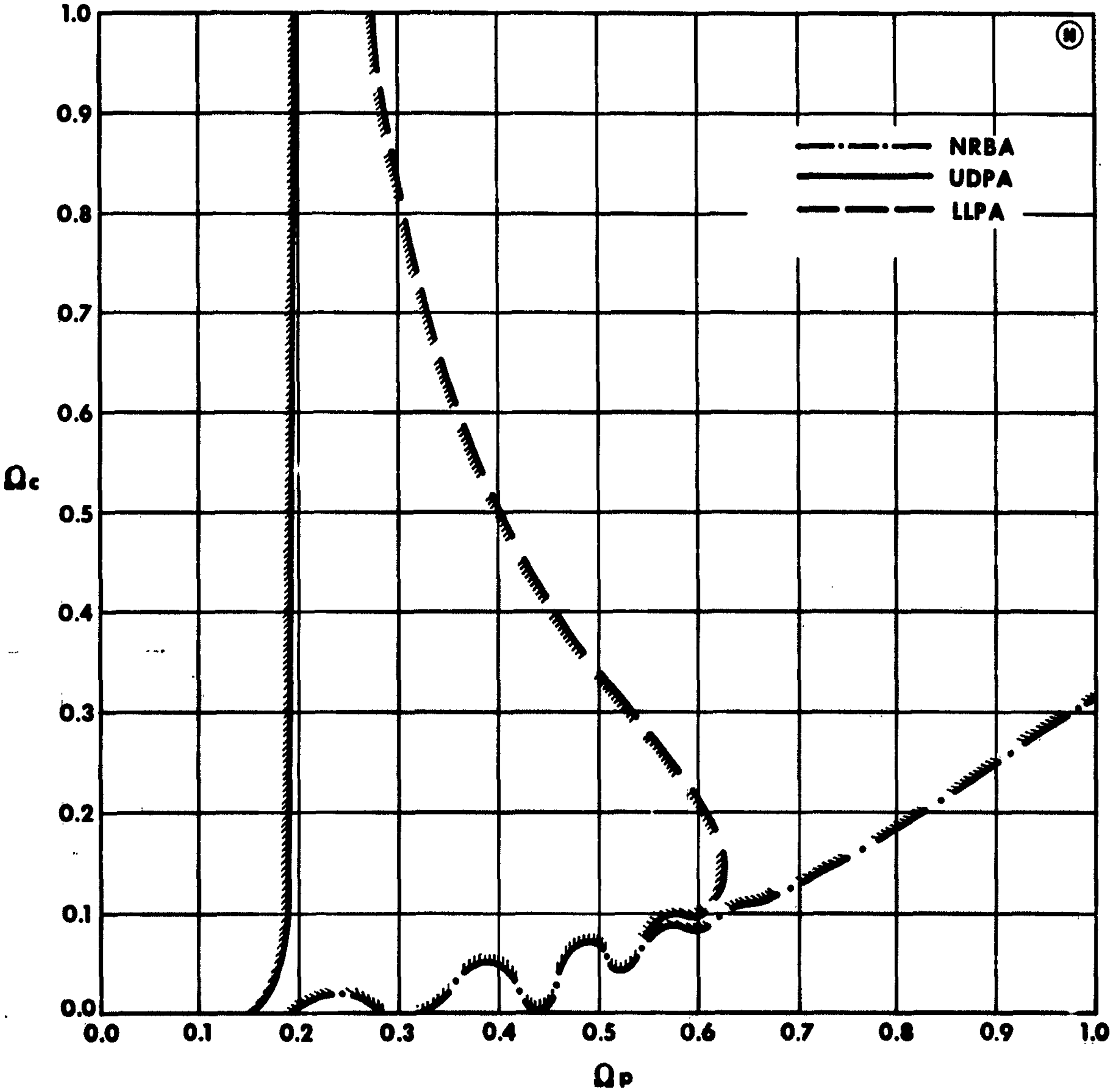

Figure 98 Comparison between Nonreflective Boundary Approximation (NRBA), Underdense Plasma Approximation (UDPA) and Low-Loss Plasma Approximation, for a Value of the Normalized Thickness of the Plasma Layer d = 10, Showing Regions where the Error in Collision Frequency is less than 1%

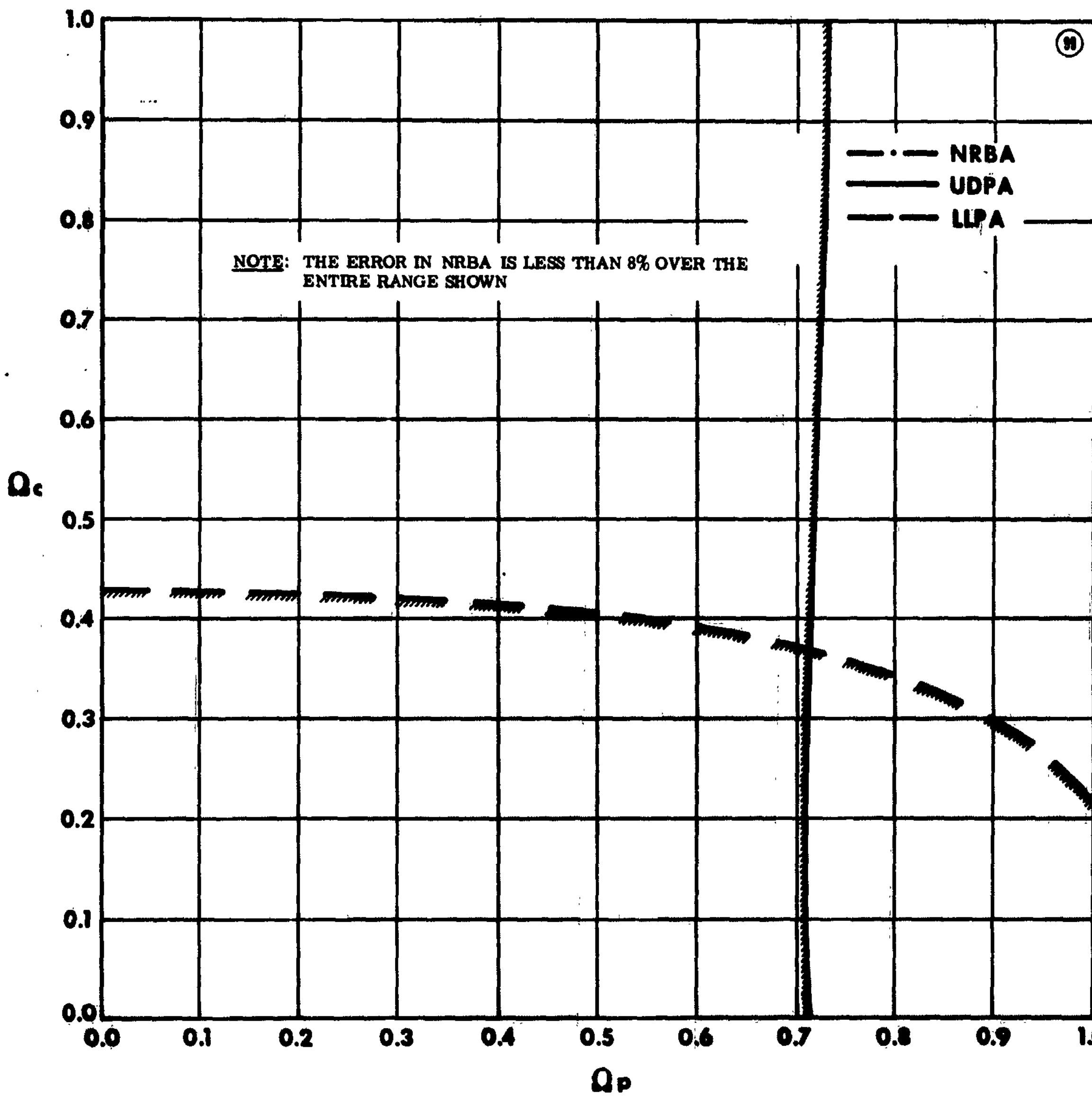

Figure 99 Comparison between Nonreflective Boundary Approximation (NRBA), Underdense Plasma Approximation (UDPA) and Low-Loss Plasma Approximation, for a Value of the Normalized Thickness of the Plasma Layer d = 1, Showing Regions where the Error in Plasma Frequency is less than 8%

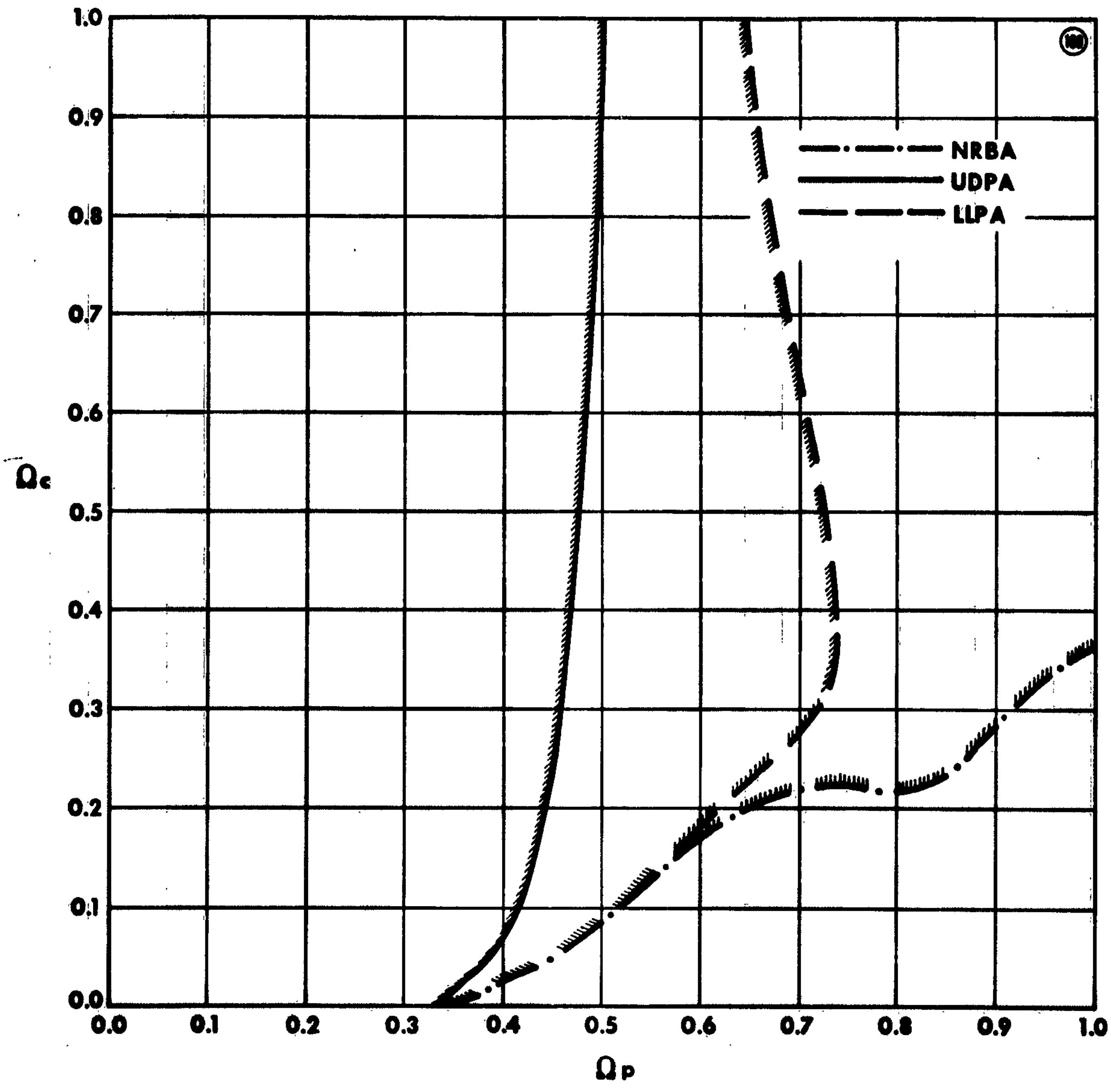

Figure 100 Comparison between Nonreflective Boundary Approximation (NRBA), Underdense Plasma Approximation (UDPA) and Low-Loss Plasma Approximation, for a Value of the Normalized Thickness of the Plasma Layer d = 1, Showing Regions where the Error in Collision Frequency is less than 8%

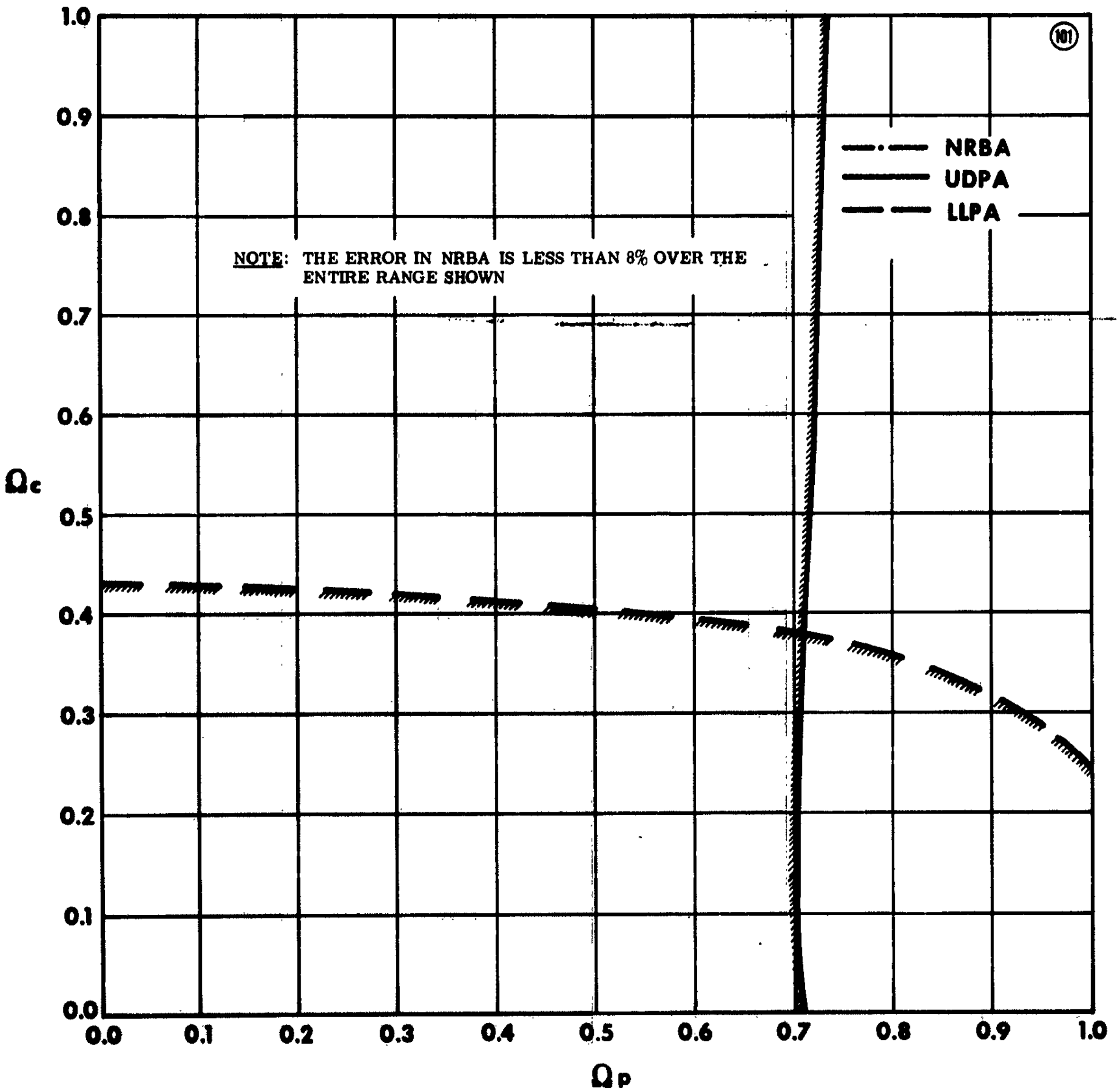

Figure 101 Comparison between Nonreflective Boundary Approximation (NRBA), Underdense Plasma Approximation (UDPA) and Low-Loss Plasma Approximation, for a Value of the Normalized Thickness of the Plasma Layer d = 3, Showing Regions where the Error in Plasma Frequency is less than 8%

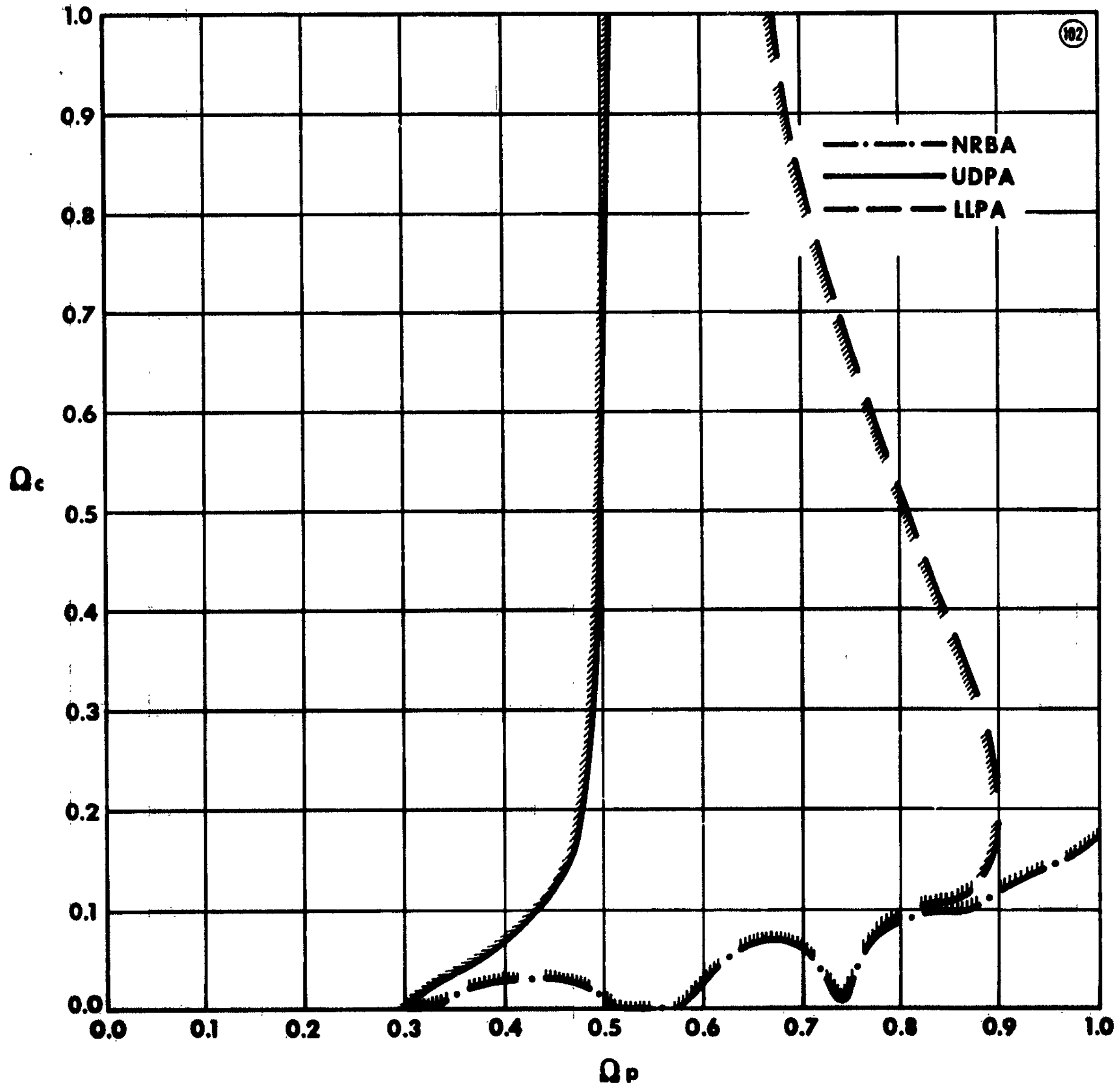

Figure 102 Comparison between Nonreflective Boundary Approximation (NRBA), Underdense Plasma Approximation (UDPA) and Low-Loss Plasma Approximation , for a Value of the Normalized Thickness of the Plasma Layer d = 3, Showing Regions where the Error in Collision Frequency is less than 8%

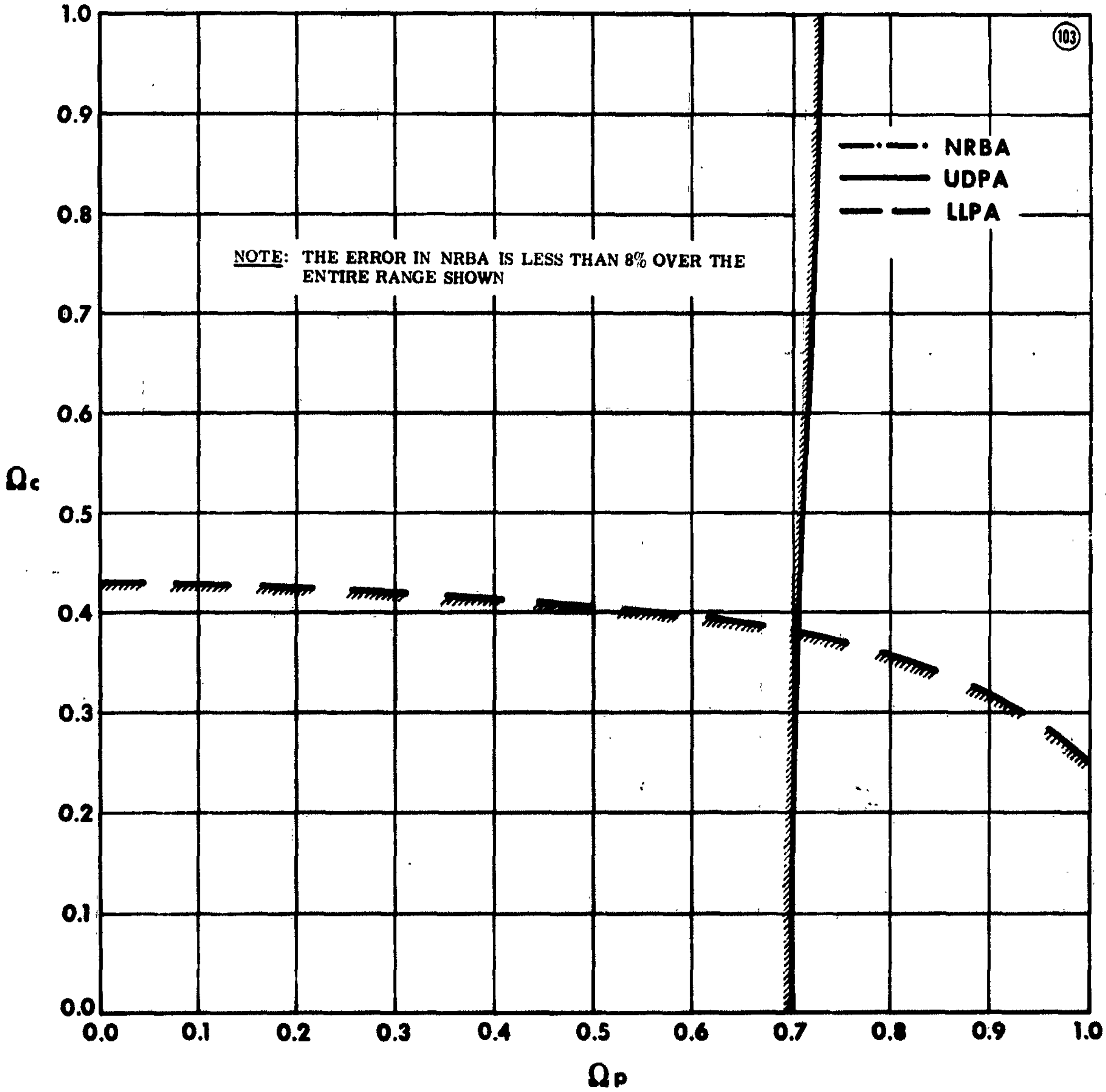

Figure 103 Comparison between Nonreflective Boundary Approximation (NRBA), Underdense Plasma Approximation (UDPA) and Low-Loss Plasma Approximation, for a Value of the Normalized Thickness of the Plasma Layer d = 5, Showing Regions where the Error in Plasma Frequency is less than 8%

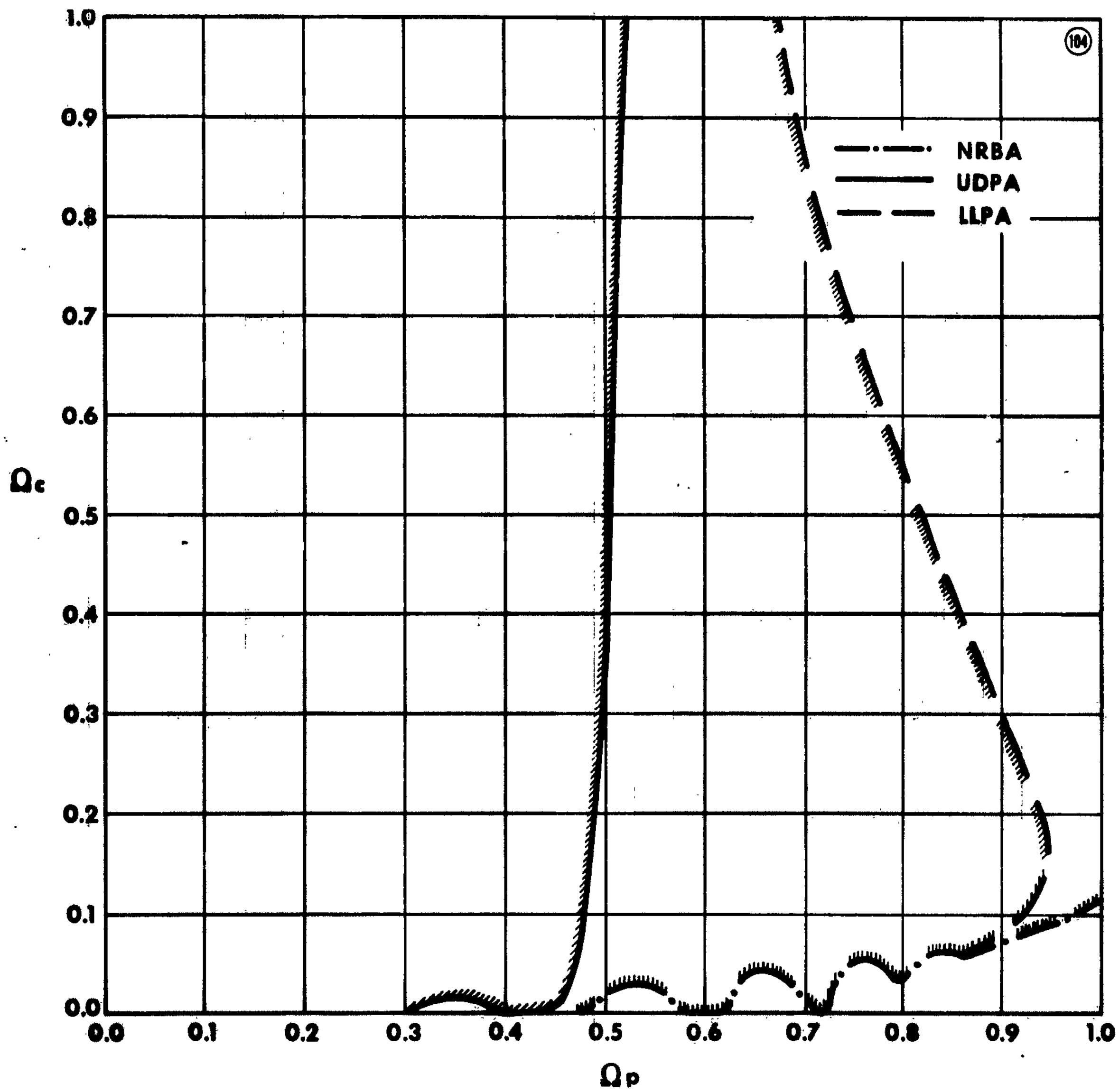

Figure 104 Comparison between Nonreflective Boundary Approximation (NRBA), Underdense Plasma Approximation (UDPA) and Low-Loss Plasma Approximation, for a Value of the Normalized Thickness of the Plasma Layer d = 5, Showing Regions where the Error in Collision Frequency is less than 8%

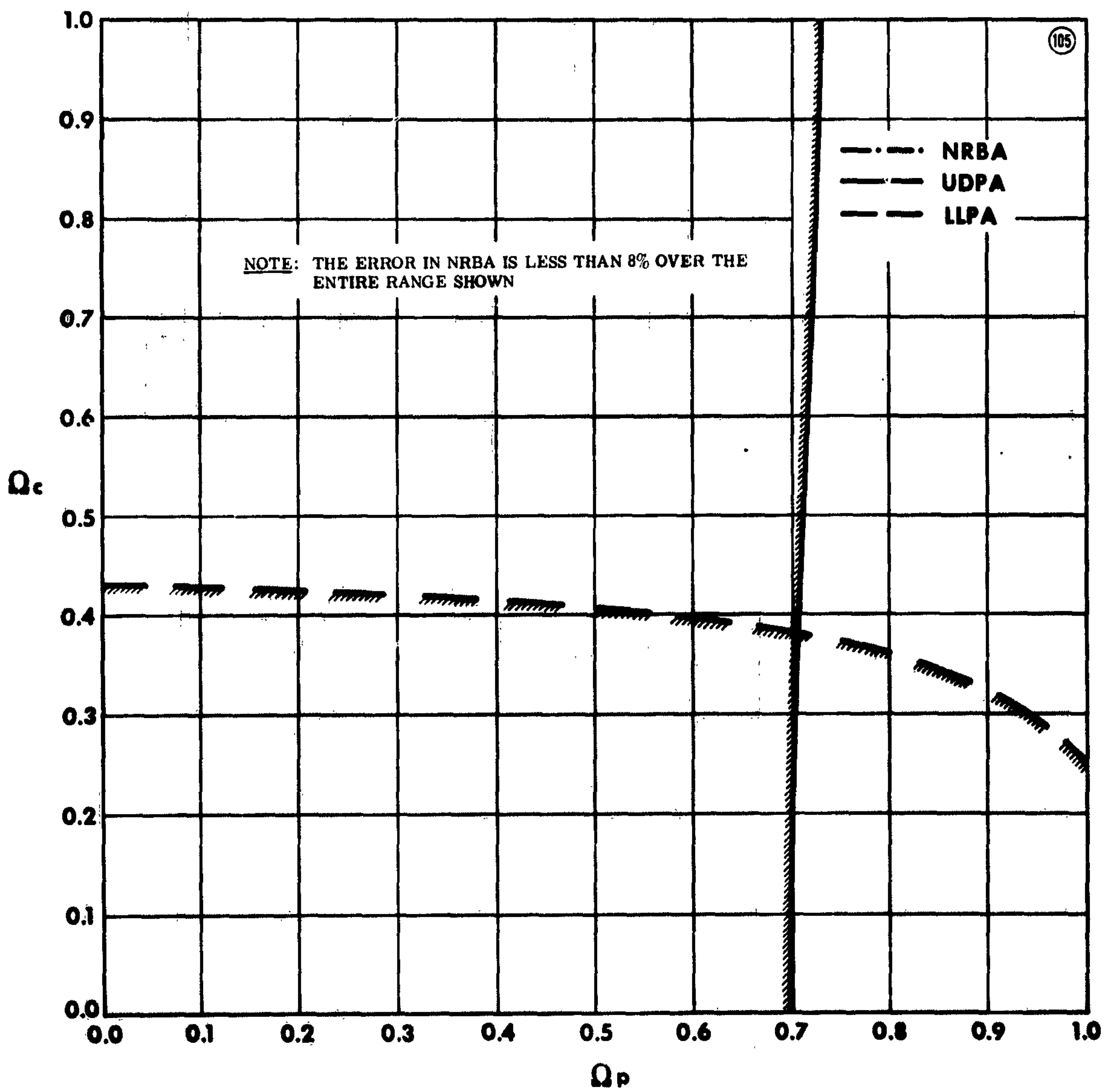

Figure 105 Comparison between Nonreflective Boundary Approximation (NRBA), Underdense Plasma Approximation (UDPA) and Low-Loss Plasma Approximation, for a Value of the Normalized Thickness of the Plasma Layer d = 10, Showing Regions where the Error in Plasma Frequency is less than 8%

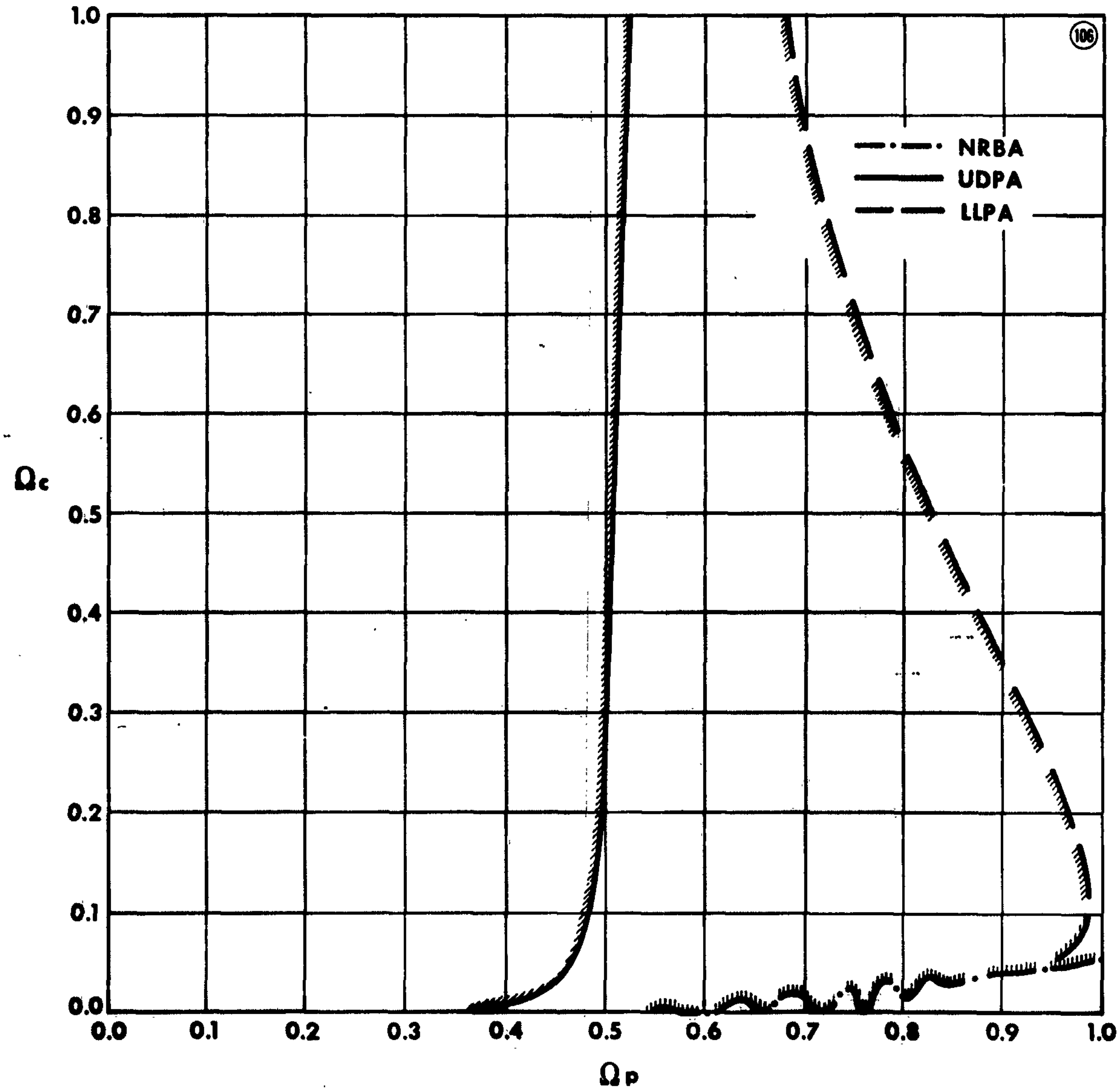

Figure 106 Comparison between Nonreflective Boundary Approximation (NRBA), Underdense Plasma Approximation (UDPA) and Low-Loss Plasma Approximation, for a Value of the Normalized Thickness of the Plasma Layer d = 10, Showing Regions where the Error in Collision Frequency is less than 8%

DISTRIBUTION LIST
for Analysis Reports on the
HYPERVELOCITY RANGE RESEARCH PROGRAM

Recipient	Copy No.
Commanding General U. S. Army Missile Command Redstone Arsenal, Alabama ATTN: ORDXM-RRX	1
Los Angeles Procurement District U.S. Army 55 South Grand Avenue Pasadena, California ATTN: F.K. Whitburn, Contracting Officer	2
Director Advanced Research Projects Agency Washington 25, D. C. ATTN: F. Koether ATTN: E. Haynes ATTN: C. McLain ATTN: Major J. Kiernan	 3-5 6 7 8
Aerojet-General Corporation P.O. Box 296 Azusa, California ATTN: Technical Library	9
Aeronutronics Division, Ford Motor Co. Ford Road Newport Beach, California ATTN: Technical Information Services	10
Aerospace Corporation 2400 E. El Segundo Bvld El Segundo, California ATTN: D. Bitondo ATTN: Manager of Penetration Aids	 11 12
Aerospace Corporation P.O. Box 95085 Los Angeles 45, California ATTN: J. Logan	13
Aerospace Corporation San Bernardino, California ATTN: Mr. R. Fowler ATTN: H. Myers	 14 15
Avco-Everett Research Laboratory 2385 Revere Beach Parkway Everett 49, Massachusetts ATTN: Dr. Bennett Kivel	16
U.S. Air Force Ballistic Systems Division AF Unit Post Office Los Angeles 45, California ATTN: Major W. Levy ATTN: Lt. K.G. Jefferson	 17 18
HQ BSD (AFSC) AF Unit Post Office Los Angeles 45, California ATTN: BSRVD	19
USAF Cambridge Research Laboratories Laurence Hanscom Field Bedford, Massachusetts ATTN: CRRELR, Stop 29	20
Director USAF Office of Scientific Research Washington 25, D.C. ATTN: Mechanics Division/ Major Terrell	21
Director Ames Research Center Moffett Field, California ATTN: H. Allen	22
Applied Physics Laboratory The John Hopkins University 8621 Georgia Avenue Silver Spring, Maryland ATTN: G. Seielstad	23
Applied Physics Laboratory Sylvania Elec. Products Waltham, Massachusetts ATTN: R. Row	24
Armour Research Foundation 10 W. 35th Street Chicago 16, Illinois ATTN: Fluid Dynamics Research Division	25
Commanding General U.S. Army Air Defense Command Colorado Springs, Colorado ATTN: Advanced Projects Division, G-3	26

DISTRIBUTION LIST (continued)

Recipient	Copy No.
Commanding General U.S. Army Ballistics Research Laboratories Aberdeen Proving Gound, Maryland	
ATTN: C.H. Murphy	27
ATTN: B.J. Karpov	28
Commanding General U.S. Army Elec. and Communications Command Research and Development Fort Monmouth, New Jersey	29
Commanding General U.S. Army Materiel Command Washington 25, D. C.	30
Commanding General U.S. Army Missile Command Redstone Arsenal, Alabama	
ATTN: AMSMI-RB	31
ATTN: AMSMI-RRX	32
ATTN: AMSMI-RNR	33
ATTN: AMCPM-ZER-R	34
Security Office, Army Missile Command Pacific Field Office Box 56, Navy 824 c/o FPO, San Francisco, California	
ATTN: Dr. S. Edelberg	35
Commanding General U.S. Army Research and Development Washington 25, D. C.	
ATTN: Intl. Division	36
ATTN: Physical Sciences Division	37
Commanding Officer U.S. Army Signal Missile Support Agency White Sands Missile Range, New Mexico	
ATTN: SIGWS-MM-1	38
ATTN: MEW	39
U.S. Army Technical Intelligence Agency Arlington Hall Station Arlington 12, Virginia	
ATTN: ORDLI	40
ARO, Inc. von Karman Facility Tullahoma, Tennessee	
ATTN: J. Lukasiewicz	41
Avco Corporation Research and Advanced Development Division Wilmington, Massachusetts	
ATTN: Technical Library	42
Avco-Everett Research Laboratory 2385 Revere Beach Parkway Everett, Massachusetts	
ATTN: Technical Library	43
Barnes Engineering Company 30 Commerce Road Stamford, Connecticut	
ATTN: H. Yates	44
Battelle Memorial Institute 505 King Avenue Columbus 1, Ohio	
ATTN: Battelle-DEFENDER	45
Bell Telephone Laboratories, Inc. Whippany, New Jersey	
ATTN: C.W. Hoover, Room 2B-105	46
ATTN: C.E. Paul	47
ATTN: John McCarthy	48
Bendix Corporation Systems Division 3300 Plymouth Road Ann Arbor, Michigan	
ATTN: Systems Analysis and Math Dept.	49
ATTN: Flight Sciences Department	50
Boeing Airplane Company P.O. Box 3707 Seattle, Washington	
ATTN: Org. 2-5732/J. Klaimon	51
Brown Engineering Company Huntsville, Alabama	
ATTN: Technical Library	52
California Institute of Technology Pasadena, California	
ATTN: Prof. L. Lees	53
Central Intelligency Agency 2930 E Street, N.W. Washington, D. C.	
ATTN: OCR Standard Distribution	54-56

DISTRIBUTION LIST (continued)

Recipient	Copy No.
Communication and Propagation Laboratory Stanford Research Institute Menlo Park, California	
ATTN: Mr. Ray L. Leadabrand, Head Propagation Group	57
ATTN: Dr. Carson Flammer	58
Defense Documentation Center Cameron Station Alexandria, Virginia	59-78
Cornell Aeronautical Laboratory 4455 Genesee Street Buffalo 21, New York	
ATTN: J. Lotsof	79
ATTN: W. Wurster	80
ATTN: Applied Physics Dept.	81
Defense Research Corporation 4050 State Street Santa Barbara, California	
ATTN: W. Short	82
Director Electromagnetic Warfare Laboratory Wright-Patterson Air Force Base Dayton, Ohio	
ATTN: ASRN/W. Bahret	83
Electro-Optical Systems, Inc. 300 N. Halstead Street Pasadena, California	
ATTN: R. Denison	84
General Applied Sciences Laboratories Merrick and Stewart Avenues Westbury, Long Island, New York	
ATTN: M. Bloom	85
General Dynamics Corporation Astronautics Division San Diego, California	
ATTN: Chief Librarian, Mail Zone 6-157	86
General Electric Company Re-entry Vehicles Division 3198 Chestnut Street Philadelphia, Pennsylvania	
ATTN: L. I. Chaseen, Room 3446	87
Geophysics Corporation of America Burlington Road Bedford, Massachusetts	88
Heliodyne Corporation 2365 Westwood Blvd Los Angeles 64, California	89
Institute for Defense Analyses 1666 Connecticut Avenue N. W. Washington 9, D. C.	
ATTN: Dr. J. Menkes	90
ATTN: Dr. L. Biberman	91
ATTN: Dr. R. Fox	92
ATTN: Dr. J. Martin	93
ATTN: Mr. D. Katcher, JASON Library	94
Institute of Science and Technology The University of Michigan P. O. Box 618 Ann Arbor, Michigan	
ATTN: BAMIRAC Library	95
Jet Propulsion Laboratory 4800 Oak Grove Drive Pasadena, California	
ATTN: H. Denslow	96
ATTN: Library	97
Kaman Nuclear Division Colorado Springs, Colorado	
ATTN: A. Bridges	98
Director Langley Research Center Langley Field, Virginia	
ATTN: W. Erickson	99
ATTN: R. L. Trimpi	100
Lockheed Corporation Missiles and Space Division Sunnyvale, California	
ATTN: Ray Munson	101
Melpar, Inc. Applied Science Division 11 Galen Street Watertown 72, Massachusetts	
ATTN: Librarian	102

DISTRIBUTION LIST (continued)

Recipient	Copy No.
Martin Aircraft Company Orlando, Florida ATTN: J. Mays	103
Director Marshall Space Flight Center Huntsville, Alabama ATTN: M-AERO-TS	104
Massachusetts Institute of Technology Lincoln Laboratory P.O. Box 73 Lexington 73, Massachusetts ATTN: M. Herlin ATTN: R. Slattery ATTN: V. Guethlen	 105 106 107
Chief U.S. Navy Bureau of Weapons Washington 25, D.C. ATTN: RMWC-322	108
Chief of Naval Operations Washington 25, D. C ATTN: OP-07T10	109
Commander U.S. Naval Ordnance Laboratory White Oak, Silver Spring, Maryland ATTN: Technical Library	110
Director U.S. Naval Research Laboratory Washington 25, D.C. ATTN: Code 2027	111
New York University Department of Aero Engineering University Heights New York 53, New York ATTN: L. Arnold	112
North American Aviation Space and Information Systems Division 12214 Lakewood Blvd Downey, California ATTN: E. Allen	113
Princeton University Princeton, New Jersey ATTN: Prof. E. Frieman ATTN: Prof. S. Bogdonoff	 114 115
Purdue University School Aero and Engineering Sciences LaFayette, Indiana ATTN: I. Kvakovsky	116
Radio Corporation of America Missiles and Surface Radar Division Mooretown, New Jersey	117
The Rand Corporation 1700 Main Street Santa Monica, California ATTN: Library	118
Raytheon Manufacturing Company Missile Systems Division Bedford, Massachusetts ATTN: I. Britton, Librarian	119
Rome Air Development Center Griffiss Air Force Base Rome, New York ATTN: P. Sandler	120
The Martin Company Aerospace Division, Mail No. T-38 P.O. Box 179, Denver, Colorado ATTN: R. E. Compton, Jr.	121
Space Technology Laboratories, Inc. 1 Space Park Redondo Beach, California ATTN: Leslie Hromas	122
The Warner and Swasey Company Control Instrument Division 32-16 Downing Street Flushing 54, New York	123
University of California San Diego, California ATTN: Prof. N. M. Kroll	124
University of California Lawrence Radiation Laboratory Livermore, California ATTN: C. Craig	125
University of Chicago Laboratories for Applied Science Chicago 37, Illinois ATTN: L. M. Biberman	126

DISTRIBUTION LIST (concluded)

Recipient	Copy No.
University of Michigan Ann Arbor, Michigan ATTN: Prof. K. M. Case	127
University of Michigan Radiation Laboratory 201 Catherine Ann Arbor, Michigan ATTN: R. J. Leite	128
Valley Forge Space Technical Center General Electric Company P. O. Box 8555 Philadelphia 1, Pennsylvania ATTN: K. Wau ATTN: J. Farber	 129 130
Director Weapon Systems Evaluation Group Pentagon, Room 1E-800 Washington 25, D. C.	131
AVCO Corporation Research and Advanced Development Division 201 Lowell Street Wilmington, Massachusetts ATTN: Dr. Wentink	132
U. S. Army Liaison Office Canadian Armament Research and Development Establishment P. O. Box 1427 Quebec, P. Q., Canada ATTN: Lt. Col. E. W. Kreischer	133
British Joint Mission British Embassy 3100 Massachusetts Avenue, N. W. Washington, D. C. ATTN: Mr. F. I. Reynolds, Defense Research Staff	134
Australian Embassy 2001 Connecticut Avenue N. W. Washington, D. C. ATTN: D. Barnsley, Defense Research and Development Rep.	135
GM Defense Research Laboratories	136 and above

GM Defense Research Laboratories, General Motors Corp., Santa Barbara, Calif.

A COMPARISON OF SEVERAL APPROXIMATIONS FOR THE DETERMINATION OF PLASMA LAYER PROPERTIES FROM THE MEASURED ELECTROMAGNETIC TRANSMISSION COEFFICIENT, by S. V. Zivanovic, H. M. Musal, Jr., R. I. Primich and J. Allen TR63-217G. Dec 1963, 126 pp, incl. 106 illus., 12 refs.

Several commonly used approximations of the transmission coefficient of a uniform plasma slab are critically examined and compared with a new approximation developed in this report. It is shown that the new approximation, in addition to being very suitable for use on digital computers, gives much higher accuracy than any other one over most useful

1. Plasma physics
2. Mathematical computers – Applications
3. Electrons – Density
4. Electromagnetic waves – Transmission

I. DA-04-495-ORD-3567(Z)
II. TR63-217G
III. Zivanovic, S. V.; Musal, H. M.; Primich, R. I.; and Allen, J.

(Descriptors) Plasma physics, Plasma sheath, Electromagnetic waves, Microwaves, Electron density

GM Defense Research Laboratories, General Motors Corp., Santa Barbara, Calif.

A COMPARISON OF SEVERAL APPROXIMATIONS FOR THE DETERMINATION OF PLASMA LAYER PROPERTIES FROM THE MEASURED ELECTROMAGNETIC TRANSMISSION COEFFICIENT, by S. V. Zivanovic, H. M. Musal, Jr., R. I. Primich and J. Allen TR63-217G. Dec 1963, 126 pp, incl. 106 illus., 12 refs.

Several commonly used approximations of the transmission coefficient of a uniform plasma slab are critically examined and compared with a new approximation developed in this report. It is shown that the new approximation, in addition to being very suitable for use on digital computers, gives much higher accuracy than any other one over most useful

1. Plasma physics
2. Mathematical computers – Applications
3. Electrons – Density
4. Electromagnetic waves – Transmission

I. DA-04-495-ORD-3567(Z)
II. TR63-217G
III. Zivanovic, S. V.; Musal, H. M.; Primich, R. I.; and Allen, J.

(Descriptors) Plasma physics, Plasma sheath, Electromagnetic waves, Microwaves, Electron density

GM Defense Research Laboratories, General Motors Corp., Santa Barbara, Calif.

A COMPARISON OF SEVERAL APPROXIMATIONS FOR THE DETERMINATION OF PLASMA LAYER PROPERTIES FROM THE MEASURED ELECTROMAGNETIC TRANSMISSION COEFFICIENT, by S. V. Zivanovic, H. M. Musal, Jr., R. I. Primich and J. Allen TR63-217G. Dec 1963, 126 pp, incl. 106 illus., 12 refs.

Several commonly used approximations of the transmission coefficient of a uniform plasma slab are critically examined and compared with a new approximation developed in this report. It is shown that the new approximation, in addition to being very suitable for use on digital computers, gives much higher accuracy than any other one over most useful

1. Plasma physics
2. Mathematical computers – Applications
3. Electrons – Density
4. Electromagnetic waves – Transmission

I. DA-04-495-ORD-3567(Z)
II. TR63-217G
III. Zivanovic, S. V.; Musal, H. M.; Primich, R. I.; and Allen, J.

(Descriptors) Plasma physics, Plasma sheath, Electromagnetic waves, Microwaves, Electron density

GM Defense Research Laboratories, General Motors Corp., Santa Barbara, Calif.

A COMPARISON OF SEVERAL APPROXIMATIONS FOR THE DETERMINATION OF PLASMA LAYER PROPERTIES FROM THE MEASURED ELECTROMAGNETIC TRANSMISSION COEFFICIENT, by S. V. Zivanovic, H. M. Musal, Jr., R. I. Primich and J. Allen TR63-217G. Dec 1963, 126 pp, incl. 106 illus., 12 refs.

Several commonly used approximations of the transmission coefficient of a uniform plasma slab are critically examined and compared with a new approximation developed in this report. It is shown that the new approximation, in addition to being very suitable for use on digital computers, gives much higher accuracy than any other one over most useful

1. Plasma physics
2. Mathematical computers – Applications
3. Electrons – Density
4. Electromagnetic waves – Transmission

I. DA-04-495-ORD-3567(Z)
II. TR63-217G
III. Zivanovic, S. V.; Musal, H. M.; Primich, R. I.; and Allen, J.

(Descriptors) Plasma physics, Plasma sheath, Electromagnetic waves, Microwaves, Electron density

values of plasma and collision frequencies.

A series of charts shows the regions of validity of each approximation in the plasma frequency-collision frequency plane for various amounts of error and slab thicknesses.

values of plasma and collision frequencies.

A series of charts shows the regions of validity of each approximation in the plasma frequency-collision frequency plane for various amounts of error and slab thicknesses.

values of plasma and collision frequencies.

A series of charts shows the regions of validity of each approximation in the plasma frequency-collision frequency plane for various amounts of error and slab thicknesses.

values of plasma and collision frequencies.

A series of charts shows the regions of validity of each approximation in the plasma frequency-collision frequency plane for various amounts of error and slab thicknesses.